Epigenetic regulation of histone three lysine twenty seven tri methylation dictates mesenchymal stem cell lineage commitment, lifespan and murine skeletal development

Sarah Elizabeth Hemming BHthSc (Hons)

The Discipline of Medicine

School of Medicine

Faculty of Health Sciences

The University of Adelaide

Supervisors

Prof. Stan Gronthos

Dr. Dimitrios Cakouros

Table of contents

Declaration

I certify that this work contains no material which has been accepted for the award of any other degree or diploma in any university or other tertiary institution and, to the best of my knowledge and belief, contains no material previously published or written by another person, except where due reference has been made in the text. I give consent to the copy of my thesis, when deposited at the University Library, being made available for loan and photocopying, subject to the provisions of the Copyright Act 1968. I also give permission for the digital version of my thesis to be made available on the web, via the University's digital research repository, the Library catalogue and also through web search engines, unless permission has been granted by the University to restrict access for a period of time

Signed:

Sarah Hemming

Date: 11-04-2016

Acknowledgments

Firstly I would like to thank my supervisors Stan and Jim for all you help and support over the last four years. You have seen me grow from an honours student to an accomplished PhD student, with many life accomplishments along the way and you both have always encouraging me to succeed. This thesis is not only a reflection of my achievement but yours also. I would like to acknowledge the Australia Postgraduate Award (APA) and Dawes Top-up scholarship, this financial assistant allowed me to focus on my PhD.

I would like to thank the present and past members of the Mesenchymal Stem Cell Laboratory and the Multiple Myeloma Group, your guidance and support has been amazing. I would like to personally recognise the time and help I received from Sharon Paton, Esther Camp-Dotlic, Kim Hynes, Mary Mathews, Kate Vandyke, Steven Fitter and Duncan Hewett. I would like to extend a big thankyou to Ruth and Agatha from Adelaide Microscopy. Thank you, Kencana for helping optimise my antibodies for immunohistochemistry and David Haynes for allowing me to use your laboratory.

I would like to thank my family (Mum, Dad, Matt, Katie and Simon) for your love, support and encouragement throughout my postgraduate studies. Most importantly, I would like to thank my loving and tolerant husband Matt, who throughout this PhD has seen the best and worst of me and still loves me any way. Thank you to Matt's family for all your support and encouragement throughout my PhD.

This has by far been the hardest thing I have accomplished and I couldn't have done it without all of you. Thank you.

Abbreviations

3D	Three dimensional
+/+	Wildtype *Ezh2* alleles
+/-	One wildtype *Ezh2* allele and one floxed *Ezh2* allele
-/-	Two floxed *Ezh2* alleles
Adip	Adipogenic
AIPOQ	Adiponectin
ALK PHOS	Alkaline phosphatase
BFR	Bone formation rate
BFR/BS	Bone formation rate/ Bone surface
BMD	Bone mineral density
BMP	Bone morphogenetic proteins.
BMSC	Bone marrow derived stromal/stem cell
BMSSC	Bone marrow stromal cell
bp	Base pair
BRDU	5-bromo-2deoxyuridine
BS	Bone surface
BSA	Bovine serum albumin
BSP	Bone sialoprotein
BV	Bone volume
BV/TV	Bone volume/ Tissue volume
CamKII	Calcium-calmodulin dependent protein kinase-II
CBFA1	Core binding factor-1 (Gene)
CBFA1	Core binding factor-1 (Protein)
CDK1	cyclin dependent kinase 1
cDNA	Complementary deoxyribonucleic acid

C/EBP-α	CCAAT/Enhancer binding protein alpha (Gene)
C/EBP-α	CCAAT/Enhancer binding protein alpha (protein)
CFU	Colony forming unit
CFU-F	Colony forming unit-fibroblast
ChIP	Chromatin immunoprecipitation
ChIP-Seq	Chromatin immunoprecipitation sequencing
ChIP-on-ChIP	Chromatin immunoprecipitation on Chromatin immunoprecipitation
COL1A1	Collagen type 1A1
Cont	Control
COX2	Cyclooxygenase 2
CTan	Comprehensive TeX Archive Network
Ct.Th	Cortical thickness
DLX5	Distal-less homeobox 5
DMEM	Dulbecco's modified eagle medium
DMSO	Dimethyl sulphoxide
DNA	Deoxyribonucleic acid
DNAse	Deoxyribonuclease
dNTP	Deoxyribonucleotide triphosphate
DNMTs	DNA methyltransferases
DTT	Dithiothreitol
EB	Elution buffer
EDTA	Ethylenediaminetetra-acetic acid
ESC	Embryonic Stem Cells
EZH2	Human enhancer of zeste homolog 2 (Gene)
EZH2	Human & mouse enhancer of zeste homolog 2 (Protein)

Ezh2	Mouse enhancer of zeste homolog 2 (Gene)
$Ezh2^{+/+}$	Tg.Prx-1 Cre +:Ezh2 wt/wt
$Ezh2^{+/-}$	Tg.Prx-1 Cre +:Ezh2 fl/wt
$Ezh2^{-/-}$	Tg.Prx-1 Cre +:Ezh2 fl/fl
FACS	Fluorescence activated cell sorting
FCS	Foetal calf serum
fl	Lox P (flox sites)
g	The number of times the gravitational force
g	Grams
GAPDH	Glutaraldehyde 3-phosphate dehydrogenase
GFP	Green fluorescent protein
GREM1	Gremlin 1
GSK3	Glycogen synthase kinase 3
H&E	Haematoxylin and eosin
HATS	Histone acetyltransferases
HDACs	Histone deacetylases
HBSS	HANKS balanced salt solution
HEPES	4-(2-hydroxyethyl)-1-piperazineethanesulfonic acid
HET	Heterozygous
hMSC	Human mesenchymal stem cell
HMTS	Histone methyltransferases
HOM	Homozygous
HSC	Haematopoietic Stem Cell
H3K4	Histone three lysine four
H3K27	Histone three lysine twenty seven

H3K36	Histone three lysine thirty six
H3K79	Histone three lysine seventy nine
H3K9	Histone three lysine nine
H_2O_2	Hydrogen peroxide
IGF	Insulin growth factor
IgG	Immunoglobulin G
IHH	Indian hedge hog
IL-1	Interleukin 1
IL-6	Interleukin 6
IP	Immunoprecipitation
iPSC	Induced Pluripotent Stem Cells
JMJD3	Jumonji domain-containing protein 3
JNK	The c-Jun NH2-terminal kinases
KLF4	Kruppel-like factor 4
LEPR	Leptin receptor
LRP	Lipoprotein related proteins
KMD6A	Lysine demethylase 6A
KDM6b	Lysine demethylase 6B
M	Molar
MAR	Mineral apposition rate
M-CSF	Macrophage colony stimulating factor
Me1	Mono-methylation
Me2	Di-methylation
Me3	Tri-methylation
MEM	Minimum essential medium

Micro-CT	Micro-computed tomography
MITR	Myocyte enhancer factor-2 interacting transcription factor
mm	Miller mitres
MPP	Multipotent progenitor cells
mRNA	Messenger ribonucleic acid
mRNA	Messenger ribonucleic acid
MSC	Mesenchymal Stem Cell
MX1	Myxovirus resistance-1
α-MEM	α-modified Eagle's medium
µM	Micro molar
µm	Microns
NCOR	Nuclear compressor
N	Number
N.Adip/Mar.Ar	Number of adipocytes in marrow area
N.Ob/B.Pm	Number of osteoblasts on bone perimeter
NOD	Normal osteoblast donor
nM	Nano molar
NRecon	high-speed volumetric reconstruction software
Ob	Osteoblast
OC	Osteoclast
OC	Osteocalcin chapter 3
OCN	Osteocalcin
OCR	Osteochondral reticular cells
OCT4	Octamer-binding transcription factor 4
OPG	Osteoprotegerin

OPN	Osteopontin
Oste	Osteogenic
OSX	Osterix
PBND	PCR buffer with non-ionic detergents
PBS	Phosphate buffered saline
PCR	Polymerase chain reaction
PDGFRα	Platelet-derived growth factor receptor α
pRUF-EZH2	pRUF-IRES-GFP-EZH2 vector
PK	Proteinase K
Pm	Perimeter
PPARγ2	Peroxisome proliferator-activated receptor gamma
pRUF-GFP	pRUF-IRES-GFP vector
pRUF-KDM6A	pRUF-IRES-GFP-KDM6A vector
PTHRP	Parathyroid hormone-related protein
RANK	Receptor activator of nuclear factor kappa-B
RANKL	Receptor activator of nuclear factor kappa-B ligand
rcf	relative centrifugal force or x g-force
RNA	Ribonucleic acid
ROI	Region of interest
rpm	revolutions per minute
RT	Room temperature
RT-PCR	Real-time polymerase chain reaction
RUNX2	Run related transcription factor
SDEV	Standard deviation
SEM	Standard error of the mean

Sem	Scanning electron microscope
SHH	Sonic hedge hog
siRNA	Small interfering RNA
SOX9	Sex-determining region SRY of the Y chromosome 9
STRO-1	stromal precursor cell surface antigen
Tb.Th	Trabecular thickness
Tb.Sp	Trabecular spacing
TF	Transcription factor
TNF	Tumour necrosis factor
TRAP	Tartrate-resistant acid phosphatase 5
TS	Tissue surface
TSS	Transcription start site
TV	Tissue volume
Tween 20	Polyethylene glycol sorbitan monolaurate
UTX	Ubiquitously transcribed tetra-tricopeptide repeat X
UV	Ultra violet
VSVG	Vesicular stomatitis virus G-protein
WT	Wild type
WNT	wingless-type
w/v	Weight per volume

List of publications

Publications generated during my PhD:

Stem Cells Dev. 2015 Jun 1;24(11):1297-308. doi: 10.1089/scd.2014.0471. Epub 2015 Feb 25. **Cakouros D, Isenmann S, Hemming SE, Menicanin D, Camp E, Zannettino AC, Gronthos S**. Novel basic helix-loop-helix transcription factor hes4 antagonizes the function of twist-1 to regulate lineage commitment of bone marrow stromal/stem cells.

Stem Cells. 2014 Jul; 32(7):1991-2. doi: 10.1002/stem.1710. **Hemming S, Cakouros D, Gronthos S**. Detachment of mesenchymal stem cells with trypsin/EDTA has no effect on apoptosis detection.

Chapter 1

Sarah Elizabeth Hemming, Dimitrios Cakouros and Stan Gronthos. "Epigenetic regulation of mesenchymal stem cell growth and multi-potential differentiation". In: The Biology and Therapeutic Applications of Mesenchymal Cells. Ed K. Atkinson. John Wiley and Sons, Hoboken, New Jersey, USA. 2015, currently in press.

Chapter 2

Hemming S, Cakouros D, Isenmann S, Cooper L, Menicanin D, Zannettino A, Gronthos S. EZH2 and KDM6A act as an epigenetic switch to regulate mesenchymal stem cell lineage specification. Stem Cells. 2014 Mar;32(3):802-15. doi: 10.1002/stem.1573.

Chapter 3

Sarah Hemming, Dimitrios Cakouros, Kate Vandyke, Melissa Davis, Andrew Zannettino, Stan Gronthos. Identification of novel EZH2 targets in osteogenesis. Summited Stem to Cell Reports 2015.

Chapter 4

Sarah Hemming, Dimitrios Cakouros, John Codrington, Kate Vandyke, Andrew Zannettino, Stan Gronthos. EZH2 regulates osteoblast and adipogenic differentiation, bone microarchitecture and bone remodelling in mice. Summited to Journal of Bone and Mineral Research (JBMR).

Conference and awards

Conference Proceedings:

2015

2015 ASSCR

ASSCR, Crown Plaza, Hunter Valley, New South Wales, Australia.

Poster**;** *Methyltransferase Ezh2 regulates newborn skeletal development.*

Sarah Hemming**,** Dimitrios Cakouros, Andrew Zannettino Stan Gronthos.

Winner of the best PhD poster presenter ASSCR 2015.

2015 SAHMRI Research Showcase.

South Australian Health and Medical Research Institute (SAHMRI), Adelaide, Australia**.**

Poster; *Epigenetic modifiers: controlling MSC osteogenic differentiation.*

Sarah Hemming, Dimitrios Cakouros, Melissa Davis, Kate Vandyke, Stan Gronthos.

2015 ASMR Conference

National Wine Centre, Adelaide, Australia.

2015 Keystone and Transcriptional Stem Cell and Epigenetics Meeting

Keystone, Colorado, United States of America.

Poster; *Epigenetic modifiers: controlling MSC osteogenic differentiation.*

Sarah Hemming, Dimitrios Cakouros, Melissa Davis, Kate Vandyke, Stan Gronthos.

2015 Justin Ichiada's ALS Laboratory

Eli and Edythe Broad CIRM Centre for Regenerative Medicine and Stem Cell Research.

University of South California (USC), Los Angeles, USA.

Presented; *Epigenetic Modifiers and Mesenchymal Stem Cells* talk to the Broad CIRM centre.

2014 Florey post-graduate conference

National Wine Centre, Adelaide Australia.

The Faculty of Health Sciences, The University of Adelaide.

Poster; *Epigenetic modifiers: controlling MSC osteogenic differentiation.*

Sarah Hemming, Dimitrios Cakouros, Melissa Davis, Kate Vandyke, Stan Gronthos.
Awarded a Florey poster prize ($300)

2014 ASSCR

ASSCR, Mantra Lorne, Victoria, Australia.
Poster**;** *Epigenetic modifiers: controlling MSC osteogenic differentiation*.
Sarah Hemming**,** Dimitrios Cakouros, Melissa Davis, Kate Vandyke, Stan Gronthos.
Awarded the National Stem Cell Foundation of Australia Conference Education Award. Award covered the travel and registration cost to the conference.

2014 Adelaide Australian and New Zealand Cell and Developmental Biology Meeting

The University of South Australia, Adelaide, Australia.
Poster; *Epigenetic modifiers: controlling MSC osteogenic differentiation*.
Sarah Hemming, Dimitrios Cakouros, Melissa Davis, Kate Vandyke, Stan Gronthos.

2014 ANZSCDB meeting

Australia and New Zealand Society for Cell and Developmental Biology, University of South Australia, Adelaide, Australia.
Poster; *Epigenetic modifiers: controlling MSC osteogenic differentiation*. Sarah Hemming, Dimitrios Cakouros, Melissa Davis, Kate Vandyke, Stan Gronthos.

2013 ASSCR

ASSCR, Brisbane Convention Centre, Brisbane, Queensland, Australia.
Poster; *EZH2 and KDM6A act as an epigenetic switch to regulate Mesenchymal Stem Cell lineage specification***.**
Sarah Hemming, Dimitrios Cakouros, Sandra Isenmann, Lachlan Cooper, Danijela Menicanin, Andrew Zannettino, Stan Gronthos.
I was awarded the National Stem Cell Foundation of Australia Conference Education Award covering travel and registration cost of the conference**.**

2013 Centre for stem cell research (CSCR) postgraduate research day

CSCR, The National Wine Centre, Adelaide, Australia.
Provided by The Robinson Institute, the University of Adelaide.

Poster; *EZH2 and KDM6A act as an epigenetic switch to regulate Mesenchymal Stem Cell lineage specification***.**

Sarah Hemming, Dimitrios Cakouros, Sandra Isenmann, Lachlan Cooper, Danijela Menicanin, Andrew Zannettino, Stan Gronthos. I was awarded Second Place poster prize winner ($500).

2013 ANZOR meeting

ANZOR, Flinder St, Adelaide, Australia.

2013 Three minute thesis competition

Competed in the Faculty of Health Sciences heats.

Title; *Good old Bone*.

Sarah Hemming

2013 ANZSCDB meeting

Australia and New Zealand Society for Cell and Developmental Biology, University of South Australia, Adelaide, Australia

Oral presentation; *EZH2 and KDM6A act as an Epigenetic switch to regulate Mesenchymal Stem Cell Lineage Specification*. Sarah Hemming.

Awarded best PhD student oral presentation

2013 ASMR

Poster Presentation at the 2013 ASMR meeting, for the Australian Society for Medical Research at the Adelaide Convention Centre, Australia.

Poster; *The role of Ezh2 in mesenchymal stem cell growth and multi-differentiation.*

Hemming, S.E**.,** Cakouros, D. and Gronthos, S.

2012 ASSCR

Poster Presentation at the 2012 ASSCR, for the 5th Australasian Society for Stem Cell Research, Adelaide Convention centre, Australia.

Poster; *The role of Ezh2 in mesenchymal stem cell growth and multi-differentiation.*

Hemming, S.E**.,** Cakouros, D. and Gronthos, S.

2012 Health Science Post graduate conference

Poster Presentation at the 2012 Health Science Post graduate conference,
The Adelaide Wine Centre, Australia.
Poster; *The role of Ezh2 in mesenchymal stem cell growth and multi-differentiation.*
Hemming, S.E**.,** Cakouros, D. and Gronthos, S.

2012 Combio

Adelaide Convention Centre, Adelaide, Australia.
Combio containing the Australian society for biochemistry and molecular biology (ASBMB)
Poster; *The role of Ezh2 in mesenchymal stem cell growth and multi-differentiation*.
Hemming, S.E**.,** Cakouros, D. and Gronthos, S.

Accomplishments

2015-Awarded the Medicine travel grant - $5000 for overseas travel.
2014-Awarded best poster prize at Florey Post-Graduate Conference. Awarded $300.
2014-Awarded a National Stem Cell Foundation of Australia Conference Education Award covering travel and registration cost of the ASSCR conference.
2013-Awarded second place for best poster presentation for PhD Student at the Centre for Stem cell research, research day. Awarded $500.
2013-Awarded a National Stem Cell Foundation of Australia Conference Education Award covering travel and registration cost of the ASSCR conference.
2013-Awarded Best PhD oral presentation at the ANZSCDB meeting 2013, at the University of South Australia. Awarded $200.
2015-Awarded the Medicine travel grants 2015. Awarded $5000 for overseas travel.
2015-ASSCR national meeting. Awarded the ASSCR 2015 PhD poster prize $500.
2015-Medical Sciences demonstrator for first yea physiology student's semester 2.
2015-2016 South Australian ASMR committee member.
2016-ASSCR Policy, Ethics and Translation, subcommittee member.

Abstract

Epigenetic modifiers are increasingly being implicated as playing major roles in many cellular and biological processes, such as cell growth, differentiation, lifespan, self-renewal, cancer, and metastasis. Epigenetic modifying proteins such as Enhancer of Zeste homology 2 (EZH2), Lysine demethylase 6A (KDM6A) regulates chromatin structure through the addition or removal histone three lysine twenty seven (H3K27) tri methylation (me3) modification. The presence of H3K27me3 on the promoter of genes leads to the recruitment of chromatin condensation complexes, chromatin compaction and repression of genes transcription. H3K27 demethylases remove the H3K27me3 modification allowing the recruitment of activating transcriptional complexes, opening up of chromatin and gene expression. The Project is based on our initial profiling of histone methylation patterns of genes associated with differentiation and the expression of epigenetic modifying enzymes in MSC clonal populations by cDNA microarray analysis. Our initial studies on the function of EZH2 lineage commitment of human BMSC, suggests that EZH2 is a negative regulator of osteogenesis and a positive regulator of adipogenesis. However, the direct role of the H3K7me3 epigenetic modifiers EZH2 and KDM6A and or KDM6B in BMSC differentiation is unclear, illustrating the importance of determining the epigenetic signatures associated with differentiation and maintenance of MSC. Additionally, EZH2 mutations in one allele of EZH2 methyltransferase SET domain have been identified in patents with Weaver Syndrome. These patients exhibit excess bone growth, aging and mental retardation suggesting the importance of EZH2 in human bone development. Furthermore, with the current use of MSC for Phase II/III clinical trials it's important to understanding of the molecular pathways and epigenetic changes that regulate maintenance and differentiation of MSC aiding in treatment of skeletal tissue disorders/diseases. Therefore this PhD project identifies that EZH2 and KDM6A acts as a switch regulating

MSC lineage commitment. Presence of EZH2 and its H3K27me3 on osteogenic genes such as RUNX2 prevent MSC osteogenic differentiation and intern allows the progression of adipogenic differentiation of MSC. During osteogenesis we believe KDM6A play a role in removing the H3K27me3 off genes critical for osteogenic differentiation. Furthermore during osteogenic differentiation, EZH2 and its H3K27 modifications must be removed from genes such as RUNX2, ZBTB16, MX1 and FHL1 allowing the activation of these genes which are important for osteogenic differentiation. EZH2 conditional deletion in early limb bud mesenchyme reveals EZH2 plays a critical role in skeletal patterning, bone microarchitecture and remodelling.

Student declaration

This work contains no material which has been accepted for the award of any other degree or diploma in any university or other tertiary institution to Sarah Hemming and, to the best of my knowledge and belief, contains no material previously published or written by another person, except where due reference has been made in the text. I give consent to this copy of my thesis when deposited in the University Library, being made available for loan and photocopying, subject to the provisions of the Copyright Act 1968.

The author acknowledges that copyright of published works contained within this thesis (as listed below*) resides with the copyright holder(s) of those works. I also give permission for the digital version of my thesis to be made available on the web, via the University's digital research repository, the Library catalogue, and also through web search engines, unless permission has been granted by the University to restrict access for a period of time.

***Sarah Elizabeth Hemming, Dimitrios Cakouros and Stan Gronthos. "Epigenetic regulation of mesenchymal stem cell growth and multi-potential differentiation". In: The Biology and Therapeutic Applications of Mesenchymal Cells. Ed K. Atkinson. John Wiley and Sons, Hoboken, New Jersey, USA. 2015, currently in press**

***Hemming, S. *et al.* "EZH2 and KDM6A act as an epigenetic switch to regulate mesenchymal stem cell lineage specification". *Stem cells (Dayton, Ohio)* 32, 802-815, doi:10.1002/stem.1573 (2014).**

***Hemming, S. *et al.* "Identification of novel EZH2 targets in mesenchymal stem/stromal cells which regulate osteogenesis". *Journal of Biological Chemistry. Summited November 2015*.**

Chapter:1

Introduction

Chapter 1 incorporates the book chapter Sarah Elizabeth Hemming, Dimitrios Cakouros, Stan Gronthos. “Epigenetic regulation of mesenchymal stem cell growth and multi-potential differentiation”. In: The Biology and Therapeutic Applications of Mesenchymal Cells. Ed K. Atkinson. John Wiley and Sons, Hoboken, New Jersey, USA. 2015, currently in press.

Statement of Authorship

Title of Paper	Epigenetic regulation of mesenchymal stem cell growth and multi-potential differentiation
Publication Status	☐ Published ☑ Accepted for Publication ☐ Submitted for Publication ☐ Publication Style
Publication Details	Sarah Elizabeth Hemming, Dimitrios Cakouros, Stan Gronthos "Epigenetic regulation of mesenchymal stem cell growth and multi-potential differentiation". In: The Biology and Therapeutic Applications of Mesenchymal Cells. Ed K. Atkinson. John Wiley and Sons, Hoboken, New Jersey, USA. 2015, currently in press.

Principal Author

Name of Principal Author (Candidate)	Sarah Elizabeth Hemming		
Contribution to the Paper	First Author Literature interpretation Manuscript development		
Overall percentage (%)	50%		
Signature		Date	26/11/2015

Co-Author Contributions

By signing the Statement of Authorship, each author certifies that:
the candidate's stated contribution to the publication is accurate (as detailed above);
permission is granted for the candidate in include the publication in the thesis; and
the sum of all co-author contributions is equal to 100% less the candidate's stated contribution.

Name of Co-Author	Dimitrios Cakouros		
Contribution to the Paper	Manuscript evaluation Literature interpretation Supervised development of work Contribution to review design		
Overall percentage (%)	20%		
Signature		Date	26/11/2015

Name of Co-Author	Stan Gronthos		
Contribution to the Paper	Manuscript evaluation Literature interpretation Supervised development of work Contribution to review design Funding		
Overall percentage (%)	30%		
Signature		Date	4/12/2015

1 Introduction

1.1 Stem Cells

Stem cells are defined by their self-renewal ability, their capacity to differentiate into multiple specialized cell types and their potential to reconstitute an entire tissue [1]. Stem cells can be segregated into three broad groups, Embryonic Stem Cells (ESC), Induced Pluripotent Stem Cells (iPSC) and Postnatal Stem Cells (PSC). ESC are derived from the blastocyst of a developing embryo and have the capacity to generate cells from all three germ layers and to develop into any tissue that constitutes the mature organism [2].

In 2006 Yamanaka and colleagues identified that mouse fibroblast can be reprogramed to an embryonic like stem cells with the addition of transcription factor OCT4, KLF4, SOX9 and MYC[3] [3]. This discovery revolutionised the way we study stem cell biology allowing us to investigate reprograming/epigenetic networks, understanding diseases using patient's fibroblast to generate iPSC of the diseased tissue and using patient derived iPSC in drug screening for a more tailored personalised health approached. However, the efficiency of directed differentiation and the issues concerning tumourgenicity of iPSC following implantation in vivo remains to be resolved. Therefore there is still great interest in alternative stem cells other than iPSC.

Postnatal stem cells, such as bone marrow derived haematopoietic stem cells (HSC) and mesenchymal stromal/ stem cells (MSC) are tissue specific, which are restricted in their differentiation potentials to form mature blood cells and stromal tissues, respectively. The use of PSC for therapeutic purposes has been a topic of enormous interest given the ethical, immunological and tumorigenic considerations associated with ESC and iPSC.

1.1.1 Mesenchymal stromal/ stem cells

MSC are adult stem cells that can differentiate into osteogenic, adipogenic, chondrogenic, or myogenic lineages. Owing to their ease of isolation from multiple tissues [4-6, 7, 8-11] and unique characteristics including suppression of allogenic immune responses, MSCs have been widely regarded as potential candidates for human tissue engineering and repair. Bone marrow derived MSC (BMSC) are tissue specific postnatal stem cells which are restricted in their differentiation potentials to form functional skeletal tissues and myelosupportive stroma [12, 13]. Mesenchymal stem-like cells have also been identified in other tissues such as peripheral adipose, umbilical cord blood, amniotic fluid, placenta, dental pulp, periodontal ligament, tendons, synovial membrane and skeletal muscle [4-11, 14-16]. However, these different MSC-like populations exhibit wide variations in their multi-differentiation potentials, hematopoietic supportive properties and proliferation capacities. This variation is most likely due to the different developmental origins and tissue specific nature of the different MSC-like populations, which may be under the direct control of epigenetic patterning.

BMSC were first identified as clonogenic stromal precursor cells, termed colony forming unit-fibroblastic (CFU-F) within bone marrow aspirates of rodents [17], and subsequently in other species including humans [18]. A common feature of the ex vivo expanded progeny of CFU-F is their heterogeneity with respect to morphology, ability to undergo self-renewal, myelosupportive capacity, lifespan and multi-differentiation potential [4, 19-21]. These observations have led to the proposal that the stromal component within bone marrow is comprised of a hierarchy [22] of immature stem cells, committed progenitor cells and mature functional stromal populations. Since the vast majority of CFU-F demonstrate limited growth and differentiation potential, the general term describing BMSC only refers to the *ex vivo*

expanded progeny of a minor subset of long lived multipotential CFU-F. This population of CFU-F have the potential to form osteoblasts, adipocytes, chondrocytes, smooth muscle cells and myelosupportive fibroblasts under inductive conditions *in vitro* or when transplanted *in vivo* (Figure 1)

Whilst attempts have been made to establish an immunophenotype specific to MSC-like populations (HLA-ABC+/ CD73+/ CD105+/ CD29+/ CD13+/ CD44+/ CD90+/ CD45-/ CD34-/ CD31-/ CD14- [23, 24], the cell surface markers used are generic to a wide range of cultured fibroblastic cells and some vascular and haematopoietic cell populations with different growth and developmental potentials. Moreover, none of the positive selection markers (HLA-ABC+/ CD73+/ CD105+/ CD29+/ CD13+/ CD44+/ CD90+) are capable of distinguishing between immature and committed stromal cell lineages. The identification of multi-potential clonogenic MSC from aspirates of human bone marrow has been achieved based on their high expression of the stromal precursor cell surface antigen, STRO-1, which is down regulated in committed stromal lineages. Purification of STRO-1^{bright} BMSC was achieved by dual fluorescence activated cell sorting based on their co-expression of the perivascular markers, CD106 and CD146, and lack of expression of the haematopoietic markers, CD34, CD14, CD45, and Glycophorin-A [6, 25-27]. Therefore, the development of immunoselection protocols to obtain purified populations of BMSC have allowed the identification of putative regulatory genes critical for maintaining the MSC population following *ex vivo* expansion [28-30]. These include, the catalytic subunit of telomerase, TERT, and the basic helix-loop-helix transcription factors, Twist-1 and Twist-2 [28, 31-33](Figure 1).

Figure 1. Stromal Hierarchy of Differentiation
BMSC contain a heterogeneous population of stem cell progenitors and committed lineage progenitors. Immature, multipotent, self-renewing MSC express high levels of STRO-1 and lack expression of lineage specific master regulatory genes. Committed lineage progenitors down regulate STRO-1, TWIST-1 and TERT expression and express higher of specific master regulatory genes such as PPARγ2, RUNX2, SOX9 as BMSC differentiate into mature adipocytes, osteoblasts, chondrocytes respectively (114).

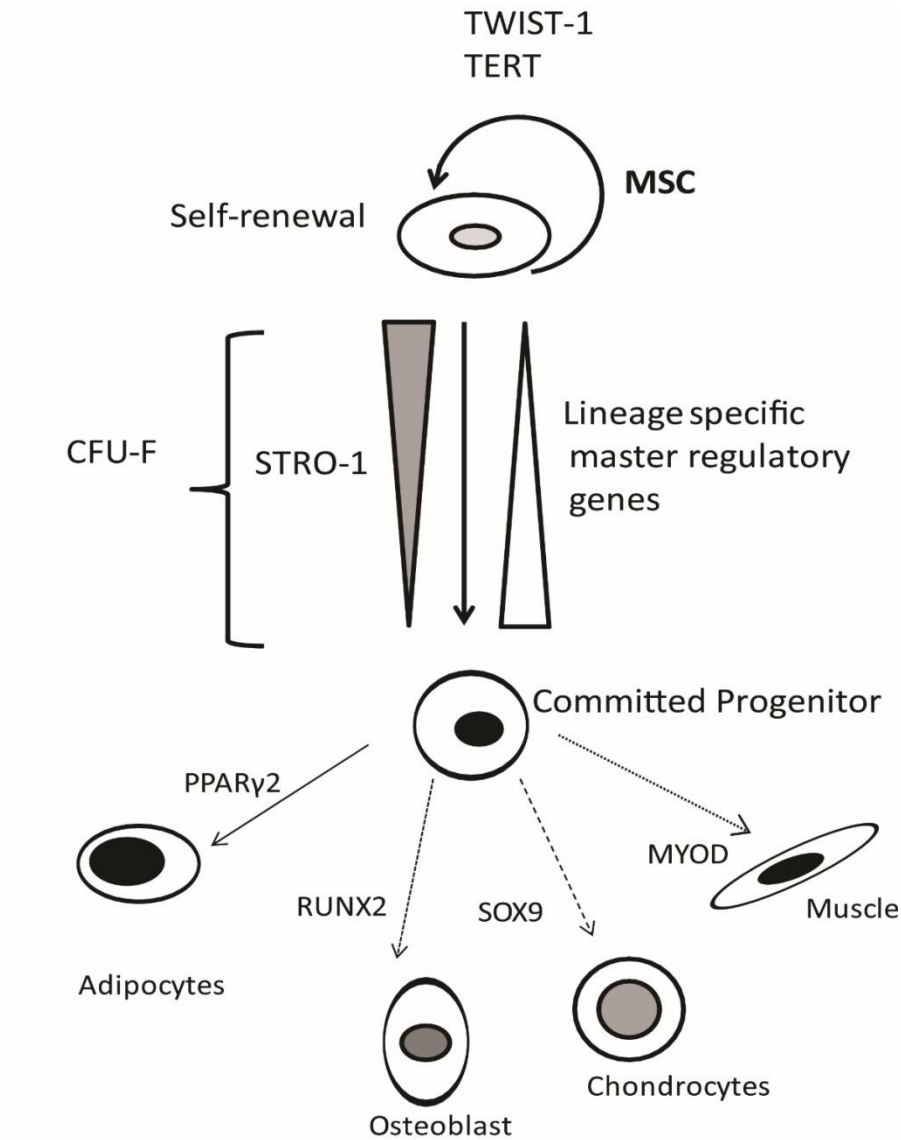
TWIST-1
TERT
MSC
Self-renewal
CFU-F
STRO-1
Lineage specific
master regulatory
genes
Committed Progenitor
PPARγ2
MYOD
Muscle
RUNX2
SOX9
Adipocytes
Chondrocytes
Osteoblast

Figure 2. BMSC populations in the bone and marrow.

Multiple distinct populations of multipotential BMSC and MSC like populations have been identified in the bone. These BMSC and MSC-like populations have the potential differentiate into osteoblast, chondrocyte, adipocyte and stromal cells.

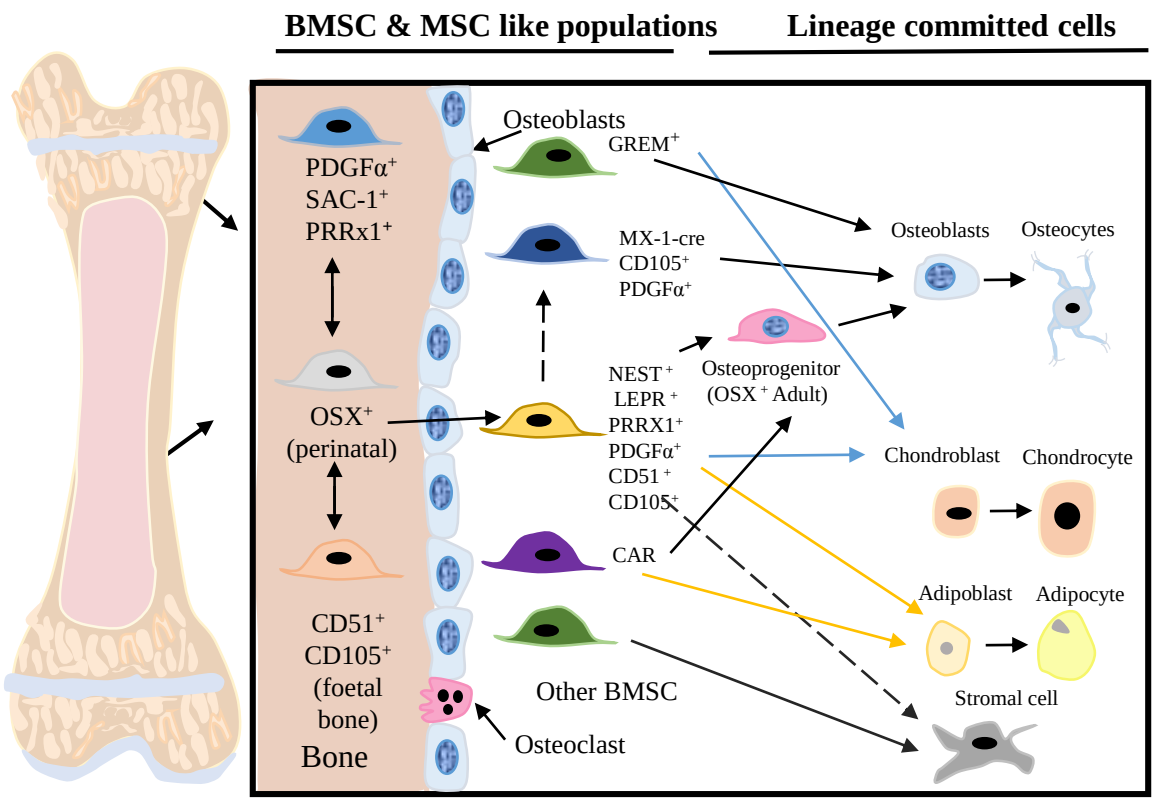
BMSC & MSC like populations
Lineage committed cells
Osteoblasts
GREM+
PDGFα+
SAC-1+
PRRx1+
MX-1-cre
CD105+
PDGFα+
Osteoblasts
Osteocytes
NEST+
LEPR+
PRRX1+
PDGFα+
CD51+
CD105+
Osteoprogenitor
(OSX+ Adult)
OSX+
(perinatal)
Chondroblast
Chondrocyte
CAR
Adipoblast
Adipocyte
CD51+
CD105+
(foetal
bone)
Bone
Other BMSC
Stromal cell
Osteoclast

BMSC lineage determination is regulated by a complex network of signalling pathways and expression of transcription factors. Signalling pathways such as WNT, Notch, Bone Morphogenic Protein (BMP) [34] and key transcription factors (TF) Runt-Related Transcription Factor 2 (RUNX2), Peroxisome Proliferator-Activated Receptor Gamma 2 (PPARγ2) and Sex Determining Region Y-box -9 (SOX9) have been implicated as being critical for drivers of MSC lineage commitment (Figure 1). Understanding the processes which drive BMSC lineage commitment may one day allow us to manipulate BMSC to maintain an immature phenotype during ex vivo expansion and direct their differentiation down specific lineages required for cellular therapies.

1.1.2 BMSC and skeletal development.

BMSC play a critical role during skeletal tissue development and are critical components of the HSC supportive niche [35, 36]. Multiple distinct populations of multipotent BMSC and unipotent MSC-like population have been identified within the bone and bone marrow to contribute to the formation of bone fat and cartilage tissues. Foetal MSC populations characterised by surface markers $CD51^{+}$,$CD105^{+}$,$CD90^{-}$,$CD45^{-}$,$Tie2^{-}$ play an important role in endochondral bone ossification, supporting the growth of the marrow vasculature and HSC progenitor cell population [37](Figure 2A).

A primitive MSC population expressed early in foetal development expresses Osterix (OSX). Osterix is often used as a marker of osteoprogentiors however, these early OSX+ MSC are short lived and are replace by definitive BMSC during later foetal development [38]. Paired-related homeobox-1 ($Prrx1^{+}$) is expressed on a subset of limb bud mesenchyme, which constitute many of the MSC populations in the developing bone and marrow [39]. Other studies have identified a BMSC Platelet-Derived Growth Factor Receptor α ($PDGFR\alpha^{+}$), Sca-

1^+,$CD45^-$,$Ter119^-$ population which are capable of differentiating into osteoblasts reticular cells and adipocytes in vivo [40, 41]. MSC-like populations positive for Myxovirus resistance-1 ($MX\text{-}1^+$) differentiate into osteogenic progenitors that maintain osteoblast pool at steady state and after tissue stress [42]. Another BMSC population exhibiting surface markers $PDGFR\alpha^+$,$CD51^+$,$CD45^-$,$Ter119^-$,$CD31^-$ are multipotential, self-renewing and can reconstitute a bone marrow niche [43].

Murine lineage tracing experiments have been used to identify new BMSC or MSC-like populations and trace their lineage commitment during development, facture healing and bone homeostasis. Lineages tracing using transgenic mice expressing GFP under the control of the Nestin promoter have identified a $NESTIN^+$ presinusoidal mesenchymal stem BMSC population [44-46]. $NESTIN^+$ BMSC can self-renew and have high CFU-F activity with the potential to differentiate into all major mesenchymal lineages. These cells are associated with HSC in the marrow and regulate haematopoietic activity [46-48].

A subset of MSC-like reticular cells expressing high levels of CXCL12 (CAR cells) have been identified. These CAR cells are bipotent differentiating into adipocytes and osteoblasts [49], and play a role in HSC cycling and self-renewal. Like mouse CAR cells, human STRO-l+ BMSC express high levels of CXCL12, with an increased capacity to support human HSC [25, 30, 50, 51]

Recently, perisinusoidal MSC-like cells expressing Leptin Receptor (LEPR) were found to form multipotent CFUFs [52]. Lineage tracing of $LEPR^+$ population revealed that this population contributed to the osteogenic and adipogenic lineages in adult mice but not during development. However this $LEPR^+$ MSC-like population does not undergo chondrogenic differentiation in vivo. Furthermore, a population of BMSC expressing $NESTIN^+$ $LEPR^+$

OSX^+ contribute to skeletal tissue regeneration after injury. More recently, a new population of osteochondroreticular stem cells have been identified. These $Gremlin1^+$ (GREM1) OCR stem cells are active during development, give rise to trabecular bone, cartilage, and reticular marrow stromal cells [47].

It therefore appears that different populations of BMSC and MSC-like stem cell populations contribute to the bone, fat and cartilage in the developing and postnatal skeletal tissue. Lineage tracing has allowed the identification of new BMSC and MSC-like populations and identifying there function in the bone development and regeneration after injury. However, questions still remain about the multipotential and self-renewal capacity of these BMSC and MSC-like population and how they regulate specific processes in bone development. Do these populations work independent of each other or in cooperation with other BMSC or MSC-like population in order for normal bone development to occur? Furthermore, it is unclear if all BMSC and MSC-like populations originate from a common progenitor stem cell. Therefore it is important investigate the functions of the stem population and understand their role in bone formation and repair and identify the existence of similar populations in human skeletal tissues.

1.2 Bone development

Intramembranous ossification occurs in the “flat bones” of the ilium, mandible, scapulae and skull. Intramembranous bone formation is medicated by the inner periosteal osteogenic layer where bone is synthesised without the mediation of the cartilage phase. Intramembranous ossification occurs within fibrous connective tissues where residing BMSC differentiate into osteoblasts which secrete a predominantly collagen type I based un-calcified bone matrix called osteoid.

The second process of bone formation is endochondral ossification, where during embryogenesis the mesenchymal cells of the neural crest in the craniofacial region (middle ear bones and temporal bones) or mesoderm within long bones (tibia, femora and humerus) undergo condensation and chondrogenic differentiation (Figure 3A). Endochondral ossification allows the formation of a cartilaginous scaffold, which dictates the boundaries of the developing limb. The MSC of developing limb bud condense and differentiate into chondroblasts, which form a collagen type II cartilaginous matrix and proteoglycans such as Aggrecan (Figure 3B).

Chondroblasts differentiate into chondrocytes and the centre of the cartilage model undergoes a process call hypertrophy. This process allows the calcification of the surrounding cartilaginous matrix. Mesenchymal stem cells in the perichondrium divide and form osteoblasts, which develop a compact bone collar around the calcified cartilage shaft (Figure 3B). Capillary's and osteoblasts invade the core of the cartilaginous shaft forming a primary (1°) ossification centre (Figure 3C). The remaining cartilage provides a template for osteoblasts to lay down new bone. As the bone is synthesised osteoblasts become trapped within the bone and mature into osteocytes, trapped within lacunae with multiple cytoplasmic extensions in canaliculi throughout the bone matrix forming a connective, sensory-like network. Bone development then extends towards the epiphyses from the primary ossification centre. The same process of ossification occurs at the epiphyses as secondary (2°) ossification centres (Figure 3D).

Trabecular bone also known as spongy bone form in the secondary ossification centre. Within the secondary ossification centre, osteoclasts reabsorb bone within the diaphysis creating the medullary cavity when the bone marrow forms.

Figure 3. Endochondral ossification.
(A) Mesenchymal stem cell condense and differentiate to form a cartilage template. (B) Bone collar is deposited on the outside of the cartilage template. The periosteum is the outer side of the bone. (C) The primary ossification centre develops within the centre of the cartilage template. (D) The cartilage template is replaced with bone. Cartilage growth plate remains at the endo of the bones. Secondary ossification centre forms in the top of the bone to for the epiphysis.

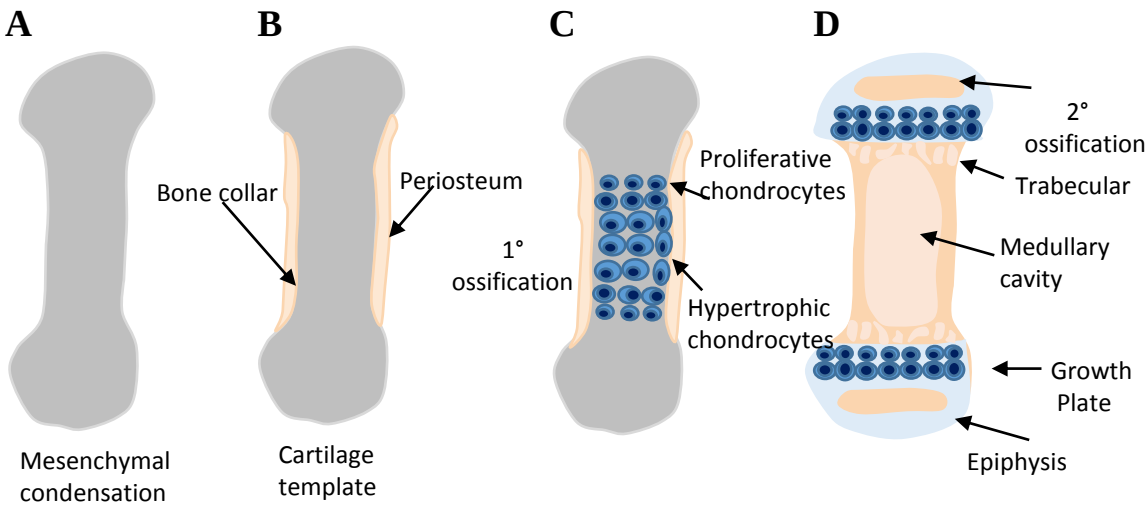
A
B
C
D
Bone collar
Periosteum
Proliferative chondrocytes
1° ossification
Hypertrophic chondrocytes
2° ossification
Trabecular
Medullary cavity
Growth Plate
Epiphysis
Mesenchymal condensation
Cartilage template

When the secondary ossification is complete the cartilage is fully replaced by bone. Only two sites cartilage is found within the long bone. A region of cartilage remains over the surface of the epiphyses called articular cartilage.

Another area of cartilage remains between the epiphyses and diaphysis known as the growth plate, growth region or epiphyseal plate. Longitudinal growth occurs at the growth plate where cartilage differentiates and proliferates at the epiphyseal and metaphyseal areas allowing the mineralization and formation of new bone. The long bones contain two growth plates, one at the proximal end and the other at the distal end of the bone. The growth plate consists of defined cartilage zones, which can be characterised according to their morphology and function with the presence of collagen type X in the extracellular matrix.

The first is the resting/reserve cartilage zone, which is located beneath the secondary bony epiphysis. The second zone under the resting cartilage zone is the proliferative zone followed by the hypertrophic zone (Figure 4A). The resting zone contains stem-like cells derived from BMSC give rise to clones of the proliferative zone (Figure 4B). These resting cartilage cells produce a plate-orientation factor which regulates the alignment of the proliferative clone into columns [53].

Directly under the resting cartilage zone is the proliferative zone. Transcription factors such sex determining region Y box (SOX) 9, 2, 6, Indian hedgehog (IHH) and parathyroid hormone-related protein (PTHRP) promotes differentiation of proliferating chondrocytes (Figure 4B). These chondrocytes are flattened and align in longitudinal columns perpendicular to the bone. The chondrocyte at the top of every column is defined as the primary cartilage cell or proliferative clone. Longitudinal growth plate growth is equal to the rate of production of new chondrocytes are the top of the proliferative zone multiplied by the maximum size of the chondrocytes at the bottom of the hypertrophic zone [54].

Figure 4. Structure of the growth plate
(A) The developing growth plate consists of define cartilage zones. The first zone is the resting/reserve zone (R). The cells are small and spherical often existing as single or paired cells. These cells give rise to flat proliferative clones, which proliferate to produce the distinct columns of the proliferative zone (P). The final zone is the hypertrophic zone (H). This zone contains larger cuboidal shaped cells, which lose cellularity as they become closer to the bottom of the zone. These cells begin to die and mineralise as they enter the metaphysis and primary spongiosa. (B) Signalling molecules and transcription factors which regulate chondrogenic differentiation. Green arrow represents activation and red bar represents inhibition.

A

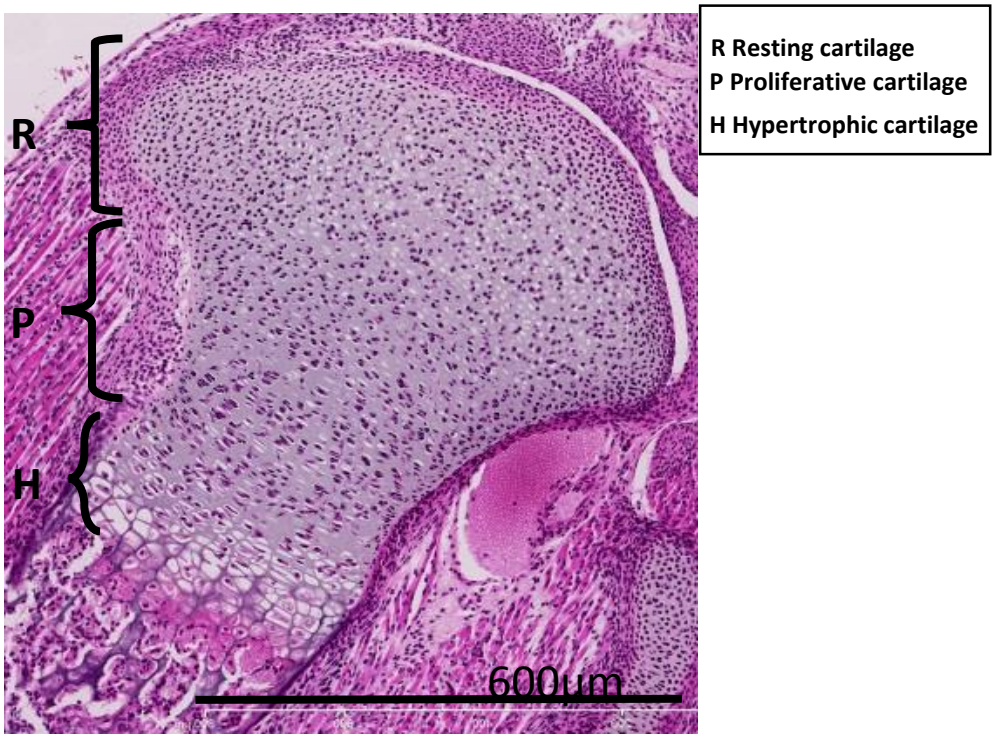
R
P
H
600um
R Resting cartilage
P Proliferative cartilage
H Hypertrophic cartilage

B

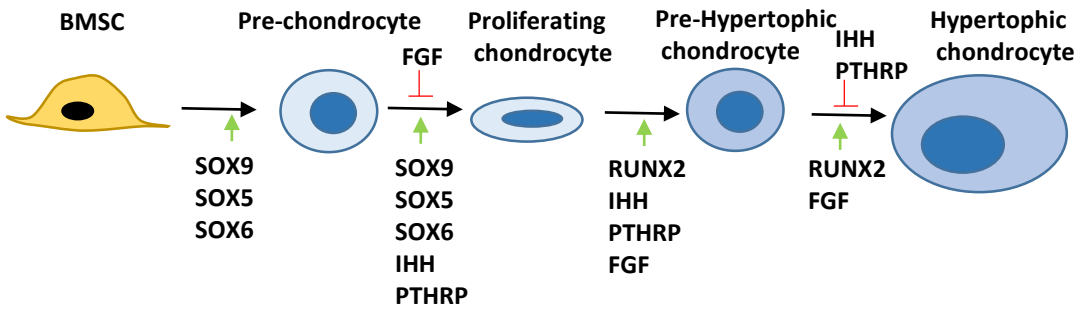
BMSC
Pre-chondrocyte
Proliferating chondrocyte
Pre-Hypertophic chondrocyte
Hypertophic chondrocyte
FGF
IHH
PTHRP
SOX9
SOX5
SOX6
SOX9
SOX5
SOX6
IHH
PTHRP
RUNX2
IHH
PTHRP
FGF
RUNX2
FGF

The flattened proliferative chondrocytes give way to larger spherical cartilage cells in the hypertrophic zone. These changes in cell morphology are quite defined allowing clear identification of the end of the proliferative zone and the beginning of the hypertrophic zone. Differentiation of proliferative chondrocytes into hypertrophic chondrocytes is regulated by the expression of RUNX2 and Fibroblast Growth Factors (FGF), and can be inhibited by expression on IHH and PTHRP (Figure 4B). As chondrocytes progress through to the hypertrophic zone they can be up to five times larger than when they started in the proliferative zone [55]. The last hypertrophic chondrocytes of each column appear nonviable with extensive fragmentation of the cell membrane and the nuclear envelope with loss of all cytoplasmic components except a few mitochondria and scattered endoplasmic reticulum. Calcium and phosphorus mineral granules are present in the mitochondria of hypertrophic chondrocytes at the top and middle half of the zone [56-58]. Hypertrophic chondrocytes in the bottom of the zone lack calcium and is suggested that mitochondrial calcium may be involved in cartilage calcification.

Under the hypertrophic zone is the mineralisation zone or 1° spongiosa when hyperopic chondrocytes differentiate into osteoblasts which migrate and mature forming trabeculae in the 2 ° spongiosa (Figure 5). Whilst, the process of endochondral bone formation has been well defined, it is still unclear which BMSC populations are responsible for all these processes.

1.3 Bone structure and composition

Bone is an important structure which provides stability, support and protection to organs and allows the anchoring of muscles to aid in movement. The developed long bone consists of consists of epiphyses and metaphyses at each end of the diaphysis. ***Epiphyses*:** epiphyses the articular cartilage lines the top surface of the epiphyses end of the bone. ***Diaphysis*:** the

Figure 5. Long bone structure
The top region of the long bone is define as the epiphysis. Each long bone contains a proximal and distal epiphysis. 2º ossification occurs within the epiphysis. Directly under the epiphysis is the cartilaginous growth plate a region of longitudinal growth. The metaphysis is located directly under the growth plate and this region contains the 1ºand 2º spongiosa and trabeculae. The middle region of the bone is the diaphysis. The outer surface of the bone is made up of dense layers of calcified bone, known as the cortex/cortical bone, which encases the bone marrow in the medullary cavity. The medullary cavity contains the haematopoietic stem cells and mature erythrocytes (red marrow). In aged mice this marrow becomes filled with adipocytes (yellow marrow) and less haematopoietic stem cells and mature erythrocytes.

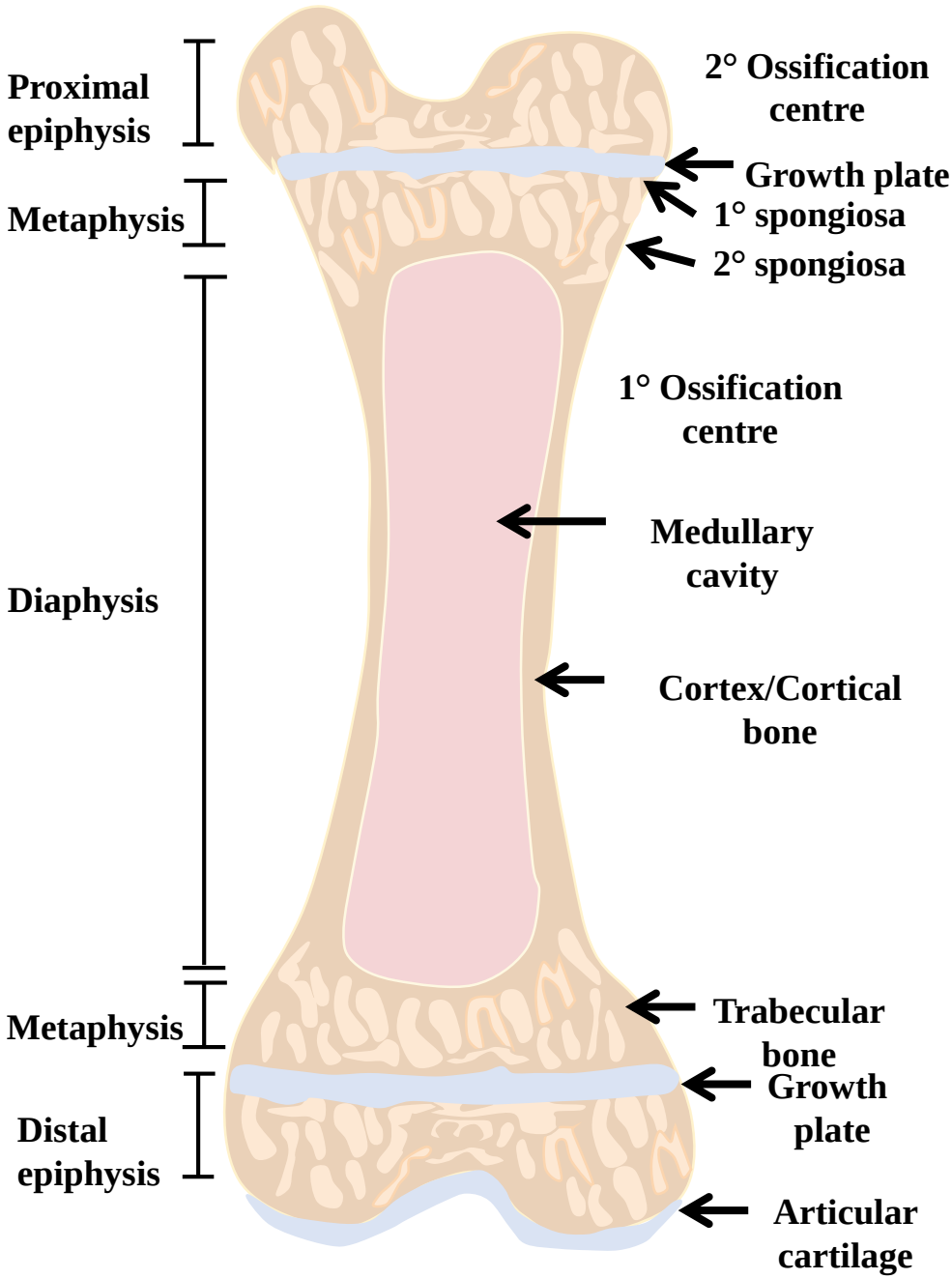
Proximal epiphysis
Metaphysis
Diaphysis
Metaphysis
Distal epiphysis
2° Ossification centre
Growth plate
1° spongiosa
2° spongiosa
1° Ossification centre
Medullary cavity
Cortex/Cortical bone
Trabecular bone
Growth plate
Articular cartilage

cylindrical middle of the bone. ***Metaphysis*:** the region located between the midshaft and the end of the bone (Figure 5).

In the medullary cavity at the metaphysis and epiphysis of long bones, the marrow space is filled with a rigid sponge-like meshwork of thin, calcified bone struts, known as trabecular or cancellous bone. Mature trabecular or "spongy bone" is located in the secondary (2°) spongiosa and consists of delicate bars and sheets of trabeculae which form an intersecting lattice like network gives supporting strength to the ends of the weight-bearing bone. Trabecular bone forms rod and plate like structures, which allow space for blood vessels and marrow within the interior of the bone. Even though trabecular bone only constitutes 20% of total bone mass, trabecular bone has nearly ten times the surface area of compact bone.

Compact bone forms the thick-walled tube of the shaft (or diaphysis) of long bones, which surrounds the marrow cavity (or medullary cavity). A thin layer of compact bone also covers the epiphyses of long bones. The outside of the cortical bone is covered by the periosteum a dense a layer of dense connective tissue. A thin layer of cells is present on the inner side of the cortical facing the marrow cavity and is called the endosteum. These surfaces have osteogenic potential and following injury cells in these layers differentiated into osteoblasts aiding in bone repair.

Bone matrix consists of collagen fibres (about 90% of the organic substance) and ground substance. The hardness of the matrix is due to its content of inorganic salts (hydroxyapatite; about 75% of the dry weight of bone), which become deposited between collagen fibres. The organic matrix is composed primarily of the protein collagen type I, which provides flexibility however only 10% of adult bone mass is collagen. Bone is made of a minor percentage of

non-collagenous matrix proteins such as Osteocalcin (OCN), Bone Sialoprotein (BSP), Osteopontin (OPN) [59]. Calcification begins a few days after the deposition of organic bone substance (or osteoid) by the osteoblasts. Bone is composed of calcium/phosphate crystals in the form of hydroxyapatite. During bone repair such as fracture repair the collagen fibres are laid down in a random organisation called woven bone and during fracture remodelling the woven bone is reabsorbed and replaced by mature lamellar bone (Figure 6A&B). In addition to its mechanical functions, the bone is a major store of calcium and phosphate critical in balancing bone homeostasis and body metabolism, and therefore the balance between bone formation and bone reabsorption is tightly regulated.

1.3.1 Bone modelling and remodelling

The shape of bones can change by removal or addition of bone to the appropriate surfaces by the coordinated action of osteoblasts and osteoclasts in response to stimuli from soluble factors, extracellular matrix components and biomechanical forces. Bone homeostasis is dependent on the balance between bone formation and bone resorption. Bones are constantly being remodeled thought life, to maintain bone strength and calcium and phosphate homeostasis. The process of osteoclasts reabsorption of old bone and osteoblast mediated formation of new bone is tightly regulated. However when the balance of bone remodelling is altered it often leads to the development of bone associated diseases such as osteopenia, osteoporosis and osteolytic disease caused by multiple myeloma and many cancers which metastasizes to the bone.

Bone remodeling requires secretion of macrophage colony stimulating factor (M-CSF) by BMSC and bone lining cells, osteoblasts and adipocytes. This stimulates HSC differentiation

Figure 6. Lamella and woven bone structure.

(A) Lamellae are made up of parallel collagen fibres, which run parallel to each other.

(B) Woven bone is when collagen fibrils are laid down in a disorganised fashion.

A

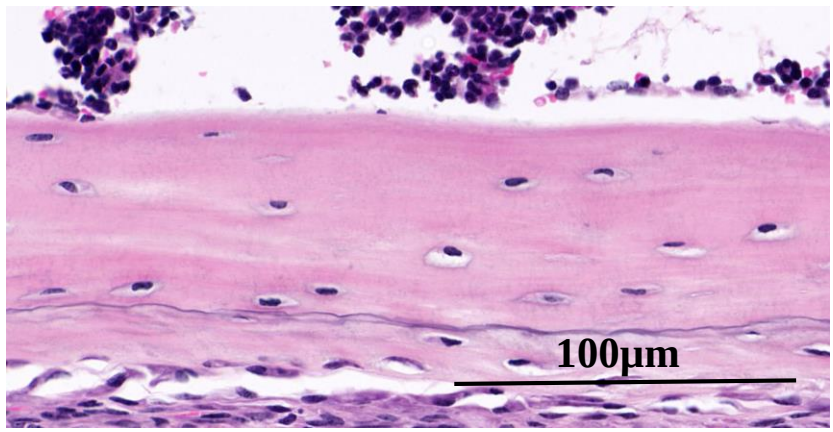

B

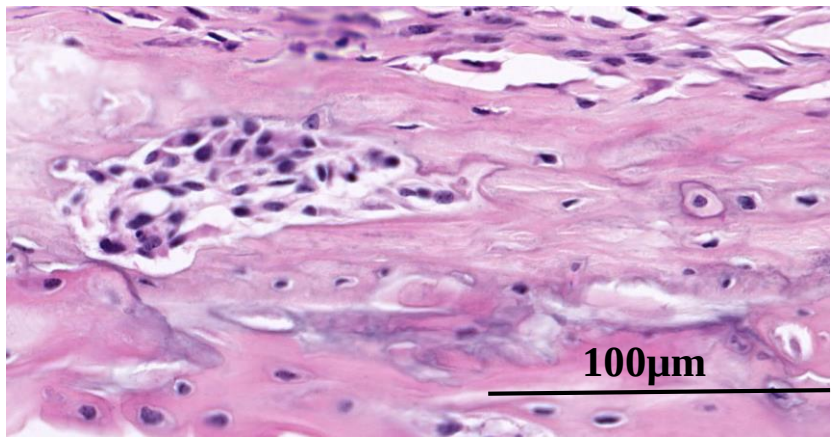

into mononuclear monocyte-macrophage osteoclast precursors (preosteoclasts). Preosteoclast maturation into osteoclasts requires the presence of Rank Ligand (RANKL) ligand secreted from BMSC and osteoblasts, which binds RANK receptor expressed on preosteoclasts. Preosteoclasts fuse together to form large multi-nucleated osteoclasts, which bind to the bone matrix and mediate site mediated bone reabsorption. At the completion of bone resorption differentiated osteoblasts are recruited to synthesize new bone [60] (Figure 7).

Osteoclastogenesis can be controlled by BMSC and osteoblasts, which can inhibit bone reabsorption by producing a membrane bound and or secreted form of Osteoprotegerin (OPG) which binds RANKL with high affinity inhibiting its activation of RANK receptors on osteoclasts [61]. If the binding between RANK and RANKL is interrupted by OPG, the osteoclast precursor cannot differentiate and fuse to form mature resorbing osteoclasts. OPG thus acts as a decoy receptor in the RANK-RANKL signalling system inhibiting osteoclast formation [62]. Furthermore OPG section can be regulated by the hormone estrogen, which stimulates osteoblast and stromal cells to express the RANK antagonist.

Estrogen can directly inhibit RANK activated JNK pathways in osteoclast precursors, inhibiting there activation. Post-menopausal women with osteoporosis have elevated expression of RANKL on the osteoblasts which stimulate the activation of osteoclast and bone reabsorption [63]. Estrogen deficiencies leads to the expression of cytokines Interleukin 1 (IL-1) and Tumour Necrosis Factor (TNF) promoting Interleukin 6 (IL-6) which stimulates osteoclastogenesis. TNF and IL-1 further contribute to osteoclastogenesis though the stimulation of increased levels of RANKL in osteoblast and stromal cells. In contrast to estrogen, glucocorticoids promote bone resorption and Parathyroid Hormone (PTH), prostaglandin E2, and basic fibroblast growth factor all suppress the expression of OPG.

Figure 7. Bone remodeling.
Bone lining osteoblasts can stimulate osteoclast differentiation through the expression of Macrophage Colony Stimulating Factor (M-CSF). Hematopoietic stem cells are stimulate to differentiate in the presence of M-CSF producing committed stem cells (monocytes). These cells further mature into multinucleated osteoclast with the presence of RANKL expressed by osteoblasts. Osteoclasts express RANK which detects the presence of RANKL and promotes osteoclastogenesis. Remodeling can also be negatively regulated by the expression of Osteoprotegerin (OPG) released from osteoblasts and stromal cells. OPG binds RANKL preventing RANKL/RANK osteoclast activation. Parathyroid hormone (PTH) can inhibit osteoclast differentiation by stimulating the production of OPG. Sclerosis secreted by the osteocytes stimulates osteoclastogenesis. Chemokines IL-2 and 6 and Tumor necrosis factor TNF promotes RANKL expression from osteoblasts and stimulate osteoclastogenesis. Estrogen can block RANK signaling inhibiting osteoclastogenesis.

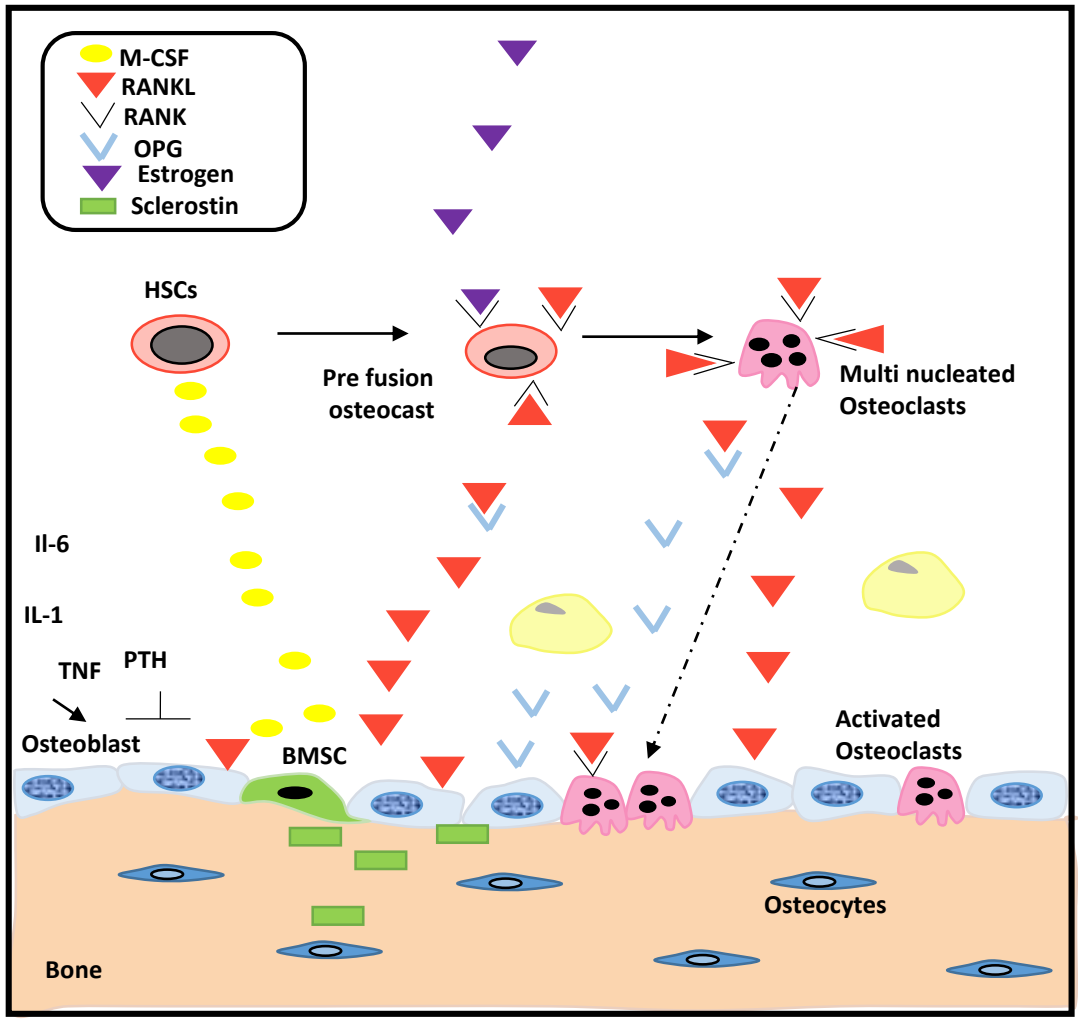
M-CSF
RANKL
RANK
OPG
Estrogen
Sclerostin
HSCs
Pre fusion
osteocast
Multi nucleated
Osteoclasts
Il-6
IL-1
TNF
PTH
Osteoblast
BMSC
Activated
Osteoclasts
Osteocytes
Bone

A key process of remodeling is the differentiation of osteoblasts from BMSC to synthesis new bone once osteoclasts have reabsorbed the old bone. Extracellular molecules secreted from osteoclasts and from the matrix during bone reabsorption stimulate osteogenesis. Factors such as, wingless-type MMTV integration site (WNT) proteins, BMPs, Insulin Growth Factors (IGF)s, FGF stimulate the expression of osteogenic associated gene transcription thought the expression of transcription factors such as DLX5, RUNX2, and OSTERIX in BMSC [64]. These TF regulate genes such as Osteocalcin, OPN, Osteonectin, BSP, Type I collagen, Alkaline Phosphatase, which are critical for osteoblast differentiation and bone synthesis [65, 66].

Wnt signaling can activate osteogenesis thought the canonical and non-canonical pathway. The canonical Wnt, WNT3a the frizzled receptors expressed by BMSC. This receptor binding activates co-receptor lipoprotein related proteins (LRP) five and six inhibiting the glycogen synthase kinase 3 (GSK3) complexes. This inhibition of GSK3 allows the stabilization of cytoplasmic β-catenin, which translocates into the nucleus activating osteogenic gene. Osteogenesis can be activate thought the Non-canonical WNTs, including WNT1, WNT5a, and WNT7b. WNT5a signal through β-catenin-independent pathways involving calcium-dependent enzymes such as calcium-calmodulindependent protein kinase-II (CaMKII). Activation of CAMKII inhibits PPARγ2 repressing adipogenesis and promotes osteogenesis [67]. Additionally BMP signalling though the type IB BMP receptor stimulates BMSC osteogenesis by the activation of DLX5 and RUNX2. [66] (Figure 8).

Osteoblasts and osteoclasts can be regulated by signalling molecules, but by direct osteoblast-osteoclast interactions. These interactions are mediated through transmembrane tyrosine kinase EphB receptors expressed by osteoblasts with membrane bound EphrinB

Figure 8. Canonical and non-canonical Wnt pathway
The Wnt pathway can be inhibited by binding of WIF1 and SFRP to Wnt preventing the activation of Fizzled receptors and coactivators. This allows the association of Axin, APC and GSK-3β leading to phosphorylation of β-catenin. B-catenin s marked for degradation by the proteasome leading to decrease in bone formation and increase bone resorption. The Wnt canonical pathway is define by the binding of Wnt5a to the FZD receptor and binding of coactivator LRP5/6. This leads to phosphorylation of Axin and inhibition of GSK-3β phosphorylation of β-catenin. B-catenin translocates into the nucleus activating genes involved in bone formation and inhibition of bone reabsorption, The Non-canonical Wnt pathway is mediated through binding of Wnt5a to ROR2 and the FZD receptor. This signaling leads to the activation of RAC which activates IP3 and Ca2+ release. RAC activates the JNK pathway activating RUNX2. RAC activates ROCK which activates NFATc1 which promotes osteoclastogenesis.

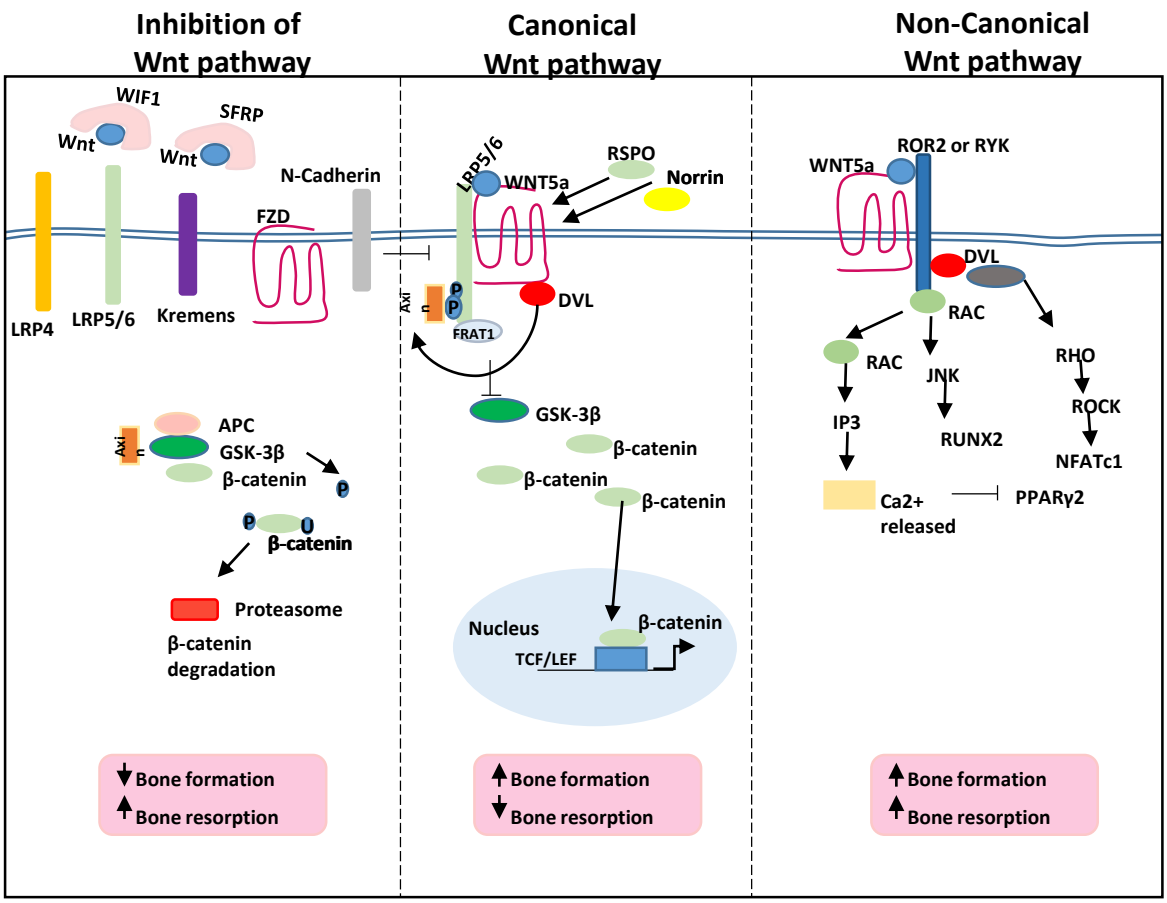
Inhibition of Wnt pathway
Canonical Wnt pathway
Non-Canonical Wnt pathway
WIF1
Wnt
SFRP
Wnt
N-Cadherin
FZD
LRP4
LRP5/6
Kremens
APC
GSK-3β
β-catenin
P
P
β-catenin
Proteasome
β-catenin degradation
Axin
LRP5/6
WNT5a
RSPO
Norrin
DVL
P
P
FRAT1
Axin
GSK-3β
β-catenin
β-catenin
β-catenin
Nucleus
β-catenin
TCF/LEF
ROR2 or RYK
WNT5a
DVL
RAC
RAC
JNK
RHO
ROCK
IP3
RUNX2
NFATc1
Ca2+ released
PPARγ2
Bone formation
Bone resorption
Bone formation
Bone resorption
Bone formation
Bone resorption

ligands expressed by osteoclasts [68-70]. Bidirectional signalling through EphB4 forward signalling in osteoblasts promotes bone formation, whereas reverse signalling through its high affinity, binding ligand, ephrinB2 expressed by osteoclasts, inhibits osteoclastogenesis and bone reabsorption [68, 69].

Whilst the interplay between osteoblasts and osteoclasts has been well studied, there is increasing evidence that other cells in the bone and marrow niche are important for regulating bone remodeling. Recently studies have identified that osteocytes play a role in bone remodeling. Communication between neighboring osteocytes through their cytoplasmic processes allows osteocytes to convert mechanical signals into biochemical signals. Osteocytes secrete growth factors such as Sclerostin which indirectly inhibits BMP mediated bone formation through inhibition of Wnt signaling. During bone remodeling local osteocytes undergo apoptosis decreasing local Sclerostin levels. As Sclerostin is a Wnt inhibitor, reduction in localised Sclerostin levels allows the activation of Wnt and promotion of differentiated preosteoblasts to form new mineralised bone.

Bone marrow adipocytes derived from BMSC may also play an important role in the bone remodeling process. The regulatory network mediating adipogenic differentiation is highly regulated and complex. CEBP-α and PPARγ2 are transcription factors critical for the initiation of adipogenic differentiation[71]. These transcription factors stimulate a cascade of other factors enhancing adipogenic differentiation through the acquisition of lipid. CEBP-α has been identified to activate PPARγ2 activation, however PPARγ2 is regulated by multiple factors and signalling pathways complicating how PPARγ2 is transcriptionally regulated. From the literature it appears that adipocytes can be promoters or inhibitors of bone

remodeling (Figure 9). Another possible molecular mechanism is the interaction of PPARγ2 with the TGF-β/Smad3 signalling, which inhibits osteoblast differentiation [72].

PPARγ2 may also inhibit osteogenesis indirectly through its stimulation of adipogenesis from marrow progenitors that can give rise to either osteoblasts or adipocytes[73].To determine the role of PPARγ2 in more differentiated osteoblastic cells than bone marrow cells, we used calvarial cells whose spontaneous differentiation is known to follow not only the osteogenic pathway but also the adipogenic pathway [74]. Furthermore several BMP molecules have been implicated in stimulating adipogenic and osteogenic pathways depending on receptor activation. Activation of type1A BMP receptor on MSC induces PPARγ2 expression promoting adipocyte differentiation. Insulin and IGF1 can activate both adipogenic and osteogenic differentiation of MSC. Changes in Leptin secretion is associated with increased number of adipocytes in the marrow and have been shown to disrupt normal coordination between osteoblasts and osteoclasts [75, 76].

Although Adiponectin has been reported to inhibit osteogenesis and promote adipogenesis, some studies provide evidence that adiponectin can promote Cyclooxygenase 2 (COX2) expression in BMSC promoting osteogenic differentiation [77]. Furthermore adipokines including Omentin-1, Resistin, and Visfatin have also been shown to modulate osteoblast and/or osteoclast differentiation [78, 79]. Adipocytes can also express RANKL and OPG when co-cultured with HSC and facilitate osteoclast differentiation [80].

Figure 9. Adipogenic regulation of osteoblasts and osteoclasts
Adipocytes regulate osteoclastogenesis and osteogenesis. RANKL secreted from osteoblasts activate preosteoclasts though RANK mediated binding. Pre-osteoclasts differentiate into osteoblasts with the expression of RUNX2, DLX5 and OSTERIX. PPARγ2 expression in adipocytes promotes osteoclasts and inhibits osteoblasts. Chemerin expression promotes osteoclastogenesis and inhibits osteogenesis. Leptin inhibits osteoclastogenesis and promotes osteogenesis. Adiponectin promotes osteoclastogenesis whilst in some instances promotes and inhibits osteogenesis.

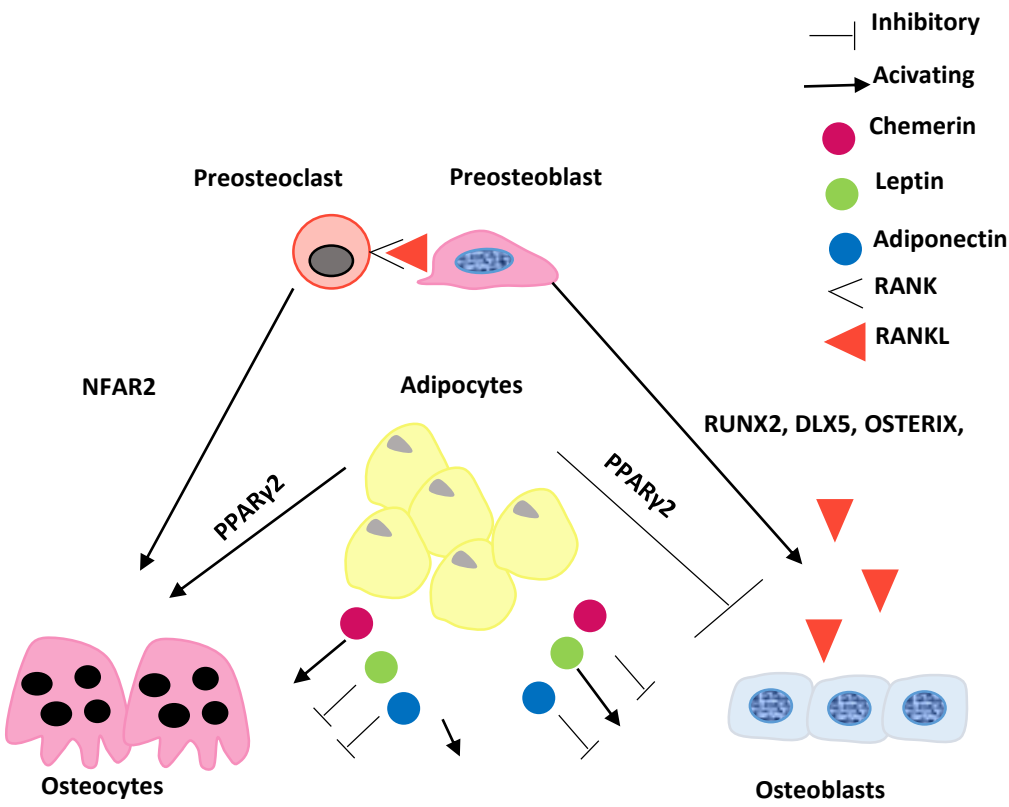
Inhibitory
Acivating
Chemerin
Leptin
Adiponectin
RANK
RANKL
Preosteoclast
Preosteoblast
NFAR2
Adipocytes
RUNX2, DLX5, OSTERIX,
PPARγ2
PPARγ2
Osteocytes
Osteoblasts

Given the discrepancies within the literature, the true role of adipocytes in bone remodelling has yet to be determined. Therefore, it appears that a complex network of cellular signals and interactions from multiple cells types are required for the balance of bone formation and reabsorption [81]. These findings suggest that the whole bone microenvironment, not just the osteoblast-osteoclast interactions may be critical for regulation of bone homeostasis and bone repair. It is therefore critical to understand the molecular mechanisms that control the expression of master regulatory genes critical for BMSC lineage specification during bone development, modelling and remodelling. The activation of these signalling pathways and expression of transcription factors are dependent on the regulation of chromatin, allowing the activation or suppression of lineage specific factors their downstream targets. Therefore, it is important to identify which epigenetic modifications are critical for the regulation of BMSC growth and lineage-specification.

1.4 Epigenetic modifiers regulate gene expression through DNA methylation and posttranslational modifications.

Epigenetics is the cellular modification of reversible and heritable changes in gene expression that occur without changes in the DNA code [82]. Epigenetic modifications such as DNA methylation, post-translational modifications including histone modifications and chromatin remodellers regulate the structure of chromatin, determining the accessibility of genes to transcription factors and other modulators involved in gene regulation. Chromatin is formed through the compaction of large amount of DNA where 145-146 base pairs of DNA are wrapped around a nucleosome, consisting of an octamer of histone subunit [83, 84]. Nucleosomes are joined together by linker histone 1 (H1) and a small region of DNA, which form a “beads on a string like structure”. Each histone subunit has a specific sequence of

amino acids in a tail like structure defined as a “histone tail” which protrudes out for the nucleosomes and can be post-translationally modified (Figure 10).

The functional state of chromatin can be modified through C5 methylation of DNA at cytosines within CpG dinucleotides and the post-translational modification of histone proteins and residues within the histone tails (Figure 10). DNA methylation is commonly located at the cytosine of the dinucleotides sequence CpG and is often located at genes, which have tissue-restricted expression and become stably silent.

The activity of DNA methyltransferases (DNMTs), is critical for genome stability, X inactivation, genomic imprinting and regulating key developmental genes during cellular differentiation [85-95]. With the development of Methyl-DNA Immunoprecipitation Microarray Hybridization and bisulphite sequencing [96, 97] investigations examining the role and patterns of DNA methylation in different process such as development, stem cell self-renewal and pluripotency have yielded enormous information showing methylation of developmental genes as a cell becomes more restricted in its multipotent capacity and less stem cell like[98, 99].

Post-translational modification of histones is another level of transcriptional regulation that can result in repression or activation of gene expression. The structure of chromatin can be regulated through methylation, acetylation, phosphorylation, sumoylation and ubiquliantion of histone tails. Post-translational modification of 28 known residues gives rise to over 100 million differentially modified nucleosomes within cells accounting for the great diversity of signals and gene expression outcomes[100]. The regulation of DNA through epigenetic

Figure 10. Compaction of DNA through the formation of chromatin
DNA is compacted within a cell through chromatin. 145-146bp DNA is wrapped around a nucleosome structure consisting of an octamer of histone subunits, 2 copies of H2 A, H2 B, H3 and H4. H1 "linker histone" anchors the DNA wrapped around the nucleosome in place. A region of DNA is present in between nucleosomes known as linker DNA. Histone tails protrude out of the histone subunits and these are regions of post-translational modifications which dictate a more open ("beads on a string") or closed chromatin structure. Nucleosomes are further compacted to form a 30 nm closed chromatin fibre structure. The structure can be further condensed to chromosomes (114).

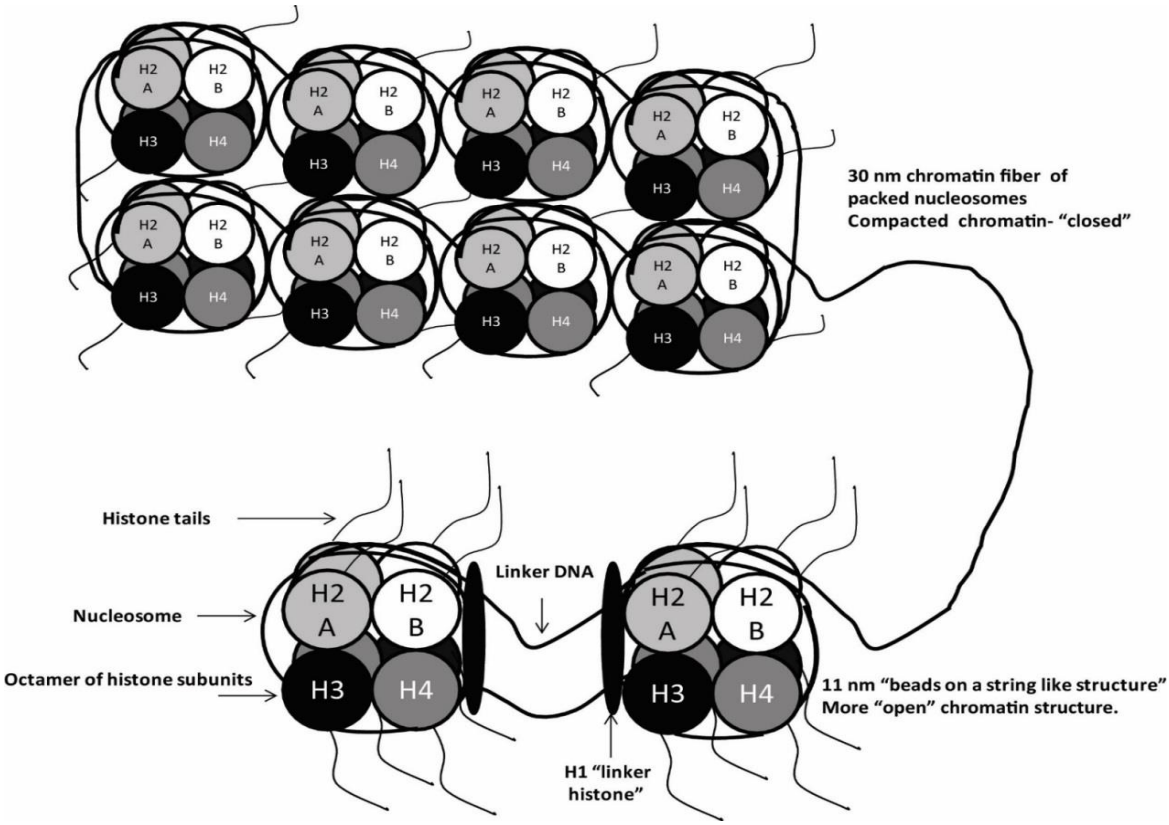
H2 A
H2 B
H3
H4
30 nm chromatin fiber of packed nucleosomes
Compacted chromatin- "closed"
Histone tails
Nucleosome
Octamer of histone subunits
Linker DNA
11 nm "beads on a string like structure"
More "open" chromatin structure.
H1 "linker histone"

modifications allows the specification and maintenance of cellular identity in a wide range of cell types [90, 101]. Acetylation of histones by histone acetyl-transferases (HATS) leads to the activation of transcription, whereas, histone methylation by histone methyltransferases (HMTs) can regulate gene activation or repression depending on which residues are methylated. Histones can be mono- (me1), di- (me2) or tri-methylated (me3) on lysine residues and me1 or me2 on arginine residues. Methylation of histone 3 lysine 4 (H3K4), lysine 36 (H3K36) and lysine 79 (H3K79) are associated with active transcription and methylation of Histone 3 lysine 9 (H3K9) and lysine 27 (H3K27) is associated with gene repression [102] (Figure 11 A&B). With the development of Chromatin Immunoprecipitation (ChIP) techniques researchers can now identify histone proteins that are associated with a particular region of the genome.

Recent investigations of embryonic stem cells (ESC) using microarray and ChIP techniques have revealed the presence of both H3K27me3 and H3K4me3 specific modification patterns on chromatin termed “bivalent domains”. The presence of both these bivalent domains within ESC genomes allows the silencing of developmental regulators whist, keeping them poised for activation. Upon ESC differentiation these bivalent domains become univalent, allowing the activation of genes that drive lineage commitment [103]. Methyltransferases and demethylases are thought to be responsible for the switch between repressive H3K27 domains and active H3K4 domains. Different combinations of histone modifications can influence the recruitment of different effector proteins and transcription factors to chromatin

Furthermore, the interplay between the different epigenetic modifying enzymes (HATs, HDACs, DNMTs, MBD, and HMTs) is critical for normal gene transcription suggesting the importance of epigenetic gene regulation in many cellular processes.

Figure 11. Chromatin modifying proteins modulate chromatin structure.
DNA accessibility is dictated by chromatin structure, chromatin can be compacted or opened up leading to repression or activation of genes through DNA and post-translational histone modifications (PTMs). **A)** 5 methyl cytosine methylation (5M) of DNA by DNA methyltransferases (DNMTs). Histone three lysine 27 Histone methylation by histone methyltransferases (HMT) can tri methylate Histone three lysine nine and 27 (H3K27me3 (Ezh2)) and the removal of H3K9 acetylation (ac) by histone deacetylatases (HDACs). All these epigenetic modifications facilitate in the compaction of the chromatin structure and gene repression. **B)** Removal of 5M from DNA by DNA demethylases (dMTase). The removal of H3K9me3 and H3K27me3 is mediated by UTX and JMJD3 histone demethylases (HDMTs). The addition of H3K4me3 and H3K420me1 methylation by HMTs and H3K9ac by acetyltransferases (HATs), lead to the opening up of chromatin and activation of gene transcription. Chromatin remodelers (CR) are recruited to chromatin by a combination of DNA and PTM leading to either the chromatin activation or condensation (114).

A

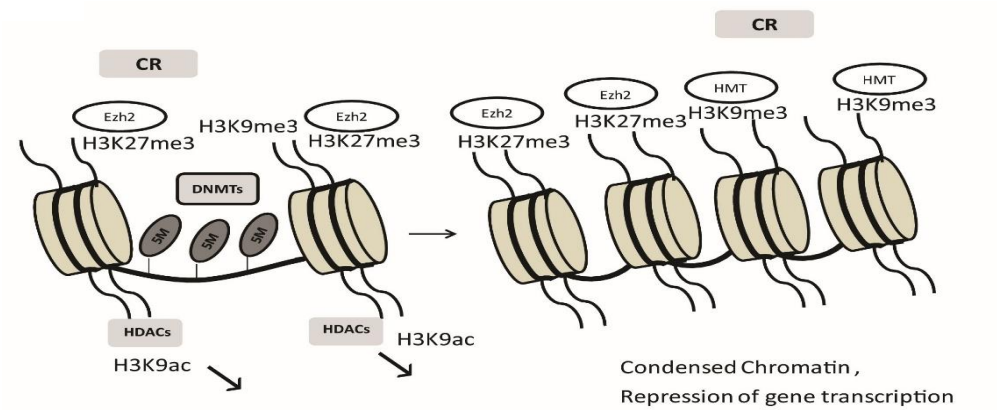
CR
Ezh2
H3K27me3
H3K9me3
Ezh2
H3K27me3
DNMTs
5M
5M
5M
HDACs
HDACs
H3K9ac
H3K9ac
CR
Ezh2
H3K27me3
Ezh2
H3K27me3
HMT
H3K9me3
HMT
H3K9me3
Condensed Chromatin ,
Repression of gene transcription

B

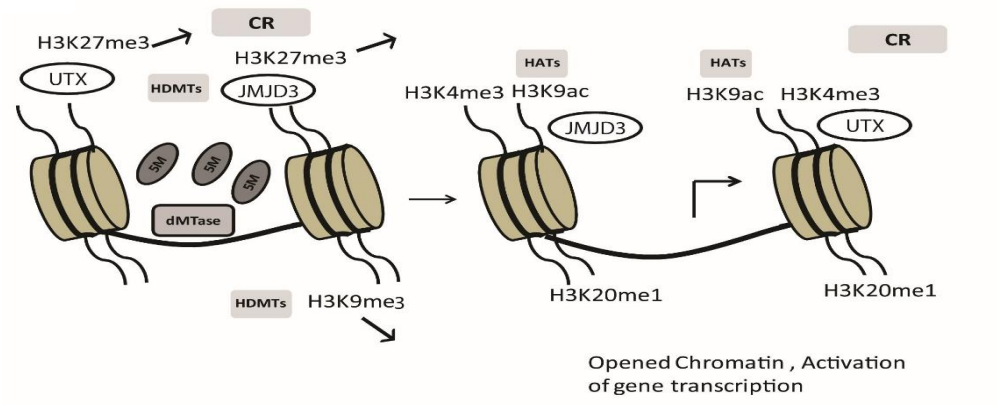
H3K27me3
CR
H3K27me3
UTX
HDMTs
JMJD3
5M
5M
5M
dMTase
HDMTs
H3K9me3
HATs
H3K4me3
H3K9ac
JMJD3
H3K20me1
CR
HATs
H3K9ac
H3K4me3
UTX
H3K20me1
Opened Chromatin , Activation
of gene transcription

Figure 12. Epigenetic Regulation of MSC Maintenance and Cell Fate
EZH2 and KDM6A dictate a switch between stemness and differentiation.

In multipotential immature MSCs EZH2 tri methylates the lysine 27 residue on the histone three tail (H3K27me3) leading to repression of osteogenic genes. As MSC differentiate EZH2 and its H3K27me3 modification is removed from osteogenic genes by UTX allowing methyltransferase MLL2 to methylate H3K4me3 activating gene expression.

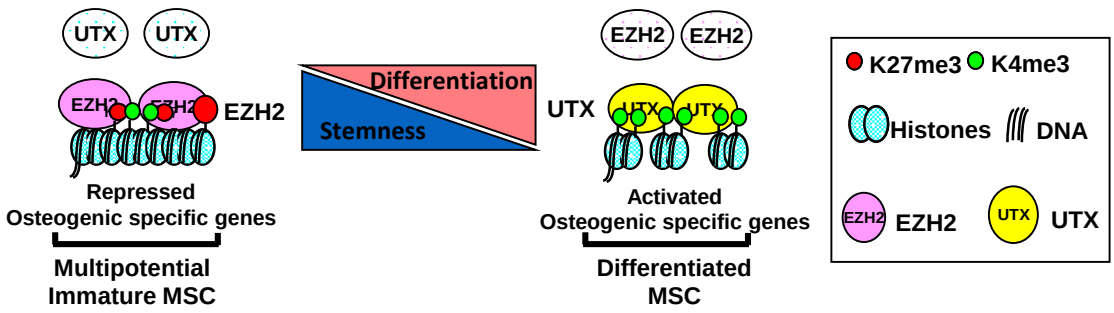
UTX
UTX
EZH2
EZH2
EZH2
Repressed
Osteogenic specific genes
Multipotential
Immature MSC
Differentiation
Stemness
EZH2
EZH2
UTX
UTX
UTX
Activated
Osteogenic specific genes
Differentiated
MSC
K27me3
K4me3
Histones
DNA
EZH2
EZH2
UTX
UTX

1.5 Histone methylation regulates BMSC differentiation

1.5.1 Epigenetic regulation of H3K27me3 and H3K4me3 in osteogenic differentiation

BMSC osteogenic differentiation is controlled by key signalling pathways and transcription factors, which can be regulated through epigenetic modifications [104]. Besides DNA methylation, gene repression can be mediated through posttranslational modification of histones. A common repressive histone methylation is H3K27me3. Studies have found that the H3K27 methyltransferase, Enhancer of Zeste Homolog two (EZH2), a component of the poly comb repressor complex 2 (PCR2), can interact with DNMTs to promote gene repression [105]. EZH2 has been widely implicated as a regulator of developmental processes and differentiation associated genes [106, 107]. EZH2 activity can lead to either mono, di or tri methylation of the K27 residue of H3 tails (H3K27me1/2/3), and is associated with heterochromatin, chromatin compaction and repression of gene transcription [108-110]. EZH2 influences chromatin structure through adding a me3 modification to H3K27, where this mark is recognised by PRC1, which recruits effector proteins such as chromatin remodelers involved in compaction of chromatin [111]. EZH2 deficiencies in mice lead to peri-natal lethality due to deformities in morphological movement of ESC in the developing embryo, highlighting the importance of EZH2 in development and perhaps stem cell maintenance. EZH2 has been implicated in anteroposterior axis specification and proximodistal axis elongation during murine limb development through the dis-regulation of the Hox genes [112]. More recently Dudakovic and colleagues demonstrated that EZH2 promotes osteoblast maturation during sskeletal development in mice [113].

Studies from our laboratory demonstrated that over-expression of EZH2 in human BMSC inhibited osteogenic differentiation, while siRNA knockdown of EZH2 or treatment with the methyltransferase inhibitor, DZNep, promoted osteogenic differentiation, identifying a direct

role for EZH2 in regulating human BMSC bone cell differentiation [114]. Furthermore, EZH2 was found to bind and methylate the promoter regions of *RUNX2* and *OSTEOPONTIN* using ChIP analysis [114], suggesting that EZH2 may be a key regulator for MSC cell fate determination. During MSC differentiation, cyclin dependent kinase 1 (CDK1) represses EZH2 methyltransferase activity through the phosphorylation of residue threonine 487, thus promoting BMSC osteogenic differentiation in vitro [115]. ChIP-on-chip analysis of adipocytes and osteoblast revealed that the myocyte enhancer factor-2 interacting transcription factor (MITR or HDAC9c) is bound by EZH2 in adipocytes but not in osteoblasts. During osteogenesis EZH2 binding to MITR is repressed allowing to MITR to complex with PPARγ2, thereby directly interrupting PPARγ-2 activity [116]. These observations have led to the hypothesis that the known H3K27 demethylase (HDMs) KDM6A (Lysine demethylase 6A also known as UTX: ubiquitously transcribed tetra-tricopeptide repeat X) and Jumonji domain-containing protein 3 (JMJD3 also known as KDM6B lysine demethylase 6B) could also be pivotal in dictating the lineage specificity of BMSC (Figure 12).

Histone methylases and demethylases control the level of methylation present within a cell. An increase in H3K27 demethylation leads to the recruitment of gene activating factors and activation of gene transcription. KDM6A and KDM6B have both been identified as having potential roles in regulating BMSC osteogenic differentiation [114, 117-120].

KDM6A over–expression in BMSC was found to promote osteogenic differentiation, while siRNA knockdown of KDM6A resulted in decreased osteogenesis *in vitro* and *in vivo* [114]. Supporting Hemming et al, 2014, UTX has be implicated in regulating osteogenic differentiate in MC3T3-E1 cells and primary osteoblasts. Expression of UTX promotes osteogenesis whilst shRNA or treatment with an H3K27me3 demethylase inhibitor (GSK-J1)

inhibited osteogenic differentiation. Furthermore silencing of UTX increased *Runx2* and *Osterix* promoter H3K27me3 [121]. However, the role of KDM6B in osteogenic differentiation is thought to act by regulating RUNX2 and Osterix expression in osteoblasts [118, 120], which is regulated by MIR146A during osteogenic differentiation [119]. JMJD3 homozygous deletion in mice identifies that JMJD3 is coactivator of RUNX2 and promotes chondrocyte proliferation and hypertrophy during endochondral ossification [122]. However it is still unclear of JMJD3 role in skeletogenesis. Therefore, it is still unclear whether KDM6A and KDM6B work synergistically or individually to regulate osteogenic differentiation. While it is well established that BMP, Wnt, and Notch signalling pathways all play important roles in osteoblast differentiation [34], these two demethylases could play different roles in regulating osteogenic differentiation based on the cellular signals they encounter leading to specialised effects on cellular differentiation.

H3K4 methylation has been shown to positively regulate transcription by recruiting nucleosome remodelling enzymes and histone acetylases [123]. H3K4 methylation is mediated by SET domain-containing methyltransferases, such as mixed lineage leukaemia 1-5 (MLL1-5), SET1A/B and SET7/9. H3K4 is critical for gene activation, where this histone modification mark is widely expressed on genes involved in differentiation, growth and self-renewal [124]. The balance of H3K4 methylation is controlled by H3K4 HMTs and H3K4 HDMs. MLL proteins often associate in a complex with H3K27 demethylase KDM6A/KDM6A or KDM6B/KDM6B and PAX transactivation domain-interacting protein (PTIP; nuclear protein associated with active chromatin), allowing the rapid removal of the repressive methylation and the application of the active methylation H3K4 [125].

Opening up of chromatin allowing the gene transcription is regulated by active histone modifications such as H3K4me3. Hassan and colleagues identified that H3K4me3 and hyper acetylation mediated by HOXA10 induces chromatin remodelling facilitating in RUNX2 mediated activation leading to activation of RUNX2 target genes such as Osteocalcin [126]. H3K4 HDMs are associated with removal of the H3K4 active methylation modification involved in transcriptional activation. Jumonji domain-containing histone demethylases such as the JARID1 family of HDMs (JARID1A−D) remove H3K4me3 and H3K4me2 modifications. JARID1A inhibits osteogenesis through the demethylation of the TSS of RUNX2, Osterix, Osteocalcin and alkaline phosphatase in human adipose-derived MSC [127]. The Nucleolar protein 66 is also known to have H3K4me3/2/1 demethylase activity, and has been found to demethylate the promoter region of Osterix and interact directly with Osterix preventing activation of its downstream target genes [128]. Furthermore in human adipose derived MSC, osteogenic differentiation is regulated by H3K4 demethylase Retinoblastoma binding protein 2 (RBP2). Knockdown of RBP2 increased H3K4me3 and promoted alkaline phosphatase, Osteocalcin and Osterix expression. Furthermore, RBP2 directly associates with the RUNX2 protein, where knockdown of RPB2 leads to activation of RUNX2 [127].

These studies have identified the role of H3K27me3 and H3K4me3 modifications are directly involved in MSC osteogenic differentiation, but have yet to determine the sequential and temporal activities of these epigenetic modifiers during the process of osteogenesis.

1.5.2 Epigenetic regulation of H3K27me3 and H3K4me3 in adipogenic differentiation

The H3K27 methyltransferase, EZH2 is also known to promote adipogenesis by repressing Wnt-1,-6,-10a and -10b leading to disruption of Wnt/β-catenin signalling rather than directly

regulating *PPARγ2* [129]. In human studies, over-expression of EZH2 in BMSC promoted adipogenic differentiation, while siRNA knockdown inhibited adipogenic differentiation [114]. Over expression of H3K27 demethylase, KDM6A, inhibited adipogenesis, while siRNA knockdown promoted adipogenic differentiation of BMSC [114] possibly by demethylating Wnt associated genes therefore inhibiting adipogenesis indirectly. Ye and colleagues identified that knockdown of H3K27me3 demethylase KDM6B/KDM6B and H3K4me3 demethylase KDM4B inhibited adipogenesis further supporting the role of demethylases in adipogenic differentiation [117].

Activating methylation modifications such as H3K4 play a critical role in activation of key adipogenic differentiation genes. MLL3 and MLL4 are mono- and di-methyltransferases targeting H3K4, which are required for enhancer activation, gene activation and differentiation and are critical for PPARγ2 and C/EBP-α expression during adipogenesis [125, 130-132]. Moreover, H3K4 di-methylation, a mark of poised genes, has been shown to be present on the promoters of the adipose associated genes, apM1, glut4, gpd1, and leptin in pre-adipocytes [124, 133].

While it has been shown that some epigenetic modifiers act by direct activation or repression of *PPARγ2*, other modifiers such as EZH2 regulate adipogenesis indirectly through the inhibition of signalling pathways that promote osteo/chondrogenesis [129]. Furthermore, the recruitment of epigenetic modifiers to the chromatin by other molecules can act as another level of control to further regulate the expression of adipose associated genes. Collectively, these studies depict the complexity H3K27me3 and H3K4me3 epigenetic modifications involved in adipogenic differentiation, where methylases and demethylases appear to be pivotal for the switch between osteogenic or adipogenic lineage commitment.

1.5.3 Epigenetic regulation of chondrogenic differentiation

While studies examining the epigenetic regulation of human MSC chondrogenic differentiation are scant, one report has shown that the chondrogenic specific gene, collagen type II loses H3K27me3 and gains H3K4 and H3K36 active methylation during early chondrogenic induction [134]. Methyltransferase Ezh2 is required for neural crest-derived cartilage formation in mice. Conditional ablation of *Ezh2* prevents the early steps of the osteochondrogenic differentiation program in mesenchymal progenitor cells [135]. Furthermore demethylases JMJD3 is important for chondrogenic proliferation and hypertrophy [122].

With limited studies using MSC derived chondrocytes the impact of epigenetic modifiers on regulating chondrogenic differentiation is unclear. It is predicated that many modifications will be critical in regulating chondrogenic differentiation and maintain healthy chondrogenic tissue. Collectively, these studies have shown that epigenetic modifiers play a role in articular and synovial derived chondrocytes and further investigation could lead to opportunity to manipulate cells with greater chondrogenic differentiation capacity for cartilage regeneration.

These studies have identified the EZH2 and other epigenetic modifiers in driving MSC lineage commitment. It has identified the direct regulation of key transcription factors RUNX2, SOX9, and PPARγ2 for BMSC differentiation as targets of epigenetic modifiers. Collectively, these findings suggest a greater level of complexity driving MSC lineage determination. However, the roles of EZH2 regulating novel genes important for osteogenic differentiation and regulating skeletal development are still unclear.

1.6 H3K27me3 human diseases.

1.6.1 Weaver Syndrome

Weaver syndrome is a rare congenital syndrome which was first described in 1974. Weaver syndrome is caused by heterozygous mutation in the EZH2 gene (601573) on chromosome 7q36. These patients' exhibits generalized overgrowth, advanced bone age, macrocephaly and abnormal facial deformities. Only 40 cases of weaver syndrome have been identified to date [136]. It is suggested that only heterozygous mutations exist in human due to embryonic lethality of a homozygous deletion such as seen in global Ezh2 knockout mice [137]. Recent studies using conditional knockout in limb bud mesenchyme have identified EZH2 plays a role in limb bud patterning and ablation of EZH2 impairs limb development [138]. EZH2 ablation in early mesenchyme causes acceleration of osteoblast maturation in the cranium leading to craniosynostosis [113]. However the effect of *Ezh2* deletion in endochondral bone development, bone homeostasis and remodelling in mice has not been well described. Furthermore how Ezh2 regulates increase bone aging in these weaver patients is still undefined.

1.6.2 Kabuki Syndrome

Kabuki syndrome (KS) is characterized by a recognizable facial gestalt, a high incidence of internal malformations, hypertonia, feeding difficulties in infancy, postnatal failure to thrive , skeletal deformities, postnatal growth impairment (short stature) and mild to moderate developmental delay [139]. This rare congenital anomaly syndrome, was first described by Niikawa and Kuroki in 1981.64,65. Kabuki syndrome is caused by a nonsense mutation in MLL2 or a mmutation in KDM6A/UTX located on Xp11.3 and cases Kabuki syndrome (KS2, MIM 300867) [139]. Global UTX homozygous knockout female mice exhibit pronounced

growth retardation, neural tube closure defects (cranioschisis), and cardiac malformations reveals [140]. However, these studies have used a global UTX knockout revealing the importance of UTX in early embryonic development. Therefore it is suggested that defects in neural tube closure defects and cardiac defects may explain why only heterozygous mutations are reported in kabuki syndrome. Investigating the role of KDM6A in bone development using a limb bud mesenchyme driver PRRX-1 or osteoprogenitor marker OSX could identify the role of KDM6A in skeletogenesis. Understanding how EZH2 and KDM6A regulate murine skeletal development will allow more information about the cause of EZH2 and KDM6A mutation in human patients. Furthermore, these studies will help identify the role of EZH2 and KDM6A in MSC lineage specification during bone development, homeostasis, remodelling, aging and repair.

1.7 Conclusion

Epigenetic modifications play a critical role in gene activation and repression in many cellular processes. Tri methylation of histone 27 by methyltransferase EZH2 facilitates with chromatin compaction leading to gene repression whilst, demethylases KDM6A and KDM6B removal of H3K27me3 facilitate with the unravelling of chromatin and incitation of gene transcription. Human heterozygous EZH2 and KDM6A mutations lead to skeletal deformities suggesting the importance of these epigenetic modifiers in human skeletal development. EZH2 has been shown to be involved in regulating human and murine MSC differentiation. Specifically, in human MSC CDK1 inhibits EZH2 activity promoting osteogenic differentiation. However the direct role of the H3K7me3 epigenetic modifiers EZH2 and KDM6A and or KDM6B in BMSC differentiation is unclear, illustrating the importance of determining the epigenetic signatures associated with differentiation and maintenance of MSC. This project aims to investigate the function of EZH2 and KDM6A in human BMSC

lineage determination. We aim to identify known or novel genes regulated by EZH2 and its H3K27me3 during human osteogenic differentiation. Furthermore, we aim to identify the role Ezh2 in murine bone formation and remodeling.

1.8 Aims:

1. To investigate the function of H3K27 methyltransferase EZH2 and demethylases KDM6A in MSC osteogenic and adipogenic differentiation *in vitro* and *in vivo*.
2. To identify known or novel osteogenic genes regulated by EZH2 during MSC osteogenic differentiation.
3. Investigate the function of EZH2 in embryonic and early postnatal murine skeletal development and remodelling *in vivo* by the tissue specific ablation of EZH2 in limb bud mesenchyme.

1.8.1 Hypotheses:

1. KDM6A promotes osteogenic differentiation whilst EZH2 inhibits human osteogenic differentiation *in vitro* and *in vivo.*
2. EZH2 regulates osteogenic genes through its H3K27me3 during MSC to osteoblast differentiation.
3. Tissue specific ablation of EZH2 in MSC will impair limb development whilst promoting bone formation in mice during embryonic and early postnatal skeletal development repair *in vivo*.
4. Ezh2 will promote bone aging through dysregulation of bone remodelling.

1.9 References

[1] Orlando V. Polycomb, epigenomes, and control of cell identity. Cell. 2003;112:599-606.

[2] Daadi MM, A.-L. Maag, and G.K. Steinberg. . Adherent Self-Renewable Human Embryonic Stem Cell-Derived Neural Stem Cell Line: Functional Engraftment in Experimental Stroke Model. PLOS one. 2008;3:1644.

[3] Takahashi K, Yamanaka S. Induction of pluripotent stem cells from mouse embryonic and adult fibroblast cultures by defined factors. cell. 2006;126:663-76.

[4] Pittenger MF, Mackay AM, Beck SC, Jaiswal RK, Douglas R, Mosca JD, et al. Multilineage potential of adult human mesenchymal stem cells. Science. 1999;284:143-7.

[5] Rogers I, Casper RF. Umbilical cord blood stem cells. Best Practice & Research Clinical Obstetrics & Gynaecology. 2004;18:893-908.

[6] Shi S, Gronthos S. Perivascular niche of postnatal mesenchymal stem cells in human bone marrow and dental pulp. Journal of Bone and Mineral Research. 2003;18:696-704.

[7] Igura K, Zhang X, Takahashi K, Mitsuru A, Yamaguchi S, Takahashi T. Isolation and characterization of mesenchymal progenitor cells from chorionic villi of human placenta. Cytotherapy. 2004;6:543-53.

[8] Schipani E, Kronenberg HM. Adult mesenchymal stem cells. 2009.

[9] Crisan M, Yap S, Casteilla L, Chen C-W, Corselli M, Park TS, et al. A perivascular origin for mesenchymal stem cells in multiple human organs. Cell stem cell. 2008;3:301-13.

[10] Gronthos S MM, Brahim J, et al. . Postnatal human dental pulp stem cells (DPSCs) in vitro and in vivo. Proc Natl Acad Sci U S A. 2000;97:3625-13630.

[11] Seo B-M, Miura M, Gronthos S, Bartold PM, Batouli S, Brahim J, et al. Investigation of multipotent postnatal stem cells from human periodontal ligament. 2004;364:149-55.

[12] Bianco P, Gehron Robey P. Marrow stromal stem cells. Journal of Clinical Investigation. 2000;105:1663-8.

[13] Owen M. Marrow stromal stem-cells Journal of Cell Science. 1988:63-76.

[14] De Bari C, Dell'Accio F, Tylzanowski P, Luyten FP. Multipotent mesenchymal stem cells from adult human synovial membrane. Arthritis & Rheumatism. 2001;44:1928-42.

[15] Kuznetsov SA, Mankani MH, Gronthos S, Satomura K, Bianco P, Robey PG. Circulating Skeletal Stem Cells. The Journal of Cell Biology. 2001;153:1133-40.

[16] Li CD, Zhang WY, Li HL, Jiang XX, Zhang Y, Tang PH, et al. Mesenchymal stem cells derived from human placenta suppress allogeneic umbilical cord blood lymphocyte proliferation. Cell research. 2005;15:539-47.

[17] Friedenstein.Aj, Chailakh.Rk, Lalykina KS. Development of fibroblast colonies in monolayer culture of guinea-pig bone-marrow and spleen cells. Cell and Tissue Kinetics. 1970;3:393-&.

[18] Castromalaspina H, Gay RE, Resnick G, Kapoor N, Meyers P, Chiarieri D, et al. Characterization of human bone-marrow fibroblast colony-forming cells (CFU-F) and their progeny Blood. 1980;56:289-301.

[19] Gronthos S, Chen SQ, Wang CY, Robey PG, Shi ST. Telomerase accelerates osteogenesis of bone marrow stromal stem cells by upregulation of CBFA1, osterix, and osteocalcin. Journal of Bone and Mineral Research. 2003;18:716-22.

[20] Kuznetsov SA, Krebsbach PH, Satomura K, Kerr J, Riminucci M, Benayahu D, et al. Single-colony derived strains of human marrow stromal fibroblasts form bone after transplantation in vivo. Journal of bone and mineral research. 1997;12:1335-47.

[21] Sacchetti B, Funari A, Michienzi S, Di Cesare S, Piersanti S, Saggio I, et al. Self-renewing osteoprogenitors in bone marrow sinusoids can organize a hematopoietic microenvironment. Cell. 2007;131:324-36.

[22] Owen M, Friedenstein AJ. Stromal stem-cells marrow-derived osteogenic precursors Ciba Foundation Symposia. 1988;136:42-60.

[23] Dominici M, Le Blanc K, Mueller I, Slaper-Cortenbach I, Marini F, Krause D, et al. Minimal criteria for defining multipotent mesenchymal stromal cells. The International Society for Cellular Therapy position statement. Cytotherapy. 2006;8:315-7.

[24] Patel DM, Shah J, Srivastava AS. Therapeutic Potential of Mesenchymal Stem Cells in Regenerative Medicine. Stem Cells International. 2013;2013:1-15.

[25] Gronthos S, Zannettino ACW, Hay SJ, Shi ST, Graves SE, Kortesidis A, et al. Molecular and cellular characterisation of highly purified stromal stem cells derived from human bone marrow. Journal of Cell Science. 2003;116:1827-35.

[26] Zannettino ACW, Paton S, Kortesidis A, Khor F, Itescu S, Gronthos S. Human multipotential mesenchymal/stromal stem cells are derived from a discrete subpopulation of STRO-1(bright)/CD34(-)/CD45(-)/glycophorin-A-bone marrow cells. Haematologica-the Hematology Journal. 2007;92:1707-8.

[27] Gronthos S, Zannettino AC. A method to isolate and purify human bone marrow stromal stem cells. Methods Mol Biol. 2008;449:45-57.

[28] Isenmann S, Arthur A, Zannettino ACW, Turner JL, Shi ST, Glackin CA, et al. TWIST Family of Basic Helix-Loop-Helix Transcription Factors Mediate Human Mesenchymal Stem Cell Growth and Commitment. Stem Cells. 2009;27:2457-68.

[29] Menicanin D BM, W ZAC, et al. Identification of a common gene Expression Signature Associated with Immature Clonal Mesenchymal Cell Populations Derived from Bone Marrow and Dental Tissues. Stem Cells and Development. 2010;19:501-1510.

[30] Kortesidis A, Zannettino A, Isenmann S, Shi S, Lapidot T, Gronthos S. Stromal-derived factor-1 promotes the growth, survival, and development of human bone marrow stromal stem cells. Blood. 2005;105:3793-801. Epub 2005 Jan 27.

[31] Shi ST, Gronthos S, Chen SQ, Reddi A, Counter CM, Robey PG, et al. Bone formation by human postnatal bone marrow stromal stem cells is enhanced by telomerase expression. Nature Biotechnology. 2002;20:587-91.

[32] Simonsen JL, Rosada C, Serakinci N, Justesen J, Stenderup K, Rattan SIS, et al. Telomerase expression extends the proliferative life-span and maintains the osteogenic potential of human bone marrow stromal cells. Nat Biotech. 2002;20:592-6.

[33] Cakouros D, Isenmann S, Cooper L, Zannettino A, Anderson P, Glackin C, et al. Twist-1 Induces Ezh2 Recruitment Regulating Histone Methylation along the Ink4A/Arf Locus in Mesenchymal Stem Cells. Molecular and Cellular Biology. 2012;32:1433-41.

[34] Lin GL, Hankenson KD. Integration of BMP, Wnt, and notch signaling pathways in osteoblast differentiation. Journal of Cellular Biochemistry. 2011;112:3491-501.

[35] Morrison SJ, Scadden DT. The bone marrow niche for haematopoietic stem cells. Nature. 2014;505:327-34.

[36] Ehninger A, Trumpp A. The bone marrow stem cell niche grows up: mesenchymal stem cells and macrophages move in. The Journal of Experimental Medicine. 2011;208:421-8.

[37] Chan CK, Chen C-C, Luppen CA, Kim J-B, DeBoer AT, Wei K, et al. Endochondral ossification is required for haematopoietic stem-cell niche formation. Nature. 2009;457:490-4.

[38] Mizoguchi T, Pinho S, Ahmed J, Kunisaki Y, Hanoun M, Mendelson A, et al. Osterix marks distinct waves of primitive and definitive stromal progenitors during bone marrow development. Developmental cell. 2014;29:340-9.

[39] Logan M, Martin JF, Nagy A, Lobe C, Olson EN, Tabin CJ. Expression of Cre Recombinase in the developing mouse limb bud driven by a Prxl enhancer. Genesis. 2002;33:77-80.

[40] Houlihan DD, Mabuchi Y, Morikawa S, Niibe K, Araki D, Suzuki S, et al. Isolation of mouse mesenchymal stem cells on the basis of expression of Sca-1 and PDGFR-α. nature protocols. 2012;7:2103-11.

[41] Morikawa S, Mabuchi Y, Kubota Y, Nagai Y, Niibe K, Hiratsu E, et al. Prospective identification, isolation, and systemic transplantation of multipotent mesenchymal stem cells in murine bone marrow. The Journal of experimental medicine. 2009;206:2483-96.

[42] Park D, Spencer JA, Koh BI, Kobayashi T, Fujisaki J, Clemens TL, et al. Endogenous bone marrow MSCs are dynamic, fate-restricted participants in bone maintenance and regeneration. Cell stem cell. 2012;10:259-72.

[43] Pinho S, Lacombe J, Hanoun M, Mizoguchi T, Bruns I, Kunisaki Y, et al. PDGFRα and CD51 mark human nestin+ sphere-forming mesenchymal stem cells capable of hematopoietic progenitor cell expansion. The Journal of experimental medicine. 2013;210:1351-67.

[44] Kunisaki Y, Bruns I, Scheiermann C, Ahmed J, Pinho S, Zhang D, et al. Arteriolar niches maintain haematopoietic stem cell quiescence. Nature. 2013;502:637-43.

[45] Mendelson A, Frenette PS. Hematopoietic stem cell niche maintenance during homeostasis and regeneration. Nature medicine. 2014;20:833-46.

[46] Méndez-Ferrer S, Michurina TV, Ferraro F, Mazloom AR, MacArthur BD, Lira SA, et al. Mesenchymal and haematopoietic stem cells form a unique bone marrow niche. nature. 2010;466:829-34.

[47] Worthley DL, Churchill M, Compton JT, Tailor Y, Rao M, Si Y, et al. Gremlin 1 identifies a skeletal stem cell with bone, cartilage, and reticular stromal potential. Cell. 2015;160:269-84.

[48] Mignone JL, Kukekov V, Chiang AS, Steindler D, Enikolopov G. Neural stem and progenitor cells in nestin-GFP transgenic mice. Journal of Comparative Neurology. 2004;469:311-24.

[49] Sugiyama T, Kohara H, Noda M, Nagasawa T. Maintenance of the hematopoietic stem cell pool by CXCL12-CXCR4 chemokine signaling in bone marrow stromal cell niches. Immunity. 2006;25:977-88.

[50] Bensidhoum M, Chapel A, Francois S, Demarquay C, Mazurier C, Fouillard L, et al. Homing of in vitro expanded Stro-1-or Stro-1+ human mesenchymal stem cells into the NOD/SCID mouse and their role in supporting human CD34 cell engraftment. Blood. 2004;103:3313-9.

[51] Gonçalves R, da Silva CL, Cabral JM, Zanjani ED, Almeida-Porada G. A Stro-1+ human universal stromal feeder layer to expand/maintain human bone marrow hematopoietic stem/progenitor cells in a serum-free culture system. Experimental hematology. 2006;34:1353-9.

[52] Zhou BO, Yue R, Murphy MM, Peyer JG, Morrison SJ. Leptin-receptor-expressing mesenchymal stromal cells represent the main source of bone formed by adult bone marrow. Cell stem cell. 2014;15:154-68.

[53] Abad V, Meyers JL, Weise M, Gafni RI, Barnes KM, Nilsson O, et al. The role of the resting zone in growth plate chondrogenesis. Endocrinology. 2002;143:1851-7.

[54] Kember NF. Cell division in endochondral ossification. A study of cell proliferation in rat bones by the method of tritiated thymidine autoradiography. J Bone Joint Surg Br. 1960;42B:824-39.

[55] Brighton CT, Sugioka Y, Hunt RM. Cytoplasmic Structures of Epiphyseal Plate Chondrocytes. quantitative evaluation using electron micrographs of rat costochondral junctions with special reference to the fate of hypertrophic cells. 1973;55:771-84.

[56] Sapolsky AI, Howell DS, Woessner JF, Jr. Neutral proteases and cathepsin D in human articular cartilage. J Clin Invest. 1974;53:1044-53.

[57] Brighton CT, Hunt RM. Mitochondrial calcium and its role in calcification. Histochemical localization of calcium in electron micrographs of the epiphyseal growth plate with K-pyroantimonate. Clin Orthop Relat Res. 1974:406-16.

[58] Kuhlman RE. phosphatases in epiphyseal cartilage; their possible role in tissue synthesis. J Bone Joint Surg Am. 1965;47:545-50.

[59] Zohar R. Signals between cells and matrix mediate bone regeneration: INTECH Open Access Publisher; 2012.

[60] Hadjidakis DJ, Androulakis II. Bone remodeling. Annals of the New York Academy of Sciences. 2006;1092:385-96.

[61] Warren JT, Zou W, Decker CE, Rohatgi N, Nelson CA, Fremont DH, et al. Correlating RANK Ligand/RANK Binding Kinetics with Osteoclast Formation and Function. Journal of cellular biochemistry. 2015.

[62] Nelson CA, Warren JT, Wang MW-H, Teitelbaum SL, Fremont DH. RANKL employs distinct binding modes to engage RANK and the osteoprotegerin decoy receptor. Structure. 2012;20:1971-82.

[63] Eghbali-Fatourechi G, Khosla S, Sanyal A, Boyle WJ, Lacey DL, Riggs BL. Role of RANK ligand in mediating increased bone resorption in early postmenopausal women. Journal of Clinical Investigation. 2003;111:1221.

[64] Thommesen L, Stunes AK, Monjo M, Grøsvik K, Tamburstuen MV, Kjøbli E, et al. Expression and regulation of resistin in osteoblasts and osteoclasts indicate a role in bone metabolism. Journal of cellular biochemistry. 2006;99:824-34.

[65] Ortuño MJ, Susperregui AR, Artigas N, Rosa JL, Ventura F. Osterix induces Col1a1 gene expression through binding to Sp1 sites in the bone enhancer and proximal promoter regions. Bone. 2013;52:548-56.

[66] Kim Y-J, Lee M-H, Wozney JM, Cho J-Y, Ryoo H-M. Bone morphogenetic protein-2-induced alkaline phosphatase expression is stimulated by Dlx5 and repressed by Msx2. Journal of Biological Chemistry. 2004;279:50773-80.

[67] Muruganandan S, Roman A, Sinal C. Adipocyte differentiation of bone marrow-derived mesenchymal stem cells: cross talk with the osteoblastogenic program. Cellular and molecular life sciences. 2009;66:236-53.

[68] Zhao C, Irie N, Takada Y, Shimoda K, Miyamoto T, Nishiwaki T, et al. Bidirectional ephrinB2-EphB4 signaling controls bone homeostasis. Cell metabolism. 2006;4:111-21.

[69] Arthur A, Panagopoulos RA, Cooper L, Menicanin D, Parkinson IH, Codrington JD, et al. EphB4 enhances the process of endochondral ossification and inhibits remodeling during bone fracture repair. J Bone Miner Res. 2013;28:926-35.

[70] Arthur A, Zannettino A, Panagopoulos R, Koblar SA, Sims NA, Stylianou C, et al. EphB/ephrin-B interactions mediate human MSC attachment, migration and osteochondral differentiation☆☆☆. Bone. 2011;48:533-42.

[71] Farmer SR. Transcriptional control of adipocyte formation. Cell metabolism. 2006;4:263-73.

[72] Alliston T, Choy L, Ducy P, Karsenty G, Derynck R. TGF-β-induced repression of CBFA1 by Smad3 decreases cbfa1 and osteocalcin expression and inhibits osteoblast differentiation. The EMBO journal. 2001;20:2254-72.

[73] Beresford J, Bennett J, Devlin C, Leboy P, Owen M. Evidence for an inverse relationship between the differentiation of adipocytic and osteogenic cells in rat marrow stromal cell cultures. Journal of cell science. 1992;102:341-51.

[74] Garcia T, Roman-Roman S, Jackson A, Theilhaber J, Connolly T, Spinella-Jaegle S, et al. Behavior of osteoblast, adipocyte, and myoblast markers in genome-wide expression analysis of mouse calvaria primary osteoblasts in vitro. Bone. 2002;31:205-11.

[75] Evans BA, Bull MJ, Kench RC, Fox RE, Morgan LD, Stevenson AE, et al. The influence of leptin on trabecular architecture and marrow adiposity in GH-deficient rats. Journal of Endocrinology. 2011;208:69-79.

[76] Astudillo P, Ríos S, Pastenes L, Pino AM, Rodríguez JP. Increased adipogenesis of osteoporotic human-mesenchymal stem cells (MSCs) characterizes by impaired leptin action. Journal of cellular biochemistry. 2008;103:1054-65.

[77] Lee HW, Kim SY, Kim AY, Lee EJ, Choi JY, Kim JB. Adiponectin stimulates osteoblast differentiation through induction of COX2 in mesenchymal progenitor cells. Stem Cells. 2009;27:2254-62.

[78] Xie H, Xie P-L, Luo X-H, Wu X-P, Zhou H-D, Tang S-Y, et al. Omentin-1 exerts bone-sparing effect in ovariectomized mice. Osteoporosis International. 2012;23:1425-36.

[79] Xie H, Tang S-Y, Luo X-H, Huang J, Cui R-R, Yuan L-Q, et al. Insulin-like effects of visfatin on human osteoblasts. Calcified Tissue International. 2007;80:201-10.

[80] Goto H, Osaki M, Fukushima T, Sakamoto K, Hozumi A, Baba H, et al. Human bone marrow adipocytes support dexamethasone-induced osteoclast differentiation and function through RANKL expression. Biomedical Research. 2011;32:37-44.

[81] Sims NA, Gooi JH. Bone remodeling: Multiple cellular interactions required for coupling of bone formation and resorption. Seminars in cell & developmental biology: Elsevier; 2008. p. 444-51.

[82] Holliday R. Epigenetics-an overview Developmental Genetics. 1994;15:453-7.

[83] Luger K, Rechsteiner TJ, Flaus AJ, Waye MMY, Richmond TJ. Characterization of nucleosome core particles containing histone proteins made in bacteria. Journal of Molecular Biology. 1997;272:301-11.

[84] Luger K, Mader AW, Richmond RK, Sargent DF, Richmond TJ. Crystal structure of the nucleosome core particle at 2.8 A resolution. Nature. 1997;389:251-60.

[85] Riggs AD. X inactivation, differentiation, and DNA methylation. Cytogenet Cell Genet. 1975;14:9-25.

[86] Holliday R, Pugh JE. DNA modification mechanisms and gene activity during development. Science. 1975;187:226-32.

[87] Miniou P, Jeanpierre M, Blanquet V, Sibella V, Bonneau D, Herbelin C, et al. Abnormal methylation pattern in constitutive and facultative (X inactive chromosome) heterochromatin of ICF patients. Hum Mol Genet. 1994;3:2093-102.

[88] Okano M, Xie S, Li E. Cloning and characterization of a family of novel mammalian DNA (cytosine-5) methyltransferases. Nat Genet. 1998;19:219-20.

[89] Bird A. DNA methylation patterns and epigenetic memory. Genes & Development. 2002;16:6-21.

[90] Jaenisch R, Bird A. Epigenetic regulation of gene expression: how the genome integrates intrinsic and environmental signals. Nature Genetics. 2003;33:245-54.

[91] Li E, Beard C, Jaenisch R. Role for DNA methylation in genomic imprinting. Nature. 1993;366:362-5.

[92] Caspary T, Cleary MA, Baker CC, Guan XJ, Tilghman SM. Multiple mechanisms regulate imprinting of the mouse distal chromosome 7 gene cluster. Mol Cell Biol. 1998;18:3466-74.

[93] Li E. Chromatin modification and epigenetic reprogramming in mammalian development. Nature Reviews Genetics. 2002;3:662-73.

[94] Shock LS, Thakkar PV, Peterson EJ, Moran RG, Taylor SM. DNA methyltransferase 1, cytosine methylation, and cytosine hydroxymethylation in mammalian mitochondria. Proc Natl Acad Sci U S A. 2011;108:3630-5. doi: 10.1073/pnas.1012311108. Epub 2011 Feb 14.

[95] Ulaner GA, Vu TH, Li T, Hu JF, Yao XM, Yang Y, et al. Loss of imprinting of IGF2 and H19 in osteosarcoma is accompanied by reciprocal methylation changes of a CTCF-binding site. Hum Mol Genet. 2003;12:535-49.

[96] Warnecke PM, Stirzaker C, Song J, Grunau C, Melki JR, Clark SJ. Identification and resolution of artifacts in bisulfite sequencing. Methods. 2002;27:101-7.

[97] Grunau C, Clark SJ, Rosenthal A. Bisulfite genomic sequencing: systematic investigation of critical experimental parameters. Nucleic Acids Res. 2001;29:E65-5.

[98] Bock C, Beerman I, Lien W-H, Smith ZD, Gu H, Boyle P, et al. DNA methylation dynamics during in vivo differentiation of blood and skin stem cells. Molecular cell. 2012;47:633-47.

[99] Smith ZD, Meissner A. DNA methylation: roles in mammalian development. Nature Reviews Genetics. 2013;14:204-20.

[100] Mikkelsen TS, Xu Z, Zhang X, Wang L, Gimble JM, Lander ES, et al. Comparative Epigenomic Analysis of Murine and Human Adipogenesis. Cell. 2010;143:156-69.

[101] Fisher AG. Cellular identity and lineage choice. Nat Rev Immunol. 2002;2:977-82.

[102] Bernstein BE, Meissner A, Lander ES. The mammalian epigenome. Cell. 2007;128:669-81.

[103] Bernstein B, Mikkelsen T, Xie X, Kamal M, Huebert D, Cuff J, et al. A Bivalent Chromatin Structure Marks Key Developmental Genes in Embryonic Stem Cells. Cell. 2006;125:315-26.

[104] Deng ZL, Sharff KA, Tang N, Song WX, Luo J, Luo X, et al. Regulation of osteogenic differentiation during skeletal development. Front Biosci. 2008;13:2001-21.

[105] Viré E, Brenner C, Deplus R, Blanchon L, Fraga M, Didelot C, et al. The Polycomb group protein EZH2 directly controls DNA methylation. Nature. 2006;439:871-4.

[106] Chambeyron S, Bickmore WA. Chromatin decondensation and nuclear reorganization of the HoxB locus upon induction of transcription. Genes & Development. 2004;18:1119-30.

[107] Perry P, Sauer S, Billon N, Richardson WD, Spivakov M, Warnes G, et al. A dynamic switch in the replication timing of key regulator genes in embryonic stem cells upon neural induction. Cell Cycle. 2004;3:1645-50.

[108] Francis NJ, Kingston RE, Woodcock CL. Chromatin compaction by a polycomb group protein complex. Science. 2004;306:1574-7.

[109] Ringrose L, Ehret H, Paro R. Distinct contributions of histone H3 lysine 9 and 27 methylation to locus-specific stability of polycomb complexes. Mol Cell. 2004;16:641-53.

[110] Ringrose L, Paro R. Epigenetic regulation of cellular memory by the polycomb and trithorax group proteins. Annual Review of Genetics. 2004;38:413-43.

[111] Sparmann A, van Lohuizen M. Polycomb silencers control cell fate, development and cancer. Nature Reviews Cancer. 2006;6:846-56.

[112] Wyngaarden LA, Delgado-Olguin P, Su IH, Bruneau BG, Hopyan S. Ezh2 regulates anteroposterior axis specification and proximodistal axis elongation in the developing limb. Development. 2011;138:3759-67.

[113] Dudakovic A, Camilleri ET, Xu F, Riester SM, McGee-Lawrence ME, Bradley EW, et al. Epigenetic Control of Skeletal Development by the Histone Methyltransferase Ezh2. J Biol Chem. 2015.

[114] Hemming S, Cakouros D, Isenmann S, Cooper L, Menicanin D, Zannettino A, et al. EZH2 and KDM6A Act as an Epigenetic Switch to Regulate Mesenchymal Stem Cell Lineage Specification. Stem Cells. 2014;32:802-15. doi: 10.1002/stem.573.

[115] Wei Y, Chen Y-H, Li L-Y, Lang J, Yeh S-P, Shi B, et al. CDK1-dependent phosphorylation of EZH2 suppresses methylation of H3K27 and promotes osteogenic differentiation of human mesenchymal stem cells. Nature Cell Biology. 2010;13:87-94.

[116] Chen YH, Yeh FL, Yeh SP, Ma HT, Hung SC, Hung MC, et al. Myocyte Enhancer Factor-2 Interacting Transcriptional Repressor (MITR) Is a Switch That Promotes Osteogenesis and Inhibits Adipogenesis of Mesenchymal Stem Cells by Inactivating Peroxisome Proliferator-activated Receptor -2. Journal of Biological Chemistry. 2011;286:10671-80.

[117] Ye L, Fan Z, Yu B, Chang J, Al Hezaimi K, Zhou X, et al. Histone Demethylases KDM4B and KDM6B Promotes Osteogenic Differentiation of Human MSCs. Cell Stem Cell. 2012;11:50-61.

[118] Yang D, Okamura H, Nakashima Y, Haneji T. Histone Demethylase Jmjd3 Regulates Osteoblast Differentiation via Transcription Factors Runx2 and Osterix. Journal of Biological Chemistry. 2013;288:33530-41.

[119] Huszar JM, Payne CJ. MIR146A inhibits JMJD3 expression and osteogenic differentiation in human mesenchymal stem cells. FEBS Letters. 2014;588:1850-6.

[120] Xu J, Yu B, Hong C, Wang C-Y. KDM6B epigenetically regulates odontogenic differentiation of dental mesenchymal stem cells. International Journal of Oral Science. 2013;5:200-5.

[121] Yang D, Okamura H, Teramachi J, Haneji T. Histone Demethylase Utx Regulates Differentiation and Mineralization in Osteoblasts. Journal of cellular biochemistry. 2015.

[122] Zhang F, Xu L, Xu L, Xu Q, Li D, Yang Y, et al. JMJD3 promotes chondrocyte proliferation and hypertrophy during endochondral bone formation in mice. Journal of molecular cell biology. 2015;7:23-34.

[123] Santos-Rosa H, Schneider R, Bernstein BE, Karabetsou N, Morillon A, Weise C, et al. Methylation of histone H3K4 mediates association of the Isw1p ATPase with chromatin. Molecular Cell. 2003;12:1325-32.

[124] Musri MM, Corominola H, Casamitjana R, Gomis R, Parrizas M. Histone H3 lysine 4 dimethylation signals the transcriptional competence of the adiponectin promoter in preadipocytes. J Biol Chem. 2006;281:17180-8. Epub 2006 Apr 13.

[125] Cho YW, Hong T, Hong S, Guo H, Yu H, Kim D, et al. PTIP associates with MLL3- and MLL4-containing histone H3 lysine 4 methyltransferase complex. J Biol Chem. 2007;282:20395-406. Epub 2007 May 11.

[126] Hassan MQ, Tare R, Lee SH, Mandeville M, Weiner B, Montecino M, et al. HOXA10 Controls Osteoblastogenesis by Directly Activating Bone Regulatory and Phenotypic Genes. Molecular and Cellular Biology. 2007;27:3337-52.

[127] Ge W, Shi L, Zhou Y, Liu Y, Ma GE, Jiang Y, et al. Inhibition of osteogenic differentiation of human adipose-derived stromal cells by retinoblastoma binding protein 2 repression of RUNX2-activated transcription. Stem Cells. 2011;29:1112-25. doi: 10.002/stem.663.

[128] Sinha KM, Yasuda H, Coombes MM, Dent SY, de Crombrugghe B. Regulation of the osteoblast-specific transcription factor Osterix by NO66, a Jumonji family histone demethylase. Embo J. 2010;29:68-79. doi: 10.1038/emboj.2009.332. Epub Nov 19.

[129] Wang L, Jin Q, Lee JE, Su Ih, Ge K. Histone H3K27 methyltransferase Ezh2 represses Wnt genes to facilitate adipogenesis. Proceedings of the National Academy of Sciences. 2010;107:7317-22.

[130] Musri MM, Gomis R, Parrizas M. A chromatin perspective of adipogenesis. Organogenesis. 2010;6:15-23.

[131] Lee JE, Wang C, Xu S, Cho YW, Wang L, Feng X, et al. H3K4 mono- and di-methyltransferase MLL4 is required for enhancer activation during cell differentiation. Elife (Cambridge). 2013;2:e01503.:10.7554/eLife.01503.

[132] Lee J-E, Ge K. Transcriptional and epigenetic regulation of PPARγ expression during adipogenesis. Cell & Bioscience. 2014;4:29.

[133] Okamura M, Inagaki T, Tanaka T, Sakai J. Role of histone methylation and demethylation in adipogenesis and obesity. Organogenesis. 2010;6:24-32.

[134] Herlofsen SR, Bryne JC, Høiby T, Wang L, Issner R, Zhang X, et al. Genome-wide map of quantified epigenetic changes during in vitro chondrogenic differentiation of primary human mesenchymal stem cells. BMC genomics. 2013;14:105.

[135] Schwarz D, Varum S, Zemke M, Scholer A, Baggiolini A, Draganova K, et al. Ezh2 is required for neural crest-derived cartilage and bone formation. Development. 2014;141:867-77. doi: 10.1242/dev.094342.

[136] Gibson William T, Hood Rebecca L, Zhan Shing H, Bulman Dennis E, Fejes Anthony P, Moore R, et al. Mutations in EZH2 Cause Weaver Syndrome. American Journal of Human Genetics. 2012;90:110-8.

[137] O'Carroll D, Erhardt S, Pagani M, Barton SC, Surani MA, Jenuwein T. The Polycomb-Group Gene Ezh2 Is Required for Early Mouse Development. Molecular and Cellular Biology. 2001;21:4330-6.

[138] Wyngaarden LA, Delgado-Olguin P, Su IH, Bruneau BG, Hopyan S. Ezh2 regulates anteroposterior axis specification and proximodistal axis elongation in the developing limb. Development. 2011;138:3759-67. doi: 10.1242/dev.063180. Epub 2011 Jul 27.

[139] Banka S, Lederer D, Benoit V, Jenkins E, Howard E, Bunstone S, et al. Novel KDM6A (UTX) mutations and a clinical and molecular review of the X-linked Kabuki syndrome (KS2). Clin Genet. 2015;87:252-8.

[140] Thieme S, Gyárfás T, Richter C, Özhan G, Fu J, Alexopoulou D, et al. The histone demethylase UTX regulates stem cell migration and hematopoiesis. Blood. 2013;121:2462-73.

Chapter:2

EZH2 and KDM6A act as an epigenetic switch to regulate mesenchymal stem cell lineage specification

Chapter Summary:

The chapter is based on our initial profiling of histone methylation patterns of genes associated with differentiation and the expression of epigenetic modifying enzymes in MSC clonal populations by cDNA microarray analysis. Our initial studies on the function of EZH2 lineage commitment of human BMSC, suggests that EZH2 is a negative regulator of osteogenesis and a positive regulator of adipogenesis. However, the direct role of the H3K7me3 epigenetic modifiers EZH2 and KDM6A and or KDM6B in BMSC differentiation is unclear, illustrating the importance of determining the epigenetic signatures associated with differentiation and maintenance of MSC. We aim to address to investigate the function of human H3K27 methyltransferase EZH2 and demethylases KDM6A in MSC osteogenic and adipogenic differentiation *in vitro* and *in vivo*.

*Please note that Figure some data from figure 1, 2 and 3 were generated in honours. The subsequent figures 4-7 and manuscript generation were completed during my PhD candidature.

This chapter is published: Stem Cells. 2014 Mar;32(3):802-15. doi: 10.1002/stem.1573. **Hemming S, Cakouros D, Isenmann S, Cooper L, Menicanin D, Zannettino A, Gronthos S.** EZH2 and KDM6A act as an epigenetic switch to regulate mesenchymal stem cell lineage specification. Stem Cells. 2014 Mar;32(3):802-15. doi: 10.1002/stem.1573

Statement of Authorship

Title of Paper	EZH2 and KDM6A act as an Epigenetic switch to regulate Mesenchymal Stem Cell Lineage Specification
Publication Status	☑ Published ☐ Accepted for Publication ☐ Submitted for Publication ☐ Publication Style
Publication Details	Stem Cells. 2014 Mar; 32(3):802-15. doi: 10.1002/stem.1573. Hemming S, Cakouros D, Isenmann S, Cooper L, Menicanin D, Zannettino A, Gronthos S. EZH2 and KDM6A act as an epigenetic switch to regulate mesenchymal stem cell lineage specification.

Principal Author

Name of Principal Author (Candidate)	Sarah Elizabeth Hemming		
Contribution to the Paper	First Author Generation of data Manuscript preparation Analysis of data		
Overall percentage (%)	78%		
Signature		Date	26-11-2015

Co-Author Contributions

By signing the Statement of Authorship, each author certifies that:
the candidate's stated contribution to the publication is accurate (as detailed above);
permission is granted for the candidate in include the publication in the thesis; and
the sum of all co-author contributions is equal to 100% less the candidate's stated contribution.

Name of Co-Author	Dimitrios Cakouros		
Contribution to the Paper	Manuscript evaluation Data interpretation Supervised development of work Contribution to experimental design		
Overall percentage (%)	8%		
		Date	26/11/15

Name of Co-Author	Lachlan Cooper
Contribution to the Paper	Manuscript evaluation Data interpretation Statical analysis of data
Overall percentage (%)	2%
Signature	Date: 26/11/2015

Name of Co-Author	Danijela Menicanin
Contribution to the Paper	Manuscript evaluation Ectopic bone implants Histological analysis
Overall percentage (%)	2%
Signature	Date: 26-11-15

Name of Co-Author	Andrew Zannettino
Contribution to the Paper	Manuscript evaluation Data interpretation Equipment/Laboratory use
Overall percentage (%)	2%
Signature	Date: 26/11/15

Name of Co-Author	Stan Gronthos
Contribution to the Paper	Manuscript evaluation Data interpretation Supervised development of work Contribution to experimental design Funding
Overall percentage (%)	8%
Signature	Date: 26/11/15

2 EZH2 and KDM6A act as an Epigenetic switch to regulate Mesenchymal Stem Cell Lineage Specification

Sarah Hemming[1], Dimitrios Cakouros[1], Sandra Isenmann[1], Lachlan Cooper[1], Danijela Menicanin[1], Andrew Zannettino[2,3], Stan Gronthos[1,3]

1. Mesenchymal Stem Cell Laboratory, School of Medical Sciences, Faculty of Health Sciences, University of Adelaide, Adelaide, SA.

2. Myeloma Research Laboratory, School of Medical Sciences, Faculty of Health Sciences, University of Adelaide, Adelaide, SA.

3. Centre for Stem Cell Research, Robinson Institute, University of Adelaide, SA, Australia

Corresponding author

Prof. Stan Gronthos

Medical School South Level 4, School of Medical Sciences, Faculty of Health Sciences, University of Adelaide, Adelaide 5005, South Australia, Australia.

Phone: +61-8-82223460

Fax: +61-882223139

Email: stan.gronthos@adelaide.edu.au

Running Title: EZH2 and KDM6A regulate MSC differentiation

Key Words: Mesenchymal Stem cells, Adipocytes, Osteoblasts, Epigenetics, Epigenetic Modifier, Chromatin.

Hemming, S., Cakouros, D., Isenmann, S., Cooper, L., Menicanin, D., Zannettino, A. & Gronthos, S. (2014). EZH2 and KDM6A act as an epigenetic switch to regulate mesenchymal stem cell lineage specification.
Stem Cells, 32(3), 802-15.

NOTE:
This publication is included on pages 66 - 76 in the print copy of the thesis held in the University of Adelaide Library.

It is also available online to authorised users at:

http://dx.doi.org/10.1002/stem.1573

Chapter:3

Identification of novel EZH2 targets in mesenchymal stem/stromal cells which regulate osteogenesis

Chapter summary:

The results of chapter 2 identified the role of EZH2 in human BMSC lineage specification. EZH2 knockout or inhibition of H3K27me3 activity promotes osteogenesis whilst inhibiting osteogenesis. Conversely, EZH2 over-expression promotes adipogenesis and inhibits osteogenesis. Enhanced expression of KDM6A promotes osteogenic differentiation however, knockdown of KDM6A promotes adipogenic differentiation of BMSC. In BMSC EZH2 actively binds *RUNX2* and *OPN* preventing osteogenic differentiation. EZH2 and H3K27me3 removal from the promoters of *RUNX2* and *OPN* by KDM6A is critical for osteogenic lineage specification.

We identified the role of EZH2 in lineage specification however it is unclear if EZH2 regulates other genes involved in osteogenic differentiation. We hypothesis, that EZH2 represses key osteogenic drivers in mesenchymal stem cells and are removed during osteogenesis. This chapter aims to use a bioinformatics approach to identify known and novel regulators of osteogenesis targeted by EZH2 in human MSC.

Sarah Hemming, Dimitrios Cakouros, Kate Vandyke, Melissa Davis, Andrew Zannettino, Stan Gronthos. Identification of novel EZH2 targets in osteogenesis. Summited to the Journal of Biological Chemistry, November 2015.

Statement of Authorship

Title of Paper	Identification of novel EZH2 targets in mesenchymal stem/ stromal cells which regulate osteogenesis
Publication Status	☐ Published ☐ Accepted for Publication ☑ Submitted for Publication ☐ Publication Style
Publication Details	Sarah Hemming, Dimitrios Cakouros, Kate Vandyke, Melissa J. Davis, Andrew C.W. Zannettino, Stan Gronthos. Identification of novel EZH2 targets in mesenchymal stem/ stromal cells which regulate osteogenesis. Summited to Journal of Biological Chemistry.

Principal Author

Name of Principal Author (Candidate)	Sarah Elizabeth Hemming
Contribution to the Paper	First Author Generation of data Manuscript preparation Analysis of data
Overall percentage (%)	74%
Signature	Date: 26-11-15

Co-Author Contributions

By signing the Statement of Authorship, each author certifies that:
the candidate's stated contribution to the publication is accurate (as detailed above);
permission is granted for the candidate in include the publication in the thesis; and
the sum of all co-author contributions is equal to 100% less the candidate's stated contribution.

Name of Co-Author	Dimitrios Cakouros
Contribution to the Paper	Manuscript evaluation Data interpretation Supervised development of work Contribution to experimental design
Overall percentage (%)	7%
Signature	Date: 26/11/15

Name of Co-Author	Kate Vandyke
Contribution to the Paper	Manuscript evaluation Data interpretation Bioinformatics analysis Stastical analysis
Overall percentage (%)	5%
Signature	Date: 26/11/15

Name of Co-Author	Melissa Davis
Contribution to the Paper	Manuscript evaluation Data interpretation Bioinformatics analysis
Overall percentage (%)	5%
Signature	Date: 01/12/2015

Name of Co-Author	Andrew Zannettino
Contribution to the Paper	Manuscript evaluation Data interpretation Equipment/Laboratory use
Overall percentage (%)	2%
Signature	Date: 26/11/15

Name of Co-Author	Stan Gronthos
Contribution to the Paper	Manuscript evaluation Data interpretation Contribution to experimental design. Funding.
Overall percentage (%)	7%.
Signature	Date: 26/11/15

3 Identification of novel EZH2 targets in mesenchymal stem/stromal cells which regulate osteogenesis

Sarah Hemming1,2, Dimitrios Cakouros1,2, Kate Vandyke2,3,4, Melissa J. Davis5, Andrew C.W. Zannettino2,3, Stan Gronthos1,2,*

1Mesenchymal Stem Cell Laboratory, School of Medicine, Faculty of Health Sciences, University of Adelaide, Adelaide, SA, Australia.
2South Australian Health and Medical Research Institute, Adelaide, SA, Australia.
3Myeloma Research Laboratory, School of Medicine, Faculty of Health Sciences, The University of Adelaide, Adelaide, SA, Australia.
4SA Pathology, Adelaide, SA, Australia.
5Cancer Systems, Biology Systems and Computational Biology Laboratory, Melbourne School of Engineering, The University of Melbourne, VIC, Australia.

*Corresponding author
Prof. Stan Gronthos
School of Medicine, Faculty of Health Sciences, University of Adelaide, Adelaide 5005, South Australia, Australia.
Phone: (+61-8-8128 4395)
Fax: (+61-8-8313 5384)
Email: stan. gronthos@adelaide. edu. au

Running Title: Novel EZH2 targets in osteogenesis

Key Words: Enhancer of Zeste homolog two, EZH2, H3K27, H3K4, mesenchymal stem cells, MSC, epigenetics, osteogenesis, chromatin

3.1 Abstract

Histone three lysine twenty seven (H3K27) methyltransferase enhancer of zeste homolog two (EZH2) is a critical epigenetic modifier which regulates gene transcription through the trimethylation of the H3K27 residue leading to chromatin compaction and gene repression. EZH2 has previously been identified to regulate human bone marrow derived mesenchymal stem cells (MSC) lineage specification. MSC lineage specification is regulated by the presence of EZH2 and its H3K27me3 modification or the removal of the H3K27 modification by lysine demethylases 6A and 6B (KDM6A and KDM6B). This study uses a bioinformatics approach to identify novel genes regulated by EZH2 during MSC osteogenic differentiation. Here we have identified ZBTB16, MX1 and FHL1. MX1 and FHL1 are expressed at low levels in MSC and EZH2 together with H3K27me3 is present along the TSS of their respective promoters. During osteogenesis, these genes become actively expressed coinciding with the disappearance of EZH2 and H3K27me3 on the transcription start site of these genes and the enrichment of the active H3K4me3 modification. Over expression of EZH2 down regulated the expression of *ZBTB16*, *MX1* and *FHL1* during osteogenesis. Small interfering RNA (siRNA) targeting MX1 and FHL1 revealed these genes are important for osteogenic differentiation and lead to down regulation of key osteogenic transcription factor RUNX2 and its downstream targets osteopontin and osteocalcin. These findings highlight that EZH2 not only acts through the direct regulation of signalling modules and lineage specific transcription factors but targets many novel genes important for MSC lineage determination.

3.2 Introduction

Osteogenic differentiation of bone marrow mesenchymal stem/stromal cells (MSCs) (1,2) is associated with the repression of adipogenic differentiation (3-5). This reciprocal relationship between adipogenesis and osteogenesis is modulated by molecules such as Msx2, which promote osteogenesis and suppress adipogenesis (6,7). Conversely osteogenic differentiation can be inhibited by the activation of protein kinase A, which upregulates peroxisome proliferator-activated receptor gamma 2 (PPARγ2) in turn inhibits runt-related transcription factor 2 (RUNX2) and osteopontin (OP), promoting adipogenesis (8). RUNX2, a key lineage specific transcription factor, and signalling pathways molecules such as WNT and bone morphogenic protein (BMP) play a critical role in dictating MSC osteogenic differentiation (9-13).

Recent investigations have identified the epigenetic regulation of chromatin as a key mechanism in dictating lineage-specific differentiation of MSC. The structure of chromatin can be regulated through methylation, acetylation, phosphorylation, sumoylation and ubiquination of histone tails. Methyltransferases and demethylases are thought to be responsible for the switch between repressive H3K27 domains and active H3K4 domains. Given the diverse array of histone modifications, their various combinations form the “histone code” which can influence the recruitment of effector proteins and transcription factors to chromatin, determining the functional state of chromatin (14-16). The epigenetic modifier enhancer of zeste homolog two (EZH2) exists within a multi-subunit complex known as the

polycomb repressor complex 2 (PRC2), which contains suppressor of zeste-12 (SUZ12), yin yang 1 (YY1) and embryonic ectoderm development (EED) (17). EZH2 is a histone three lysine twenty seven (H3K27) methyltransferase that contains a carboxy-terminal catalytic SET domain responsible for the mono, di or tri methylation modification of H3K27 residues of histone tails (18). EZH2 H3K7 tri methylation (me3) modification facilitates the recruitment of the PRC1 during chromatin remodelling, compaction of chromatin and gene repression (19-21). During development, EZH2 is required for neural crest-derived cartilage and bone formation and anterior/posterior skeletal patterning in mice (22,23). In postnatal skeletal tissue, reports have identified EZH2 as having a role in regulating MSC lineage differentiation. EZH2 was found to promote adipogenesis by disrupting Wnt/β-catenin signaling through the direct repression of pro-osteogenic *Wnt* genes *Wnt1*, *-6*, *-10a*, and *-10b* in mouse peripheral pre-adipocytes (24). More recently, enforced expression of EZH2 in human bone marrow derived MSC promoted adipogenesis *in vitro* and inhibited osteogenic differentiation potential *in vitro* and *in vivo* (25). Conversely, inhibition of EZH2 enzymatic activity and knockdown of EZH2 gene expression inhibited adipogenesis and promoted osteogenic differentiation by MSC (25). Regulation of EZH2 has been reported to be regulated via phosphorylation at Thr 487 by cyclin dependent kinase 1 (CDK1). CDK1 phosphorylation suppresses EZH2 activity, promoting MSC osteoblast differentiation *in vitro* (26). Chromatin immunoprecipitation (ChIP) analysis has revealed that the presence of EZH2 and its H3K27me3 associated modification are reduced at the transcription start site (TSS) of key osteogenic transcription factor *RUNX2* during osteogenic differentiation (25,26). However, it is still unclear whether EZH2 directly targets other critical genes and pathways during MSC osteogenic differentiation. The present study aimed to identify novel EZH2 targets in osteogenesis through a bioinformatics approach using publically available ChIP-on-chip, ChIP-Seq and microarray data sets.

3.3 Experimental procedures

Bioinformatic analysis

Bioinformatic analysis was performed to assess gene expression and EZH2 occupancy and H3K27 and H3K4 methylation in three independent datasets which compared primary cultured human bone marrow derived MSC versus *in vitro* differentiated osteoblasts (OB) differentiated with dexamethasone 100nM (Dex) and 10mM β-glycerophosphate and with the addition of 50 µg/ml ascorbic acid for 28 days (GSE9451 (27); (26)) or 50 nM ascorbic acid for 16 days (GSE27900 (28)). GSE951 data set contained three independent MSC lines. These MSC lines were differentiated under osteogenic inductive conditions to generate paired osteoblasts for microarray analysis.

ChIP data sets: ChIP-on-chip data for genes bound by EZH2 in undifferentiated MSC and not bound by EZH2 in OB were obtained from Wei et al. (26). H3K27me3 and H3K4me3 ChIP-Seq data were obtained from GEO (Gene Expression Omnibus, http://www.ncbi.nlm.nih.gov.geo/, NCBI; data set GSE35573) (28). A list of all genes identified in either of these studies was generated to generate a results profile for each gene. Datasets were parsed and reformatted using a set of custom Perl Scripts. Gene annotation was retrieved from the Gene Ontology Database (www.geneontology.org).

Microarray data sets: In order to assess the differential expression of the genes

identified in the ChIP datasets, two datasets were used, both conducted on Affymetrix GeneChip Human Genome U133 plus 2.0 arrays. Microarray (Affymetrix U133A) GEO dataset GSE9451 (27) were normalised using RMA (RMA Express program http://rmaexpress.bmbolstad.com/). For GSE9451, raw microarray data (.CEL files) were downloaded from ArrayExpress (EMBL-EBI) and were normalised by RMA using the bioconductor package (affy) (29) and R (version 3.03) and $\log_2$ transformed. Genes which were not expressed (signal < $\log_2 100$) in either MSC or OB were excluded from further analysis. Initially, expression of the genes identified differentially expressed genes (adjusted p-value ≤ 0.05) were identified using linear models for microarray data (LIMMA (30-32)) in MultiExperiment Viewer (MeV (33)). Initially, genes that were significantly > 2-fold up or down regulated with OB differentiation in GSE9451 were identified.

Isolation and culture of mesenchymal stem cells (MSCs)

Bone-marrow aspirates were isolated from the posterior iliac crest of healthy human adult donors, following informed consent (SA Pathology normal bone marrow donor program, Royal Adelaide Hospital Human Ethics Number 940911a). MSC were isolated and cultured using plastic adherence (34). Culture media: Alpha modified Eagle's medium (α-MEM) (Sigma Aldrich Inc., St Louis, MO, USA, http://www.sigmaaldrich.com/safc.html) supplemented with 10% (v/v) foetal calf serum (FSC) (SAFC Biosciences, Melbourne, VIC, AUS, http://www.sigmaaldrich.com/safc.html), 50U/mL, 5µg/mL penicillin, streptomycin (Sigma Aldrich Inc. ,Louis, MO, USA,http://www.sigmaaldrich.com/safc.html), 1mM sodium pyruvate (Sigma Aldrich Inc. , St Louis, MO, http://www.sigmaaldrich.com/safc.html), 100µM L-ascorbic acid (Wako Pure Chemical industries, Richmond, VA, USA), 2mM L-glutamine (JRH Biosciences/Sigma, Lenexa, KS, USA, http://www.sigmaaldrich.com/safc.html) and 10mM HEPES (Sigma Aldrich Inc., Louis, MO, USA http://www.sigmaaldrich.com/safc.html), and cultured at 37oC, >90% humidity and 5% CO2. Osteogenic differentiation media: α-MEM supplemented with 10% (v/v) FCS, 2mM L-Glutamine, 1mM sodium pyruvate, 10mM HEPES buffer and 50U/mL penicillin-streptomycin, 100µM L-ascorbic acid, 0.1µM dexamethasone and 2.6mM potassium di-hydrogen phosphate (KH2PO4) (34).

Retroviral transduction over-expression

The human *EZH2* coding region of the gene was ligated into pRUF-IRES-GFP retroviral vector using PCR primers to amplify the coding region with Xho1 restriction sites (25). The pRUF-IRES-GFP-*EZH2* construct was transfected into the HEK293T viral packaging cell line together with PGP and VSVG (viral envelope proteins, SBI System Biosciences, Mountain View, CA, USA, https://www.systembio.com/) and viral supernatant was used for infection of MSCs and sorted by fluorescence-activated cell sorting (FACS: Beckman Coulter Epics Ultra cell sorter, Lane Cove, NSW, AUS, https://www.beckmancoulter.com/). MSC were passaged and at passage 5 were seeded for osteogenic differentiation assays and RNA assays.

siRNA transfection

Passage 5 MSC were seeded in either 24 well plates (1.9cm^2) at 3x10^4 or 96 well plates (0. 32cm^2) at 3x10^3 cells per well. Early the next day, MSC were treated with 12 pmol siRNA (Life Technologies, Scoresby VIC, AUS). Negative control siRNA (4390843), EZH2 #1 (s4916), EZH2 #2 (s4918), FHL1 #1 (n261445)

FHL1 #2 (n261446), MX1 #1 (s9100) and MX1 #2 (s9099) siRNAs with Lipofectamine RNAi MAX were used for this study (Invitrogen/Life Technologies, Scoresby VIC, AUS, http://www.thermofisher.com.au/). siRNA were added to cells as specified by the manufacturer. Seventy two hours post transfection, media were removed and either culture growth media or osteogenic inductive media were added (25).

***In vitro* osteogenic differentiation assay**

siRNA- treated MSC in 96 well plates were cultured in either non inductive culture media or osteogenic inductive media for 14 days with media changes twice weekly. Mineral formation by human MSCs under osteogenic differentiation was identified by 1% alizarin red (PH 4. 3) (Sigma Aldrich Inc, St Louis, MO, USA) staining of hydroxyapatite deposits. Extracellular calcium levels were assessed by Calcium Arsenazo III assay (Thermo Scientific/ Life technologies, Scoreby, VIC, AUS, http://www.thermofisher.com.au/) in replicate samples and normalised to DNA content per well by pico-green incorporation (Life technologies, Scoreby, VIC, AUS).

Real-Time Polymerase Chain Reaction Analysis

Culture expanded MSCs infected with pRUF-IRES-GFP and pRUF-IRES-GFP-*EZH2* were seeded at $5.64x10^4$ per/well in 6 well plates in the presence of either non-inductive or osteogenic inductive media as previously described (25). siRNA-treated MSC were cultured in the presence of non-inductive or osteogenic inductive media in 24 well plates. Total RNA was extracted using TRIzol reagent (Invitrogen/Life Technologies, Scoresby VIC, AUS, http://www.thermofisher.com.au/) and converted to cDNA by reverse transcription. Gene expression was assessed by real-time polymerase chain reaction (RT-PCR) amplification using specific primer sets (Table 1), SYBR Green/Rox PCR master mix (Qiagen, Doncaster, Chadstone Centre, VIC, Australia, http://www.qiagen.com/) and Rotor-Gene 6000 Real-Time Thermal Cycler (Corbett Research, Mortlake, NSW, Australia, http://www.corbettlifescience.com/). Changes in gene expression were calculated relative to β-actin using the 2-dCT method (25,35).

ChIP analysis

Passage 5 MSC were seeded at $2x10^6$ cells per flask (75 cm^2) and induced under normal growth medium and or osteogenic differentiation media for 14 days. ChIP was adapted from the Abcam (Abcam, Melbourne, VIC, AUS, http://www.abcam.com/) cross-linking chromatin immunoprecipitation (X-ChIP) protocol. Briefly, chromatin was cross-linked with final of 0.75% formaldehyde Adherent cells were detached using 1x trypsin EDTA and remaining cells were scraped from the bottom of the flask. Cells was lysed with 400µl of FA lysis buffer (50mM HEPES KOH pH7.5, 140mM NaCl,1mM EDTA pH8,1%triton x-100,0.1% Sodium deoxycholate, 0.1% SDS and protease inhibitors). DNA was sheared with probe sonication on ice. Sonicated sample were used for immunoprecipitation (36).

Immunoprecipitation

Antibodies against anti-rabbit H3K27me3 (1 µg, Merck, Millipore 07-449, Bayswater, VIC, AUS, http://www.merck.com.au/), anti-human EZH2 mouse monoclonal (1 µg, Millipore AC22 17-662), anti–human H3K4me3 rabbit polyclonal (1 µg, Abcam ab8580-100) and anti-human IgG rabbit polyclonal control (1 µg Millipore, Bayswater, VIC, AUS) were used for immunoprecipitation. Immunoselected genomic DNA was used for real time PCR (RT-PCR) using primers targeting

the promoters of genes of interest (Table 2) as previously described (37).

Statistical Analysis

Statistical analysis was carried out GraphPad Prism 6 (GraphPad Software, La Jolla, CA, http://www.graphpad.com/). One-way ANOVA with Dunnett's multiple comparison test were used to assess statistical significance for siRNA and BrdU assays. Two-way ANOVA with Sidak's multiple comparison test were used for ChIP and EZH2 over expression studies. (*) denotes statistical significance at p value ≤ 0.05.

3.4 Results

Identification of novel EZH2 targets during MSC osteogenic differentiation.

Initially, we examined three independent datasets in order to identify novel genes that may be switched on during osteogenic differentiation by removal of EZH2 binding and its associated H3K27me3 mark. We identified 99 genes that were reported to be bound by EZH2 in MSC but not following osteogenic differentiated *in vitro* (26) and were found to have a loss of the repressive modification H3K27me3 during osteogenic differentiation of MSCs in the independent ChIP-Seq data set GSE35576 (28).

Assessment of differential gene expression in the independent microarray dataset GSE9451 (27) identified that, of these 99 genes, 6 genes (*ZBTB16, HOPX, ROR2, MYADM, FHL1, MX1*) were significantly upregulated (> 2-fold change; $p \leq 0.05$, LIMMA), while no genes were significantly downregulated, under osteogenic differentiation when compared with undifferentiated MSC (Figure 1). Of these, two (*ZBTB16, FHL1*) gained the activating modification H3K4me3 under osteogenic differentiation, one gene lost the H3K4me3 mark in OB (*HOPX*), one gene (*MYADM*) had the H3K4me3 mark in both MSC and OB and two genes (*MX1, ROR2*) did not have the H3K4me3 mark in either MSC or OB (Table 3). These findings suggest that *ZBTB16, HOPX, ROR2, MYADM, FHL1* and *MX1* are potential EZH2 targets that may play a role in regulating osteogenic cell fate determination. Three of these genes were selected for subsequent validation studies.

EZH2 directly represses ZBTB16, MX1 and FHL1 gene expression in undifferentiated MSC.

In order to confirm the bioinformatics analysis, manual ChIP analysis was performed for three of the identified genes using anti-EZH2, -H3K27me3, -H3K4me3 or IgG control antibodies on genomic DNA isolated from human MSC cultured under normal growth conditions or in osteogenic inductive media. Primers targeting the TSS of *ZBTB16, MX1* and *FHL1* were used to assess the presence of epigenetic modifying enzymes and modifications. *P16* was used as the positive control and *GAPDH* was used as the negative control for the EZH2 and H3K27me3 ChIP analysis (Supplementary Figure 1A&B). *GAPDH* was used as the positive control and the *IL2* was used as the negative control for the H3K4me3 ChIP (Supplementary Figure 1C).

The TSS of *ZBTB16, MX1* and *FHL1* were significantly enriched for EZH2 binding in undifferentiated MSC compared with MSC cultured under osteogenic conditions (Figure 2A). This correlated to a significant enrichment of the gene silencing mark H3K27me3 at the TSS of *ZBTB16, MX1* and *FHL1* in undifferentiated MSC compared with OB (Figure 2B). In contrast, the active mark H3K4me3 was present at the TSS of all genes in OB correlating with an increase in gene expression during osteogenesis

(Figure 1). Importantly, EZH2 and the H3K27me3 modification were no longer present at the TSS of *ZBTB16*, *MX1* and *FHL1* during osteogenesis.

We have previously reported that EZH2 inhibits human MSC osteogenic differentiation in vitro and in vivo (25). In the present study, the role of EZH2 in regulating *ZBTB16*, *MX1* and *FHL1* gene expression was confirmed using stably transduced EZH2 over-expressing MSC lines and vector control MSC (Figure 3A), cultured under normal growth conditions or osteogenic inductive conditions. *EZH2* over-expressing MSC were found to exhibit significantly lower expression levels of the osteogenic master regulatory factor *RUNX2* during osteogenic differentiation when compared with vector control MSC lines (Figure 3A&B). Furthermore, *EZH2* over-expressing MSC demonstrated repressed gene expression levels of *ZBTB16*, *MX1* and *FHL1* following osteogenic induction, when compared with vector control MSC (Figure 3C).

In parallel studies, two independent siRNA were used to knockdown gene expression of *EZH2* in MSC cultured under osteogenic inductive conditions (Figure 4A). Knockdown of EZH2 in MSC increased expression of *RUNX2* (Figure 4B), and significantly increased the expression of *ZBTB16*, *MX1* and *FHL1* compared with MSC treated with scramble control siRNA (Figure 4C).

Collectively, these studies showed that *ZBTB16*, *MX1* and *FHL1* are direct targets of EZH2 binding and activity in undifferentiated MSC leading to suppression of gene expression. However, during osteogenic lineage commitment, *ZBTB16*, *MX1* and *FHL1* expression is induced due to the loss of both EZH2 binding and H3K27me3, correlating with the appearance of the H3K4me3 modification.

Targeted knockdown of MX1 and FHL1 inhibits MSC osteogenic differentiation.

ZBTB16 has previously been implicated in regulating osteogenesis in human MSC by acting upstream of *RUNX2* to promote osteogenic differentiation and the expression of key osteogenic differentiation genes (38,39). However, the direct role of MX1 and FHL1 in regulating MSC osteogenic differentiation is not as well defined. Two independent siRNA targeting different regions of MX1 or FHL1 were used to assess the role of these proteins in MSC osteogenic differentiation following transient knockdown (Figure 5A). Functionally, siRNA knockdown of MX1 or FHL1 reduced alizarin red positive mineralized deposits (Figure 5B) and reduced of extracellular calcium (Figure 5C) compared with scramble control siRNA treated MSC. RT-PCR-analysis of MX1 and FHL1 siRNA treated MSC revealed significantly reduced expression of *RUNX2*, and the mature bone associated markers, osteopontin (*OP*) and osteocalcin (*OC*) compared with control MSC, following osteogenic induction.

We next assessed the proliferation rates of MX1 and FHL-1 siRNA-treated MSC by BrdU incorporation. After 6 days of culture there were no significant differences in the proliferation rates between siRNA scramble control-treated MSC compared with MX1 or FHL1 siRNA-treated MSC (Figure 6). These data demonstrate that MX1 and FHL1 play an important role in promoting MSC osteogenic differentiation, similar to that described for ZBTB16.

3.5 Discussion

Our previous work has shown that the histone H3K27 methyltransferase EZH2 is an essential epigenetic modifying enzyme

involved in inhibiting osteogenesis (25) and is recruited to the p16/Ink4A locus in response to the bHLH transcription factor Twist-1 to repress senescence (40). Although we have illustrated that EZH2 can bind to some key osteogenic gene promoters to repress their expression, we have a limited knowledge in regards to what the targets of EZH2 are and how they are involved in inhibiting osteogenesis. To identify novel EZH2 targets that are involved in human MSC osteogenic lineage specification, we conducted a bioinformatics survey of publically available databases to identify putative EZH2 target genes suppressed in undifferentiated human bone marrow derived MSC and subsequently activated following osteogenic differentiation. The present study revealed that EZH2 directly regulated the pro-osteogenic genes *ZBTB16*, *MX1* and *FHL-1* in human bone marrow derived MSC via H3K27me3. Upon MSC osteogenic differentiation, EZH2 and H3K27me3 were removed from the promoters of these genes, correlating with the appearance of the epigenetic activation mark H3K4me3. This is in agreement with our recent studies which identified EZH2 as a suppressor of MSC osteogenic differentiation, through the regulation of key osteogenic genes, *RUNX2*, *OP* and *OC* (25). Supportive studies demonstrated that inhibition of EZH2 methyltransferase activity following treatment with DZNep, or deactivation of EZH2 through phosphorylation of Thr 487 by cyclin dependent kinase 1, resulted in the promotion of osteogenesis (25,26). Furthermore, EZH2 has been reported to regulate the β-catenin signalling pathway by targeting Wnt genes *Wnt1*, *-6*, *-10a*, and *-10b* in mouse peripheral pre-adipocytes and MSC to stimulate adipogenesis over osteogenesis (24). As these *Wnt* genes are involved in the induction of *RUNX2* and downstream osteogenic genes, their inhibition by recruitment of EZH2 to the promoter inhibits osteogenesis. Therefore, EZH2 acts to repress osteogenesis at multiple levels by directly inhibiting WNT genes, key osteogenic transcription factor RUNX2 and its downstream targets such as OP and OC, while allowing adipogenic differentiation to occur. Collectively these findings support the notion that EZH2 is a key regulator of MSC cell fate determination by selective repression of osteogenic inductive pathways.

The validity of the bioinformatics approach used here was shown by the identification of the putative EZH2 target ZBTB16, a promyelotic leukaemia zinc finger (PLZF) transcription factor. ZBTB16 is a negative regulator of cell division in embryogenesis and controls skeletal patterning through repression of HOX, BMP and Sonic Hedge Hog (Shh) expression. Deletion of *ZBTB16* in mice leads to severe skeletal deformities due to impaired limb and axial skeleton patterning leading to transformation of anterior skeletal elements into posterior structures (41-43). ZBTB16 is required for stylopod and zeugopod formation during early stages of limb development, before the initiation of cartilage condensation (44).

ZBTB16 has been found to either be deleted or mutated in patients exhibiting bone deformities. A 12-year-old male patient with skeletal defects including hypoplasia of radius and ulna, short stature, mental retardation, delayed bone age and mild facial dysmorphism was identified with a ~8 Mbp interstitial deletion in the 11q23 chromosomal region, which includes the *ZBTB16* gene. This patient also revealed a recessive missense mutation (c. 1849ARG) within the remaining *ZBTB16* allele (45,46). This study indicated that ZBTB16 may play a critical role in the development of the skeleton and bone aging. Furthermore, Ikeda et al. (2005) found *ZBTB16* was one of 24 genes upregulated during osteoblastic differentiation of OPLL cells

(39). ZBTB16 has been reported to regulate mesenchymal osteogenic and chondrogenic differentiation, acting upstream of the master transcription factors *RUNX2* and *SOX9*, respectively, in mesenchymal progenitor cell line C3H10T1/2 (47). Overexpression of ZBTB16 in C3H10T1/2 MSC line promoted osteogenic and chondrogenic differentiation whilst inhibiting adipogenic differentiation, Furthermore, these ZBTB16 over expressing C3H10T1/2 MSC readily formed bone and cartilage when implanted into an intratibial osteochondral defect model (47). Small interfering RNA knockdown of ZBTB16 in human and mouse MSC reduced osteogenic differentiation and expression of collagen 1A1 (*COL1A1*), alkaline phosphatase (*ALPL*), *RUNX2* and *OC*. Furthermore, overexpression of Zbtb16 in a murine MSC line increased Runx2 and Col1A expression during osteogenic differentiation (39). Collectively, these studies and this current study have identified ZBTB16 as a regulator of osteogenic differentiation.

Mechanistically, ZBTB16 can act through its localisation within nuclear bodies and plays a role in transcriptional activation or repression by regulating chromatin modifications and remodelling (48). ZBTB16 can act as a transcriptional repressor through the recruitment of nuclear corepressors SMRT, N-COR, SIN-3 and class 1 and class 2 histone deacetylases to the transcriptional complex (48-54). ZBTB16 mediates transcriptional repression of HoxD gene expression through chromatin remodelling through long range DNA looping and interactions with polycomb protein Bmi-1 on DNA (48). This study identified EZH2 actively binds ZBTB16 transcriptional start site and this coincides with the presence of H3K27me3 and low *ZBTB16* gene expression. However, during osteogenic differentiation EZH2 and its H3K27me3 modification is removed from the TSS followed by the addition of H3K4me3 and significant activation of *ZBTB16*. In the current study, we have demonstrated, for the first time, that over-expression of EZH2 in MSC, and thereby inhibiting osteogenic differentiation (25), was associated with reduced expression of *ZBTB16*. Conversely, siRNA mediated knockdown of EZH2 promoted osteogenic differentiation (25) and promoted expression of ZBTB16. However, this study is the first to identify ZBTB16 as an EZH2 target in human mesenchymal stem cells.

In the present study, MX1, another known regulator of osteogenesis, was identified as a putative EZH2 target. The *MX1* gene encodes a guanosine triphosphate (GTP)-metabolizing protein that participates in the cellular antiviral response, where it is induced by type I and type II interferons and antagonizes the replication process of several different RNA and DNA viruses (55,56). *In vivo* lineage tracing studies, using Mx1-Cre mice crossed with Rosa-YFP reporter mice, revealed that MX1 positive cells were predominantly osteolineage restricted with a small number of adipocytes found to have originated from MX1 positive cells during normal development and or bone fracture healing (57). While the MX1-positive cell population exhibited tri-lineage potential, differentiating into adipocytes, osteoblast and chrondrocytes *in vitro*, MX1 positive cells did not contribute to chrondrogenesis *in vivo* (57). These findings suggest a distinct role of MX1 in murine osteogenic differentiation; however, the role of MX1 in human osteogenic differentiation is not as well defined. The present study demonstrated that siRNA-mediated suppression of MX1 expression decreased osteogenic differentiation of human MSC in vitro. These findings are supported by microarray studies which have identified MX1 as being differentially upregulated in transformed bone-forming human stromal cell lines versus non-bone-forming stromal cell lines (58).

Furthermore, our data suggest that EZH2-mediated repression of MX1 expression in MSC may result in an inhibition of osteogenic differentiation, where removal of EZH2 and subsequent H3K27me3 at the TSS of *MX1* is critical for promotion of osteogenic lineage differentiation.

Another gene which was identified as a potential EZH2 target was four-and-a-half LIM domains 1 (FHL1), which encodes a member of the four-and-a-half-LIM-only protein family. FHL1 contains two conserved zinc finger domains with four highly conserved cytosine binding zinc atoms in each zinc finger. FHL-1 contains a TCF/LEF binding site which can be stimulated by β-catenin or Wnt pathway agonist lithium chloride (LiCl) inducing muscle hypertrophy and repressing chondrogenesis. (59,60). In support of our results, a recently study (61) identified that over-expression of FHL1 in murine MC3T3-E1 cells promotes osteogenesis. Transfection of Wnt3a or treatment with estrogen in MC3T3-E1 cells significantly increase *FHL1* expression and osteogenic differentiation. Over-expression of FHL1 increased alizarin red staining and extra-cellular calcium which was associated with increased expression of osteogenic genes *RUNX2*, *OP* and *OC*. Treatment with shRNAs targeting FHLl inhibited osteogenic differentiation of MC3T3-E1 cells compared to scramble control. These studies identify the role of FHL-1 in regulating muscle, chondrogenic and osteogenic lineage specification. Our study identified that FHL1 is upregulated in human OB (Figure 1B) and that knockdown of FHL1 by siRNA repressed osteogenic differentiation (Figure 3B) as previously described in murine MC3T3-E1 cells. Furthermore, this is the first study to identify FHL1 as a novel EZH2 target during osteogenesis. EZH2 may act to repress FHL1 in MSC, preventing osteogenic lineage specification, suggesting that removal of EZH2 and hence H3K27me3 is critical for osteogenic differentiation.

Through bioinformatics analysis of publically available ChIP-on-chip, ChIP-Seq and microarray data sets, we identified three novel EZH2 targets that may play a role in the suppression of osteogenesis by EZH2. With the use of over-expression studies, we verified that EZH2 directly inhibits *ZBTB16*, *MX1* and *FHL1* expression in MSC. Furthermore, siRNA knockdown of EZH2 in OB promoted the expression of *ZBTB16*, *MX1* and *FHL1*. Knockdown studies using siRNA targeting MX1 and FHL-1 identified that MX1 and FHL-1 are critical for human MSC osteogenic differentiation and for the expression of key osteogenic transcription factor RUNX2 and its downstream targets. These findings suggest that EZH2 mediated H3K27me3 of ZBTB16, MX1 and FHL1 in MSC prevent osteogenic differentiation, keeping the MSC in a more undifferentiated state. Furthermore, EZH2 doesn't only act on these genes identified in this study but regulation of RUNX2 and WNT genes are critical for the lineage specification (24-26). Recent studies from our laboratory, and others, have identified the role of the histone H3 lysine 27 demethylase KDM6A and KDM6B in regulating MSC osteogenic differentiation (25,62). We predict that these demethylase together or individually may be responsible for the removal of H3K27me3 from the TSS of ZBTB16, MX1 and FHL-1 during MSC to osteogenic lineage commitment. Furthermore as we know KDM6A and KDM6B often associate with the H3K4 methyltransferases we suggest that the recruitment of these demethylases to the TSS of these genes are critical for the removal of H3K27me3 and the subsequent addition of H3K4me3 modification. Further studies are needed to fully identify the mechanism involved in H3K27me3 removal and the addition of H3K4me3 on these key osteogenic genes. Furthermore it is still unclear how and

why is EZH2 recruited to the promoters ZBTB16, MX1 and MX1 and what factors and or signalling pathways are critical for the specific removal of EZH2 from these genes. Studies have identified EZH2 as an important regulator of the HOX genes during skeletal development and neural crest derived cartilage and bone in mice (22,23). Therefore, we predict that EZH2 may directly regulate ZBTB16, MX1 and FHL1 during murine and human skeletal development.

3.6 Acknowledgments

Funding National Health and Medical Research project grant APP1046053. KV was supported by a Mary Overton Early Career Research Fellowship (Royal Adelaide Hospital).

3.7 Conflict of Interest

The authors declare that they have no conflicts of interest with the contents of this article.

3.8 Author Contributions

SH study conception and design, acquisition of data Figures 1-6, analysis and interpretation of data, drafting the article.
DC study conception and design, acquisition of data Figures 1-6, data analysis and interpretation of data, drafting the article.
KV bioinformatics analysis and interpretation of data, drafting the article.
MD bioinformative analysis and interpretation of data, drafting the article.
ACWZ revising article critically for important intellectual content.
SG study conception and design, data analysis and interpretation of data, drafting the article, revising it critically for important intellectual content.
All authors approved the final version of the manuscript.

3.9 References

1. Pittenger, M. F., Mackay, A. M., Beck, S. C., Jaiswal, R. K., Douglas, R., Mosca, J. D., Moorman, M. A., Simonetti, D. W., Craig, S., and Marshak, D. R. (1999) Multilineage potential of adult human mesenchymal stem cells. *Science* **284**, 143-147
2. Gronthos, S., Zannettino, A. C. W., Hay, S. J., Shi, S. T., Graves, S. E., Kortesidis, A., and Simmons, P. J. (2003) Molecular and cellular characterisation of highly purified stromal stem cells derived from human bone marrow. *Journal of Cell Science* **116**, 1827-1835
3. Chou, R. H., Yu, Y. L., and Hung, M. C. (2011) The roles of EZH2 in cell lineage commitment. *American journal of translational research* **3**, 243-250
4. James, A. W., Pang, S., Askarinam, A., Corselli, M., Zara, J. N., Goyal, R., Chang, L., Pan, A., Shen, J., Yuan, W., Stoker, D., Zhang, X., Adams, J. S., Ting, K., and Soo, C. (2012) Additive effects of sonic hedgehog and Nell-1 signaling in osteogenic versus adipogenic differentiation of human adipose-derived stromal cells. *Stem cells and development* **21**, 2170-2178
5. Pei, L., and Tontonoz, P. (2004) Fat's loss is bone's gain. *The Journal of clinical investigation* **113**, 805-806
6. Cheng, S. L., Shao, J. S., Charlton-Kachigian, N., Loewy, A. P., and Towler, D. A. (2003) MSX2 promotes osteogenesis and suppresses adipogenic differentiation of multipotent mesenchymal progenitors. *The Journal of biological chemistry* **278**, 45969-45977
7. Barnes, G. L., Javed, A., Waller, S. M., Kamal, M. H., Hebert, K. E., Hassan, M. Q., Bellahcene, A., Van Wijnen, A. J., Young, M. F., Lian, J. B., Stein, G. S., and Gerstenfeld, L. C. (2003) Osteoblast-related transcription factors Runx2 (Cbfa1/AML3) and MSX2 mediate the expression of bone sialoprotein in human metastatic breast cancer cells. *Cancer Res* **63**, 2631-2637
8. Yang, D. C., Tsay, H. J., Lin, S. Y., Chiou, S. H., Li, M. J., Chang, T. J., and Hung, S. C. (2008) cAMP/PKA regulates osteogenesis, adipogenesis and ratio of RANKL/OPG mRNA expression in mesenchymal stem cells by suppressing leptin. *PloS one* **3**, e1540
9. D'Alimonte, I., Lannutti, A., Pipino, C., Di Tomo, P., Pierdomenico, L., Cianci, E., Antonucci, I., Marchisio, M., Romano, M., Stuppia, L., Caciagli, F., Pandolfi, A., and Ciccarelli, R. (2013) Wnt signaling behaves as a "master regulator" in the osteogenic and adipogenic commitment of human amniotic fluid mesenchymal stem cells. *Stem cell reviews* **9**, 642-654
10. Taipaleenmaki, H., Abdallah, B. M., AlDahmash, A., Saamanen, A. M., and Kassem, M. (2011) Wnt signalling mediates the cross-talk between bone marrow derived pre-adipocytic and pre-osteoblastic cell populations. *Experimental cell research* **317**, 745-756
11. Jung, R. E., Windisch, S. I., Eggenschwiler, A. M., Thoma, D. S., Weber, F. E., and Hammerle, C. H. (2009) A randomized-controlled clinical trial evaluating clinical and radiological outcomes after 3 and 5 years of dental implants placed in bone regenerated by means of GBR techniques with or without the addition of BMP-2. *Clinical oral implants research* **20**, 660-666
12. Bessa, P. C., Casal, M., and Reis, R. L. (2008) Bone morphogenetic proteins in tissue engineering: the road from laboratory to clinic, part II (BMP delivery). *Journal of tissue engineering and regenerative medicine* **2**, 81-96

13. Kugimiya, F., Kawaguchi, H., Kamekura, S., Chikuda, H., Ohba, S., Yano, F., Ogata, N., Katagiri, T., Harada, Y., Azuma, Y., Nakamura, K., and Chung, U. G. (2005) Involvement of endogenous bone morphogenetic protein (BMP)2 and BMP6 in bone formation. *Journal of Biological Chemistry* **280**, 35704-35712
14. Bernstein, B. E., Humphrey, E. L., Erlich, R. L., Schneider, R., Bouman, P., Liu, J. S., Kouzarides, T., and Schreiber, S. L. (2002) Methylation of histone H3 Lys 4 in coding regions of active genes. *Proceedings of the National Academy of Sciences of the United States of America* **99**, 8695-8700
15. Cao, R., Wang, L., Wang, H., Xia, L., Erdjument-Bromage, H., Tempst, P., Jones, R. S., and Zhang, Y. (2002) Role of histone H3 lysine 27 methylation in Polycomb-group silencing. *Science* **298**, 1039-1043
16. Taverna, S. D., Li, H., Ruthenburg, A. J., Allis, C. D., and Patel, D. J. (2007) How chromatin-binding modules interpret histone modifications: lessons from professional pocket pickers. *Nat Struct Mol Biol* **14**, 1025-1040
17. Sparmann, A., and van Lohuizen, M. (2006) Polycomb silencers control cell fate, development and cancer. *Nature reviews. Cancer* **6**, 846-856
18. Vire, E., Brenner, C., Deplus, R., Blanchon, L., Fraga, M., Didelot, C., Morey, L., Van Eynde, A., Bernard, D., Vanderwinden, J. M., Bollen, M., Esteller, M., Di Croce, L., de Launoit, Y., and Fuks, F. (2006) The Polycomb group protein EZH2 directly controls DNA methylation. *Nature* **439**, 871-874
19. Francis, N. J., Kingston, R. E., and Woodcock, C. L. (2004) Chromatin compaction by a polycomb group protein complex. *Science* **306**, 1574-1577
20. Ringrose, L., Ehret, H., and Paro, R. (2004) Distinct contributions of histone H3 lysine 9 and 27 methylation to locus-specific stability of polycomb complexes. *Molecular cell* **16**, 641-653
21. Ringrose, L., and Paro, R. (2004) Epigenetic regulation of cellular memory by the polycomb and trithorax group proteins. *Annual Review of Genetics* **38**, 413-443
22. Schwarz, D., Varum, S., Zemke, M., Scholer, A., Baggiolini, A., Draganova, K., Koseki, H., Schubeler, D., and Sommer, L. (2014) Ezh2 is required for neural crest-derived cartilage and bone formation. *Development (Cambridge, England)* **141**, 867-877
23. Wyngaarden, L. A., Delgado-Olguin, P., Su, I. H., Bruneau, B. G., and Hopyan, S. (2011) Ezh2 regulates anteroposterior axis specification and proximodistal axis elongation in the developing limb. *Development (Cambridge, England)* **138**, 3759-3767
24. Wang, L., Jin, Q., Lee, J. E., Su, I. h., and Ge, K. (2010) Histone H3K27 methyltransferase Ezh2 represses Wnt genes to facilitate adipogenesis. *Proceedings of the National Academy of Sciences* **107**, 7317-7322
25. Hemming, S., Cakouros, D., Isenmann, S., Cooper, L., Menicanin, D., Zannettino, A., and Gronthos, S. (2014) EZH2 and KDM6A act as an epigenetic switch to regulate mesenchymal stem cell lineage specification. *Stem cells (Dayton, Ohio)* **32**, 802-815
26. Wei, Y., Chen, Y.-H., Li, L.-Y., Lang, J., Yeh, S.-P., Shi, B., Yang, C.-C., Yang, J.-Y., Lin, C.-Y., Lai, C.-C., and Hung, M.-C. (2010) CDK1-dependent phosphorylation of EZH2 suppresses methylation of H3K27 and promotes osteogenic differentiation of human mesenchymal stem cells. *Nature Cell Biology* **13**, 87-94
27. Kubo, H., Shimizu, M., Taya, Y., Kawamoto, T., Michida, M., Kaneko, E., Igarashi, A., Nishimura, M., Segoshi, K., Shimazu, Y., Tsuji, K., Aoba, T., and Kato, Y. (2009) Identification of mesenchymal stem cell (MSC)-transcription factors by microarray and knockdown analyses, and signature molecule-marked MSC in bone marrow by

immunohistochemistry. *Genes to cells : devoted to molecular & cellular mechanisms* **14**, 407-424

28. Easwaran, H., Johnstone, S. E., Van Neste, L., Ohm, J., Mosbruger, T., Wang, Q., Aryee, M. J., Joyce, P., Ahuja, N., Weisenberger, D., Collisson, E., Zhu, J., Yegnasubramanian, S., Matsui, W., and Baylin, S. B. (2012) A DNA hypermethylation module for the stem/progenitor cell signature of cancer. *Genome research* **22**, 837-849
29. Gentleman, R. C., Carey, V. J., Bates, D. M., Bolstad, B., Dettling, M., Dudoit, S., Ellis, B., Gautier, L., Ge, Y., and Gentry, J. (2004) Bioconductor: open software development for computational biology and bioinformatics. *Genome biology* **5**, R80
30. Smyth, G. K. (2004) Linear models and empirical bayes methods for assessing differential expression in microarray experiments. *Statistical applications in genetics and molecular biology* **3**, Article3
31. Smyth, G. K. (2005) limma: Linear Models for Microarray Data. in *Bioinformatics and Computational Biology Solutions Using R and Bioconductor* (Gentleman, R., Carey, V., Huber, W., Irizarry, R., and Dudoit, S. eds.), Springer New York. pp 397-420
32. Gentleman, R., Carey, V., Huber, W., Irizarry, R., and Dudoit, S. (2006) *Bioinformatics and computational biology solutions using R and Bioconductor*, Springer Science & Business Media
33. Saeed, A., Sharov, V., White, J., Li, J., Liang, W., Bhagabati, N., Braisted, J., Klapa, M., Currier, T., and Thiagarajan, M. (2003) TM4: a free, open-source system for microarray data management and analysis. *Biotechniques* **34**, 374
34. Isenmann, S., Arthur, A., Zannettino, A. C. W., Turner, J. L., Shi, S. T., Glackin, C. A., and Gronthos, S. (2009) TWIST Family of Basic Helix-Loop-Helix Transcription Factors Mediate Human Mesenchymal Stem Cell Growth and Commitment. *Stem cells (Dayton, Ohio)* **27**, 2457-2468
35. Nguyen, T. M., Arthur, A., Hayball, J. D., and Gronthos, S. (2013) EphB and Ephrin-B interactions mediate human mesenchymal stem cell suppression of activated T-cells. *Stem Cells Dev* **22**, 2751-2764
36. Cakouros, D., Isenmann, S., Cooper, L., Zannettino, A., Anderson, P., Glackin, C., and Gronthos, S. (2012) Twist-1 induces Ezh2 recruitment regulating histone methylation along the Ink4A/Arf locus in mesenchymal stem cells. *Mol Cell Biol* **32**, 1433-1441
37. Cakouros, D., Isenmann, S., Hemming, S. E., Menicanin, D., Camp, E., Zannetinno, A. C., and Gronthos, S. (2015) Novel basic helix-loop-helix transcription factor hes4 antagonizes the function of twist-1 to regulate lineage commitment of bone marrow stromal/stem cells. *Stem Cells Dev* **24**, 1297-1308
38. Inoue, I., Ikeda, R., and Tsukahara, S. (2006) Current topics in pharmacological research on bone metabolism: Promyelotic leukemia zinc finger (PLZF) and tumor necrosis factor-alpha-stimulated gene 6 (TSG-6) identified by gene expression analysis play roles in the pathogenesis of ossification of the posterior longitudinal ligament. *Journal of pharmacological sciences* **100**, 205-210
39. Ikeda, R., Yoshida, K., Tsukahara, S., Sakamoto, Y., Tanaka, H., Furukawa, K., and Inoue, I. (2005) The promyelotic leukemia zinc finger promotes osteoblastic differentiation of human mesenchymal stem cells as an upstream regulator of CBFA1. *The Journal of biological chemistry* **280**, 8523-8530
40. Cakouros, D., Isenmann, S., Hemming, S. E., Menicanin, D., Camp, E., Zannettino, A. C., and Gronthos, S. (2015) Novel basic Helix Loop Helix Transcription Factor Hes4

Antagonizes the Function of Twist-1 to Regulate Lineage Commitment of Bone Marrow Stromal/ Stem Cells. *Stem cells and development*

41. Ivins, S., Pemberton, K., Guidez, F., Howell, L., Krumlauf, R., and Zelent, A. (2003) Regulation of Hoxb2 by APL-associated PLZF protein. *Oncogene* **22**, 3685-3697
42. Barna, M., Hawe, N., Niswander, L., and Pandolfi, P. P. (2000) Plzf regulates limb and axial skeletal patterning. *Nature genetics* **25**, 166-172
43. Xu, B., Hrycaj, S. M., McIntyre, D. C., Baker, N. C., Takeuchi, J. K., Jeannotte, L., Gaber, Z. B., Novitch, B. G., and Wellik, D. M. (2013) Hox5 interacts with Plzf to restrict Shh expression in the developing forelimb. *Proceedings of the National Academy of Sciences of the United States of America* **110**, 19438-19443
44. Barna, M., Pandolfi, P. P., and Niswander, L. (2005) Gli3 and Plzf cooperate in proximal limb patterning at early stages of limb development. *Nature* **436**, 277-281
45. Wieczorek, D., Koster, B., and Gillessen-Kaesbach, G. (2002) Absence of thumbs, A/hypoplasia of radius, hypoplasia of ulnae, retarded bone age, short stature, microcephaly, hypoplastic genitalia, and mental retardation. *Am J Med Genet* **108**, 209-213
46. Fischer, S., Kohlhase, J., Bohm, D., Schweiger, B., Hoffmann, D., Heitmann, M., Horsthemke, B., and Wieczorek, D. (2008) Biallelic loss of function of the promyelocytic leukaemia zinc finger (PLZF) gene causes severe skeletal defects and genital hypoplasia. *J Med Genet* **45**, 731-737
47. Djouad, F., Tejedor, G., Toupet, K., Maumus, M., Bony, C., Blangy, A., Chuchana, P., Jorgensen, C., and Noel, D. (2014) Promyelocytic leukemia zinc-finger induction signs mesenchymal stem cell commitment: identification of a key marker for stemness maintenance? *Stem Cell Res Ther* **5**, 27
48. Barna, M., Merghoub, T., Costoya, J. A., Ruggero, D., Branford, M., Bergia, A., Samori, B., and Pandolfi, P. P. (2002) Plzf mediates transcriptional repression of HoxD gene expression through chromatin remodeling. *Developmental cell* **3**, 499-510
49. Hong, S. H., David, G., Wong, C. W., Dejean, A., and Privalsky, M. L. (1997) SMRT corepressor interacts with PLZF and with the PML-retinoic acid receptor alpha (RARalpha) and PLZF-RARalpha oncoproteins associated with acute promyelocytic leukemia. *Proceedings of the National Academy of Sciences of the United States of America* **94**, 9028-9033
50. He, L. Z., Guidez, F., Tribioli, C., Peruzzi, D., Ruthardt, M., Zelent, A., and Pandolfi, P. P. (1998) Distinct interactions of PML-RARalpha and PLZF-RARalpha with co-repressors determine differential responses to RA in APL. *Nature genetics* **18**, 126-135
51. Grignani, F., De Matteis, S., Nervi, C., Tomassoni, L., Gelmetti, V., Cioce, M., Fanelli, M., Ruthardt, M., Ferrara, F. F., Zamir, I., Seiser, C., Grignani, F., Lazar, M. A., Minucci, S., and Pelicci, P. G. (1998) Fusion proteins of the retinoic acid receptor-alpha recruit histone deacetylase in promyelocytic leukaemia. *Nature* **391**, 815-818
52. Rosato, R. R., Wang, Z., Gopalkrishnan, R. V., Fisher, P. B., and Grant, S. (2001) Evidence of a functional role for the cyclin-dependent kinase-inhibitor p21WAF1/CIP1/MDA6 in promoting differentiation and preventing mitochondrial dysfunction and apoptosis induced by sodium butyrate in human myelomonocytic leukemia cells (U937). *Int J Oncol* **19**, 181-191
53. Lemercier, C., Brocard, M. P., Puvion-Dutilleul, F., Kao, H. Y., Albagli, O., and Khochbin, S. (2002) Class II histone deacetylases are directly recruited by BCL6 transcriptional repressor. *The Journal of biological chemistry* **277**, 22045-22052

54. David, G., Alland, L., Hong, S. H., Wong, C. W., DePinho, R. A., and Dejean, A. (1998) Histone deacetylase associated with mSin3A mediates repression by the acute promyelocytic leukemia-associated PLZF protein. *Oncogene* **16**, 2549-2556
55. Watanabe, S., Imaizumi, T., Tsuruga, K., Aizawa, T., Ito, T., Matsumiya, T., Yoshida, H., Joh, K., Ito, E., and Tanaka, H. (2013) Glomerular expression of myxovirus resistance protein 1 in human mesangial cells: possible activation of innate immunity in the pathogenesis of lupus nephritis. *Nephrology (Carlton)* **18**, 833-837
56. Patzina, C., Haller, O., and Kochs, G. (2014) Structural requirements for the antiviral activity of the human MxA protein against Thogoto and influenza A virus. *The Journal of biological chemistry* **289**, 6020-6027
57. Park, D., Spencer, J. A., Koh, B. I., Kobayashi, T., Fujisaki, J., Clemens, T. L., Lin, C. P., Kronenberg, H. M., and Scadden, D. T. (2012) Endogenous bone marrow MSCs are dynamic, fate-restricted participants in bone maintenance and regeneration. *Cell stem cell* **10**, 259-272
58. Larsen, K. H., Frederiksen, C. M., Burns, J. S., Abdallah, B. M., and Kassem, M. (2010) Identifying a molecular phenotype for bone marrow stromal cells with in vivo bone-forming capacity. *Journal of bone and mineral research : the official journal of the American Society for Bone and Mineral Research* **25**, 796-808
59. Lee, J. Y., Chien, I. C., Lin, W. Y., Wu, S. M., Wei, B. H., Lee, Y. E., and Lee, H. H. (2012) Fhl1 as a downstream target of Wnt signaling to promote myogenesis of C2C12 cells. *Molecular and cellular biochemistry* **365**, 251-262
60. Lee, H.-H., Lee, J.-Y., and Shih, L.-H. (2013) Proper Fhl1 expression as Wnt signaling is required for chondrogenesis of ATDC5 cells. *Animal Cells and Systems* **17**, 413-420
61. Wu, S. M., Shih, L. H., Lee, J. Y., Shen, Y. J., and Lee, H. H. (2015) Estrogen enhances activity of wnt signaling during osteogenesis by inducing fhl1 expression. *Journal of cellular biochemistry* **116**, 1419-1430
62. Ye, L., Fan, Z., Yu, B., Chang, J., Al Hezaimi, K., Zhou, X., Park, N.-H., and Wang, C.-Y. (2012) Histone Demethylases KDM4B and KDM6B Promotes Osteogenic Differentiation of Human MSCs. *Cell stem cell* **11**, 50-61

3.10 Tables, figures and figure legends

Table 1. Human Real Time PCR primers

Gene	**Accession No.**	**Forward Primer 5' - 3'**	**Reverse Primer 5' - 3'**
EZH2	NM_004456.4 (All variants)	gggacagtaaaaatgtgtcctgc	tgccagcaatagatgctttttg
RUNX2	NM_001271893.3	ctcttgctggtgacattgtc	cccttctctcgacgctgg
OP	NM_001040058.1	atgagagccctcacactcctcg	gtcagccaactcgtcacagtcc
OC	NM_199173.5 (All variants)	acatccagtaccctgatgctacag	gtgggtttcagcactctggt
β-ACTIN	NM_001101.3|	gatcattgctcctcctga	gtcatagtccgcctagaagcat
ZBTB16	NM_006006.4 (All variants)	ggtcgagcttcctgataac	accgcactgatcacagacaa
MX1	NM_001144925.2 (All variants|)	taccagcgagctcatcacac	catttgtggaactcgtgtcg
FHL1	NM_001159702.2 (All variants)	atgagacctttgtggccaag	cttgttgcacttcacgcaat

OP, Osteopointin; OC, Osteocalcin; β-ACTIN, Beta Actin.

Table 2. Human ChIP transcription start site primers

Gene	**Accession No.**	**Forward Primer 5'- 3'**	**Reverse Primer 5'- 3'**
GAPDH	*NM_002046.5*	cggctactagcggttttacg	aagaagatgcggctgactgt
IL2	*NM*_000586.3	attgtggcaggagttgaggt	cagtcagtctttgggggttt
INK4A	NM_000077.4	accccgattcaatttggcag	aaaaagaaatccgcccccg
ZBTB16	NM_006006.4 (All variants)	atctgctgtggcagaacctt	ttctttccttctgggctctg
MX1	NM_001144925.2 (All variants)	tcagcacagggtctgtgagt	gcgcccttgctatgattatg
FHL1	NM_001159702.2 (All variants)	acacagcctccgtgcagt	agggaaagaggggaggaag

IL2, Interleukin Two.

Table 3. Genes with upregulated expression during osteoblasts differentiation associated with loss of EZH2 binding and loss of H3K27 methylation and/or gain of H3K4 methylation

		Histone methylation marks		**GSE9451**	
GENE SYMBOL	**GENE NAME**	**MSC**	**OB**	**FOLD CHANGE**	**ADJUSTED P-VALUE**
ZBTB16	Zinc finger and BTB domain containing 16	H3K27me3	H3K4me3	4.6	0.007
FHL1	Four and a half LIM domain 1	H3K27me3	H3K4me3	1.1	0.0141
MYADM	Myeloid-associated differentiation marker	H3K27me3 + H3K4me3	H3K4me3	1.3	0.0011
HOPX	HOP homeobox	H3K27me3	-	3.2	0.0197
ROR2	Receptor tyrosine kinase-like orphan receptor 2	H3K27me3	-	3.0	0.000673
MX1	Myxovirus (influenza virus) resistance1, interferon-inducible protein p78	H3K27me3	-	1.2	0.0129

A tabulated list of 6 genes, identified by bioinformatics analysis. Listed are genes in which are bound by EZH2 in MSC but not in OB, 26 are statically significant 2-fold up-regulation of expression in OB compared with MSC ($p< 0.5$[LIMMA];GSE9451, 6 genes lost H3K27 tri-methylation (me3) following differentiation and or the gain of H3K4 following differentiation. Fold change < 2 fold are defined as up-regulated expression in OB compared to MSC. >2 fold was not differentially expressed in OB compared with MSC. Genes were excluded as not expressed in either MSC or OB (signal<100). Fold change represented in table is fold change of OB/MSC.

Figure 1. Genes with up-regulated expression and loss of EZH2 during osteoblast differentiation associated with loss of H3K27 methylation and / or gain of H3K4 methylation.

Genes up regulated expression with loss of EZH2 and H3K27me3 in OB. (A) Microarray (GSE9451) (28) expression of *ZBTB16*, *FHL1*, *MYADM*, *HOPX*, *ROR2* and *MX1* in OB compared with MSC were significant up regulated (*p < 0. 05 un-paired t-test).

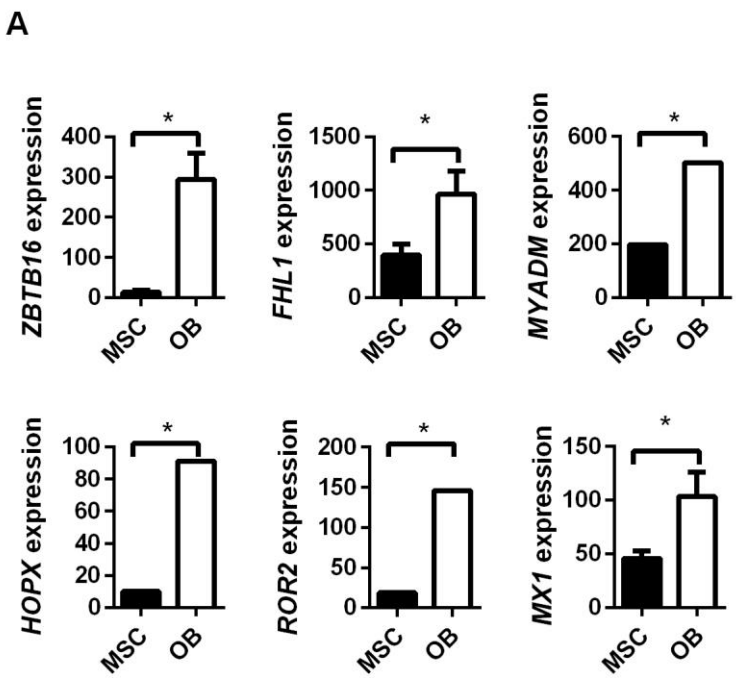
A
ZBTB16 expression
400
300
200
100
0
*
MSC
OB
FHL1 expression
1500
1000
500
0
*
MSC
OB
MYADM expression
600
400
200
0
*
MSC
OB
HOPX expression
100
80
60
40
20
0
*
MSC
OB
ROR2 expression
200
150
100
50
0
*
MSC
OB
MX1 expression
150
100
50
0
*
MSC
OB

Figure 2. EZH2, H3K27me3 and H3K4me3 ChIP analysis of MSC and Osteoblast confirmed modification patterns identified by bioinformatics analysis.

Manual ChIP analysis confirms EZH2 regulates *ZBTB16*, *MX1* and *FHL1* in osteogenic differentiation. MSC (non-differentiated) and osteogenic differentiated OB were immunoprecipitated with anti-H3K27me3, anti-EZH2, anti-H3K4me3 and anti-IgG control antibody and RT-PCR were used to measure enrichment. (A) EZH2 enrichment was present at the transcription start site (TSS) of *ZBTB16*, *MX1* and *FHL1* in MSC and was absent in OB. (B) EZH2 H3K27me3 repressive modification was present at the TSS of *ZBTB16*, *MX1* and *FHL1* and was removed in OB. (C) H3K4me3 active gene modification was not present on the TSS of *ZBTB16*, *MX1* and *FHL1* in MSC; however, the modification was present in OB. * $p < 0.05$, 2-way ANOVA with Sidak's multiple comparison test. Data is a representative of 3 independent MSC donors. Positive and negative ChIP controls are represented in Supplementary data Figure 1.

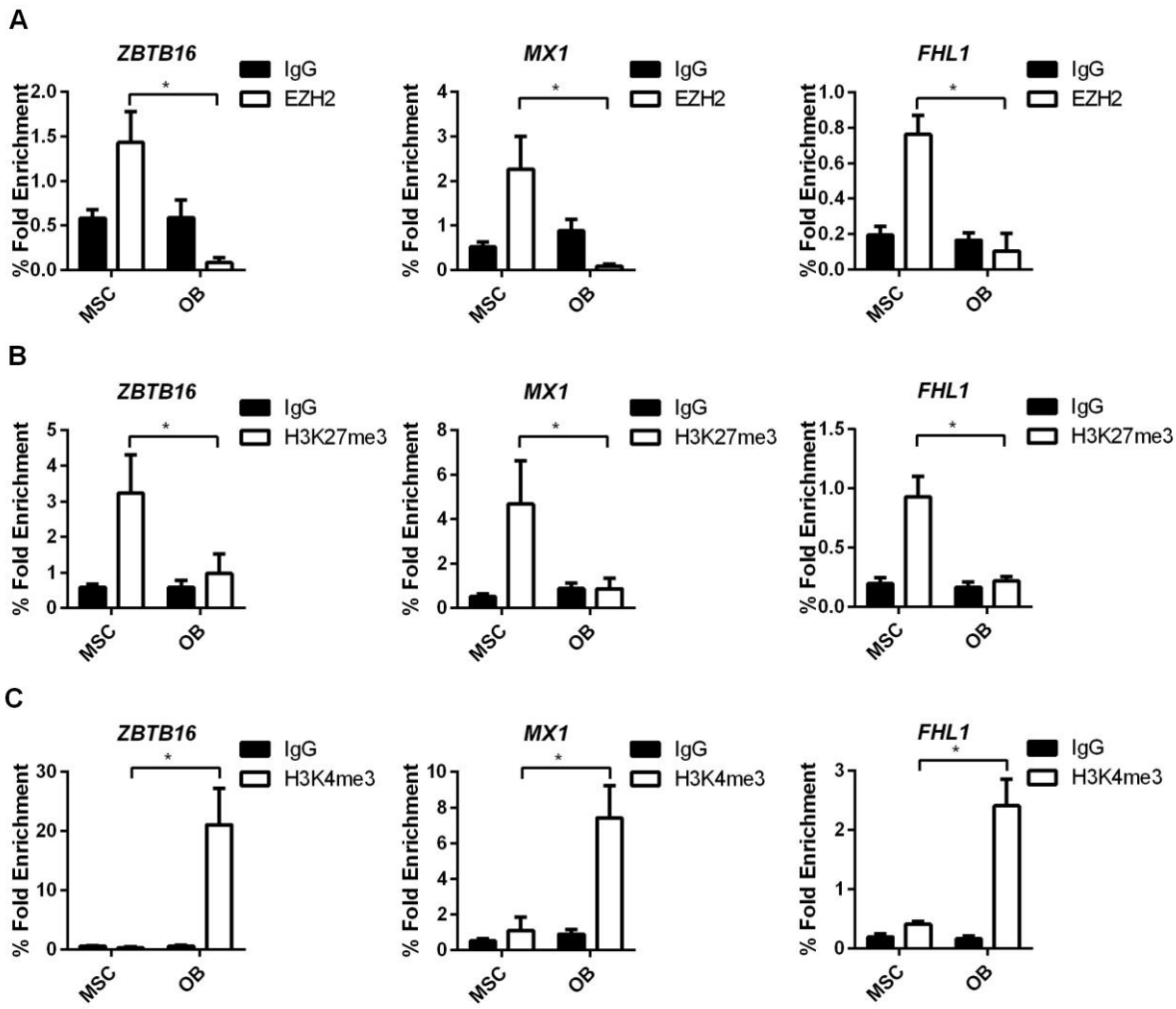
A
ZBTB16
MX1
FHL1
IgG
EZH2
% Fold Enrichment
MSC
OB
B
H3K27me3
C
H3K4me3

Figure 3. Enforced expression of EZH2 inhibits *ZBTB16*, *MX1* and *FHL1* expression in MSC and OB.

pRUF-IRES-GFP-*EZH2* over-expressing or pRUF-IRES-GFP control MSC were treated with no inductive media (MSC) or osteogenic differentiation media (OB) for 14 days. RT-PCR analysis: (A) Ezh2 overexpression. (B) Expression of *RUNX2*. (C) Expression of *ZBTB16*, *MX1* and *FHL1* were significantly down regulated in EZH2 over-expressing OB compared with control OB. * $p < 0.05$, 2-way ANOVA with Sidak's multiple comparison test. Data is a representative of 3 independent MSC donors.

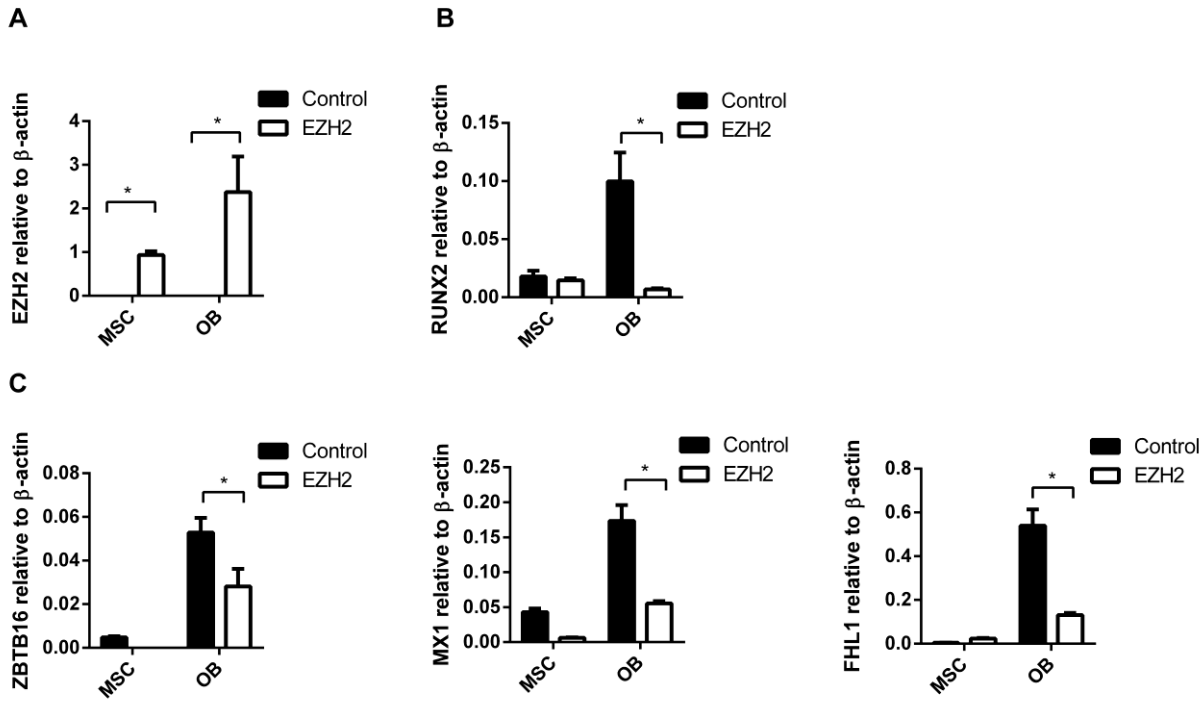
A
EZH2 relative to β-actin
Control
EZH2
MSC
OB
B
RUNX2 relative to β-actin
C
ZBTB16 relative to β-actin
MX1 relative to β-actin
FHL1 relative to β-actin

Figure 4. siRNA knockdown of EZH2 promotes expression of *ZBTB16, MX1* and *FHL1* in OB.

MSC were treated with negative control siRNA, EZH2 siRNA #1 and EZH2 siRNA #2. MSC were cultured for 14 days with osteogenic differentiation media. (A) Knockdown of *EZH2* by siRNA was confirmed by RT-PCR. (B) RT-PCR reveals a significant increase in *RUNX2* expression compared with negative control treated OB. (C) *ZBTB16*, *MX1* and *FHL1* gene expression was up-regulated in EZH2 siRNA treated OB compared with negative control treated OB. * $p < 0.05$, 1-way ANOVA with Dunnet's multiple comparison test. Data is a representative of 3 independent MSC donors.

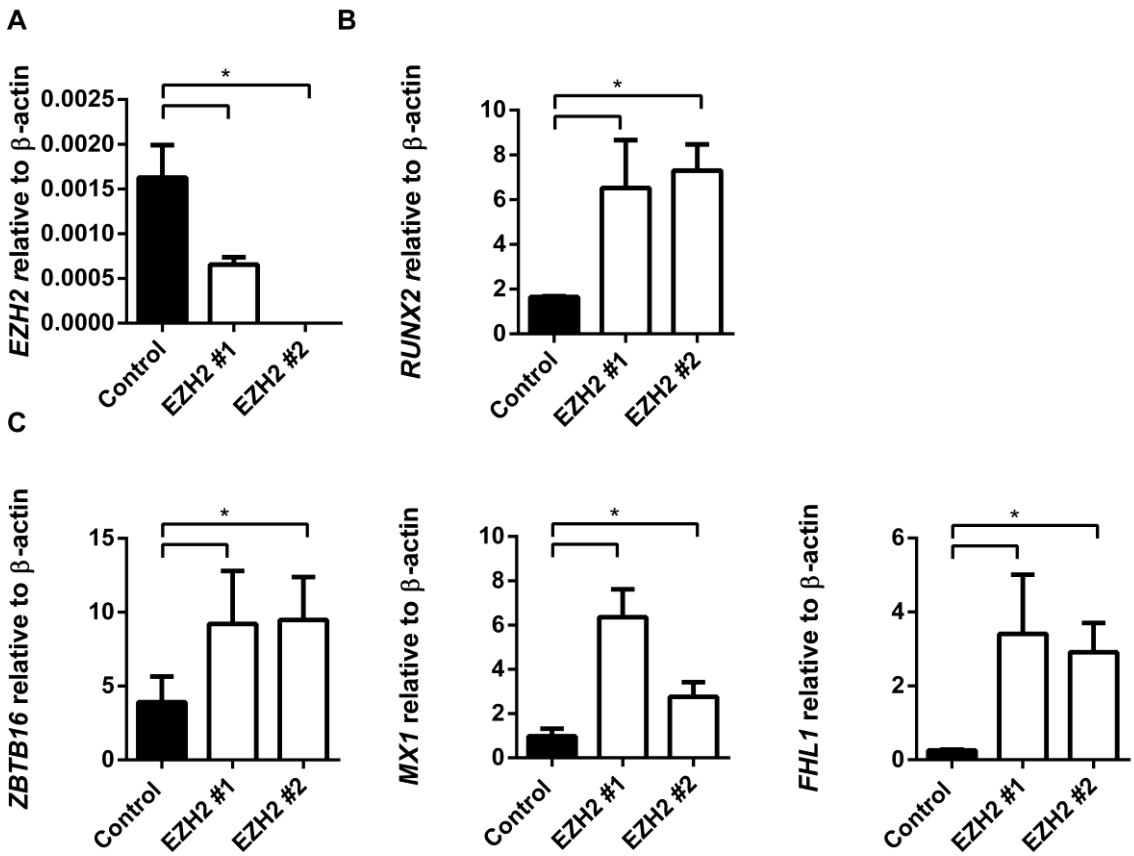
A
B
C
EZH2 relative to β-actin
RUNX2 relative to β-actin
ZBTB16 relative to β-actin
MX1 relative to β-actin
FHL1 relative to β-actin
Control
EZH2 #1
EZH2 #2
*

Figure 5. siRNA knockdown of MX1 and FHL1 inhibits osteogenesis.

MSC were treated with negative control siRNA, MX1 siRNA #1, MX1 siRNA #2, FHL1 siRNA #1 and FHL1 siRNA #2 and were cultured for 14 days under osteogenic differentiation media. (A) Knockdown of MX1 and FHL1 by siRNA was confirmed by RT-PCR at 14 days of induction. (B) Representative images of alizarin red-stained mineral (x40) showing a decrease in hydroxyl appetite mineral MX1 and FHL1 siRNA treated OB. (C) Extracellular calcium quantitated and normalized to DNA per triplicate well revealed significant decrease in calcium in siRNA treated OB (n=3 donors). (D) RT-PCR reveals a significant decrease in osteogenic marker *RUNX2*, *OP* and *OC* in MX1 and FHL1 siRNA knockdown OB. Statistical analysis for A&C were 1-way ANOVA with Dunnet's multiple comparisons test. Data is a representative of 3 independent MSC donors.

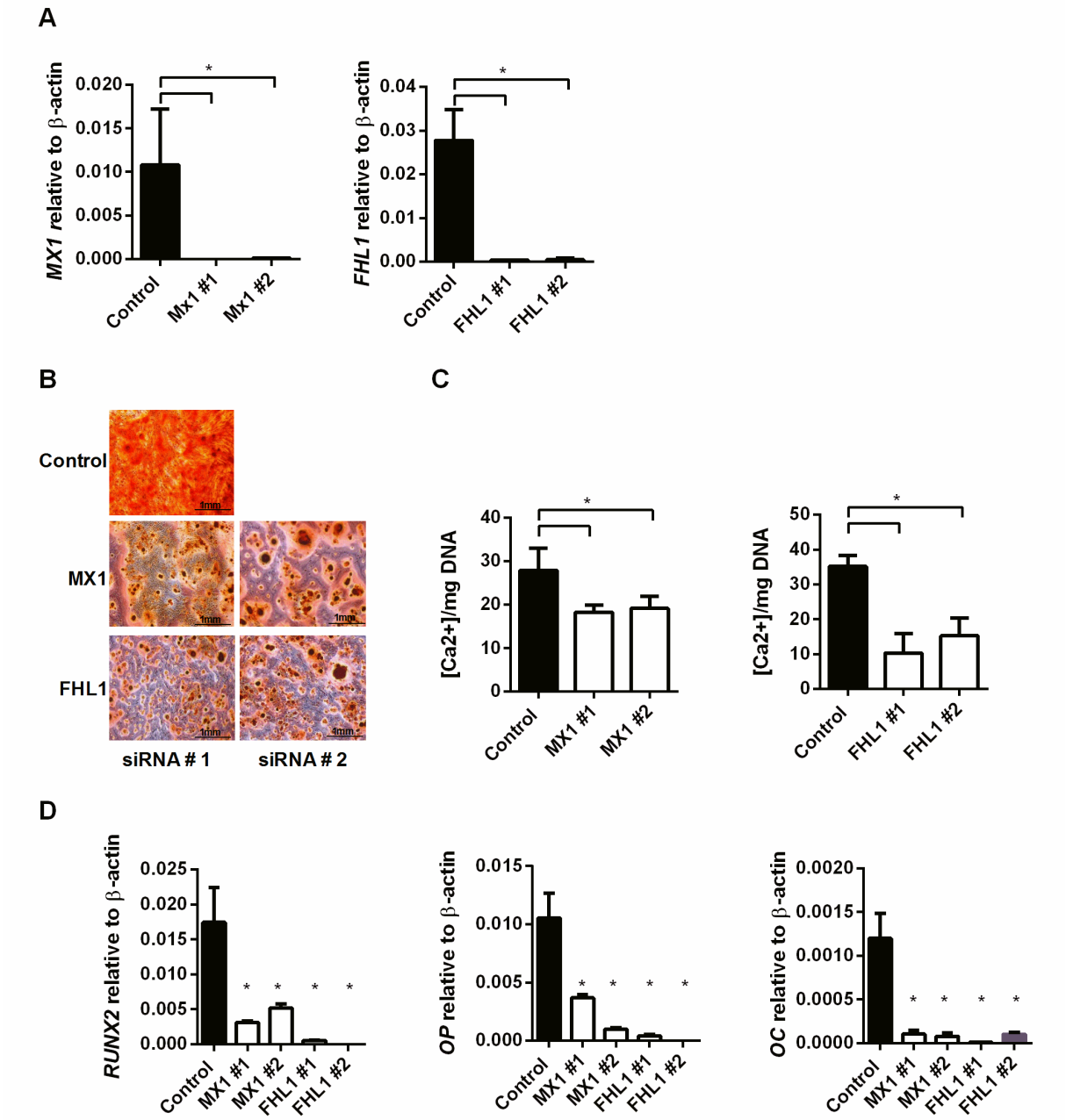
A
MX1 relative to β-actin
0.020
0.015
0.010
0.005
0.000
*
Control
Mx1 #1
Mx1 #2
FHL1 relative to β-actin
0.04
0.03
0.02
0.01
0.00
*
Control
FHL1 #1
FHL1 #2
B
Control
MX1
FHL1
1mm
siRNA # 1
siRNA # 2
C
[Ca2+]/mg DNA
40
30
20
10
0
*
Control
MX1 #1
MX1 #2
[Ca2+]/mg DNA
50
40
30
20
10
0
*
Control
FHL1 #1
FHL1 #2
D
RUNX2 relative to β-actin
0.025
0.020
0.015
0.010
0.005
0.000
Control
MX1 #1
MX1 #2
FHL1 #1
FHL1 #2
OP relative to β-actin
0.015
0.010
0.005
0.000
Control
MX1 #1
MX1 #2
FHL1 #1
FHL1 #2
OC relative to β-actin
0.0020
0.0015
0.0010
0.0005
0.0000
Control
MX1 #1
MX1 #2
FHL1 #1
FHL1 #2

Figure 6. siRNA knockdown of MX1 and FHL1 has no effect on MSC proliferation.

MSC were treated with 12 pmol of negative control siRNA, MX1 siRNA #1, MX1 siRNA #2, FHL1 siRNA #1 of FHL1 siRNA #2. MSC were treated with BrdU proliferation agent 24 hours prior to the 6 day time point. (A) At 6 days of culture the proliferation of MSC treated with either MX1 or FHL1 siRNA were no different compared to negative control siRNA (1-way ANOVA with Dunnet's multiple comparisons test). Data is a representative of 3 independent MSC donors.

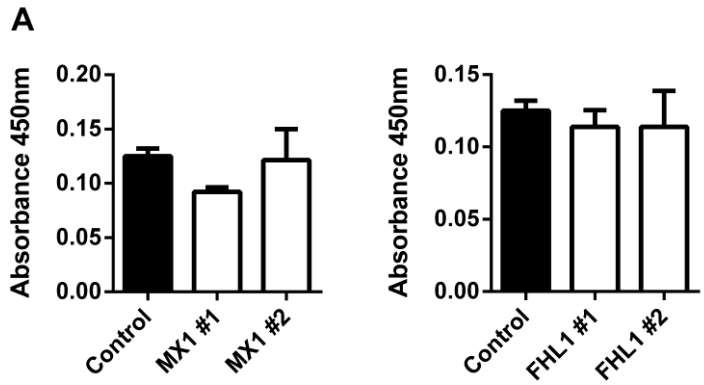
A
Absorbance 450nm
0.20
0.15
0.10
0.05
0.00
Control
MX1 #1
MX1 #2
Absorbance 450nm
0.15
0.10
0.05
0.00
Control
FHL1 #1
FHL1 #2

Supplementary Figure 1. Positive and negative ChIP controls.

(A&B) Positive control TSS of P16 showed enrichment EZH2 and H3K27me3 compared with IgG control. (C&D) Negative control TSS of GAPDH showed enrichment of EZH2 and H3K27me3 compared with IgG control. (E) Positive control for H3K4me3 was the TSS of GAPDH which showed enrichment for MSC and OB compared with IgG control. (F) Negative control for H3K4me3 TSS of IL-2 showed no enrichment for MSC and OB compared with IgG. Statistical analysis 2way ANOVA with Sidak's multiple comparisons test * $p < 0.05$. Data is a represented of 3 independent MSC donors.

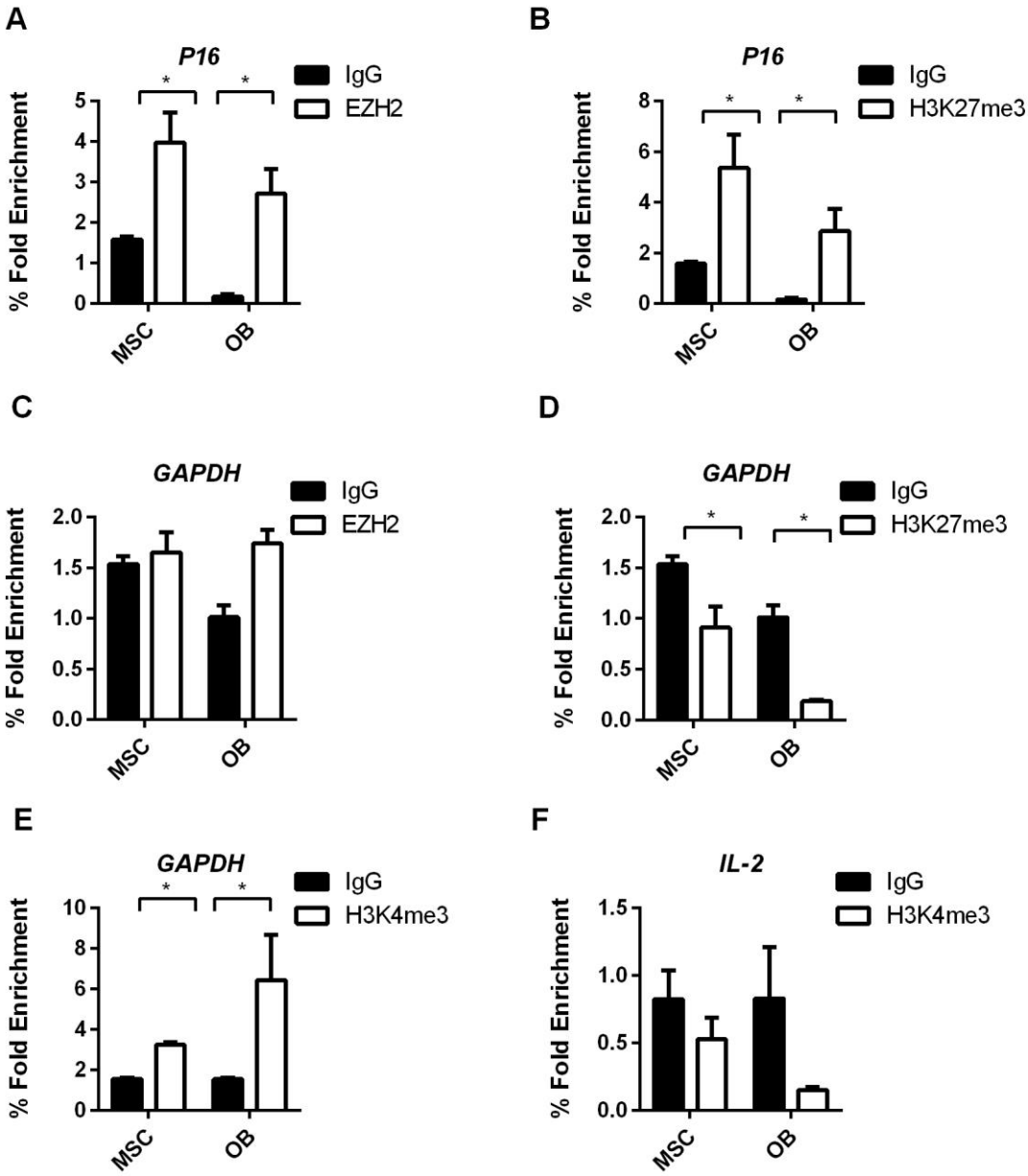
A
P16
IgG
EZH2
% Fold Enrichment
MSC
OB
B
P16
IgG
H3K27me3
% Fold Enrichment
MSC
OB
C
GAPDH
IgG
EZH2
% Fold Enrichment
MSC
OB
D
GAPDH
IgG
H3K27me3
% Fold Enrichment
MSC
OB
E
GAPDH
IgG
H3K4me3
% Fold Enrichment
MSC
OB
F
IL-2
IgG
H3K4me3
% Fold Enrichment
MSC
OB

Chapter:4

EZH2 deletion in limb bud mesenchyme effects postnatal long bone patterning, microarchitecture and remodelling.

Chapter summary:

The results of Chapter 3 identified known and novel regulators of osteogenesis targets by EZH2 in human MSC. EZH2 represses key known osteogenic drivers ZBTB16 and MX1 and novel osteogenic driver FHL1 in human BMSC. EZH2 and its repressive H3K27me3 modification are removed off the promoters of *Zbtb16*, *Mx1* and *Fhl1* during osteogenesis correlating with an increase in gene expression and appearance of the active H3K4me3 mark. It is still unclear if KDM6A and KDM6B play a role in the removal of the H3K27me3 on the promoters facilitating in gene activation. These findings led us to question the role of EZH2 in murine skeletal development.

To address this question we used conditional knockout of EZH2 in the limb bud mesenchyme. These mice were used to identify the role of EZH2 deletion in MSC in embryonic skeletal development. Secondly, these studies investigated the effect of EZH2 deletion on newborn bone development and microarchitecture. Lastly, we determined the effect of EZH2 deletion on postnatal bone formation, microarchitecture and remodelling.

Sarah Hemming, Dimitrios Cakouros, John Codrington, Kate Vandyke, Andrew Zannettino, Stan Gronthos. EZH2 regulates osteoblast and adipogenic differentiation, bone microarchitecture and bone remodelling in mice. This chapter will be summited to the Journal of Bone and Mineral Research (JBMR).

Statement of Authorship

Title of Paper	EZH2 deletion in limb bud mesenchyme effects postnatal long patterning, microarchitecture and remodelling
Publication Status	☐ Published ☐ Accepted for Publication ☑ Submitted for Publication ☑ Publication Style
Publication Details	Sarah Hemming, Dimitrios Cakouros, Kate Vandyke, John Codrington, Andrew C.W. Zannettino, Stan Gronthos. Identification of novel EZH2 targets in mesenchymal stem/ stromal cells which regulate osteogenesis. Summited to Journal Bone Mineral Research (JBMR)

Principal Author

Name of Principal Author (Candidate)	Sarah Elizabeth Hemming
Contribution to the Paper	First Author Generation of data Manuscript preparation Analysis of data
Overall percentage (%)	73%
Signature	Date 26-11-15

Co-Author Contributions

By signing the Statement of Authorship, each author certifies that:
the candidate's stated contribution to the publication is accurate (as detailed above);
permission is granted for the candidate in include the publication in the thesis; and
the sum of all co-author contributions is equal to 100% less the candidate's stated contribution.

Name of Co-Author	Dimitrios Cakouros
Contribution to the Paper	Manuscript evaluation Data interpretation Supervised development of work Contribution to experimental design Helped with animal work
Overall percentage (%)	10%
Signature	Date 26/11/15

Name of Co-Author	Kate Vandyke
Contribution to the Paper	Manuscript evaluation Data interpretation Technical advice Stastical analysis
Overall percentage (%)	5%
Signature	Date 26/11/15

Name of Co-Author	John Codrington
Contribution to the Paper	3 point mechanical bone testing Data generation Data analysis Data interpretation
Signature	Date 26/11/15

Name of Co-Author	Andrew Zannettino
Contribution to the Paper	Manuscript evaluation Data interpretation Equipment/Laboratory use
	2%
Signature	Date 26/11/15

Name of Co-Author	Stan Gronthos
Contribution to the Paper	Manuscript evaluation Data interpretation Supervised development of work Contribution to experimental design Funding
Overall percentage (%)	8%
Signature	Date 26/11/15

4 EZH2 deletion in limb bud mesenchyme effects postnatal long patterning, microarchitecture and remodelling.

Sarah Hemming[1,2], Dimitrios Cakouros[1,2], John Codrington[4] , Kate Vandyke[2,3], Andrew Zannettino[2,3], Stan Gronthos[1,2,*]

1. Mesenchymal Stem Cell Laboratory, School of Medical Sciences, Faculty of Health Sciences, University of Adelaide, Adelaide, Australia.

2. Cancer Theme, South Australian Health and Medical Research Institute (SAHMRI), Adelaide, Australia.

3. Myeloma Research Laboratory, School of Medical Sciences, Faculty of Health Sciences, University of Adelaide, Adelaide, Australia.

4. School of Mechanical Engineering, University of Adelaide, Adelaide, Australia

Corresponding author

Prof. Stan Gronthos

Medical School South Level 4, School of Medical Sciences, Faculty of Health Sciences, University of Adelaide, Adelaide 5005, South Australia, Australia.

Phone: +61-8-82223460

Fax: +61-882223139

Email: stan.gronthos@adelaide.edu.au

Running Title: Ezh2 Regulates murine skeletal development.

Key Words: Mesenchymal Stem cells, EZH2, Bone, Remodelling, Osteoblasts, Skeletal development, Knockout.

4.1 Abstract

Epigenetic regulation of adult stem cell renewal and lineage determination is of major importance to understand how the stem cell pool is maintained and how differentiation is orchestrated and specified for lineage determination. We have previously shown that the polycomb group protein, EZH2 is an essential epigenetic player in repressing osteogenesis and promoting adipogenesis, whereas the actions of EZH2 are counteracted by the demethylase, KDM6A, which promotes osteogenesis and whilst inhibiting adipogenesis in human BMSC. In this study we examined the function of either reducing EZH2 or totally eliminating EZH2 in mesenchymal tissues using a conditional knockout approach, based on the early mesenchyme marker, Prrx-1, a critical factor involved in limb bud development. Examination of skeletal formation during embyogenesis and early postnatal development found that heterozygous *Ezh2*$^{+/-}$ mice exhibit longer limbs and overall skeleton and drastically shorter limbs and skeleton for the homozygous *Ezh2*$^{-/-}$ animals. As early as E16.5, the *Ezh2*$^{-/-}$ mice displayed craniosynostosis with fusion of the sutures of the frontal and parietal bones. Upon birth and at 4 weeks, *Ezh2*$^{-/-}$ mice exhibit shorter limbs with decreased growth plate size and increased total trabecular throughout the tibia and femurs. Although *Ezh2*$^{+/-}$ animals did not display high bone volumes relative to tissue volume, their overall size, weight and skeleton was significantly larger. Strikingly EZH2 deficient animals displayed an increase in marrow adipocytes, osteoblast number and bone formation rates. Both *Ezh2*$^{+/-}$ and *Ezh2*$^{-/-}$ mice had thinner cortical bone, decreased mechanical strength associated with increases in the serum bone turnover markers, OCN, CTX-1 and TRAP. Cultured BMSC isolated from the long bones of *Ezh2*$^{+/-}$ exhibited increased osteogenic and adipogenic potential *in vitro*. Assessment of bone marrow cells flushed from the long bones of *Ezh2*$^{+/-}$ exhibited increased osteoclastogenesis *in vitro.* These studies demonstrate that Ezh2 orchestrates skeletal development and bone

remodelling *in vivo*, where deletion of *Ezh2* in primitive MSC accelerates both adipogenesis and osteogenesis, leading to aberrant adipose development and bone formation/ patterning in the hind limbs.

4.2 Introduction

Clonogenic bone marrow derived mesenchymal stem/stromal cells (BMSC) are quiescent cells that reside in the bone marrow, where a minor proportion of human MSC clones exhibit multi-lineage differentiation and the capacity for self-renewal (1-5). These cells play a critical role during skeletal tissue development and are integral components of the haematopoietic stem cell supportive niche (6). Primitive mesenchyme expressing Paired-related homeobox-1 (PRRX1) are responsible for early limb bud development and are thought to give rise to MSC-like populations within the newly formed skeleton (7), identified by various markers including $NEST^{+}$ (8), $PDGFR\alpha^{+}/Sca\text{-}1^{+}$ (9), CXCL12 (10), Myxovirus resistance-1 (MX1), Leptin Receptor (LEPR) (11) and Gremlin1 (GREM1) (12). Multipotent BMSC cell fate determination is known to be driven by key regulators of lineage associated transcription factors, RUNX2/CBFA1, PPARγ2 and SOX9 which are essential for differentiation into osteoblasts, adipocytes and chondrocytes, respectively (13-17). Similarly, BMSC self-renewal and longevity and has been shown to be mediated through various factors such as Telomerase, Twist-1/2, Nanog and Oct4 (18-21). Whilst these processes are now thought to be coordinated through different epigenetic modifications of chromatin and associated histone proteins, the precise role of epigenetic regulation of BMSC maintenance and cell fate determination have yet to be fully determined.

Epigenetic regulation of stem cell differentiation and self-renewal has been investigated mainly in embryonic stem cells with fewer studies in adult stem cells (22,23). Nucleosomes which contain 146bp of DNA wrapped around a histone octamer can be post translationally modified and remodelled. With currently roughly 28 histone modifications known, including DNA methylation and hydroxymethylation, there are many histone modifying enzymes known to regulate stem cell differentiation by regulating gene expression and dictating lineage specific gene expression (24,25). To date, the single most important epigenetic complex in stem cell differentiation is the polycomb complex. First discovered in drosophila, the polycomb proteins are transcriptional repressors required for correct spatial-temporal expression of developmental regulators (26,27). Polycomb group proteins assemble into two complexes, PRC1 and PRC2. PRC2 contains the histone 3 lysine 27 methyl transferase, Enhancer of Zeste 2, Ezh2 and Ezh1, embryonic ectoderm development, EED and suppressor of zeste 12, SUZ12 (28). H3K27me3 is the physiological substrate for the PRC1 complex which acts as a docking site for the chromodomain protein, CBX present in the PRC2 complex (28,29). This complex also includes RING1A/B, PCGF1-6 and HPH1-3. The polycomb group proteins cause compaction of nucleosomes, chromatin compaction and mediate long range chromatin interactions (30-32). In Embryonic stem cells, the chromatin landscape tends to be more open chromatin and upon differentiation there is a shift to a more closed chromatin configuration (33). This is correlated to PCG proteins being highly expressed in stem cells, which bind the promoters of transcription factors and developmental genes to inhibit differentiation in order to maintain an immature stem cell phenotype (34,35).

EZH2 is highly expressed in embryonic stem cells and required for early embryonic development (36). EZH2, EED and RING1B are essential for self-renewal and

pluripotency of mouse ESC's and maintaining a differentiation program of (22,36). In terms of adult stem cells, *Ezh2* is highly expressed in epidermal stem cells and its levels decrease upon differentiation (37). In addition EZH2 maintains the multi-potency of haemopotietic, muscle and neural stem cells (38-40). Overall, EZH2 has been shown to be involved in the differentiation of adult stem cells into myocytes, adipocytes, osteoblasts, cartilage, neurons, cardiomyocytes, haematopoietic cells, lymphocytes, epidermal and hepatocyte differentiation (41-49). Studies in mouse peripheral pre-adipocytes identified EZH2 as playing an important role in promoting adipogenic differentiation through repression of Wnt1,-6,-10a and -10b (42). In bone marrow derived mesenchymal stem cell differentiation, Wei and colleagues described that CDK1 inhibits EZH2 methyltransferase activity through the phosphorylation of T48, resulting in the promotion of osteogenesis(43). Thus EZH2 down regulation or inhibition is required for MSC osteogenic differentiation allowing the demethylation of H3K27me3 residues on *RUNX2* promoting osteogenic lineage specification. In agreement with these findings, we have reported that *EZH2* expression decreased during osteogenesis and was essential in repressing osteogenic differentiation of MSC by acting on the osteogenic master regulatory gene, *RUNX2* and its downstream bone gene target, Osteopontin (49). Conversely we found that EZH2 promoted adipogenesis and via an indirect mechanism, most probably due to its ability to inhibit the Wnt pathway which is a repressor of adipogenesis. Furthermore Twist-1 induces EZH2 expression and/or recruitment to Ink4A/Arf locus repressing senescence in MSC and osteogenesis (21,50).

The *in vivo* function of EZH2 in skeletal development has been difficult to examine mainly due to the embryonic lethality exhibited by EZH2 deficient mice (36,51). We therefore set out to examine the *in vivo* function of EZH2 in skeletal development by creating a

conditional knockout of *Ezh2* in mesenchymal tissues by crossing the *Ezh2* floxed mice with a *Prrx1* promoter-Cre driven mouse (7).

Our studies reveal that Prrx-1-EZH2 deficient mice exhibit gross craniofacial defects with premature suture closure mice were a lot smaller with smaller long bones and overall skeletal architecture and although there was an increase in trabecular bone relative to total size, however the quality of bone was compromised reflecting features of increase bone turnover. Remarkably the bone marrow of Prrx-1-EZH2 deficient mice showed a dramatic increase in bone marrow derived fat, which was associated with an increase in osteoclastogenesis, leading to abnormal bone remodelling.

4.3 Materials and Methods

4.4 Generation of EZH2 conditional knockout mouse

The Cre-loxP system was used to conditionally ablate EZH2 in limb bud mesenchyme. Mice carrying a transgene, in which exons encoding the SET domain of *Ezh2* are flanked by loxP sites, have been described (52). Homozygous animals *Ezh2*^{tm1Tara} (Ezh2 $^{fl/fl}$) from MRRC mutant mouse Regional resource Centre (MRRC, Ste, CA, USA) were backcrossed for 7 generations onto a C57BL/6 background. Backcrossed *Ezh2*$^{fl/fl}$ mice were crossed with animals carrying the Cre recombinase under the control of the paired related homeobox 1 promoter (*Prrx1)* derived enhancer (*Prrx1*-Cre transgene B6.Cg-Tg(*Prrx1*-cre$^{+/-}$)1Cjt/J from (Jackson Laboratories, Bar Harbor, ME USA, https://www.jax.org/). Offspring with the genotype *Prrx1*-cre$^{+/-}$:*Ezh2*$^{fl/fl}$ (Homozygous *Ezh2*$^{-/-}$) were compared with littermates lacking a one copy of the floxed *Ezh2 Prrx1*-cre$^{+/-}$:Ezh2$^{wt/fl}$ (Heterozygous *Ezh2*$^{+/-}$) and controls *Prrx1*-Cre$^{+/-}$:*Ezh2*$^{wt/wt}$ mice wildtype (*Ezh2*$^{+/+}$). SA Pathology Animal Ethics Approved Protocols: EZH2 breeding colony (BC06/12), Prrx1 breeding colony

(BC70a/12), EZH2 development study (103c/13), and Adelaide University Animal Ethics approved protocol (M-2013-143).

4.4.1 Genomic DNA genotyping

Mice genotypes were confirmed with tail tipping and PCR of genomic DNA. *Ezh2* primers; Enx1 3' loxP: ctgctctgaatggcaactcc and Enx1 5' of loxP: ttattcatagagccacctgg. floxed insertion band detected at 450bp and wildtype *Ezh2* gene with no floxed insertion was present at 410bp (Figure 1). *Prrx1*-cre$^{+/-}$ primers; OIMR1084: 5'gcggtctggcagtaaaaactatc3' and OIMR1085: 5'gtgaaacagcattgctgtcactt3'. The presence of Cre recombinase transgene was detected at band size of 100bp (Figure 1A). *Ezh2* genotyping PCR were performed with cycling parameters, initial denature of 94°C (5 mins), 35 cycles of denaturing at 94°C (30 secs), annealing at 62°C (30 secs), elongation at 72°C (45 secs) for *Ezh2* PCR and 35 cycles of 94°C (15 secs), 65°C (30 secs), 72°C (30 secs) for *Prrx-1* PCR. Both PCR conditions had a final elongation of 72°C (5mins) and stored at 4°C.

4.4.2 RNA extractions, cDNA synthesis and Real Time PCR

Total RNA from approximately $1.5x10^5$ mouse passage 5 BMSC was isolated using Trizol (Invitrogen, New York, Grand Island, http://www.lifetechnologies.com/au/en/home.html) according to manufacturer's instructions. Generation of cDNA and real time analysis was performed as previously described in triplicate (50,53,54). Changes in gene expression were calculated relative to β-actin using the 2^{-dCT} method. Real-time PCR primers used in this study: *Ezh2* (NM_007971.2)*:* Fwd, 5'actgctggcaccgtctgatg3', 5'tcctgagaaataatctccccacag3', *M-csf* (NM_007778.4): Fwd 5' gccaggggaaagtgaaagtt3', rev 5'catgaggagacagaccagca3', *Rankl* (NM_011613.3): Fwd 5'agccgagactacggcaagta3', rev 5'agtcctgcaaatctgcgt3', *Opg*

(NM_008764.3): Fwd 5'atgaacaagtggctgtgctg3', rev 5'rgtaggtgccaggagcacatt3', *Runx2* (NM_001289690.1): Fwd 5'cctctgacttctgcctctgg3', rev 5'tatggagtgctgctggtctg3', *Opn* (NM_001204201.1): Fwd, 5'agcaaactcttgcaagcaa3', rev 5'gattcgtcagattcatccgagt3', *Ocn* (NM_001032298.3): Fwd, 5'aagcaggagggcaataaggt3', rev 5'tcaagccatactggtgtgatagc3', *Pparγ2* (NM_001127330.2): Fwd, 5'ttttccgaagaaccatccgatt3', rev 5'atggcattgtgagacatcccc3', *C/EBPα* (NM_001287514.1): Fwd, 5'caagaacagcaacgagtaccg3', rev 5'ctcactggtcaactccagcca3', *AdipQ* (NM_009605.4): Fwd, 5'tgttcctcttaatcctgccca3', rev 5'ccaacctgcacaagttccctt3'.

4.4.3 Embryo and newborn extraction

Ezh2$^{wt/fl}$ heterozygous *Prrx1*-cre$^{+/-}$ mice were crossed with *Ezh2*$^{fl/fl}$ females. Embryonic days E16.5 and E17.5 were calculated from visualisation of a plug and mothers were humanely killed by CO_2 and cervical dislocation prior to embryo extraction. Newborn mice were humanely killed by intraperitoneal injection of 1mg/Kg of lethobarb. Embryos and newborns were tail tipped and processed for genotyping. E17.5 embryos and newborns were skinned and eviscerated and fixed and store in 95% ethanol at room temperature.

4.4.4 Western Blot

Murine BMSC were seeded at $8.0x10^3$ cells per cm^2, and cultured in regular growth medium as described above. Whole cell lysates (50 µg) were separated on SDS gel as previously described (21,55-57). Membranes were probed with anti-mouse EZH2 (Acc2; Cell signalling, Beverly, MA, USA, http://www.cellsignal.com, 1/1000 dilution), anti-rabbit H3K27me3 IgG (07-449, Merck, Millipore, Bayswater, VIC, AUS, http://www.merck.com.au/, 1/1000 dilution) and anti-mouse β-actin IgG (Sigma-Aldrich Pty Ltd, Castle Hill, NSW, AUS, http://www.sigmaaldrich.com, 1/2500 dilution)

antibodies. Secondary detection was performed using anti-rabbit- alkaline phosphatase conjugate (Merck Millipore, 1/10,000) and anti-mouse-alkaline phosphatase (Merck Millipore 1/10,000) antibodies.

4.4.5 Immunohistochemistry

Paraffin sections (5 μm) of 4 week old femora were dewaxed through histolene and ethanol solutions. Following proteinase K (PK, 200 μg/ml) antigen retrieval, the sections were incubated at 37°C for 30minutes in a humidity chamber. Sections were washed three times in 1x PBS then blocked in 0.3 v/v% H_2O_2 in methanol for 10 minutes at room temperature. Washed sections were incubated with horse anti mouse blocking serum (PK-6200, Vector laboratory, Vectastain Elite Universal ABC kit, Vector laboratory, Burlingame, CA, USA). Serum was removed and 2 μg/ml of Anti-rabbit H3K27me3 IgG (07-449, Merck, Millipore, Bayswater, VIC, AUS) or 2 μg/ml rabbit serum (negative control) was added to sections and incubated overnight. Sections were washed and incubated with a universal biotinylated secondary antibody (Vectastain Elite Universal ABC kit, Vector laboratory) for 45 minutes at room temperature. Sections were washed and incubated with an avidin biotin complex for 30 minutes and after incubation sections were washed with the peroxidase substrate AEC (SK-4200, Peroxidase substrate kit, Vector laboratory). Sections were left for 10 minutes to allow colour to develop, washed with H_20, counterstained with haematoxylin and mounted with an aqueous mounting solution.

4.4.6 Microtomography (Micro-CT)

3D microarchitecture of newborn long bones was evaluated using Micro-CT (Skyscan 1076 X-ray Microtomography SkyScan, Bruker Microct, Kontich, BEL, http://bruker-

microct.com). All whole newborn skeletons were scanned at 9µm resolution, No filter, Excitation 1767ms, Voltage 55kV, Current 120mA, rotation step 0.5 and two frame averaging. Reconstruction of the original scan data was performed using NRecon (NRecon Reconstruction 64-bit for, v.1.6.10; Bruker Microct) with a smoothing of 1, ring artefact of 8 and beam hardening of 30%. 2D, 3D morphometric parameters are calculated by CT-analyser (CTAn (v.1.15) + CTVol (v.2.3): 32-bit version (XP, Vista, Win-7) 2D/ 3D processing, analysis, visualization Bruker Micro-CT) in 2D or 3D based on a surface-rendered volume model in 2D or 3D space. Bone parameters based on the bone ASBMR established by Parfitt (58). Bone microarchitecture parameter used as previously described in (55). For the newborn tibia and region of interest (ROI) for the total whole tibial analysis define as where the tibia began and finished. Trabecular ROI was defined manually to elude the cortex (With shrink wrap settings). Tibiae images were reconstructed based on a specimen-specific threshold.

Four week old tibiae and femora were scanned at 9 µm resolution, Al 0.5mm filter, Excitation 5890ms, Voltage 48 kV, Current 110 mA, rotation step 0.6 and two frame averaging. Femurs were reconstruction using NRecon with a smoothing of 1, ring artefact of 8 and beam hardening of 30%. Reconstructed bmp files were realigned in Data Viewer (DATAVIEWER 64-bit version, V.1.5.2, Bruker Micro-CT) and VOI underwent thresholding and bone parameters were assessed using CTAn analyser. Total trabecular patterned through the femur a trabecular ROI analysed was defined as 40 slices under the proximal growth plate to a define region of bone within the proximal epiphysis. The length of the bone was determined from the first slice of the epiphysis to the end of the proximal epiphysis. Trabecular ROI was defined manually to elude the cortex (59). The midpoint of the bones was determined using the length measurement at 20 slices above and below this

point was analysed (40 slices). The medullary space was subtracted from the cortical data set to remove any trabecular present. Femur images were reconstructed based on a specimen-specific threshold. Three dimensional (3D) images were generated using Avizo fire 3D software (http://www.fei.com/software/avizo3d/) or CTVol 3D software (Burker, Skyscan).

4.4.7 Biomechanical testing

Femora's were stored at -20°C and wrapped in 1xPBS soaked gauze, then thawed overnight at 4°C and stored at room temperature for 1 hour prior to 3-point bend testing. The 3-point bend testing was undertaken using a Test Resources mechanical test machine (TestResources 800LE4, Shakopee, MN, USA)(60-62). The lower span width was 3.5 mm, the lower and upper contact anvils had radius of 1 mm. Femora were placed posterior side down (on the 2 lower anvils). Femora were place with the midpoint between the anvils located centrally along the diaphysis. A pre-loaded force of 0.5N was applied test was conducted in displacement control at a rate of 1 mm/min and load measured with a ±111N (25lb) load cell. Displacement was measured from a LVDT (±5mm) attached above the load cell. LVDT measurement corrected for compliance in the load-line by calibrating with an aluminium test piece. Load-displacement, flexural rigidity, ultimate bending moment were calculated as previously described (62)

4.4.8 Paraffin embedding

Fixed femora were decalcified in 0.5 M EDTA (EL023-5KG ChemSupply, Gillman SA, AUS, https://www.chemsupply.com.au) /0.5% paraformaldehyde (FL010-10L-P, ChemSupply) decalcification solution at 4ºC with agitation, changed three times weekly, for 3 weeks. Complete decalcification of the samples was confirmed by X-ray. The

samples were processed through sequential changes of ethanol, xylene and then embedded in paraffin. Longitudinal tissue sections (5 μm) were mounted on super frost plus slides and were stained with Safranin O/Fast Green, and Hematoxylin/ Eosin.

4.4.9 Methacrylate embedding

Mouse tibiae were embedded in methyl methacrylate (8005901000, Merk Millipore) as described (55;Fitter, 2013 #809,62-64) Fixed tibiae were dehydrated in acetone (AA008-2.5L-P, ChemSupply) (70% acetone for 1 hour; 90% acetone, 1 hour; 100% acetone, 1 hour; 100% acetone, 1 hour) at 4°C. Bones were infiltrated in 91% methyl methacrylate/9% PEG 400 (202398-500G, Sigma) under a vacuum for 1 week at room temperature in the dark. Filtration mixture was removed from bones and the samples were embedded in 10-5mL methyl methacrylate/PEG 400 (10:1) with Perkadox 16 (0.4% w/v) at 37°C for 48 hours in the dark. Blocks were mounted to round aluminium block holders with Araldite epoxy resin (Selleys, Padstow, NSW AUS, http://www.selleys.com.au/). A D-profile blade was used to section 5μm thick sections using a Leica SM2500 motorised sledge microtome (Leica Microsystems, North Ryde, NSW, AUS, http://www.leica-microsystems.com).

4.4.10 Histology

Alizan red and alcian blue staining: whole E16.5, 17.5, newborn and 4week tibias were fixed with 95% and dehydrated through acetone for two days with gentle agitation at room temperature. Alcian blue (0.3%, A5268, Sigma) in 70% ethanol and Alizarin red S (0.1%, A5533, Sigma) in 95% ethanol stains were prepared. Working solution was prepared by 1 volume of 0.3% Alcian blue, 1 volume of 0.1% Alizarin red S, 1 volume of glacial acetic acid and 17 volumes 70% Ethanol. Specimens were stained for at least 3 days with gentle

agitation at room temperature and cleared with 1% potassium hydroxide (KOH, 1050330500, Merck Millipore). The embryo was further cleared through 1:4 glycerol (GA010-2.5L-P, ChemSupply): KOH, 2:3 glycerol: KOH, 3:2 glycerol: KOH, 4:1 glycerol: KOH and finally stored 100% glycerol.

Hematoxylin and eosin staining: Paraffin embedded 5µm sections were dewaxed in xylene for 10 minutes and stained with H&E (65).

Safranin O and Fast Green staining: Methacrylate 5 µm sections were deplasticised in acetone for 15 minutes and stained with Fast Green FCF (0.2% w/v Fast Green FCF, F-7252-25G, Sigma, in H_20) and washed in 1% acetic acid dehydrated through ethanol and xylene. Slides were stained with Safranin O (0.1% w/v, S8884-25G, Sigma) and dehydrated through ethanol and xylene. Slides were coversliped with 2 x 40 mm coverslips using DePeX mounting medium.

Toludine Blue staining: Methacrylate 5 µm sections were deplasticised in acetone for 15minutes and stained with Toluidine Stain (198161-25g, Sigma) 2% (w/v) in 100 ml Toludine blue buffer, toludine buffer sodium phosphate/citrate buffer at pH 3.7. Slides were dehydrated through ethanol and xylene. Slides were coversliped and mounted with DePeX (Sigma).

4.4.11 Tartrate-resistant acid phosphatase (TRAP)

Cells were stained for TRAP activity with the Leukocyte Acid Phosphatase (TRAP, 387A-1KT, Sigma) kit as per the manufacturer's recommendations. Briefly, cells were fixed in 100 µL/well freshly-prepared citric acid/acetone/formaldehyde solution. Cells were

carefully washed 3 times in 250 µL/well RO water and were then incubated with freshly-prepared fast garnet TRAP stain for 15 – 20 minutes at 37°C in the dark. Wells were washed 4 times with 250 µL/well RO water and the plates were left to dry by evaporation. Wells were removed from slide and coversliped. Osteoclasts with 3-5, 6-10 and greater than ten were quantitated per well in duplicate wells. Cells were visualised and photographed with an Olympus CKX41 inverted microscope and an Olympus DP11 digital camera cellSens (Olympus, Notting Hill, VIC, AUS, http://www.olympus-lifescience.com/en/software/) imaging camera at 200x magnification.

4.4.12 Calcien labelling

Calcien (20mg/kg) was injected intraperitoneal at 4 days and 24 hours prior to harvesting of mice. Unstained, deplasticised sections were cover-slipped and used for measurements of bone formation. Histomorphometric analyses were conducted on blinded coded slides using OsteoMeasurexp V3.3.02 (Osteometric, Decatur, GA, http://www.osteometrics.com/software_ update.htm) software on an Olympus BX53 Microscope at 200x magnification. Methacrylate embedded tibia were sectioned, deplasticised and cover-slipped for analysis of calcien labelled bone formation. Mineral apposition rate (MA, µm/d) was evaluated as the mean distance between the calcien labelled surfaces, divided by 3 days (the interval between labelling and the death of the animals). Bone formation rate on bone surface (BFR/BS) was derived using the formula BFR = MAR × MS/BS × d/100(µm3/mm2/d).

4.4.13 Analysis of bone turnover serum markers

Mice were cardiac punctured to obtain blood samples which were centrifuged at 3000xg for 10 minutes at room temperature to collect serum frozen at -80ºC. Serum levels of

TRAP, Osteocalcin and CTX-1 were analysed using a MouseTRAP™ ELISA (TRAP 5b/SB-TR103; Immunodionostics (ids), UK http://www.idsplc.com/), Rat-Mid™ Osteocalcin EIA ELISA (AC-12F1; ids) and RatLaps™ CTX-I EIA ELISA (AC-06F1; ids) as specified by the manufacturer's instructions (http://www.idsplc.com/).

4.4.14 Microscopy imaging

NanoZoomer Slide Scanner was used to image histological sections and then viewed on NDP.view2 (http://ndp-view.software.informer.com). Alizarin red and alcian blue stained embryos were imaged on the Olympus CZXY7 (Olympus, Melbourne, VIC, AUS, http://www.olympusaustralia. com.au/) stereomicroscope and an Olympus DP21 digital camera at approximately 30 x final magnification. Calcien and differentiation images were taken using CellSens software (Olympus, Melbourne, VIC, AUS, http://www.olympusaustralia. com.au/) on the using Olympus BX53 Microscope and DP71 digital camera at 200x and 400x magnification.

4.4.15 Histomorphometric bone analysis

An area of (0.72mm^2) directly under the primary spongiosa was used to analyse the trabeculae in the secondary spongiosa Tissue immediately adjacent to the cortex was excluded from trabecular analysis. Trabecular bone volume to tissue volume (BV/TV, %), trabecular thickness (Tb.Th, μm), trabecular spacing (Tb.Sp, μm) and trabecular number (Tb.Th, /mm) were analysed. A length of 3.6mm cortical bone was analysed at the midpoint of the diaphysis determining cortical BV/TV and cortical thickness (Ct.Th, mm). Analysis of Osteoblasts numbers on trabecular bone (N.Ob/B.Pm, /mm) and adipocytes per marrow area (N.Adip/Ma.Ar, mm^2) was analysed in a region of the secondary spongiosa. Tissue immediately adjacent to the cortex was excluded from trabecular analysis.

4.4.16 Bone marrow derived MSC isolation and culture

Mice were humanely killed by carbon dioxide affixation and cervical dislocation. Mouse bone marrow stromal progenitors were isolated from flushed femora and tibiae as previous described (55). Flushed marrow was added to T175 and incubate overnight where cell suspension was collected and cryopreserved in 500µl of FSC and 500µl FSC with 20% DMSO in liquid nitrogen Briefly, both hind femora and tibiae were flushed with ice cold normal culture media and compact bone was crushed and incubated in collagenase say which type of collagenase (3mg/ml) and DNAse1 (50U/ml) (company details) for a hour at 37°C with rotation. Bone chips were filtered through a 0.75µm filter and washed with 5% Hanks buffered salt solution. Cells were seeded at $1.0x10^5$, $2.5x10^5$ and $5.0x10^5$ in duplicate in 6 week plates, and incubated for 7 days at 37°C under hypoxic conditions (5% O_2, 10% CO_2; Coy Laboratory Products, Grass Lake, MI, USA). At day 8 the CFU-F were stained with alkaline phosphatase staining kit (85L3R-1KT, Sigma) and counter stained with 1% toluidine blue. Replicate cultures were seeded at $8.0x10^3$ cells per cm^2 in normal growth media in hypoxia for 2 weeks. BMSC were passage to a minimum of 3 passages for functional and gene/ protein expression studies.

4.4.17 *In vitro* differentiation assays

Normal growth media: Murine BMSC were cultured in normal growth media, osteogenic media and adipogenic media. Normal growth media: αMEM (MEM-alpha, M4526-500ml , Sigma) was supplemented with 20% (v/v) FCS (cat), 2 mM L-Glutamine (G7513-100ml, Sigma), 1 mM Sodium Pyruvate (S8636, Sigma), and 50 U/mL penicillin, 50 µg/ml streptomycin (P4333-100ml, Sigma) and 100 µM L-ascorbate-2-phosphate (013-12061, Wako Pure Chemical Industries, Richmond, VA, USA, http://wako-chem.com). Cells were

cultured under hypoxic conditions (5% O_2, 10% CO_2; Coy Laboratory Products, Grass Lake, MI, USA) at 37°C.

Osteogenic media: αMEM supplemented with 20% (v/v) FCS , 2 mM L-Glutamine, 1 mM sodium pyruvate, 10 mM HEPES buffer, 50 U/ml penicillin, 50 μg/ml streptomycin, 100 μM L-ascorbate-2-phosphate, 10^{-7} M dexamethasone, and 1.8 mM KH_2PO_4. Mineralized bone matrix (mineral) formation was identified with Alizarin red (A5533-25G, Sigma.) staining of mineral deposits (50). Extracellular calcium was measured in triplicate samples and normalized to DNA content per well as previously described (50).

Adipogenic differentiation: αMEM supplemented with 20% (v/v) FCS (Cat) 2 mM L-Glutamine, 1 mM sodium pyruvate, 50 U/ml penicillin, 50 μg/ml streptomycin, 100 μM L-ascorbate-2-phosphate, 10^{-7} M dexamethasone, and 60 μM indomethacin (I8280, Sigma) and 1 μg/ml Insulin (Austr47219, Royal Adelaide Hospital pharmacy Adelaide, SA, AUS). Media was sterilised with a 0.2 μm bottle cap filter (CLS431161-48EA, Sigma) and cultured on BMSC for up to 14 days changing media twice weekly. Lipid formation was assessed by Nile red 25 ng/ml (N3013, Sigma) staining as previously described (50). Quantitation of lipid was performed by Nile red fluorescence staining normalized to the nucleus stain, DAPI 600 μM (D1306, Invitrogen/Life Technologies Australia, Mulgrave, VIC, AUS, https://www.lifetechnologies.com/au/en/home.html) stained nuclei per field of view in triplicate wells as previously described (50,56).

Osteoclast differentiation: Flushed cultured bone marrow (BM) cells were seeded in 96 well chamber slides or 96 well plates containing or on slices of whale dentine (55). Briefly, BM cells were cultured at 3.1 x 10^5 cells/cm^2 in 200 μL α-MEM supplemented with 75

ng/mL of macrophage colony stimulating factor (M-CSF) and Rank ligand (RANKL). Media was replaced every three days and the formation of TRAP-positive multinucleated osteoclasts was assessed after 6 days of osteoclast induction. The formation of resorption pits on dentine slices were assessed after 9 days of osteoclast induction. Dentine slices were incubated in 1x trypsin for 3 hours, washed with PBS and carbon coated for imaging by the Philips XL30 Scanning Electron Microscope (SEM) (Adelaide Microscopy, University of Adelaide) as previously described (66). Three representative fields of view were obtained using the SEM at 500x magnification and the surface area of total resorption was analysed using ImageJ software (Image J version 1.50e, http://imagej.nih.gov/ij/).

4.4.18 Statistics

Data analysis, graph generation and statistical analysis were carried out using Graphpad Prism 5. For differentiation and gene expression analysis a paired or unpaired Students T-test was used to compare *Ezh2*$^{+/+}$ and *Ezh2*$^{+/-}$ BMSC treated with control, osteogenic and adipogenic differentiation media. For analysis to detect differences between *Ezh2*$^{+/+,}$ *Ezh2*$^{+/-}$ and *Ezh2*$^{-/-}$ animals a one-way ANNOVA with a Tukey's multiple comparisons test. A Two-way ANNOVA with a Sidak's multiple comparisons test were used to determine the differences between nuclei groups in osteoclast assays and differences in alkaline positive colonies a Statistical differences (*) of $p \leq 0.05$.

4.5 Results

4.5.1 Confirmation of EZH2 and H3K27me3 deletion in cells of the developing long bones.

Our previous studies have shown that EZH2 inhibits human BMSC osteogenic differentiation by inhibiting expression of osteogenic genes via the methylation of H3K27 along the transcription start sites. Conversely, EZH2 promotes adipogenesis through the repression of inhibitors of adipogenesis and key regulators of the Wnt pathway by enzymatic modification of histone H3K27 (42,49). We have also discovered that EZH2 works in conjunction with its demethylase counterpart, KDM6A (UTX) as KDM6A promotes osteogenesis and inhibits adipogenesis by removing the H3K27 methylation mark (49). Given the importance of EZH2 in human osteoblast and adipocyte differentiation and that EZH2 knockout mice are embryonically lethal (36,51), we embarked on deciphering the *in vivo* function of EZH2 specifically in early mesenchyme to examine its effect on skeletogenesis.

Ezh2^{tm1Tara} (*Ezh2*$^{fl/fl}$) mice on a mixed background were backcrossed to 7 generations to achieve a C57BL/6 genetic background. The C57BL/6 *Ezh2*$^{fl/fl}$ females were then crossed with male B6.Cg-Tg*Prrx1*-cre1Cjt/J (*Prrx-1*-cre), transgenic driver mice. PRRX1 is expressed in early limb bud mesenchyme and a subset of craniofacial mesenchyme (7,67,68). Genotyping confirmed the generation of Prrx-1-*Ezh2*$^{wt/fl}$ heterozygous (*Ezh2*$^{+/-}$) and Prrx-1-*Ezh2*$^{fl/fl}$ homozygous (*Ezh2*$^{-/-}$) mice (Figure 1A). *Ezh2*$^{-/-}$ mice were under the expected mandolin ratio at birth and died shortly with only 3 mice surviving females until 4 weeks of age. *Ezh2*$^{+/-}$ and *Ezh2*$^{+/-}$ mice were born in the expected mandolin ratio. Knockout of EZH2 expression and activity was confirmed by analysing H3K27me3 using Western blot, RT-PCR and immunohistochemical analyses of passage five, 4 week old

hind limb compact bone derived MSC from *Ezh2*$^{+/-}$mice. The data showed a reduction in EZH2 protein and reduced expression of H3K7me3 modification compared with *Prrx-1* Cre (*Ezh2*$^{+/+}$) positive control mice (Figure 1B). Furthermore, total RNA was extracted from cultured MSC and *Ezh2* gene expression was analysed confirming *Ezh2* gene knockdown in *Ezh2*$^{+/-}$ mice (Figure 1C). Due to the presence of only three viable female *Ezh2*$^{-/-}$ mice we were unable to isolate MSC from these mice as they were used for Micro-CT and histological analysis. Therefore homozygous deletion of EZH2 was confirmed by the absence of EZH2 activity, using H3K27me3 immunohistochemistry staining of 4 week old femora. *Ezh2*$^{+/+}$ wildtype mice showed robust H3K27me3 staining of chondrocytes in the growth plate, osteoblasts lining the bone surfaces and osteocytes within the bone (Figure 1D&E). In contrast, *Ezh2*$^{+/-}$ mice showed reduced H3K27me3 staining in chondrocytes, osteoblasts and osteocytes, whereas *Ezh2*$^{-/-}$femurs showed a marked reduction in H3K27me3 expression *in situ* (Figure 1D&E). Positive EZH2 cells of the blood lineage were observed in all genotypes confirming EZH2 deletion was restricted to stromal cells where reduced H3K27me levels correlated to a dose dependent loss of EZH2 expression (Figure 1D).

4.5.2 EZH2 deletion in limb bud mesenchyme effect embryonic and postnatal skeletal patterning and size.

The phenotypic effects due to EZH2 deficiency in the mesenchymal stromal population were assessed during embryonic and postnatal skeletal development and bone homeostasis. As osteogenesis begins at E13.5 and mineralisation of the skeleton occurs from E14.5, E17.5 embryos were stained with alizarin red (bone) and alician blue (cartilage) to investigate skeletal morphology. The data showed that the wildtype E17.5 and newborn mice had normal skeletogenesis, of the fore and hind limbs, spine, ribs and the cranial

bones (Figure 2 A&B). Comparisons with Alizarin Red stained *Ezh2*$^{+/-}$ E17.5 embryos and high resolution images of newborn mice revealed an increase in overall skeleton size (Figure 2 A&B). However, *Ezh2*$^{-/-}$ E17.5 embryos exhibited a serve growth phenotype, with forelimb deformities obvious with the newborn mice (Figure 2 A&B). Given that no male *Ezh2*$^{-/-}$ mice were detected after birth we analysed the skeletons and long bones of new born female mice and Ezh2 heterozygous animals. Newborn *Ezh2*$^{+/-}$ female and male mice exhibited higher birth weights, whereas *Ezh2*$^{-/-}$ female mice weighed significantly less than *Ezh2*$^{+/+}$ control newborns (Figure 2C). Micro-CT Avizo 3D generated images of newborn mice further confirmed differences in skeletal size, and identified differences in the vertebrae and skulls (Figure 2D). *Ezh2*$^{-/-}$ mice had smaller vertebrae with a loss of the third sacral vertebrae compared with *Ezh2*$^{+/+}$ (Figure 2E). Differences in cranial bone patterning and formation was observed as early as E16.5. *Ezh2*$^{+/-}$ embryos exhibited an increase in size and mineralisation of the frontal and parietal bones. *Ezh2*$^{-/-}$ cranial defects were more prominent at E17.5 whilst still detectable at E16.5 with a distinct difference in cranial shape and increased cranial mineralisation and fusing of the frontal, parietal, and occipital sutures (Figure 2A&F and supplementary Table 1). Micro-CT imaging of newborn skulls further confirmed increased parietal and occipital bone sizes in *Ezh2*$^{+/-}$ mice with fusing of the frontal, parietal and occipital bone sutures indicative of craniosynostosis in *Ezh2*$^{-/-}$ newborns (Figure 2G and Table 3).

Interestingly, EZH2 deletion appeared to effect the formation and patterning of the fore and hind limbs. Alizarin red and alcian blue staining of *Ezh2*$^{+/-}$ fore limbs revealed longer limbs in newborn mice compared to wildtype controls (Figure 2H&I). Complete deletion of EZH2 was found to cause gross fore limb deformities and reduction in fore limb bone size at E17.5 and newborn, compared with *Ezh2*$^{+/+}$ embryos and newborns (Table 1).

Histological assessment found that the *Ezh2*$^{-/-}$ E17.5 and newborn scapula, humerus and ulna appeared markedly smaller, where *Ezh2*$^{-/-}$ humerus appeared cylindrical without the formation of the dorsal notch (Figure 2H&I). Relative to size, the forearms including humerus, radius and ulna showed more alizarin red staining in *Ezh2*$^{+-/-}$ and *Ezh2*$^{-/-}$ newborn forelimbs compared with *Ezh2*$^{+/+}$ newborn forelimbs (Figure 2I).

Changes in hind limb development were not as dramatic as the fore limbs, where the differences between femora, tibiae and fibulae lengths were smaller at E17.5 (Figure 2J & Table 2). Complete separation of tibiae and fibulae and absence of bone staining in the foot were observed only in the *Ezh2*$^{-/-}$ newborn hind limbs (Figure 2K). Quantitative analyses revealed a significant increase in all bones of the fore and hind limb in *Ezh2*$^{+/-}$ newborns, with a significant decrease in limb bone length in *Ezh2*$^{+/-}$ newborns, compared to wild type (Figure 2L-R). The length of E16.5 and E17.5 fore and hind limbs were measured using image J software and revealed increases in *Ezh2*$^{+/-}$ limb bone lengths and decreased in *Ezh2*$^{-/-}$ limb bone lengths, compared with *Ezh2*$^{+/+}$ controls (Table 1&2 and supplementary Table 1&2).

Collectively, these observations indicate that skeletal mineralisation developed at an accelerated rate in the *Ezh2*$^{+/-}$and *Ezh2*$^{-/-}$ mice, with a clear distinct patterning and growth defect that appeared to be EZH2 dose dependent. Moreover, there were less E16.5 *Ezh2*$^{-/-}$ embryos present implying that complete loss of EZH2 in the mesenchymal tissues is detrimental to embryogenesis (Data not shown).

4.5.3 Four week old mesenchymal specific deletion of *Ezh2* results in altered skeletal size and fore and hind limb mmorphology.

The effect of deleting one or both alleles of *Ezh2* in skeletal tissue was examined in 4 week old mice. X-ray analysis clearly showed that female *Ezh2*$^{+/-}$ mice were significantly larger than the wildtype mice, associated with longer limbs, spine and overall skeletal size (Figure 3A). However, loss of both *Ezh2* alleles resulted in *Ezh2*$^{-/-}$ mice with reduced body mass and significantly smaller shorter fore and hind limbs, spine and skull (Figure 3A). Moreover, significant increases in body weight were seen in 4 week old *Ezh2*$^{+/-}$ females and males compared to the *Ezh2*$^{+/+}$ mice, whereas the *Ezh2*$^{-/-}$ females were dramatically lighter than their Ezh2$^{+/+}$ counterpart reflecting their smaller overall size (Figure 3B). The same was evident for male *Ezh2*$^{+/-}$ mice, however, no male *Ezh2*$^{-/-}$ mice survived birth and therefore we have no data for these animals (Figure 3B&C).

The limbs of the female *Ezh2*$^{-/-}$ mice were somewhat abnormal and curved compared to the wildtype mice (Figure 3D). X-ray scans of 4week old fore limbs confirmed the decreased size and deformities of *Ezh2*$^{-/-}$ mice compared with *Ezh2*$^{+/+}$ mice. In contrast, *Ezh2*$^{+/-}$ fore limbs appeared slightly larger than *Ezh2*$^{+/+}$ mice (Figure 3D). The same was evident for the hind limbs, however, the effects were not as pronounced (Figure 3E). The lengths of the tibiae were measured using Image J software of histological sections. The data showed that tibiae were considerably longer for the *Ezh2*$^{+/-}$ mice, whereas the *Ezh2*$^{-/-}$ tibiae were significantly shorter compared to wildtype mice (Figure 3F). These findings were confirmed using Micro-CT 3D modelling (Figure 3G). The tibiae of *Ezh2*$^{-/-}$ mice also displayed an unusual tibial morphology with larger fibulae, running the whole length of the tibiae with abnormal attachment at the ankle (Figure 3G).

We next analysed the femora of 4 week old female mice. The length of the femora were found to be significantly increased in *Ezh2*$^{+/-}$, while *Ezh2*$^{+/-}$ mice exhibited decreased femoral length compared with wildtype control, calculated using the Micro-CT analysis (Figure 3H). The femora of *Ezh2*$^{-/-}$ mice showed an increase in size and differences in morphology of the epiphysis and diaphysis, which was considerably wider compared with *Ezh2*$^{+/+}$ femora (Figure 3I). Differences in bone shape and trabecular patterning was evident by Micro-CT scanning with trabeculae present throughout the whole shaft of the femora.

4.5.4 *Ezh2* deletion effects the size of the growth plate and cartilage zones.

As the growth plate is the area of longitudinal growth, an overall decrease in growth plate zones and length could be a contributing factor to the differences seen in tibial length for *Ezh2*$^{-/-}$ newborn mice. Assessment of growth plate size and area of the cartilage zones was performed for newborn and 4 week old mice, as measured by image J software from nanozommed imaged, Safranin O stained tissue sections (Figure 4A&B). *Ezh2* heterozygous deletion in newborn mice increased growth plate length, whilst heterozygous deletion decreased growth plate length (Figure 4C). Both *Ezh2*$^{+/-}$ and *Ezh2*$^{-/-}$ growth plates had a smaller resting cartilage zone length (Figure 4D). The proliferative and hypertrophic cartilage zone was larger in length in *Ezh2*$^{+/-}$ newborns compared with *Ezh2*$^{+/+}$ control (Figure 4E), whereas *Ezh2*$^{-/-}$ proliferative and hypertrophic cartilage zones were smaller in size when compared to *Ezh2*$^{+/+}$ newborn hypertrophic zone (Figure 4F).

Histological analysis of Safranin O stained sections showed a striking decrease in size from the epiphysis to the hypertrophic zone and significant reduction in growth plate depth in 4 week old *Ezh2*$^{-/-}$ tibiae (Figure 4G). The resting, proliferative and hypertrophic

cartilage zones were smaller in *Ezh2*$^{-/-}$ mice than *Ezh2*$^{+/-}$ and *Ezh2*$^{+/+}$ mice (Figure 4G-J). However unlike newborn mice, there were no differences in growth plate size and the cartilage zones in *Ezh2*$^{+/-}$ tibiae compared with *Ezh2*$^{+/+}$ tibial growth plates, at 4 weeks of age. These findings suggest that heterozygous deletion of EZH2 promotes early growth plate formation, however, by 4 weeks there is no difference in growth plate size and zones. However, complete ablation of EZH2 effected newborn and 4 week old growth plate development contributing to the shortening of the hind limbs.

4.5.5 Mesenchymal specific deletion of *Ezh2* results in altered hind limb bone microarchitecture.

Investigations into the role of EZH2 in bone microarchitecture revealed that trabecular bone was patterned throughout the *Ezh2*$^{-/-}$ newborn tibiae and 4 week old femora, where trabeculae were localised at the metaphysis of *Ezh2*$^{+/-}$ and *Ezh2*$^{+/+}$ long bones (Figure 5A&B). Micro-CT analysis showed that *Ezh2*$^{-/-}$ mice exhibited increased percentage of total trabecular bone proportional to tissue volume (BV/TV) within tibiae when compared to *Ezh2*$^{+/-}$ and *Ezh2*$^{+/+}$ mice (Figure 5C). However, there were no differences between trabeculae BV/TV for *Ezh2*$^{+/-}$ and *Ezh2*$^{+/+}$ newborns. Examination of trabecular parameters revealed increased trabeculae numbers (Tb.N) for *Ezh2*$^{-/-}$ mice compared to wild type mice, with no significant differences to *Ezh2*$^{+/-}$ mice (Figure 5D). Of note, no significant differences were evident between *Ezh2*$^{+/-}$ and wildtype mice except for an increased TV, BV (data not shown) and longer tibiae.

Micro-CT analysis of total trabecular bone in the femora of 4 week old female mice showed no differences in trabecular bone compared to wild type mice, when normalised to total volume for the *Ezh2*$^{+/-}$ mice. However, there was a clear increase in the percentage of trabecular bone in the femora of 4 week old *Ezh2*$^{-/-}$ mice compared to *Ezh2*$^{+/-}$ and *Ezh2*$^{+/-}$

mice (Figure 5E). Furthermore, 4 week old *Ezh2*$^{-/-}$ mice exhibited increases in trabecular number throughout the femora compared to *Ezh2*$^{+/-}$ and *Ezh2*$^{+/-}$ mice (Figure 5F), in accord with the analyses of new born tibiae. Overall, the newborn tibiae and 4 week old femora patterning defects altered the location and number of trabeculae throughout the long bones in *Ezh2*$^{-/-}$ animals.

Histological assessment of H&E stained tissue sections of 4 week old femora revealed a disorganized patterning of the cortical bone in *Ezh2*$^{-/-}$ mice compared to *Ezh2*$^{+/-}$ and *Ezh2*$^{+/-}$ mice (Figure 5G). This disorganised bone structure was similar to immature woven bone often associated with high bone turnover states. Micro-CT 3D modelling of a defined cortical bone region in the middle of the diaphysis demonstrated thinner cortical bones in *Ezh2*$^{+/-}$ and *Ezh2*$^{-/-}$ femora, compared to wild type controls (Figure 5H). Assessment of bone parameters found that *Ezh2*$^{-/-}$ mice exhibited decreased cortical BV/TV, and *Ezh2*$^{+/-}$ and *Ezh2*$^{-/-}$ mice displayed decreased cortical thickness (Ct.Th), compared to *Ezh2*$^{+/+}$ controls (Figure 5I&J).

Histomorphometric analysis of toluidine blue stained tibial sections (Figure 6A), revealed decreased BV/TV in secondary spongiosa trabeculae of *Ezh2*$^{-/-}$ mice compared with wildtype controls (Figure 6B). The secondary spongiosa trabeculae in *Ezh2*$^{-/-}$ mice were found to be significantly thicker with increased trabeculae spacing and decreased trabeculae number, when compared to *Ezh2*$^{+/+}$ and *Ezh2*$^{+/-}$ mice (Figure 6C-E). Furthermore, histomorphometric analysis of cortical bone demonstrated a decrease in percentage of cortical BV/TV and cortical thickness in *Ezh2*$^{-/-}$ and *Ezh2*$^{+/-}$ mice compared to wildtype mice, and between *Ezh2*$^{-/-}$ and *Ezh2*$^{+/-}$ mice (Figure 6F&G). Biomechanical testing was subsequently employed to assess bone structural integrity of 4 week old

femora. The data showed that the femora of 4 week old *Ezh2*$^{+/-}$ and *Ezh2*$^{-/-}$ mice exhibited decreased flexuralrigidty (stiffness), Yield load, Yield moment when compared to wildtype controls (Figure 6H-J).

4.5.6 Deletion of Ezh2 promotes increased bone formation and remodelling

To determine the effect of EZH2 deletion on bone trabeculae and cortical bone formation, mice were labelled with calcien 4 days and 24 hours prior to harvesting the limbs of 4 week old animals. Histological analysis of methacrylate embedded undecalcified tibial sections found two distinct fronts of calcien labelled newly formed secondary spongiosa trabeculae in *Ezh2*$^{+/-}$ and *Ezh2*$^{-/-}$ mice, compared to wildtype controls (Figure 7A). Quantification of trabeculae labelled with calcien in the secondary spongiosa found an increase in mineral apposition rate (MAR) and bone formation rate on bone surface (BFR/BS) in *Ezh2*$^{+/-}$ and *Ezh2*$^{-/-}$ mice compared to wildtype control mice (Figure 7B&C). A significantly higher BFR/BS was also observed in *Ezh2*$^{-/-}$ mice compared to *Ezh2*$^{+/-}$ mice. Similar studies showed that newly formed cortical bone in the middle of the diaphysis exhibited distinct calcien labelled fronts in *Ezh2*$^{+/-}$ and *Ezh2*$^{-/-}$ mice compared to wildtype control mice where the calcien labelled bone fronts had begun to merge (Figure 7D). An increase in MAR and BFR/BS was observed in *Ezh2*$^{+/-}$ and *Ezh2*$^{-/-}$ cortical bone when compared to wildtype controls (Figure 7E&F). Interestingly, both MAR and BFR/BS cortical bone parameters were significantly higher in the *Ezh2*$^{-/-}$ mice compared to the *Ezh2*$^{+/-}$ mice, associated with irregular bone mineralising fronts. Assessment of the rate of osteoclast mediated bone resorption found that *Ezh2*$^{+/-}$ and *Ezh2*$^{-/-}$ mice had significantly higher serum levels of TRAP and CTX-1, compared with control mice, while *Ezh2*$^{-/-}$ mice also expressed significantly higher serum levels of TRAP and CTX-1 compared with

Ezh2$^{+/-}$ mice (Figure 7G&H). These findings suggest a possible increase in osteoclast activity is associated with increased bone turnover rates in *Ezh2*$^{+/-}$ and *Ezh2*$^{-/-}$ mice.

Bone marrow (BM) was extracted from the long bones of *Ezh2*$^{+/-}$ and *Ezh2*$^{+/+}$ mice and treated with M-CSF and RANKL to induce osteoclast differentiation *in vitro*, in the absence of sufficient numbers of replicate Ezh2$^{-/-}$ mice. Differentiated multinucleated osteoclasts were assessed for TRAP activity and their ability to form resorption pits in dentine slices. *Ezh2*$^{+/-}$ derived bone marrow cells demonstrated a greater potential to form multinucleated TRAP positive osteoclasts compared with and *Ezh2*$^{+/+}$ mice (Figure 7I&J). Moreover, *Ezh2*$^{+/-}$ differentiated osteoclasts formed more dentin resorption pits than and *Ezh2*$^{+/+}$ differentiated osteoclasts (Figure 7K).

To determine whether EZH2 deficiency in MSC could affect the expression of pro-osteoclastic factors, gene expression levels of *M-csf*, *Rankl* and *Opg* were investigated in cultured BMSC. Real-time PCR analysis found that cultured BMSC derived from the hind limbs of *Ezh2*$^{+/-}$ mice expressed higher transcript levels of *M-csf*, *Rankl*, but no differences in *Opg* gene expression, compared to wildtype controls (Figure 7L-N). However, due to the low numbers of osteoclasts detected in histological sections we were unable to confirm an increase in osteoclast number on bone surfaces in *Ezh2*$^{+/-}$ and *Ezh2*$^{+/+}$ mice *in vivo*.

4.5.7 *Ezh2* deletion promoted osteogenic and adipogenic differentiation *in vitro* and *in vivo*.

We next examined whether differences in osteoblast numbers could contribute to the observed increases in trabeculae thickness and bone formation. Histomorphometric analysis of secondary spongiosa and cortical bone revealed an increase in the number of

cuboidal osteoblasts on the bone surfaces (N.Ob./B.Pm) in both *Ezh2*$^{+/-}$ and *Ezh2*$^{-/-}$ mice compared with *Ezh2*$^{+/+}$ controls (Figure 8A&B). These findings were supported by an increase in OCN levels detected in the serum of both *Ezh2*$^{+/-}$ and *Ezh2*$^{-/-}$ mice compared to *Ezh2*$^{+/+}$ serum samples (Figure 8C). These findings suggest that the increased number of osteoblasts in Ezh2 deficient mice could contribute to the observed increased MAR and BFR/BS and trabecular bone thickness.

The role of EZH2 deficiency in MSC differentiation *in vitro* was only assessed using *Ezh2*$^{+/-}$mice due to limited numbers of viable *Ezh2*$^{-/-}$ mice. Cultured BMSC derived from 4 week old hind limbs of *Ezh2*$^{+/-}$ mice produced significantly more alizarin red mineralised deposits and higher levels of extra cellular calcium, compared with *Ezh2*$^{+/+}$ BMSC under osteogenic inductive conditions (Figure 8D&E). Real-time PCR analysis found that *Ezh2*$^{+/-}$ BMSC expressed higher levels of the osteogenic associated genes, runt related transcription factor 2 (*Runx2),* bone gamma-carboxyglutamate protein (osteocalcin) *(Ocn),* and secreted phosphoprotein 1 (osteopontin) (*Opn*) compared to wildtype controls (Figure 8F-H). Furthermore, *Ezh2*$^{+/-}$ displayed increased numbers of clonogenic CFU-F with a greater proportion of alkaline phosphatase positive colonies, than *Ezh2*$^{+/+}$ BMSC (Figure 8I&J). The findings suggest that *Ezh2* heterozygous deletion increases the levels of BMSC osteogenic commitment and proportion of osteogenic precursors.

Histologically, the long bones of *Ezh2*$^{-/-}$ mice were filled with significantly more bone marrow adipose tissue compared to both *Ezh2*$^{+/-}$ and *Ezh2*$^{-/-}$ mice, suggesting complete ablation of EZH2 in murine MSC may promote adipogenic differentiation (Figure 9A&B). To identify if heterozygous *Ezh2* deletion promoted adipogenic differentiation *in vitro,* cultured BMSC from *Ezh2*$^{+/-}$ and *Ezh2*$^{+/+}$ mice were treated with adipogenic inductive

media. The data showed that cultured *Ezh2*$^{+/-}$ BMSC produced significantly higher levels of Nile Red and Oil Red O stained lipid-containing adipocytes, compared with wildtype control BMSC, cultured under adipogenic inductive conditions (Figure 9C&D). Real-time PCR analysis showed that *Ezh2*$^{+/-}$ BMSC expressed higher levels of adipogenic associated genes, peroxisome proliferator activated receptor gamma 2 *(Pparγ2)*, CCAAT/enhancer binding protein (*C/EBPα)* and adiponectin, C1Q and collagen domain containing (*AdipoQ)*, compared to wildtype controls (Figure 9E-G). These findings suggest that heterozygous deletion of *Ezh2* promoted both osteogenic and adipogenic differentiation *in vivo*.

4.6 Discussion

In Chapter 2 we showed, for the first time, that EZH2 acts together with KDM6A to regulate lineage commitment of human bone marrow derived MSC. EZH2 inhibits BMSC osteogenic differentiation and promotes adipogenic differentiation, while KDM6A promotes BMSC osteogenic differentiation and inhibits adipogenic differentiation. Our studies have shown that EZH2 acts directly on osteogenic genes methylating histone H3K27, whereas KDM6A removes the methylation of H3K27 promoting expression of these genes and osteogenic commitment (49). Chapter 4 investigated the *in vivo* function of EZH2 during skeletal development. Preliminary studies showed that EZH2 was the main enzyme responsible for H3K27me3 in mesenchymal derived skeletal tissues as deletion of EZH2 resulted in almost complete depletion of the modification mark, H3K27me3. Previous reports have described that the Ezh family member, Ezh1, known to be part of the PRC2 complex, can in some cases compensate for the absence of EZH2 (69). However, the presence of Ezh1 in Prrx-1-Ezh2$^{-/-}$ mice did not appear to compensate for the loss of H3K27me in mesenchymal derived skeletal tissues.

As early as E16.5, there was a marked decrease in the frequency of EZH2 deficient embryos, where all viable EZH2 deficient mice following birth were female with an overall reduction in expected mandolin numbers, illustrating that loss of EZH2 in skeletal tissue was detrimental to embryogenesis. The effects of EZH2 deficiency in early mesenchyme during embryogenesis resulted in an overall larger skeleton from E17.5 onwards, with increased bone mineralisation in femora, tibiae, vertebrae and the skull. The frontal, parietal and occipital bones were also larger with enhanced mineralisation and longer and more developed forearms and hind limbs. These effects indicated that osteogenesis occurred early during embryogenesis and at a faster rate compared with wildtype mice, and is in agreement with our previous study showing that EZH2 normally represses human BMSC osteogenic differentiation *in vitro and in vivo,* by inhibiting expression of osteogenic genes (49). The increased size and length of skeletal structures was indicative of an increased rate of skeletal development and premature formation of the skeleton. Complete deletion of *Ezh2,* however, showed a different phenotype, where the overall skeleton was significantly smaller than the wild type mice from E16.5 onwards. The tibiae, femora, forearms and hind limbs, vertebrae and skull were all significantly smaller. The frontal, parietal and occipital bone sutures were prematurely fused as the mice displayed characteristics of craniosynostosis (70,71). Complete ablation of *Ezh2* in early mesenchyme was also accompanied with dramatically increased mineralisation of the femora, tibiae, vertebrae and frontal, parietal and occipital bones to the extent where it was difficult to identify the sutures due to premature fusion. These studies confirm the findings of a recent paper by Dudakovic and colleagues reporting the role of EZH2 in skeletal development using the same *Prrx1* promoter driver (72). Their study observed a similar long bone and cranial phenotype in Prrx-1-*Ezh2*$^{-/-}$ newborn mice, however, there was no assessment of *Ezh2* heterozygous mice reported, nor the effects of Ezh2 deficiency in bone

remodelling. Complete ablation of EZH2 resulted in smaller mice with smaller skeletal structures including forearms, hind limbs, femur and tibia. Newborn growth plates also showed reduced distance from the articular surface to the hypertrophic zone. Similar to our findings, Dudakovic and colleagues showed that EZH2 deficient newborn mice displayed craniosynostosis with premature fusion of the coronal sutures. Micro-CT analysis of 3 week old tibias showed no effect on trabecular thickness but did show a decrease in trabecular spacing and trabecular number. However their analysis of the trabecular involved only the measurement of the trabeculae directly under the growth plate in the primary spongiosa. This is in contrast to our findings as we measured the trabeculae throughout the whole bone spanning from underneath the growth plate, throughout the diaphysis and the proximal epiphyseal area as we observed that the trabeculae were more dispersed and not concentrated just under the growth plate. Notably, the study by Dudakovic *et al.* did not evaluate cortical bone parameters or osteoclastogenesis. The present study observed a significant increase in osteoclast activity, which appeared to counteract the increased rate of new bone formation as evident by the calcien staining in *Ezh2* deficient mice.

Micro-CT 3D imaging of EZH2 deficient newborn mice identified osteolytic pit-like structures, where the bone in the skull appeared disorganised and porous, which was associated with a distinct craniosynostosis phenotype in $Ezh2^{-/-}$ newborn mic and as early as E17.5. The study by Dudakovic and colleagues reported that the development of craniosynostosis was due to an increased maturation of osteoblasts in the skull. Therefore, EZH2 appears to be important for the cranial bone patterning through increased osteoblast maturation and function leading to pre-fusion of the cranial sutures. It would be of interest in future experiments to investigate the effect of EZH2 deletion in cranial suture stem cells

based on their expression of the zinc finger transcription factor, Gli1, and whether interactions between these two factors lead to any functional consequences (73). In addition, previous studies in our laboratory have reported that Twist-1 induces EZH2 recruitment to preventing cellular senescence in BMSC and mutation in Twist-1 cause craniosynostosis (21). It would therefore, be of interest to determine if EZH2 and Twist-1 are co-regulated during cranial suture development particularly in Gli1 positive cells.

Postnatally, Prrx-1-Ezh2 deficient mice exhibited similar but more pronounced features as seen during embryogenesis, with *Ezh2*$^{+/-}$ mice exhibiting lager skeletal structures and Ezh2$^{-/-}$ displaying smaller skeletal structures and clinodactyly. The smaller size in *Ezh2*$^{-/-}$ skeletal structures could partly be explained by differences in growth plate formation within the tibiae of EZH2 deficient mice. Reduction in the levels of *Ezh2* had a significant effect on growth plate size and chondrocyte zones in newborn mice, however this effect was not seen at 4 weeks of age, suggesting the importance of EZH2 in the developing embryonic growth plate. Complete removal of *Ezh2* caused a reduced distance from the articular surface to the hypertrophic zone, which was less pronounced in the Ezh2$^{+/-}$ animals. The proliferative zone was also diminished in the *Ezh2*$^{-/-}$ animals, as was the hypertrophic zone. The growth plate effects in Ezh2 heterozygous mice could potentially be explained by the de-repression of HOXC8. Previously, HOXC8 has been shown to be de-repressed in *Ezh2* Wnt1 conditional knockouts causing neural crest cartilage and bone deformities (48). HOXC8 expression in endochondral growth plate promoted chondrocyte proliferation and inhibition of cartilage hypertrophy (74). Therefore, it is possible that HOXC8 is also de-repressed in the growth plate of Prrx-1-Ezh2$^{+/-}$ mice, leading to an increased proliferative zone and contribution to a larger growth plate size. Furthermore, these results indicated that in the absence of EZH2, the process of endochondral ossification is deregulated, where

the proliferation or survival of chondrocytes is compromised leading to increased hypertrophy, and shorter long bone sizes even though the amount of bone per volume has increased.

Previous studies have shown that anteroposterior limb axis formation involves specification of MSC positional identity along the axis followed by commitment and differentiation, where diffusible factors specify the positional identity of MSC (75,76). Differentiation then occurs from a proximal to distal order (44). This process was found to be under the tight control of Hox gene linear expression in particular Hox9/10/11 and 13. Moreover, EZH2 has been found to be essential in anteroposterior axial patterning as it affects many factors including Gli-3 and Hand2 expression, which is essential in this process (77,78). EZH2 has a dual role as a repressor and activator of Hox gene expression, effecting early limb formation by prevents ectopic Hox gene expression (79) and then maintaining Hox gene expression to enforce positional identities in the maturing limb bud. In a study examining the deletion of *Ezh2* in limb buds, EZH2 was found to be essential for proximodistal elongation and anterioposteior patterning of limb segments due to altered Hox gene expression patterns (44). The present study observed a similar phenotype in Prrx-1-Ezh2 deficient mice, which could be due to increased chondrogenic hypertrophy, involving the exit of cell cycle, enlarging of chondrocytes and subsequent apoptosis, resulting in the shortening of the limbs.

Micro-CT analysis showed that there was an increase in trabecular bone present throughout the whole length of the long bones, associated with increased trabeculae number. Therefore homozygous deletion of EZH2 affected the patterning of the trabeculae and substantially increased trabeculae number within the long bones, yet the overall size of the bones had

decreased due to deregulation of the growth plate possibly due to effects on proliferation or survival of chondrocytes. Calcien staining of newly formed mineralised bone surfaces supported the notion that loss of EZH2 accelerates osteogenesis for both trabecular and cortical bone. However, due to patterning defects there was less trabecular bone and number in the secondary spongiosa, which were thicker in size with increased numbers of osteoblasts on the bone surfaces. Increased numbers of osteoblasts were also present on the periosteal and endosteal surfaces of the bone with an increase in MAR and BFR/BS values, however, the bone is appeared to be formed in a disorganised manner akin to woven bone. Biomechanical testing of femurs revealed the bones were less stiff and required less load before catastrophic failure, which could be attributed to thinner and disorganised cortical bone. Higher levels of osteoblast activity in EZH2 deficient mice was confirmed by elevated serum levels of osteocalcin (OCN). However it is important to note that total osteocalcin levels were assessed containing both carboxylated and uncarboxylated forms of OCN (80). Carboxylated OCN is produced by osteoblasts, whereas uncarboxylated OCN is released during bone matrix resorption by osteoclasts. Therefore in this study we cannot deduce if the increase serum OCN is attributed solely to increased osteoblast activity, bone reabsorption or both (81,82) Furthermore we confirmed that BMSC isolated from *Ezh2*$^{+/-}$ mice exhibited higher osteogenic differentiation potential *in vitro* than wildtype BMSC, which correlated with increased gene expression levels of the osteogenic master regulatory transcription factor, *Runx2*, and its downstream bone associated gene targets, *Opn* and *Ocn*. Moreover, *Ezh2*$^{+/-}$ mice were found to exhibit a higher incidence of alkaline phosphatase positive CFU-F compared to wildtype mice, indicating that EZH2 deficiency promoted BMSC osteogenic commitment, in accord with our human BMSC studies (49).

Disorganised bone has been identified in high bone turnover states potentially suggesting deregulation of bone being laid down and/or increased rates of bone remodelling in the Ezh2$^{-/-}$ mice. Furthermore, decreased cortical bone thickness was observed in 4 week old *Ezh2*$^{+/-}$ and *Ezh2*$^{-/-}$ mice. Whilst, the increase in newly formed bone was evident by calcien staining in *Ezh2* deficient mice, there was no overall increase in cortical bone possibly due to a high resorption rate through increased osteoclast activity. Therefore, deletion of *Ezh2* in MSC may trigger increased osteoclast activity either through increased paracrine stimulation of osteoclast numbers or their recruitment to bone. Therefore increases in bone resorption activity in Ezh2 deficient mice could counteract any increases in bone formation. This notion was supported by increases in the serum levels of the resorption markers, TRAP and CTX-1, in 4 week old *Ezh2*$^{+/-}$ and *Ezh2*$^{-/-}$ mice, compared to wildtype controls. Furthermore, there was an increase in TRAP positive multinucleated *vitro* differentiated osteoclasts derived from bone marrow cells isolated from *Ezh2*$^{+/-}$ than *Ezh2*$^{+/+}$ control mice. The present study confirmed that *Ezh2*$^{+/-}$ BMSC expressed increased gene expression levels of the osteoclast inductive factors, *M-csf* and *Rankl*, however, the levels of the RANKL decoy receptor, *Opg*, were unchanged compared to control mice. This is an interesting finding and could possibly involve the de-repression of a secreted factor that activates osteoclasts when EZH2 is eliminated in MSC.

The adipogenic potential of Prrx-1-Ezh2$^{+/-}$ BMSC *in vitro* was found to be enhanced, correlating to the striking increase in bone marrow adipose tissue *in situ*, where the whole bone diaphysis was completely filled with adipocytes in new born and 4 week old Ezh2 deficient mice. However, these observations were contrary to studies showing that adipogenesis is decreased in human BMSC following *Ezh2* knockdown (49), or when *Ezh2* has been deleted specifically in pre-adipocytes in mice (42). These findings suggest that

the function of EZH2 in adipogenesis is stage specific, where deletion of *Ezh2* in the early limb bub mesenchyme stage seems to result in an overall alleviation of repression for both adipocyte and osteoblast lineages. Although the effect of EZH2 on adipogenesis has been shown to be due to its ability to inhibit the Wnt genes, which normally inhibits adipogenesis, removal of EZH2 at the MSC stage possibly alleviates repression of adipogenic genes directly or the expression of another pathway that influences adipogenesis resulting in increased adipocytes. Therefore, it is unclear which populations of BMSC derived from the early PRRX1 MSC are targeted during EZH2 deletion potentially contributing to differences in bone and fat formation. Future studies using lineage tracing may provide us with a understanding of the MSC subpopulations regulated by EZH2 during early limb bud formation and postnatal bone homeostasis. Furthermore, using known osteogenic or adipogenic cre drivers like Osterix or Adiponectin, respectively, would further confirm the role of EZH2 in osteoblast and adipocyte function in *vivo*.

Overall, reducing EZH2 or complete removal of EZH2 caused increased skeletal development and osteogenesis with a premature onset of osteogenesis during embryogenesis and cranial defects including craniosynostosis. Complete removal of Ezh2 resulted in patterning defects and smaller animals presumable due to effects on *Hox* gene patterning. There was an overall increase in bone remodelling and turnover as osteoclast activity was increased to counteract the increase in bone being formed. With EZH2 being the main enzyme responsible for H3K27me3 in mesenchymal tissue, its removal resulted in increased osteogenic gene expression driving osteogenesis. The skeletal defects described in our study following EZH2 deletion in mesenchyme tissue is similar to that seen in human patients who carry autosomal dominant mutations in *Ezh2* in a condition

known as Weaver syndrome. Their bones grow and develop more quickly both before and after birth, where adults are generally taller, display clinodactylyly especially in the fingers, a larger head (marcocephaly) and craniosynostosis (83). Their general overgrowth and advanced bone age suggests that the skeletal stem cell pool may undergo premature cellular senescence and maturation as we have previously demonstrated with genetically manipulated human BMSC and cranial bone cells isolated from Saethre-Chotzen patients who exhibit craniosynostosis and other skeletal deformities (21,49). A better understanding of the molecular pathways targeted by Ezh2 activity during BMSC maintenance and differentiation may help identify new therapeutic drug targets to treat these congenital bone disorders. These studies have also shed some light on the potential use of EZH2 inhibitors in bone related diseases such as osteoporosis. Based on our work the inhibition of EZH2 activity would be beneficial but the near complete inhibition of EZH2 would be detrimental as chondrocyte hypertrophy and MSC proliferation or survival will be affected compromising bone quality particularly in growing long bones. Furthermore, the use of EZH2 inhibitors could cause an increase in osteoclast activity and bone resorption hence anti-resporptive drugs would need to be considered in combination.

4.7 References

1. Friedenstein, A. J. (1980) Stromal mechanisms of bone marrow: Cloning in vitro and retransplantation in vivo. *Immunology of Bone Marrow Transplantation, ed.Thienfelder, S. Springer-Verlag, Berlin,* , p. 19.
2. Pittenger, M. F., Mackay, A. M., Beck, S. C., Jaiswal, R. K., Douglas, R., Mosca, J. D., Moorman, M. A., Simonetti, D. W., Craig, S., and Marshak, D. R. (1999) Multilineage potential of adult human mesenchymal stem cells. *Science* **284**, 143-147
3. Owen, M., and Friedenstein, A. J. (1988) Stromal stem-cells marrow-derived osteogenic precursors *Ciba Foundation Symposia* **136**, 42-60
4. Gronthos, S., Zannettino, A. C. W., Hay, S. J., Shi, S. T., Graves, S. E., Kortesidis, A., and Simmons, P. J. (2003) Molecular and cellular characterisation of highly purified stromal stem cells derived from human bone marrow. *Journal of Cell Science* **116**, 1827-1835
5. Sacchetti, B., Funari, A., Michienzi, S., Di Cesare, S., Piersanti, S., Saggio, I., Tagliafico, E., Ferrari, S., Robey, P. G., and Riminucci, M. (2007) Self-renewing osteoprogenitors in bone marrow sinusoids can organize a hematopoietic microenvironment. *Cell* **131**, 324-336
6. Morrison, S. J., and Scadden, D. T. (2014) The bone marrow niche for haematopoietic stem cells. *Nature* **505**, 327-334
7. Logan, M., Martin, J. F., Nagy, A., Lobe, C., Olson, E. N., and Tabin, C. J. (2002) Expression of Cre Recombinase in the developing mouse limb bud driven by a Prxl enhancer. *Genesis* **33**, 77-80
8. Mignone, J. L., Kukekov, V., Chiang, A. S., Steindler, D., and Enikolopov, G. (2004) Neural stem and progenitor cells in nestin-GFP transgenic mice. *Journal of Comparative Neurology* **469**, 311-324
9. Houlihan, D. D., Mabuchi, Y., Morikawa, S., Niibe, K., Araki, D., Suzuki, S., Okano, H., and Matsuzaki, Y. (2012) Isolation of mouse mesenchymal stem cells on the basis of expression of Sca-1 and PDGFR-α. *nature protocols* **7**, 2103-2111
10. Greenbaum, A., Hsu, Y. M., Day, R. B., Schuettpelz, L. G., Christopher, M. J., Borgerding, J. N., Nagasawa, T., and Link, D. C. (2013) CXCL12 in early mesenchymal progenitors is required for haematopoietic stem-cell maintenance. *Nature* **495**, 227-230
11. Zhou, B. O., Yue, R., Murphy, M. M., Peyer, J. G., and Morrison, S. J. (2014) Leptin-receptor-expressing mesenchymal stromal cells represent the main source of bone formed by adult bone marrow. *Cell stem cell* **15**, 154-168
12. Worthley, D. L., Churchill, M., Compton, J. T., Tailor, Y., Rao, M., Si, Y., Levin, D., Schwartz, M. G., Uygur, A., and Hayakawa, Y. (2015) Gremlin 1 identifies a skeletal stem cell with bone, cartilage, and reticular stromal potential. *Cell* **160**, 269-284
13. Komori, T. (2010) Regulation of bone development and extracellular matrix protein genes by RUNX2. *Cell and tissue research* **339**, 189-195
14. Komori, T. (2006) Regulation of osteoblast differentiation by transcription factors. *Journal of cellular biochemistry* **99**, 1233-1239
15. Ducy, P., Zhang, R., Geoffroy, V., Ridall, A. L., and Karsenty, G. (1997) Osf2/Cbfa1: a transcriptional activator of osteoblast differentiation. *cell* **89**, 747-754
16. Bi, W., Deng, J. M., Zhang, Z., Behringer, R. R., and de Crombrugghe, B. (1999) Sox9 is required for cartilage formation. *Nature genetics* **22**, 85-89
17. Tontonoz, P., Hu, E., Graves, R. A., Budavari, A. I., and Spiegelman, B. M. (1994) mPPAR gamma 2: tissue-specific regulator of an adipocyte enhancer. *Genes & development* **8**, 1224-1234
18. Shi, S. T., Gronthos, S., Chen, S. Q., Reddi, A., Counter, C. M., Robey, P. G., and Wang, C. Y. (2002) Bone formation by human postnatal bone marrow stromal stem cells is enhanced by telomerase expression. *Nature Biotechnology* **20**, 587-591
19. Simonsen, J. L., Rosada, C., Serakinci, N., Justesen, J., Stenderup, K., Rattan, S. I. S., Jensen, T. G., and Kassem, M. (2002) Telomerase expression extends the proliferative life-span and maintains the osteogenic potential of human bone marrow stromal cells. *Nat Biotech* **20**, 592-596

20. Isenmann, S., Cakouros, D., Zannettino, A., Shi, S. T., and Gronthos, S. (2007) hTERT transcription is repressed by cbfal in human mesenchymal stem cell Populations. *Journal of Bone and Mineral Research* **22**, 897-906
21. Cakouros, D., Isenmann, S., Cooper, L., Zannettino, A., Anderson, P., Glackin, C., and Gronthos, S. (2012) Twist-1 Induces Ezh2 Recruitment Regulating Histone Methylation along the Ink4A/Arf Locus in Mesenchymal Stem Cells. *Molecular and Cellular Biology* **32**, 1433-1441
22. Boyer, L. A., Plath, K., Zeitlinger, J., Brambrink, T., Medeiros, L. A., Lee, T. I., Levine, S. S., Wernig, M., Tajonar, A., and Ray, M. K. (2006) Polycomb complexes repress developmental regulators in murine embryonic stem cells. *nature* **441**, 349-353
23. Lee, T. I., Jenner, R. G., Boyer, L. A., Guenther, M. G., Levine, S. S., Kumar, R. M., Chevalier, B., Johnstone, S. E., Cole, M. F., and Isono, K.-i. (2006) Control of developmental regulators by Polycomb in human embryonic stem cells. *Cell* **125**, 301-313
24. Kouzarides, T. (2007) SnapShot: Histone-Modifying Enzymes. *Cell* **128**, 802.e801-802.e802
25. Kouzarides, T. (2007) Chromatin Modifications and Their Function. *Cell* **128**, 693-705
26. Duncan, I. M. (1982) Polycomblike: a gene that appears to be required for the normal expression of the bithorax and antennapedia gene complexes of Drosophila melanogaster. *Genetics* **102**, 49-70
27. Denell, R. (1978) Homoeosis in Drosophila. II. A genetic analysis of Polycomb. *Genetics* **90**, 277
28. Margueron, R., and Reinberg, D. (2011) The Polycomb complex PRC2 and its mark in life. *Nature* **469**, 343-349
29. Vandamme, J., Völkel, P., Rosnoblet, C., Le Faou, P., and Angrand, P.-O. (2011) Interaction proteomics analysis of polycomb proteins defines distinct PRC1 complexes in mammalian cells. *Molecular & Cellular Proteomics* **10**, M110. 002642
30. Francis, N. J., Kingston, R. E., and Woodcock, C. L. (2004) Chromatin compaction by a polycomb group protein complex. *Science* **306**, 1574-1577
31. Li, G., and Reinberg, D. (2011) Chromatin higher-order structures and gene regulation. *Current opinion in genetics & development* **21**, 175-186
32. Bulger, M., and Groudine, M. (1999) Looping versus linking: toward a model for long-distance gene activation. *Genes & development* **13**, 2465-2477
33. Zhu, J., Adli, M., Zou, J. Y., Verstappen, G., Coyne, M., Zhang, X., Durham, T., Miri, M., Deshpande, V., and De Jager, P. L. (2013) Genome-wide chromatin state transitions associated with developmental and environmental cues. *Cell* **152**, 642-654
34. Aloia, L., Di Stefano, B., and Di Croce, L. (2013) Polycomb complexes in stem cells and embryonic development. *Development* **140**, 2525-2534
35. Richly, H., Aloia, L., and Di Croce, L. (2011) Roles of the Polycomb group proteins in stem cells and cancer. *Cell Death Dis* **2**, e204
36. O'Carroll, D., Erhardt, S., Pagani, M., Barton, S. C., Surani, M. A., and Jenuwein, T. (2001) The Polycomb-group gene Ezh2 is required for early mouse development. *Molecular and Cellular Biology* **21**, 4330-4336
37. Ezhkova, E., Pasolli, H. A., Parker, J. S., Stokes, N., Su, I.-h., Hannon, G., Tarakhovsky, A., and Fuchs, E. (2009) Ezh2 orchestrates gene expression for the stepwise differentiation of tissue-specific stem cells. *Cell* **136**, 1122-1135
38. de Haan, G., and Gerrits, A. (2007) Epigenetic control of hematopoietic stem cell aging - The case of Ezh2. in *Hematopoietic Stem Cells Vi* (Kanz, L., Weisel, K. C., Dick, J. E., and Fibbe, W. E. eds.), Blackwell Publishing, Oxford. pp 233-239
39. Caretti, G., Di Padova, M., Micales, B., Lyons, G. E., and Sartorelli, V. (2004) The Polycomb Ezh2 methyltransferase regulates muscle gene expression and skeletal muscle differentiation. *Genes Dev* **18**, 2627-2638
40. Sher, F., Rößler, R., Brouwer, N., Balasubramaniyan, V., Boddeke, E., and Copray, S. (2008) Differentiation of neural stem cells into oligodendrocytes: involvement of the polycomb group protein Ezh2. *Stem Cells* **26**, 2875-2883

41. Su, I. H., Basavaraj, A., Krutchinsky, A. N., Hobert, O., Ullrich, A., Chait, B. T., and Tarakhovsky, A. (2003) Ezh2 controls B cell development through histone H3 methylation and Igh rearrangement. *Nature Immunology* **4**, 124-131
42. Wang, L., Jin, Q., Lee, J. E., Su, I. h., and Ge, K. (2010) Histone H3K27 methyltransferase Ezh2 represses Wnt genes to facilitate adipogenesis. *Proceedings of the National Academy of Sciences* **107**, 7317-7322
43. Wei, Y., Chen, Y.-H., Li, L.-Y., Lang, J., Yeh, S.-P., Shi, B., Yang, C.-C., Yang, J.-Y., Lin, C.-Y., Lai, C.-C., and Hung, M.-C. (2010) CDK1-dependent phosphorylation of EZH2 suppresses methylation of H3K27 and promotes osteogenic differentiation of human mesenchymal stem cells. *Nature Cell Biology* **13**, 87-94
44. Wyngaarden, L. A., Delgado-Olguin, P., Su, I. H., Bruneau, B. G., and Hopyan, S. (2011) Ezh2 regulates anteroposterior axis specification and proximodistal axis elongation in the developing limb. *Development.* **138**, 3759-3767. doi: 3710.1242/dev.063180. Epub 062011 Jul 063127.
45. Yu, Y. L., Chou, R. H., Chen, L. T., Shyu, W. C., Hsieh, S. C., Wu, C. S., Zeng, H. J., Yeh, S. P., Yang, D. M., Hung, S. C., and Hung, M. C. (2011) EZH2 Regulates Neuronal Differentiation of Mesenchymal Stem Cells through PIP5K1C-dependent Calcium Signaling. *Journal of Biological Chemistry* **286**, 9657-9667
46. Kamminga, L. M., Bystrykh, L. V., de Boer, A., Houwer, S., Douma, J., Weersing, E., Dontje, B., and de Haan, G. (2006) The Polycomb group gene Ezh2 prevents hematopoietic stem cell exhaustion. *Blood* **107**, 2170-2179
47. Qin, G., Chen, L., Ma, Y., Kim, E. Y., Yu, W., Schwartz, R. J., Qian, L., and Wang, J. (2012) Conditional Ablation of Ezh2 in Murine Hearts Reveals Its Essential Roles in Endocardial Cushion Formation, Cardiomyocyte Proliferation and Survival. *PLoS ONE* **7**, e31005
48. Schwarz, D., Varum, S., Zemke, M., Scholer, A., Baggiolini, A., Draganova, K., Koseki, H., Schubeler, D., and Sommer, L. (2014) Ezh2 is required for neural crest-derived cartilage and bone formation. *Development.* **141**, 867-877. doi: 810.1242/dev.094342.
49. Hemming, S., Cakouros, D., Isenmann, S., Cooper, L., Menicanin, D., Zannettino, A., and Gronthos, S. (2014) EZH2 and KDM6A Act as an Epigenetic Switch to Regulate Mesenchymal Stem Cell Lineage Specification. *Stem Cells.* **32**, 802-815. doi: 810.1002/stem.1573.
50. Isenmann, S., Arthur, A., Zannettino, A. C., Turner, J. L., Shi, S., Glackin, C. A., and Gronthos, S. (2009) TWIST Family of Basic Helix-Loop-Helix Transcription Factors Mediate Human Mesenchymal Stem Cell Growth and Commitment. *Stem cells* **27**, 2457-2468
51. Huang, X. J., Wang, X., Ma, X., Sun, S. C., Zhou, X., Zhu, C., and Liu, H. (2014) EZH2 is essential for development of mouse preimplantation embryos. *Reprod Fertil Dev* **26**, 1166-1175
52. Hirabayashi, Y., Suzki, N., Tsuboi, M., Endo, T. A., Toyoda, T., Shinga, J., Koseki, H., Vidal, M., and Gotoh, Y. Polycomb Limits the Neurogenic Competence of Neural Precursor Cells to Promote Astrogenic Fate Transition. *Neuron* **63**, 600-613
53. Nguyen, T. M., Arthur, A., Hayball, J. D., and Gronthos, S. (2013) EphB and Ephrin-B interactions mediate human mesenchymal stem cell suppression of activated T-cells. *Stem cells and development* **22**, 2751-2764
54. Cakouros, D., Isenmann, S., Hemming, S. E., Menicanin, D., Camp, E., Zannetinno, A. C. W., and Gronthos, S. (2015) Novel Basic Helix–Loop–Helix Transcription Factor Hes4 Antagonizes the Function of Twist-1 to Regulate Lineage Commitment of Bone Marrow Stromal/Stem Cells. *Stem cells and development* **24**, 1297-1308
55. Vandyke, K., Dewar, A. L., Diamond, P., Fitter, S., Schultz, C. G., Sims, N. A., and Zannettino, A. C. (2010) The tyrosine kinase inhibitor dasatinib dysregulates bone remodeling through inhibition of osteoclasts in vivo. *Journal of Bone and Mineral Research* **25**, 1759-1770
56. Fitter, S., Vandyke, K., Schultz, C. G., White, D., Hughes, T. P., and Zannettino, A. C. (2013) Plasma adiponectin levels are markedly elevated in imatinib-treated chronic

myeloid leukemia (CML) patients: a mechanism for improved insulin sensitivity in type 2 diabetic CML patients? , Endocrine Society
57. Isenmann, S., Arthur, A., Zannettino, A. C. W., Turner, J. L., Shi, S. T., Glackin, C. A., and Gronthos, S. (2009) TWIST Family of Basic Helix-Loop-Helix Transcription Factors Mediate Human Mesenchymal Stem Cell Growth and Commitment. *Stem Cells* **27**, 2457-2468
58. Parfitt, A. M., Drezner, M. K., Glorieux, F. H., Kanis, J. A., Malluche, H., Meunier, P. J., Ott, S. M., and Recker, R. R. (1987) Bone histomorphometry: standardization of nomenclature, symbols, and units. Report of the ASBMR Histomorphometry Nomenclature Committee. *J Bone Miner Res* **2**, 595-610
59. Bouxsein, M. L., Boyd, S. K., Christiansen, B. A., Guldberg, R. E., Jepsen, K. J., and Müller, R. (2010) Guidelines for assessment of bone microstructure in rodents using micro–computed tomography. *Journal of bone and mineral research* **25**, 1468-1486
60. Baron, R. (2000) Anatomy and Ultrastructure of Bone - Histogenesis, Growth and Remodeling. in *Endotext* (De Groot, L. J., Beck-Peccoz, P., Chrousos, G., Dungan, K., Grossman, A., Hershman, J. M., Koch, C., McLachlan, R., New, M., Rebar, R., Singer, F., Vinik, A., and Weickert, M. O. eds.), MDText.com, Inc., South Dartmouth MA. pp
61. Schriefer, J. L., Robling, A. G., Warden, S. J., Fournier, A. J., Mason, J. J., and Turner, C. H. (2005) A comparison of mechanical properties derived from multiple skeletal sites in mice. *J Biomech* **38**, 467-475
62. Arthur, A., Panagopoulos, R. A., Cooper, L., Menicanin, D., Parkinson, I. H., Codrington, J. D., Vandyke, K., Zannettino, A. C., Koblar, S. A., Sims, N. A., Matsuo, K., and Gronthos, S. (2013) EphB4 enhances the process of endochondral ossification and inhibits remodeling during bone fracture repair. *J Bone Miner Res* **28**, 926-935
63. Vandyke, K., Dewar, A., Fitter, S., Menicanin, D., To, L., Hughes, T., and Zannettino, A. (2009) Imatinib mesylate causes growth plate closure in vivo. *Leukemia* **23**, 2155-2159
64. McNeil, P. J., Durbridge, T. C., Parkinson, I. H., and Moore, R. J. (1997) Simple method for the simultaneous demonstration of formation and resorption in undecalcified bone embedded in methyl methacrylate. *Journal of histotechnology* **20**, 307-311
65. Mrozik, K. M., Gronthos, S., Menicanin, D., Marino, V., and Bartold, P. M. (2012) Effect of coating Straumann Bone Ceramic with Emdogain on mesenchymal stromal cell hard tissue formation. *Clin Oral Investig* **16**, 867-878
66. Cantley, M., Fairlie, D., Bartold, P., Rainsford, K., Le, G., Lucke, A., Holding, C., and Haynes, D. (2011) Inhibitors of histone deacetylases in class I and class II suppress human osteoclasts in vitro. *Journal of cellular physiology* **226**, 3233-3241
67. ten Berge, D., Brouwer, A., Korving, J., Martin, J. F., and Meijlink, F. (1998) Prx1 and Prx2 in skeletogenesis: roles in the craniofacial region, inner ear and limbs. *Development* **125**, 3831-3842
68. Lu, M. F., Cheng, H. T., Kern, M. J., Potter, S. S., Tran, B., Diekwisch, T. G., and Martin, J. F. (1999) prx-1 functions cooperatively with another paired-related homeobox gene, prx-2, to maintain cell fates within the craniofacial mesenchyme. *Development* **126**, 495-504
69. Mochizuki-Kashio, M., Aoyama, K., Sashida, G., Oshima, M., Tomioka, T., Muto, T., Wang, C., and Iwama, A. (2015) Ezh2 loss in hematopoietic stem cells predisposes mice to develop heterogeneous malignancies in an Ezh1-dependent manner. *Blood* **126**, 1172-1183
70. Anderson, P. J. (2007) The human cranial sutures in health and disease.
71. Slomic, A., Bernier, J., Morissette, J., and Renier, D. (1991) A craniometric study of bicoronal craniosynostosis (BCC). *Journal of craniofacial genetics and developmental biology* **12**, 174-181
72. Dudakovic, A., Camilleri, E. T., Xu, F., Riester, S. M., McGee-Lawrence, M. E., Bradley, E. W., Paradise, C. R., Lewallen, E. A., Thaler, R., Deyle, D. R., Larson, A. N., Lewallen, D. G., Dietz, A. B., Stein, G. S., Montecino, M. A., Westendorf, J. J., and van Wijnen, A. J. (2015) Epigenetic Control of Skeletal Development by the Histone Methyltransferase Ezh2. *J Biol Chem*

73. Zhao, H., Feng, J., Ho, T.-V., Grimes, W., Urata, M., and Chai, Y. (2015) The suture provides a niche for mesenchymal stem cells of craniofacial bones. *Nat Cell Biol* **17**, 386-396
74. Kruger, C., and Kappen, C. (2010) Expression of cartilage developmental genes in Hoxc8- and Hoxd4-transgenic mice. *PLoS One* **5**, e8978
75. Cooper, K. L., Hu, J. K.-H., ten Berge, D., Fernandez-Teran, M., Ros, M. A., and Tabin, C. J. (2011) Initiation of proximal-distal patterning in the vertebrate limb by signals and growth. *Science* **332**, 1083-1086
76. Roselló-Díez, A., Ros, M. A., and Torres, M. (2011) Diffusible signals, not autonomous mechanisms, determine the main proximodistal limb subdivision. *Science* **332**, 1086-1088
77. Mo, R., Freer, A. M., Zinyk, D. L., Crackower, M. A., Michaud, J., Heng, H., Chik, K. W., Shi, X.-M., Tsui, L.-C., and Cheng, S. H. (1997) Specific and redundant functions of Gli2 and Gli3 zinc finger genes in skeletal patterning and development. *Development* **124**, 113-123
78. Xu, B., and Wellik, D. M. (2011) Axial Hox9 activity establishes the posterior field in the developing forelimb. *Proceedings of the National Academy of Sciences* **108**, 4888-4891
79. Vargesson, N., Clarke, J., Vincent, K., Coles, C., Wolpert, L., and Tickle, C. (1997) Cell fate in the chick limb bud and relationship to gene expression. *Development* **124**, 1909-1918
80. Hauschka, P. V., Lian, J. B., Cole, D., and Gundberg, C. M. (1989) Osteocalcin and matrix Gla protein: vitamin K-dependent proteins in bone. *Physiol Rev* **69**, 990-1047
81. Brennan-Speranza, T. C., and Conigrave, A. D. (2015) Osteocalcin: An Osteoblast-Derived Polypeptide Hormone that Modulates Whole Body Energy Metabolism. *Calcified tissue international* **96**, 1-10
82. Ferron, M., and Lacombe, J. (2014) Regulation of energy metabolism by the skeleton: osteocalcin and beyond. *Archives of biochemistry and biophysics* **561**, 137-146
83. Gibson, William T., Hood, Rebecca L., Zhan, Shing H., Bulman, Dennis E., Fejes, Anthony P., Moore, R., Mungall, Andrew J., Eydoux, P., Babul-Hirji, R., An, J., Marra, Marco A., Consortium, F. C., Chitayat, D., Boycott, Kym M., Weaver, David D., and Jones, Steven J. (2012) Mutations in EZH2 Cause Weaver Syndrome. *American Journal of Human Genetics* **90**, 110-118

4.8 Tables, figures and figure legends

Table 1 E17.5 Fore limb bone length measurements.

Measurements	*Ezh2*$^{+/+}$	*Ezh2* $^{+/-}$	*Ezh2*$^{-/-}$
Scapular (S) Length (mm)	2.8	3.1	2.1
Humerus (H) Length (mm)	2.7	3.5	2.8
Ulna (U) Length (mm)	3.8	4.2	2.2
Radius (R) Length (mm)	2.6	3.3	2.1

S=Scapular, H=Humerus, U=Ulna, R=Radius.
Data represents mean ± SEM of 5 *Ezh2*$^{+/+}$, 5 *Ezh2*$^{+/-}$ and 4 *Ezh2*$^{-/-}$ fore limbs

Table 2. E17.5 hind limb bone length measurements.

Measurements	*Ezh2*$^{+/+}$	*Ezh2* $^{+/-}$	*Ezh2*$^{-/-}$
Femur (F) Length (mm)	1.9	2.4	2.1
Tibia (T) Length (mm)	2.2	2.9	2.2
Fibular (f) Length (mm)	2.2	2.7	2.1
Femur Width (mm)	0.8	1	0.7

F=Femur, T=Tibia, f=Fibular, FW=Femur width.
Data represents mean ± SEM of 5 *Ezh2*$^{+/+}$, 5 *Ezh2*$^{+/-}$ and 4 *Ezh2*$^{-/-}$ hind limbs

Table 3. Newborn Skull length measurements.

Measurements	+/+	+/-	-/-
Nasal Bone (NB) Length (cm)	1.7	1.9	1.9
Frontal Bone Length (FB) (cm)	3.4	3.8	undefined
Parietal Bone Length (PB) (cm)	1	1.3	undefined
Occipital Bone Length (OB) (cm)	1.2	1.2	undefined
NB to OB pole Length (NB-OB) (cm)	7.8	8.7	7.87

Data represents mean ± SEM of 4 *Ezh2*$^{+/+}$, 4 *Ezh2*$^{+/-}$ and 3 *Ezh2*$^{-/-}$ skulls

Supplementary Table 1. E16.5 Fore limb bone length measurements

Measurements	*Ezh2*$^{+/+}$	*Ezh2* $^{+/-}$	*Ezh2*$^{-/-}$
Scapular (S) Length (mm)	2.1	2.6	1.6
Humerus (H) Length (mm)	2.4	2.8	2.19
Ulna (U) Length (mm)	2.3	3.1	1.9
Radius (R) Length (mm)	2	2.5	1.65
Humerus Width (mm)	0.9	1.1	0.61

S=Scapular, H=Humerus, U=Ulna, R=Radius.
Data represents mean ± SEM of 5 *Ezh2*$^{+/+}$, 5 *Ezh2*$^{+/-}$ and 4 *Ezh2*$^{-/-}$ fore limbs

Supplementary Table 2. E16.5 hind limb bone length measurements

Measurements	*Ezh2*$^{+/+}$	*Ezh2* $^{+/-}$	*Ezh2*$^{-/-}$
Femur (F) Length (mm)	1.8	2	1.8
Tibia (T) Length (mm)	1.9	2.3	2.2
Fibular (f) Length (mm)	1.8	1.9	1.9
Femur Width (mm)	0.8	0.9	0.7

F=Femur, T=Tibia, f=Fibular, FW=Femur width
Datarepresents mean ± SEM of 5 *Ezh2*$^{+/+}$, 5 *Ezh2*$^{+/-}$ and 4 *Ezh2*$^{-/-}$ hind limbs.

Supplementary Table 3. E17.5 Skull length measurements

Measurements	*Ezh2*$^{+/+}$	*Ezh2* $^{+/-}$	*Ezh2*$^{-/-}$
Nasal Bone (NB)Length (mm)	2.4	2.6	2.4
Frontal Bone (FB) Length (mm)	5	5.2	undefined
Parietal Bone (PB) Length (mm)	2	2.7	undefined
Occipital Bone (OB) Length (mm)	1.7	1.9	undefined
NB to OB pole (NB-OB) Length (mm)	12.2	12.9	13.1

Data mean ± SEM of 5 *Ezh2*$^{+/+}$, 5 *Ezh2*$^{+/-}$ and 4 *Ezh2*$^{-/-}$ hind limbs

Figure 1. Confirmation of the generation of *Ezh2* conditional knockout mice.

(A) Representative agarose gel depicting PCR analysis of genomic DNA confirming *Ezh2* floxed alleles at 450bp. Heterozygous mice expressed one wildtype (400bp) and one floxed Ezh2 allele (450bp). Primers to Cre recombinase detected Cre at 100bp. (B) Western Blot analysis of *Ezh2* and H3K27me3 protein levels in $Ezh2^{+/-}$ BMSC derived from 4 week old mice, compared with wildtype $Ezh2^{+/+}$ BMSC. (C) Real-time PCR analysis of *Ezh2* transcripts in BMSC derived from 4 week old $Ezh2^{+/-}$ and $Ezh2^{+/+}$ mice. Immunohistochemical analysis of H3K27me3 expression in femora harvested from 4 week old $Ezh2^{+/+}$, $Ezh2^{+/-}$ and $Ezh2^{-/-}$ mice on (D) proliferative chondrocytes (round dot arrow) and blood cells (dashed arrow), and (E) bone and osteoblasts lining the bone surfaces (black arrow). Representative images of 3 $Ezh2^{+/+}$ or $Ezh2^{+/-}$ mice. (D) Representative images of 4 $Ezh2^{+/+}$, $Ezh2^{+/-}$ mice and 3 $Ezh2^{-/-}$ independent mice. The data represent mean values ± SEM of 3 independent mice per genotype (significance *$p \leq 0.05$, unpaired t-test).

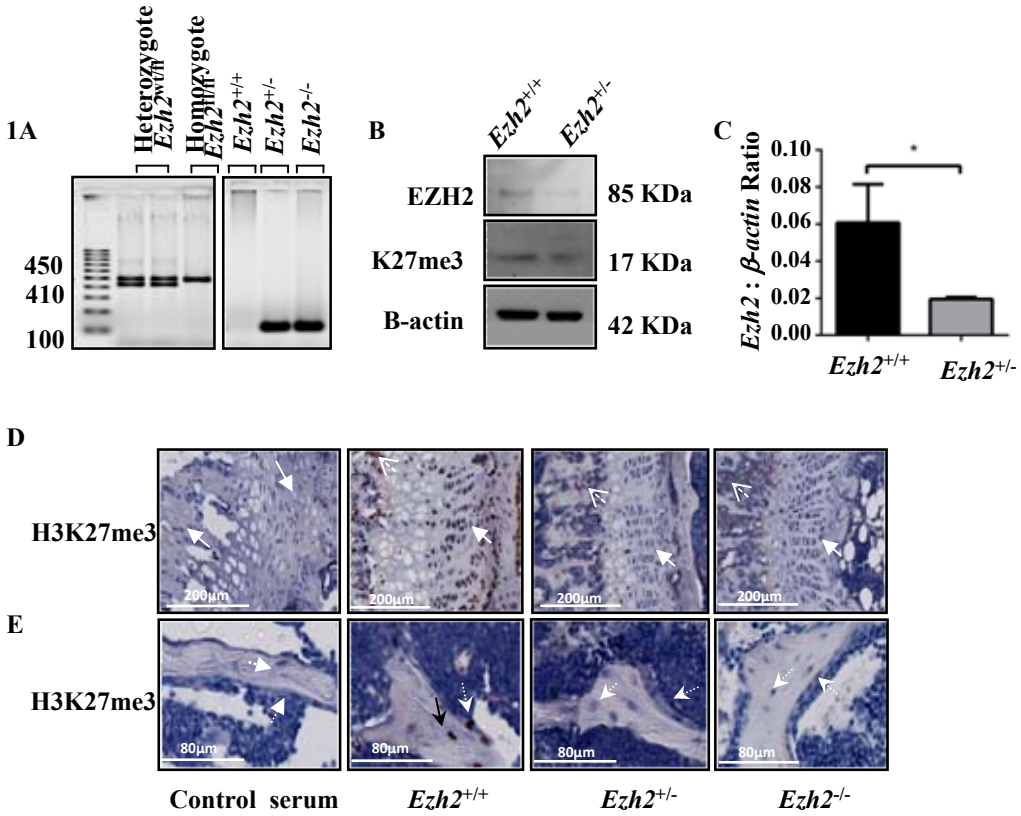
1A
Heterozygote
Ezh2wt/fl
Homozygote
Ezh2fl/fl
Ezh2+/+
Ezh2+/-
Ezh2-/-
450
410
100
B
Ezh2+/+
Ezh2+/-
EZH2
85 KDa
K27me3
17 KDa
B-actin
42 KDa
C
Ezh2 : β-actin Ratio
0.10
0.08
0.06
0.04
0.02
0.00
*
Ezh2+/+
Ezh2+/-
D
H3K27me3
200µm
E
H3K27me3
80µm
Control serum
Ezh2+/+
Ezh2+/-
Ezh2-/-

Figure 2. *Ezh2* deletions affect the size and skeletal development in E17.5 and newborn mice.

(A) Alizarin red and alcian blue staining of whole E17.5 embryos. (B) Images comparing size differences and skeletal phenotype in *Ezh2*$^{+/+}$, *Ezh2*$^{+/-}$, *Ezh2*$^{-/-}$ mice. (C) Weights of female and male newborn mice. (D) Micro-CT Aviso generated 3D images of newborn skeletons assessing vertebrae and skull formation. (E) Alizarin red and alcian blue stained lumbar (L) and sacral (S) vertebrae of *Ezh2*$^{-/-}$ mice which lack the third sacral vertebrae (S3). (F) Alizarin red and alcian blue stained skulls depicting differences in cranial bone patterning at E17.5. (G) Avizo 3D imaging of the skulls revealing craniosynthosis in *Ezh2*$^{-/-}$ mice and increased parietal and occipital bone size in *Ezh2*$^{+/-}$ newborns. Alizarin red staining of differences in length of (H) E17.5 fore limbs, (I) newborn fore limbs, (J) E17.5 hind limbs, (K) newborn hind limbs. (I) Image J quantitation of newborn scapular length, (M) Humerus length, (N) Ulna length, (O) Radius length, (P) Femur length, (Q) Tibia length and (R) Fibular length. Representative images of 4 replicate embryos or newborn per genotype or representative image of 3 replicate embryos or newborn per genotype (A,B,D,E,F,G,H,I,J,K). The data represent mean values ± SEM of 5 *Ezh2*$^{+/-}$ or *Ezh2*$^{+/+}$ female and male and 3 *Ezh2*$^{-/-}$ female mice in (C), or the mean ± SEM of 4 independent mice per genotype (L-R). Statistical significance is represented as *$p \leq 0.05$, unpaired t-test (C) and a one-way ANNOVA with a Tukey's multiple comparisons test (L-R).

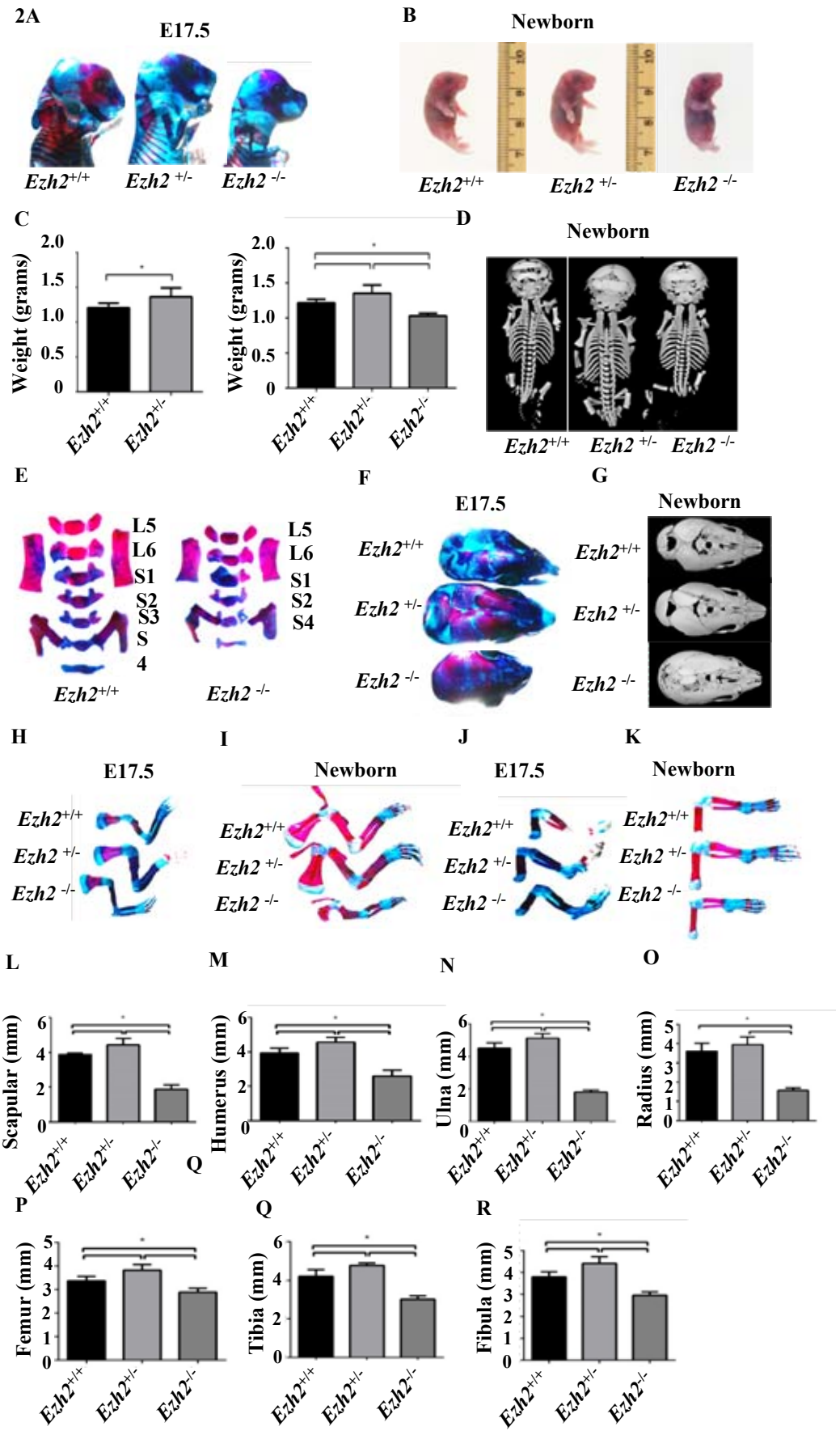
2A
E17.5
Ezh2+/+
Ezh2 +/-
Ezh2 -/-
B
Newborn
Ezh2+/+
Ezh2 +/-
Ezh2 -/-
C
Weight (grams)
2.0
1.5
1.0
0.5
0
Ezh2+/+
Ezh2+/-
Ezh2-/-
D
Newborn
Ezh2+/+
Ezh2 +/-
Ezh2 -/-
E
L5
L6
S1
S2
S3
S
4
S4
Ezh2+/+
Ezh2 -/-
F
E17.5
Ezh2+/+
Ezh2 +/-
Ezh2 -/-
G
Newborn
Ezh2+/+
Ezh2 +/-
Ezh2 -/-
H
E17.5
Ezh2+/+
Ezh2 +/-
Ezh2 -/-
I
Newborn
Ezh2+/+
Ezh2 +/-
Ezh2 -/-
J
E17.5
Ezh2+/+
Ezh2 +/-
Ezh2 -/-
K
Newborn
Ezh2+/+
Ezh2 +/-
Ezh2 -/-
L
Scapular (mm)
6
4
2
0
Ezh2+/+
Ezh2+/-
Ezh2-/-
M
Humerus (mm)
6
4
2
0
Ezh2+/+
Ezh2+/-
Ezh2-/-
N
Ulna (mm)
6
4
2
0
Ezh2+/+
Ezh2+/-
Ezh2-/-
O
Radius (mm)
5
4
3
2
1
0
Ezh2+/+
Ezh2+/-
Ezh2-/-
P
Femur (mm)
5
4
3
2
1
0
Ezh2+/+
Ezh2+/-
Ezh2-/-
Q
Tibia (mm)
6
4
2
0
Ezh2+/+
Ezh2+/-
Ezh2-/-
R
Fibula (mm)
5
4
3
2
1
0
Ezh2+/+
Ezh2+/-
Ezh2-/-

Figure 3 *Ezh2* deletion effects 4 week skeletal size and for and hind limb morphology.
(A) X-ray micrographs of 4 week old mice showing differences in skeletal size between *Ezh2*$^{+/+}$, Ezh2$^{+/-}$, *Ezh2*$^{-/-}$ mice. (B&C) Weight comparisons between *Ezh2*$^{+/-,}$ female and male mice, Ezh2$^{-/-}$ female mice and *Ezh2*$^{+/+}$ control males and females. (D) X-ray of fore limbs revealed size and limb deformities between *Ezh2*$^{+/+}$, Ezh2$^{+/-}$, *Ezh2*$^{-/-}$ mice (E) X-ray of hind limbs identifies differences in size and morphology (F) Tibial length was significantly increased in *Ezh2*$^{+/-}$ and reduced in *Ezh2*$^{-/-}$ mice. (G) Avizo 3D imaging of *Ezh2*$^{+/+}$, Ezh2$^{+/-}$, *Ezh2*$^{-/-}$ tibias. (H) Femora length was significantly increased in *Ezh2*$^{+/-}$ and reduced in *Ezh2*$^{-/-}$ mice. (I) Micro-CT image of 4 week old femurs revealed visual differences in size with *Ezh2*$^{-/-}$ compared with *Ezh2*$^{+/+}$ control mice. (A, D, E) Representative images of 3 replicate mice per genotype or (G&I) are representative image of 5 *Ezh2*$^{+/-}$, 5 *Ezh2*$^{+/+}$ or 3 *Ezh2*$^{-/-}$ replicate mice. Graphs depict mean ± SEM of 5 *Ezh2*$^{+/-}$ or 5 *Ezh2*$^{+/+}$ female and male and 3 *Ezh2*$^{-/-}$ female mice (B, C, F, H). Statistical significance is represented as *$p \leq 0.05$, unpaired t-test (C) and a one-way ANNOVA with a Tukey's multiple comparisons test (B, F, H).

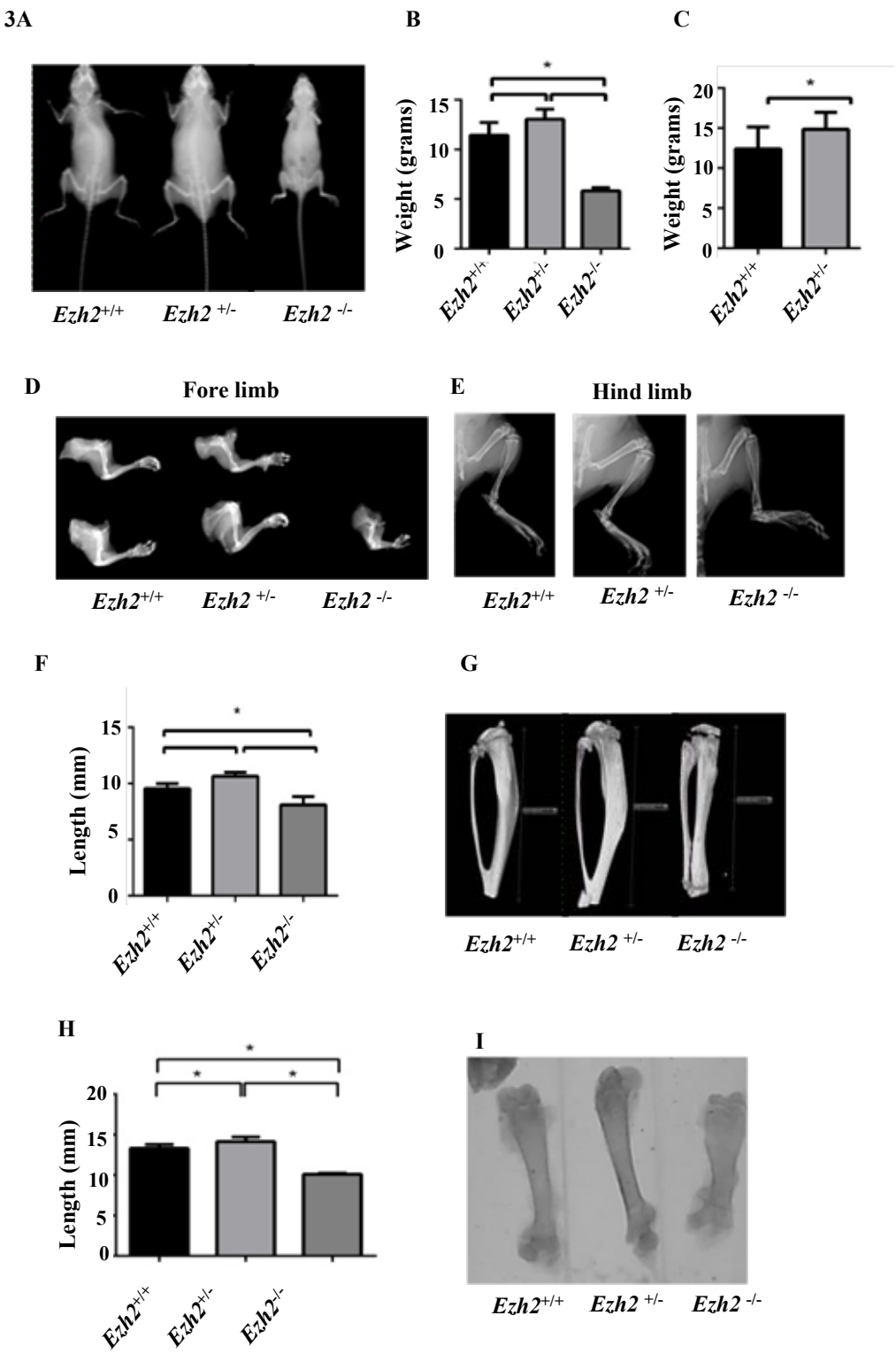
3A
B
C
Weight (grams)
15
10
5
0
20
*
Ezh2+/+
Ezh2 +/-
Ezh2 -/-
D
Fore limb
E
Hind limb
F
Length (mm)
G
H
I

Figure 4. *Ezh2* deletions affect the size of the growth plates and the cartilage zone size.

(A) Safarin O stained newborn growth plates. Arrows identify resting (solid arrow), proliferative (dashed arrow) and hypertrophic (round dot arrow) cartilage in images. (B) 4 week old *Ezh2*$^{+/+}$, *Ezh2*$^{+/-}$, *Ezh2*$^{-/-}$ safarin O stained growth plate. Quantitation of newborn growth plate zones reveals difference in size and cartilage zones (C) Growth plate length, (D) resting cartilage zone length, (E) proliferative cartilage zone length, (F) hypertrophic cartilage zone length. 4 week old *Ezh2*$^{-/-}$ has smaller growth plate length (G), resting cartilage zone (H), proliferative zone (I) and hypertrophic zone (J) compared with *Ezh2*$^{+/+}$, *Ezh2*$^{+/-}$ mice. (A) Representative image of 4 *Ezh2*$^{+/-}$, *Ezh2*$^{+/+}$ and 4 *Ezh2*$^{-/-}$ replicate mice or (B) Representative image of 5 *Ezh2*$^{+/-}$, 5 *Ezh2*$^{+/+}$ or 3 *Ezh2*$^{-/-}$ replicate mice. Graphs depict mean ± SEM of 5 *Ezh2*$^{+/-}$ or 5 *Ezh2*$^{+/+}$ female and 3 *Ezh2*$^{-/-}$ female mice (C-J). Statistical significance is represented as *$p \leq 0.05$, (C-J) a one-way ANNOVA with a Tukey's multiple comparisons test.

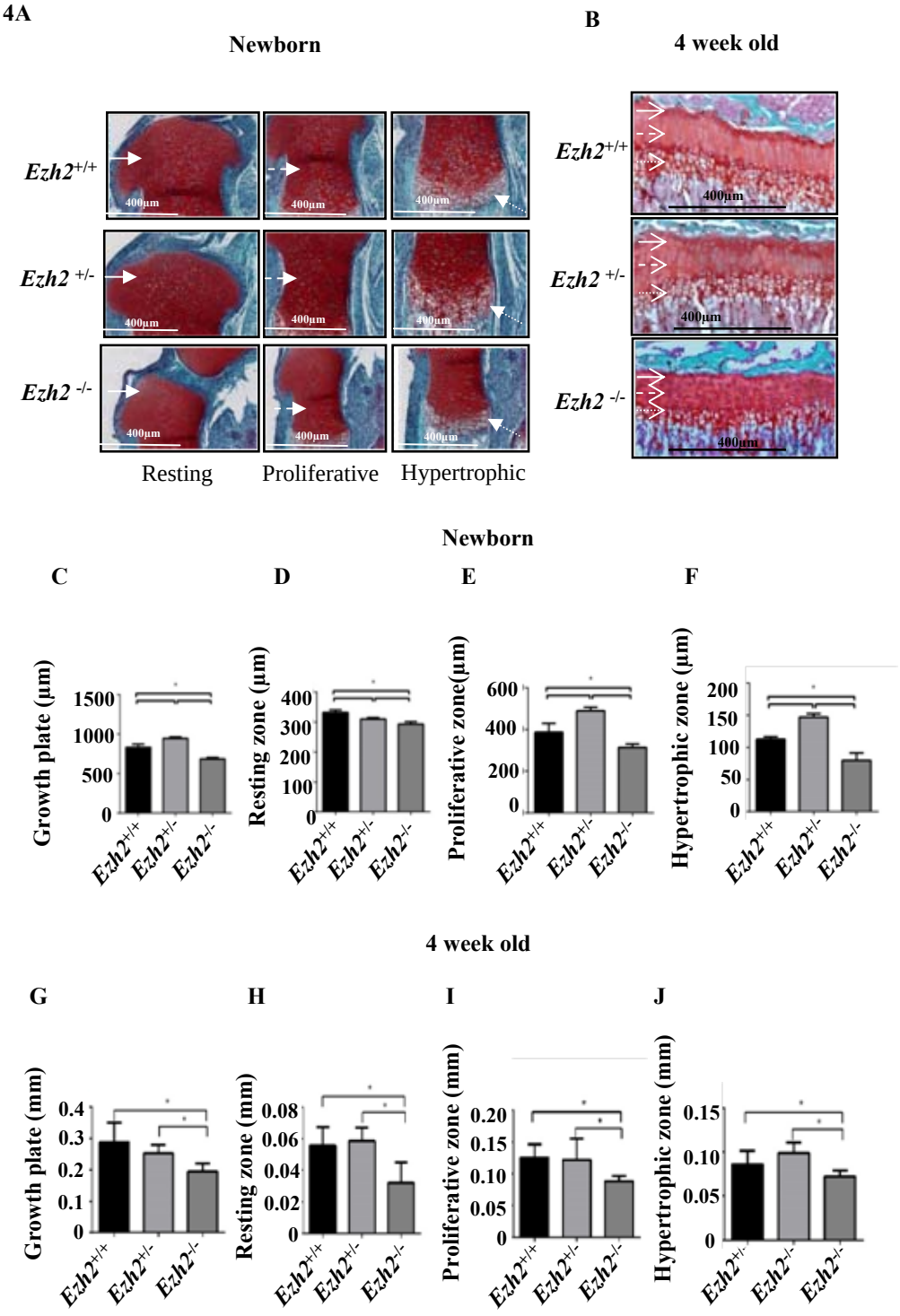
4A
Newborn
B
4 week old
Ezh2+/+
Ezh2 +/-
Ezh2 -/-
400µm
Resting
Proliferative
Hypertrophic
Newborn
C
D
E
F
Growth plate (µm)
Resting zone (µm)
Proliferative zone(µm)
Hypertrophic zone (µm)
4 week old
G
H
I
J
Growth plate (mm)
Resting zone (mm)
Proliferative zone (mm)
Hypertrophic zone (mm)

Figure 5. Micro-CT analysis identified EZH2 deletion effects trabecular patterning and cortical thickness.

(A) Micro-CT image of newborn tibias revealing differences in trabecular patterning (B) Micro-CT CTVol 3D image of quantitated trabecular thought the whole 4 week femora. (C) Micro-CT quantitated the percentage of total bone volume to total volume (BV/TV) the newborn tibia. (D) The number of trabeculae (Tb.N) throughout the newborn tibia. (E) The total trabecular within the femora was normalised to total volume (BV/TV) and trabecular number (Tb.N) patterning throughout the femora (F). (G) H&E stained femora cortical bone organisation. (H) CTVol 3D model of 4 week femora cortical bone. Cortical bone volume analysed by Micro-CT and identified a decrease in BV/TV (I) and cortical thickness (J). (A, B, G, H) Representative images of 5 *Ezh2*$^{+/-}$, 5 *Ezh2*$^{+/+}$ or 3 *Ezh2*$^{-/-}$ replicate mice. Graphs depict mean ± SEM of 5 *Ezh2*$^{+/-}$ or 5 *Ezh2*$^{+/+}$ female and 3 *Ezh2*$^{-/-}$ female mice (C, D, E, F, I, J). Statistical significance is represented as *$p \leq 0.05$, (C-J) a one-way ANNOVA with a Tukey's multiple comparisons test.

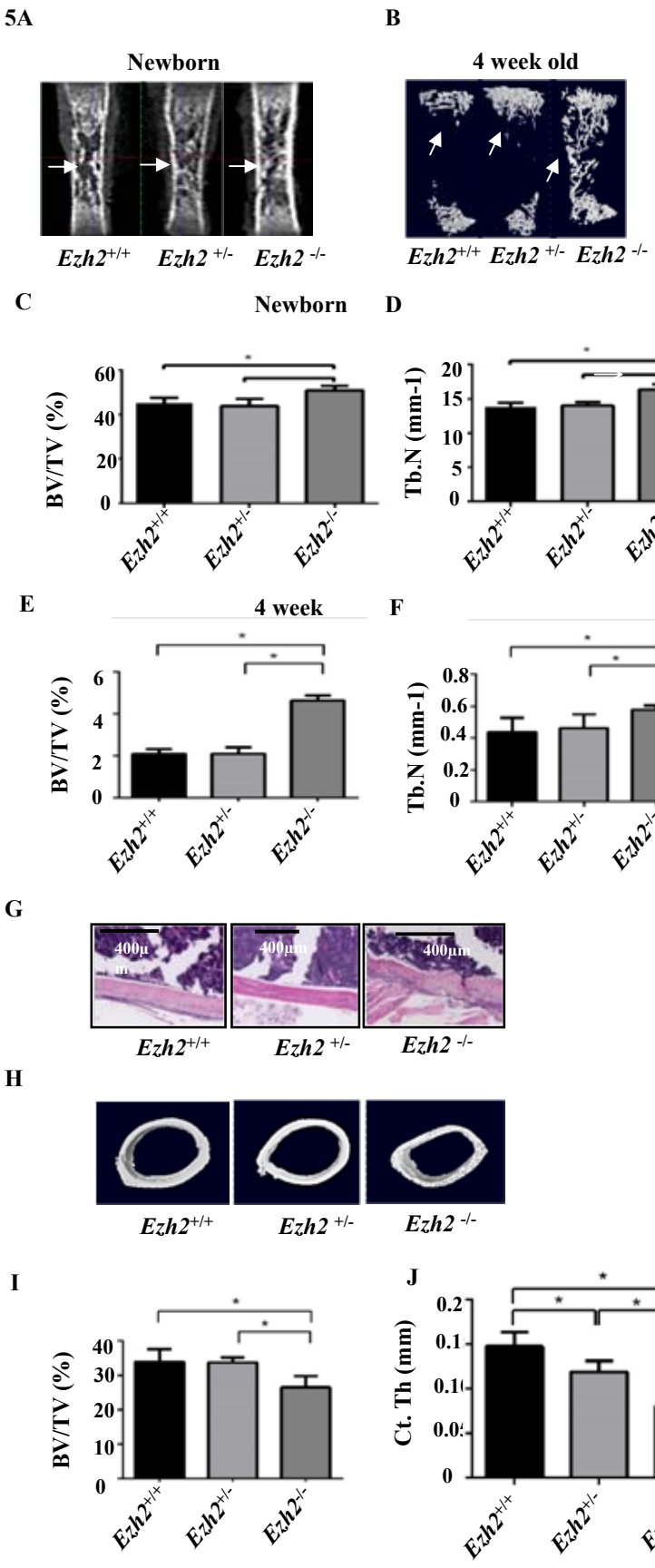
5A
B
Newborn
4 week old
Ezh2+/+ Ezh2 +/- Ezh2 -/-
Ezh2+/+ Ezh2 +/- Ezh2 -/-
C
Newborn
D
BV/TV (%)
Tb.N (mm-1)
E
4 week
F
BV/TV (%)
Tb.N (mm-1)
G
400µm
Ezh2+/+ Ezh2 +/- Ezh2 -/-
H
Ezh2+/+ Ezh2 +/- Ezh2 -/-
I
J
BV/TV (%)
Ct. Th (mm)

Figure 6. EZH2 deletion effects bone microarchitecture and bone strength.
(A) Histomorphometric analyses of the secondary spongiosa in the 4 week old tibias. Quantitated differences in trabecular bone volume to tissue volume (BV/TV) (B), trabecular number (Tb.N) (C), trabecular thickness (Tb.Th) (D) and trabecular separation (E). Quantitated differences in cortical (BV/TV) (F) and cortical thickness (G). Three point bending tests reveal changes in femora flexural rigidity (stiffness), decrease in yield load and yield moment at point of catastrophic failure (H-J). (A) Representative image of 5 *Ezh2*$^{+/-}$, 5 *Ezh2*$^{+/+}$ or 3 *Ezh2*$^{-/-}$ replicate mice. Graphs depict mean ± SEM of 5 *Ezh2*$^{+/-}$ or 5 *Ezh2*$^{+/+}$ female and 3 *Ezh2*$^{-/-}$ female mice (B-J). Statistical significance is represented as *$p \leq 0.05$, (C-J) a one-way ANNOVA with a Tukey's multiple comparisons test

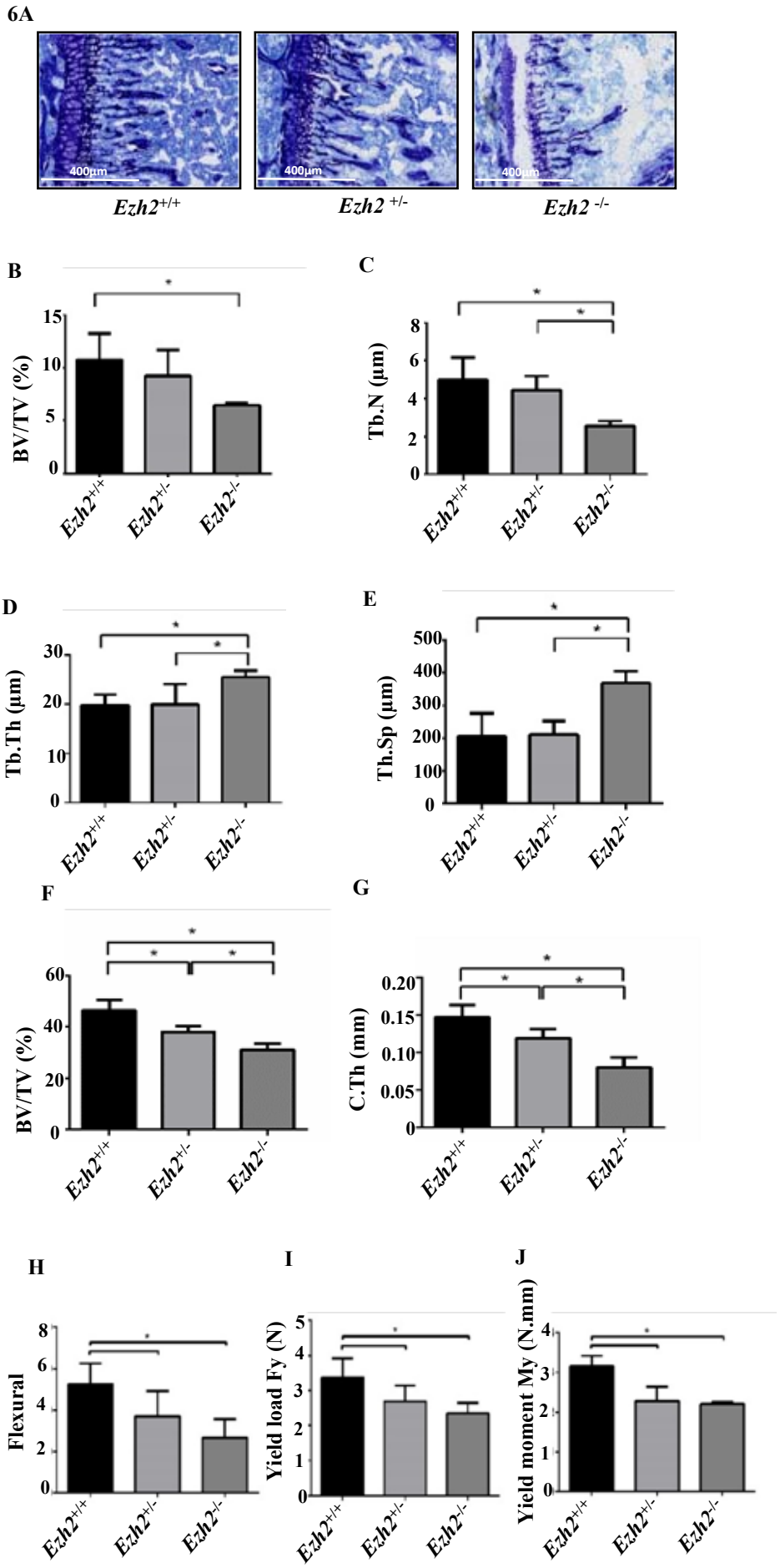
6A
400µm
400µm
400µm
Ezh2+/+
Ezh2 +/-
Ezh2 -/-
B
BV/TV (%)
15
10
5
0
C
Tb.N (µm)
8
6
4
2
0
D
Tb.Th (µm)
30
20
10
0
E
Th.Sp (µm)
500
400
300
200
100
0
F
BV/TV (%)
60
40
20
0
G
C.Th (mm)
0.20
0.15
0.10
0.05
0
H
Flexural
8
6
4
2
0
I
Yield load Fy (N)
5
4
3
2
1
0
J
Yield moment My (N.mm)
4
3
2
1
0
Ezh2+/+
Ezh2+/-
Ezh2-/-

Figure 7. EZH2 deletion increases bone formation and osteoclast differentiation and activity.
(A) Representative image of calcien labelling of newly formed trabecular bone in 4 week old methacrylate embedded tibias. Mineral apposition rate (MAR) and bone formation rate on bone surface (BFR/BS) were calculated (B&C). (D) Representative image of calcien labelling of newly formed cortical bone in 4 week old methacrylate embedded tibias. (E&F) Cortical MAR and BFR/BS. (G&H) TRAP and CTX-1 levels detected in serum compared with *Ezh2*$^{+/+}$ serum. (I-K) *In vitro* bone marrow cells from 4 week old hind limbs were differentiated into more multinucleated TRAP positive osteoclasts and formed more pits on whale dentine slides compared with *Ezh2*$^{+/+}$ bone marrow cells. (L-N) *M-Csf, Rankl* and *Opg* expression on BMSC extracted from 4 week old hind limbs. (A, D) Representative images of 5 *Ezh2*$^{+/-}$, 5 *Ezh2*$^{+/+}$ or 3 *Ezh2*$^{-/-}$ replicate mice or representative images of 3 *Ezh2*$^{+/-}$ and 3 *Ezh2*$^{+/+}$ replicate mice (J&K). Graphs depict mean ± SEM of 5 *Ezh2*$^{+/-}$ or 5 *Ezh2*$^{+/+}$ female and 3 *Ezh2*$^{-/-}$ mice (B, C, E, F) or mean ± SEM of 3 *Ezh2*$^{+/-}$, 3 *Ezh2*$^{+/+}$ or 2 *Ezh2*$^{-/-}$ mice (G&H) or mean ± SEM of 3 *Ezh2*$^{+/-}$ and 3 *Ezh2*$^{+/+}$ mice (I, L, M, N). Statistical significance represented as * ($p < 0.05$). Statistical significance is represented as *$p \leq 0.05$, (B, C, E, F, G, H) a one-way ANNOVA with a Tukey's multiple comparisons test , (I) a two-way ANNOVA with a Sidak's multiple comparisons test and (L-N) unpaired t-test.

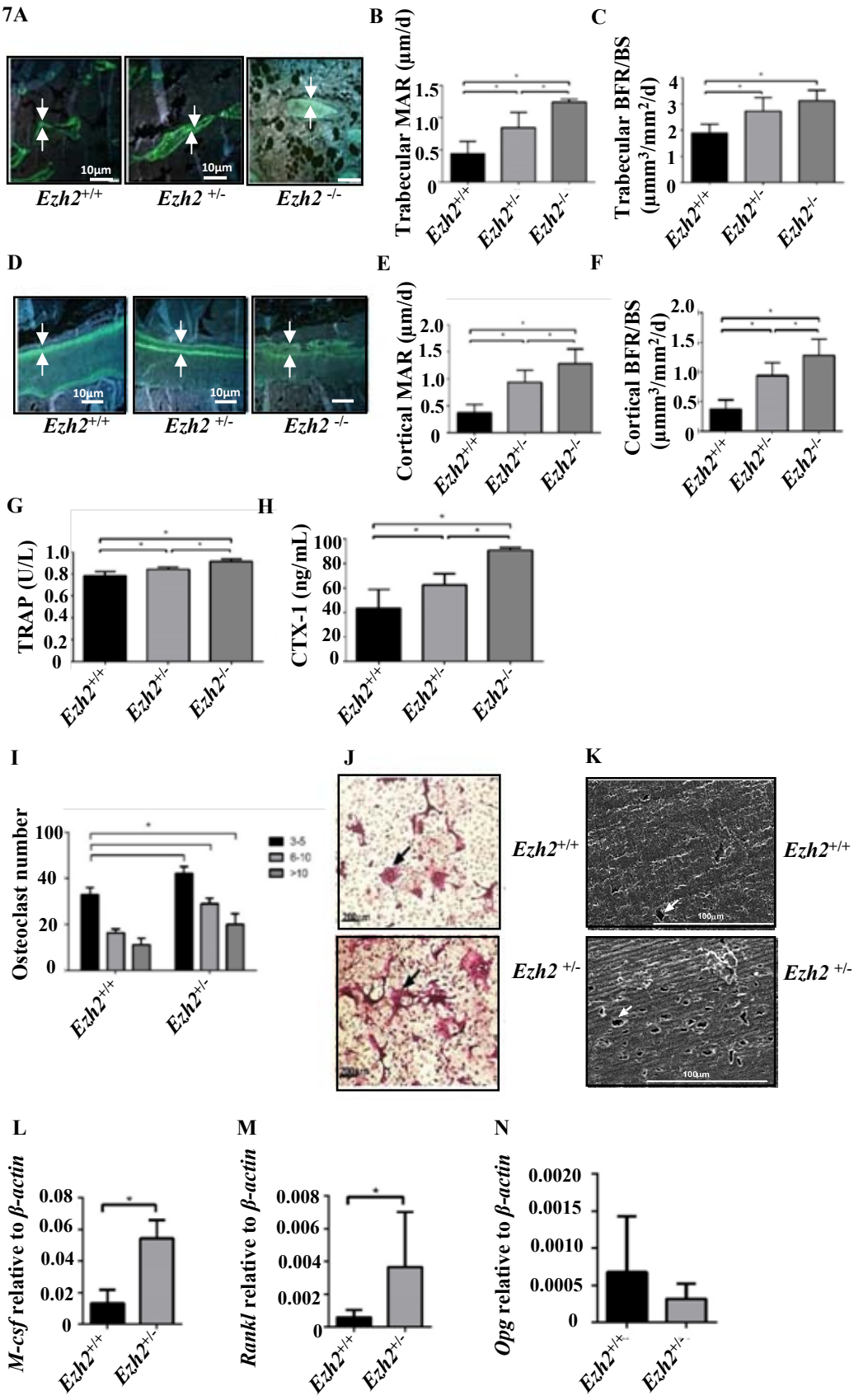
7A
B
C
D
E
F
G
H
I
J
K
L
M
N
10μm
Ezh2+/+
Ezh2 +/-
Ezh2 -/-
Trabecular MAR (μm/d)
Trabecular BFR/BS (μmm3/mm2/d)
Cortical MAR (μm/d)
Cortical BFR/BS (μmm3/mm2/d)
TRAP (U/L)
CTX-1 (ng/mL)
Osteoclast number
3-5
6-10
>10
100μm
M-csf relative to β-actin
Rankl relative to β-actin
Opg relative to β-actin

Figure 8. EZH2 deletion increases osteoblast number and osteogenic differentiation *in vitro.*
(A) Histomorphometric analysis revealed differences in trabecular osteoblasts number on bone perimeter (N.Ob/B.Pm) and (B) cortical bone. (C) Total OCN present in 4 week old serum. (D) Osteogenic differentiated hind limb BMSCs produced alizarin red stained mineral at 7 days of osteogenic induction. (E) Osteogenic differentiated BMSC produced extracellular calcium which was normalised to DNA. (F-H) Expression of *Runx2*, *Osteoclacin* (*Ocn*) and *Osteopontin (Opn*) in osteogenic differentiated BMSC extracted from 4 week old hind limbs. (I). Colony forming unit fibroblast potential of BMSC extracted from 4 week old hind limbs (J). Percentage of alkaline positive CFU-F colonies from 4 week old hind limb BMSC (D). Representative image of 3 $Ezh2^{+/-}$, 3 $Ezh2^{+/+}$ replicate mice. Graphs depict mean ± SEM of 5 $Ezh2^{+/-}$ or 5 $Ezh2^{+/+}$ female and 3 $Ezh2^{-/-}$ female mice (A, B, C) or mean ± SEM of 3 $Ezh2^{+/-}$ and 3 $Ezh2^{+/+}$ mice (E, F-J). Statistical significance is represented as *$p \leq 0.05$, (A, B, C) a one-way ANNOVA with a Tukey's multiple comparisons test, (E, F, G, H, I) unpaired t-test and a two-way ANNOVA with a Sidak's multiple comparisons test (J).

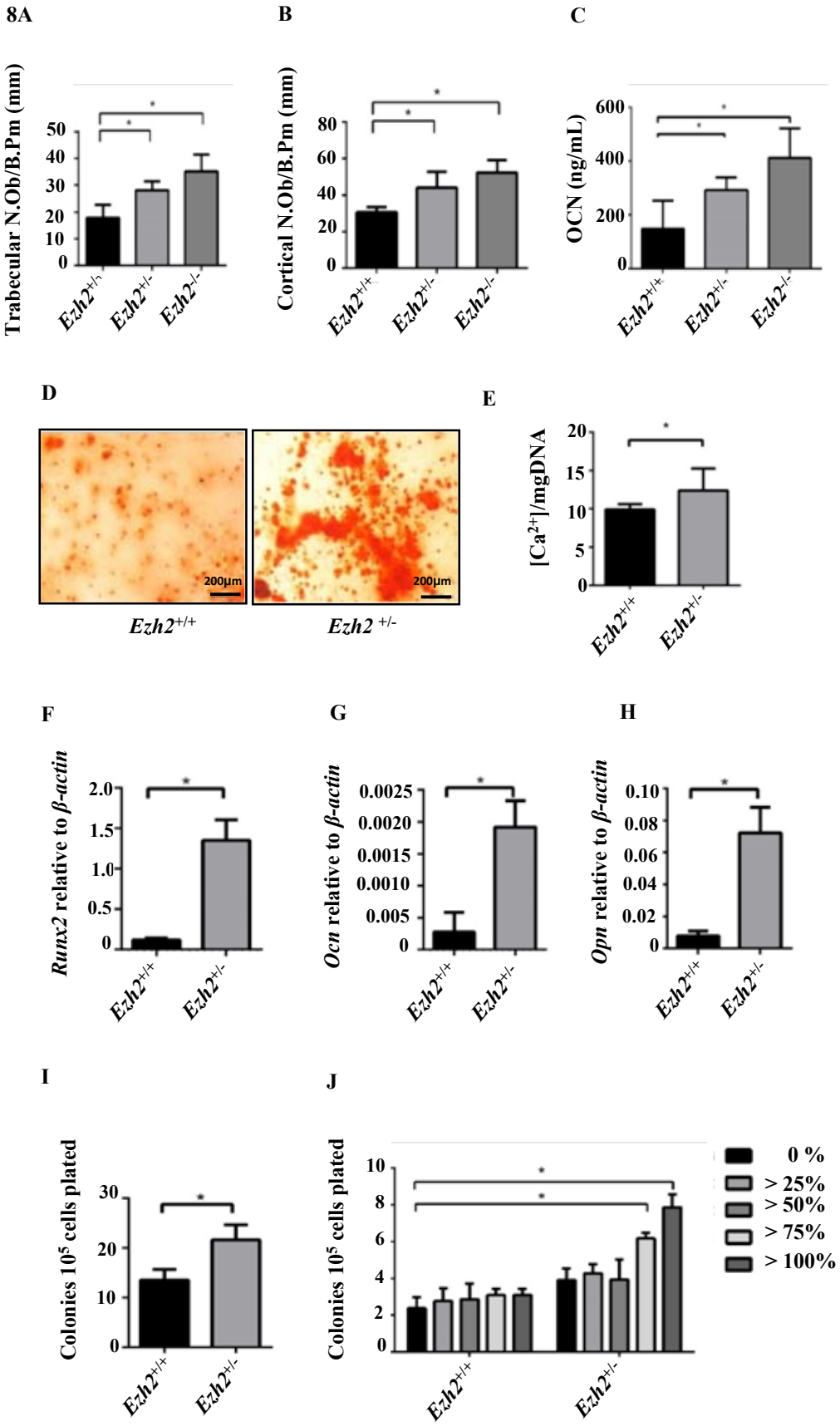
8A
Trabecular N.Ob/B.Pm (mm)
50
40
30
20
10
0
Ezh2+/+
Ezh2+/-
Ezh2-/-
B
Cortical N.Ob/B.Pm (mm)
80
60
40
20
0
C
OCN (ng/mL)
600
400
200
0
D
200µm
200µm
Ezh2+/+
Ezh2 +/-
E
[Ca2+]/mgDNA
20
15
10
5
0
F
Runx2 relative to β-actin
2.0
1.5
1.0
0.5
0
G
Ocn relative to β-actin
0.0025
0.0020
0.0015
0.0010
0.005
0
H
Opn relative to β-actin
0.10
0.08
0.06
0.04
0.02
0
I
Colonies 10^5 cells plated
30
20
10
0
J
Colonies 10^5 cells plated
10
8
6
4
2
0
0 %
> 25%
> 50%
> 75%
> 100%

Figure 9. EZH2 deletion increases adipogenic differentiation *in vitro* and *in vivo*.

(A) Representative image of the increase in marrow fat observed in 4 week old mice. (B) Analysis of marrow fat in the secondary spongiosa of 4 week old tibias (C) BMSC differentiated under adipogenic inductive conditions for 7 days stained with nile red (arrow lipid) and Dapi (arrow nuclei). (D) Nile red stained lipid containing adipocytes were normalised to total nuclei present. (E-G). Expression of adipogenic genes *Pparγ2*, *C/ebpα*, A*diponectin* (*AdipQ*) were asses in adipogenic differentiated BMSC. (A, C) Representative images of 5 *Ezh2*$^{+/-}$, 5 *Ezh2*$^{+/+}$ or 3 *Ezh2*$^{-/-}$ replicate mice or representative image of 3 *Ezh2*$^{+/-}$ and 3 *Ezh2*$^{+/+}$ mice. Graphs depict mean ± SEM of 5 *Ezh2*$^{+/-}$ or 5 *Ezh2*$^{+/+}$ female and 3 *Ezh2*$^{-/-}$ female mice (B) or mean ± SEM of 3 *Ezh2*$^{+/-}$and 3 *Ezh2*$^{+/+}$ mice (D, E, F, G). Statistical significance is represented as *$p \leq 0.05$, (B) a one-way ANNOVA with a Tukey's multiple comparisons test and (D-G) unpaired t-test and a two-way ANNOVA

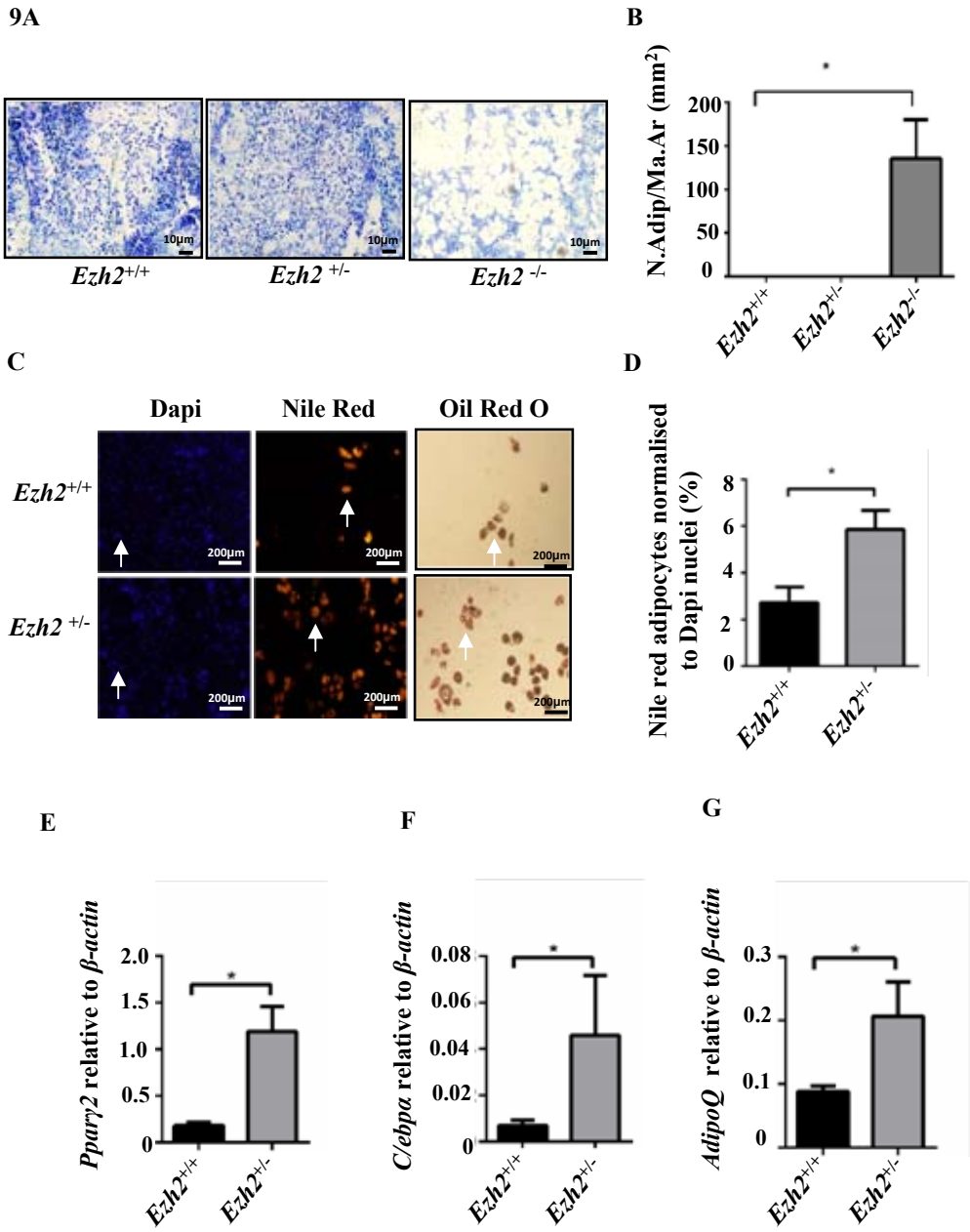
9A
B
10µm
Ezh2+/+
Ezh2 +/-
Ezh2 -/-
N.Adip/Ma.Ar (mm2)
200
150
100
50
0
C
D
Dapi
Nile Red
Oil Red O
200µm
Nile red adipocytes normalised to Dapi nuclei (%)
8
6
4
2
0
E
F
G
Pparγ2 relative to β-actin
2.0
1.5
1.0
0.5
C/ebpa relative to β-actin
0.08
0.06
0.04
0.02
AdipoQ relative to β-actin
0.3
0.2
0.1

Chapter 5

Discussion and Future Directions

5 Discussion and Future Directions

Multipotential MSC-like populations have been widely regarded as potential candidates for different clinical indications, owing to their ease of isolation from different tissues (1-7) and unique characteristics including tissue regeneration, suppression of allogenic immune responses and pro-angiogenic properties. Bone marrow derived MSC (BMSC) are tissue specific postnatal stem cells, which are restricted in their differentiation potential to skeletal tissues and myelosupportive stroma (8,9). Cell lineage determination is regulated by a complex network of signalling pathways such as WNT, Notch, BMP (10), and expression of key lineage specific transcription factors including, RUNX2, PPARγ2, SOX9, implicated as being critical drivers of MSC lineage osteogenic, adipogenic and chondrogenic commitment, respectively (10-16). The activation of these signalling pathways and transcription factors are dependent on the regulation of chromatin, allowing the activation or suppression of lineage specific factors and their downstream targets. Therefore, it is important to identify the role of epigenetic modifiers in the regulation of BMSC growth and lineage-specification.

Epigenetics is often defined as "the study of changes in organisms caused by modification of gene expression rather than alteration in DNA sequence" (17). The complex study of epigenetics encompasses DNA methylation, chromatin remodelers, histone modifications and non-coding RNAs (18-23). The Polycomb Repressor Complex 2 (PCR2) is one of the most studied histone modifying complexes currently identified (24-26). Methyltransferase EZH2 exists within the PCR2 and is responsible for H3K27me3 modification promoting chromatin compaction and gene repression. The H3K27me3 modification can be removed by demethylases KDM6A and KDM6B often associated within a complex containing H3K4 methyltransferases facilitating in gene transcription. Previous studies have implicated EZH2 in maintaining the stem cell phenotype of hematopoietic stem cells, epidermal skin cells,

myoblasts, chondrocytes, osteoblasts, pre-adipocytes, embryonic stem cells, and multipotent neural progenitor cells of the cerebral cortex in vitro differentiation (27-37). However, the direct role of EZH2 and KDM6A in regulating MSC lineage commitment and skeletal development is not as defined.

The present thesis investigated the roles of EZH2 and KDM6A in regulating human BMSC lineage specification, with a focus on understanding the role of EZH2 in vivo during skeletal development, bone formation and remodelling. We hypothesised that H3K27me3 demethylase KDM6A facilitates human BMSC osteogenic differentiation, whilst EZH2 inhibits osteogenic differentiation in vitro and in vivo. EZH2 activity suppresses osteogenic associated genes through its H3K27me3 mark in uncommitted BMSC, while KDM6A removes this mark to initiate osteogenic differentiation. Furthermore, tissue specific ablation of EZH2 in uncommitted MSC would promote accelerated bone formation during embryonic and early postnatal skeletal development in vivo.

In Chapter 2, retroviral mediated over-expression of either EZH2 or KDM6A in human BMSC demonstrated that these epigenetic modifiers act as an epigenetic switch to regulate osteogenic and adipogenic differentiation (35). We found that EZH2 over-expression inhibited osteogenesis and promoted adipogenesis in human BMSC in vitro. Conversely, KDM6A over-expression promoted osteogenesis and inhibited adipogenesis in human BMSC in vitro. Similar effects on bone formation in vivo were observed when EZH2 and KDM6A over-expressing BMSC were seeded with an osteoconductive carrier then implanted subcutaneously into immunocompromised mice. Confirmatory studies showed that siRNA mediated knockdown of EZH2, or chemical induced inhibition of methyltransferase activity, resulted in the promotion of osteogenesis and inhibition of adipogenesis in BMSC. In

contrast, siRNA mediated knockdown of KDM6A inhibited osteogenesis and promoted adipogenesis in human BMSC. These results were consistent with previous studies identifying that CDK1 phosphorylates EZH2 preventing its H3K27me3 activity and promoting osteogenic differentiation in human BMSC (36). EZH2 inhibition in human MSC allowed the removal of EZH2 and its H3K27me3 mark from the promoter of the osteogenic transcription factor, RUNX2 (36). The present studies supported these previous findings, confirming EZH2 directly methylates the promoter of RUNX2 and OCN preventing human BMSC osteogenic differentiation. However, EZH2 did not appear to target known adipogenic associated genes in human BMSC to inhibit BMSC.

EZH2 has been previously identified as a promoter of adipogenesis repressing Wnt1, -6, -10a, and -10b genes in murine peripheral pre-adipocytes. Deletion of EZH2 in murine pre-adipocytes promoted Wnt/beta-catenin signalling and inhibiting adipogenesis (37). Similarly, we found that siRNA knockdown or enzymatic inhibition of EZH2 inhibited adipogenic differentiation in human BMSC, where H3K27me3 methylation patterns on adipogenic gene promoters were largely unaffected by EZH2 and KDM6A. Therefore, future studies will investigate EZH2 regulation of Wnt genes in human BMSC. Interestingly, cultured BMSC isolated from the long bones of Prrx-1-Ezh2+/- exhibited increased osteogenic and adipogenic potential in vitro. Strikingly, EZH2 deficient animals displayed an increase in marrow adipocytes. These findings suggested that Ezh2 deletion promoted adipogenic differentiation, contrary to previous literature and Chapter 2, where deletion of Ezh2 inhibited adipogenic differentiation in human BMSC and murine pre-adiopcytes (35,37). The differences could be attributed to targeted deletion in early limb bud mesenchymal cells, whereas previous studies have used more committed pre-adipocytes and mixed populations of BMSC committed progenitors in vitro. Lineage tracing experiments could be used to identify and follow the

progeny of MSC. This approach could help determine the presence of a subpopulation of MSC or adipogenic precursor cells derived from the original limb bud mesenchyme. In addition, changes in signalling within the niche in vivo could impact on the adipogenic potential of the MSC within the limb, or that cell fate determination for different MSC subpopulations is based on alternate molecular pathways. Future experiments performing EZH2, H3K27me and H3K4me ChIP-Seq and or RNA-Seq analyses on human or murine Ezh2+/+, Ezh2+/-, Ezh2-/- BMSC following adipogenic differentiation, could identify unique adipogenic genes targets by EZH2. Furthermore, to assess the role of EZH2 in osteogenic, adipogenic and chondrogenic differentiation, Ezh2 floxed mice could be bred with either osteogenic (Osterix), adipogenic (Adiponectin) or chondrogenic (Collagen type II) cre driver mice to confirm the role of EZH2 in osteoblast, adipocyte and chondrocyte function in vivo, respectively.

During the course of this thesis, other studies have confirmed that KDM6A and KDM6B promote osteogenic differentiation (38-40). These reports together with the present study suggest KDM6A and KDM6B demethylate key osteogenic gene such as RUNX2, allowing the activation of its downstream targets to promote bone cell differentiation (38,39,41). Similar to EZH2, it is possible that both KDM6A and KDM6B remove the H3K27me3 mark off WNT genes contributing to the progression of osteogenesis. To identify if the WNT genes are demethylases targets during MSC differentiation, MSC could be transfected with dominant negative KDM6A and KDM6B mutants using over-expression viral vectors. ChIP analysis of H3K27me3 methylation on the WNT gene promoters in MSC, adiopcytes and osteoblasts would then be assessed to help identify the role of methylation in MSC lineage determination. It is also important to determine whether KDM6A and KDM6B work independently or synergistically to promote osteogenic differentiation, where some evidence

suggests that KDM6B is playing an earlier role during osteogenic (40). Transfecting MSC with both KDM6A and KDM6B or with combinations of their corresponding dominant negative mutants could reveal whether these two demethylases have independent or synergistic roles in MSC lineage commitment. Naturally occurring KDM6A mutations have been identified in patients with Kabuki syndrome, who exhibit skeletal deformities such as short stature and craniofacial deformities demonstrating the important the role of KDM6A in human skeletal development (42-46). KDM6A plays a role in posterior patterning, regulating HOX genes similar to EZH2 during skeletal development (47,48). Collectively, these findings suggest that the H3K27me3 demethylases KDM6A and perhaps KDM6B have a critical functional role in human skeletal development. To support this notion, future studies will require the generation of conditional KDM6A and KDM6B knockout mice targeting MSC (Prrx-1-Cre or MX1-Cre), osteoblast progenitors (Osterix-Cre), osteoblasts (Osteocalcin-Cre) or osteocytes (DMP-1-Cre), in order to determine the role of these demethylases during skeletal development and the effect on different stages of osteogenic differentiation in vivo. Furthermore, single and double knockout of KDM6A and KDM6B could determine the unique and combinatorial role of these demethylases in skeletal development. It would be interesting to asses if treatment of KDM6A conditional knockout mice with EZH2 inhibitors could rescue the skeletal growth phenotype. These animal studies could possibly lead to the treatment of Kabuki patients with EZH2 inhibitors to alleviate some of the symptoms, which are currently being used in clinical trials for cancer (49,50).

This current study and previous studies have yet to determine how EZH2 and KDM6A or KDM6B are recruited to the promoters of lineage specific genes during MSC lineage commitment. The current literature indicates RNA transcripts, DNA methylation, pre-existing histone modification and transcription factors can influence the chromatin state (51). The

presence or absence of other histone modifications on the promoter of these genes may provide a clue as to the mechanisms of recruitment. As phosphorylation of EZH2 is important for osteogenic differentiation, other post-translational protein modifications such as ubiquitylation may play a role in the regulation of EZH2 and KDM6A during lineage specification (36,52). Therefore, it is critical to investigate the processes of recruiting epigenetic modifiers in multiple cell types under different environmental conditions. Whilst Chapter 1 identified the role of EZH2 and KDM6A in human BMSC lineage specification, it remains unclear if EZH2 regulated other known or novel genes involved during BMSC osteogenic differentiation.

This question was partly addressed in Chapter 3 using a bioinformatics approach to identify known or novel osteogenic gene targets regulated by EZH2 in human BMSC. The strategy involved interrogation of publically available EZH2 ChIP-on-ChIP, H3K27me3/H3K4me3 ChIP-Seq data sets and gene expression microarray datasets in human MSC and osteoblasts (36,53,54). These bioinformatics analyses identified 99 genes that contained bound EZH2 and the repressive H3K27me3 mark on their respective promoters in MSC, which were subsequently removed following osteogenic differentiation. However, only six genes, ZBTB16, HOPX, ROR2, MYADM, FHL1 and MX1, were significantly upregulated (none down regulated) in MSC following osteogenic differentiation. Of this cohort of putative EZH2 targets, two genes, ZBTB16 and FHL1, demonstrated both EZH2 and H3K27me3 removal and a gain in the active H3K4 mark on their promoters during osteogenic differentiation. In addition, MX1 was found to lose EZH2 and H3K27me3 and gain the active H3K4 mark during osteogenic differentiation by manual ChIP analysis. These genes were 2 fold up regulated in osteoblasts compared to MSC, suggestive of a functional role in BMSC osteogenic differentiation. Previous studies have identified ZBTB16 as a promoter of

osteogenic differentiation in human MSC (55). Similarly, FHL1 has been reported to promote osteogenesis in the murine cell line, MC3T3-E1 (56,57) and MX1 has been demonstrated to have an important role during murine osteochondral differentiation (58,59). Using the EZH2 over-expressing BMSC generated in Chapter 2 we showed that EZH2 repressed expression of ZBTB16, FHL1 and MX1 in osteoblasts correlating with the reduced osteogenic differentiation potential of these lines. Direct siRNA mediated knockdown of MX1 and FHL1 in human BMSC inhibited osteogenic differentiation, similar to that previously reported for ZBTB16 (55). Furthermore, these proteins are known to play a functional role in murine skeletal development, where ZBTB16 controls skeletal patterning through repression of HOX, BMP and Sonic Hedge Hog (Shh) expression (60-62). MX1 is expressed in a subset of murine MSC which differentiate into osteogenic progenitors that maintain the osteoblast pool under steady state and tissue stress conditions (58). However, the role of FHL1 during skeletal development in vivo remains to be determined.

Our study is the first study to identify ZBTB16, MX1 and FHL1 as novel EZH2 targets during human BMSC osteogenic differentiation, identifying the potential importance of epigenetic regulation of osteogenic lineage specific genes. Moreover, this is the first to report describing that MX1 and FHL-1 are direct regulators of osteogenesis in human BMSC. The findings in Chapter 3 and previous studies (55,56,58,59,61,63-65) implicate ZBTB16, MX1 and FHL1 as regulators, of murine and human osteogenic differentiation. Future investigations could assess the expression of ZBTB16, MX1 and FHL1 during skeletal development in Prrx-1-Ezh2 conditional knockout mice generated in Chapter 4. Furthermore, breeding osteogenic Cre driver mice such as Osterix and Osteocalcin with the Ezh2fl/fl mice could determine the role of EZH2 in regulating ZBTB16, MX1 and FHL1 in committed osteogenic precursor during skeletal development.

Further investigation are needed to assess the role of EZH2 in regulating HOPX, ROR2 and MYADM during MSC to osteogenic differentiation. These genes are promising targets of osteogenic differentiation as ROR2, a receptor tyrosine kinase-like orphan associates with Wnt5a, a transmembrane receptor mediating the non-canonical WNT pathway (66,67). Activation of the non-canonical pathway allows the upregulation of bone formation and reabsorption independent of β-catenin signalling (68). Over-expression of ROR2 in human MSC promotes osteoblast differentiation through the activation of Osterix (69). ROR2/WNT5a signalling activates the JNK pathway promoting RANK ligand activation and osteoclastogenesis and mice deficient in ROR2 have impaired osteoclast formation (70). Thesis findings suggest EZH2 could be involved in osteoblast and osteoclast activation through regulation of ROR2 through the non-canonical WNT pathway. Additionally, ROR2 mutations in this gene can cause brachydactyly type B, a skeletal disorder characterized by hypoplasia/aplasia of distal phalanges and nails. Mutations in this gene can also cause the autosomal recessive form of Robinow syndrome, which is characterized by skeletal dysplasia, generalized limb bone shortening, segmental defects of the spine, brachydactyly and a dysmorphic facial appearance (66,71). Similar to ROR2, HOPX regulates WNT gene expression though BMP activation of SMADS, which represses WNT gene expression in cardiomyocytes (72). HOPX expression has been linked to contributing to stem cell quiescence and tumour suppressor function (73-75). MYADM expression was previously shown to regulate hematopoietic differentiation, where inhibition of MYADM with antisense oligonucleotides inhibited c-kit+ Lin- in bone marrow cells, however, its role in MSC differentiation has not been defined (76).

Previous studies have generated conditional knockout EZH2 mice in early limb bud mesenchymal, which resulted in serve skeletal patterning due to deregulation of HOX genes (77). However, this study failed to identify the role of EZH2 in embryonic postnatal bone growth and remodelling. In Chapter 4 we examined the function of either reducing EZH2 or totally eliminating EZH2 in mesenchymal tissues using a conditional knockout approach, based on the early mesenchyme marker, Prrx-1, a critical factor involved in limb bud development and a subset of craniofacial bones (78). Examination of skeletal development during embryogenesis found that heterozygous Prrx-1-Ezh2+/- mice exhibited longer limbs and overall skeleton, in contrast to the drastically shorter limbs and skeleton observed for the homozygous Ezh2-/- animals, correlating with pattering defects seen previously (77). As early as E16.5 Prrx-1-Ezh2-/- mice display craniosynostosis with fusion of the sutures of the frontal and parietal bones, supporting the reported cranial phenotype in newborn Prrx-1 Ezh2-/- mice recently published during the course of this thesis (79). This recent study also reported that EZH2 effected limb size, growth plate size and secondary spongiosa bone formation was effected in the tibiae of 3 week old mice (79). Similarly, the present study demonstrated that Prrx-1-Ezh2-/- mice exhibit shorter limbs with decreased growth plate size, with increased total trabecular bone throughout the tibiae and femora at birth and 4 weeks of age. Closer analysis of the secondary spongiosa revealed a decrease in trabecular bone to volume, number and separation however these trabecular present are thicker, supporting previous observation (79). Collectively, these findings suggest that EZH2 deletion in PRRX1 limb bud mesenchyme effects limb patterning and promoting trabeculae patterning throughout the long bones. However a decreased growth plate size and percentage secondary spongiosa trabecular bone was observed, where the trabeculae were thicker with greater number of osteoblast lining the trabecular bone and an increase in MAR. Therefore, Ezh2 deficiency appeared to

affect the patterning and trabeculae microarchitecture, while promoting osteoblast differentiation and activity in the long bones.

Investigations of Prrx-1-Ezh2+/- animals revealed heterozygous deletion of Ezh2 did not alter trabecular bone relative to tissue volume, however, overall size, weight and skeleton was significantly larger. EZH2 deficient animals displayed an increased osteoblast number and bone formation rates. Both Ezh2+/- and Ezh2-/- mice had thinner cortical bone, decreased mechanical strength associated with increased levels of the serum bone turnover markers, OCN, CTX-1 and TRAP. Also assessment of bone marrow cells flushed from the long bones of Ezh2+/- exhibited increased osteoclastogenesis in vitro. These observations suggested that deletion of Ezh2 in MSC triggered an increase in osteoclast activity either through increased paracrine stimulation of osteoclast numbers or their recruitment to bone tissue. Therefore, increases in bone resorption activity in Ezh2 deficient mice could counteract any increases observed in bone formation. In support of this, cultured BMSC isolated from Ezh2 deficient mice exhibited increased gene expression levels of the pro-osteoclastic factors, RANKL and M-CSF. Future experiments could involve the establishment of co-cultures of Ezh2+/+, Ezh2+/- and Ezh2-/- BMSC with osteoclast precursors as we have previously reported (80), in order to assess the functional support of osteoclastogenesis by different stromal cells.

The skeletal defects described in our study following EZH2 deletion in mesenchyme tissue are similar to that seen in human patients who carry autosomal dominant mutations in Ezh2 in a condition known as Weaver syndrome. These patients exhibit excess bone growth, aging and cranial deformities (81). We suggest the general overgrowth is contributed to increase osteoblasts maturation, whilst advanced bone age may be contributed to depletion or senescence of the skeletal stem cell pool. The use of KDM6A and KDM6B inhibitors could

possibly rescue the growth and skeletal effects seen in the Weaver syndrome patients, however the effectiveness would need to be investigated further in pre-clinical animal models.

EZH2 deletion has been identified in osteoblast maturation, whilst EZH2 plays a role in preventing cellular senesce with Twist-1 in MSC in vitro. (35,36,82). To address the role of EZH2 in normal bone aging, ongoing studies in our laboratory have housed Ezh2+/-, Ezh2+/+ mice up to 2 years of age, in order to assess the role of EZH2 deficiency in maintaining the skeletal stem cell pool and bone integrity during aging. Bone parameters will be determined over time for each mouse genotype as reported in Chapter 4. The skeletal stem cells will be isolated as described previously (83,84) and assessed for global presence of Ezh2, H3K27me and H3K4me by ChIP-Seq, then correlated to changes in gene expression patterns following RNA-Seq analysis under normal growth and osteogenic conditions. A better understanding of the molecular pathways targeted by EZH2 activity during BMSC maintenance and differentiation may help identify new therapeutic drug targets to treat these and other congenital bone disorders. These studies have also shed light on the potential use of EZH2 inhibitors in bone related diseases such as osteoporosis, characterised by low bone density and high fracture risk (85,86).

Based on our work the inhibition of EZH2 activity would be beneficial to stimulate bone formation, but complete inhibition of EZH2 would be detrimental as chondrocyte hypertrophy and MSC proliferation or survival will be affected compromising the bone quality. It also suggests that the use of EZH2 inhibitors could cause an increase in osteoclast activity and bone resorption, hence anti-resorptive drugs such as bisphosphanates would need to be considered in combination. To determine the role of EZH2 in the development of osteoporosis, adult female Prrx-1-, Osterix-Ezh2+/- or Ezh2+/+mice could be ovariectomised

to induce osteoporosis due to oestrogen deficiency (87,88). Similarly, Ezh2+/- and Ezh2+/+ mice could also be used to assess the role of EZH2 during endochondral ossification and remodelling in a long bone fracture repair model (89). These experiments may shed some light on the potential role of EZH2 in bone repair under pathological conditions, and assess the possibility of using EZH2 inhibitors to treat patients with non-union fractures and bone loss due to osteoporosis.

In conclusion this study has characterised the role of EZH2 and KDM6A in human BMSC lineage commitment, and has identified that EZH2 represses known and novel osteogenic genes to inhibit MSC osteogenic differentiation. EZH2 was also found to be important for murine skeletal patterning, bone formation and remodelling in vivo. These studies lay the foundations for further investigations into the molecular mechanisms of EZH2 mediated MSC differentiation and lifespan during skeletal development, postnatal bone homeostasis and under pathological conditions.

5.1 References

1. Pittenger, M. F., Mackay, A. M., Beck, S. C., Jaiswal, R. K., Douglas, R., Mosca, J. D., Moorman, M. A., Simonetti, D. W., Craig, S., and Marshak, D. R. (1999) Multilineage potential of adult human mesenchymal stem cells. Science 284, 143-147

2. Rogers, I., and Casper, R. F. (2004) Umbilical cord blood stem cells. Best Practice & Research Clinical Obstetrics & Gynaecology 18, 893-908

3. Shi, S., and Gronthos, S. (2003) Perivascular niche of postnatal mesenchymal stem cells in human bone marrow and dental pulp. Journal of Bone and Mineral Research 18, 696-704

4. Igura, K., Zhang, X., Takahashi, K., Mitsuru, A., Yamaguchi, S., and Takahashi, T. (2004) Isolation and characterization of mesenchymal progenitor cells from chorionic villi of human placenta. Cytotherapy 6, 543-553

5. Gronthos S, M. M., Brahim J, et al. . (2000) Postnatal human dental pulp stem cells (DPSCs) in vitro and in vivo. Proc Natl Acad Sci U S A. 97, 3625-13630.

6. Seo, B.-M., Miura, M., Gronthos, S., Bartold, P. M., Batouli, S., Brahim, J., Young, M., Robey, P. G., Wang, C. Y., and Shi, S. (2004) Investigation of multipotent postnatal stem cells from human periodontal ligament. The Lancet 364, 149-155

7. De Bari, C., Dell'Accio, F., Tylzanowski, P., and Luyten, F. P. (2001) Multipotent mesenchymal stem cells from adult human synovial membrane. Arthritis & Rheumatism 44, 1928-1942

8. Bianco, P., and Gehron Robey, P. (2000) Marrow stromal stem cells. Journal of Clinical Investigation 105, 1663-1668

9. Owen, M. (1988) Marrow stromal stem-cells Journal of Cell Science, 63-76

10. Lin, G. L., and Hankenson, K. D. (2011) Integration of BMP, Wnt, and notch signaling pathways in osteoblast differentiation. Journal of Cellular Biochemistry 112, 3491-3501

11. Bi, W., Deng, J. M., Zhang, Z., Behringer, R. R., and de Crombrugghe, B. (1999) Sox9 is required for cartilage formation. Nature genetics 22, 85-89

12. Delorme, B., Ringe, J., Pontikoglou, C., Gaillard, J., Langonne, A., Sensebe, L., Noel, D., Jorgensen, C., Haupl, T., and Charbord, P. (2009) Specific lineage-priming of bone marrow mesenchymal stem cells provides the molecular framework for their plasticity. Stem Cells. 27, 1142-1151. doi: 1110.1002/stem.1134.

13. Takada, I., Kouzmenko, A. P., and Kato, S. (2009) Wnt and PPARγ signaling in osteoblastogenesis and adipogenesis. Nature Reviews Rheumatology 5, 442-447

14. Tontonoz, P., Hu, E., Graves, R. A., Budavari, A. I., and Spiegelman, B. M. (1994) mPPAR gamma 2: tissue-specific regulator of an adipocyte enhancer. Genes & development 8, 1224-1234

15. Day, T. F., Guo, X., Garrett-Beal, L., and Yang, Y. (2005) Wnt/β-catenin signaling in mesenchymal progenitors controls osteoblast and chondrocyte differentiation during vertebrate skeletogenesis. Developmental cell 8, 739-750

16. Komori, T. (2010) Regulation of bone development and extracellular matrix protein genes by RUNX2. Cell and tissue research 339, 189-195

17. Margueron, R., Trojer, P., and Reinberg, D. (2005) The key to development: interpreting the histone code? Current Opinion in Genetics & Development 15, 163-176

18. Taverna, S. D., Li, H., Ruthenburg, A. J., Allis, C. D., and Patel, D. J. (2007) How chromatin-binding modules interpret histone modifications: lessons from professional pocket pickers. Nat Struct Mol Biol 14, 1025-1040

19. Felsenfeld, G. (2014) A brief history of epigenetics. Cold Spring Harbor perspectives in biology 6, a018200

20. Bell, J. T., and Spector, T. D. (2011) A twin approach to unraveling epigenetics. Trends in Genetics 27, 116-125

21. Goldberg, A. D., Allis, C. D., and Bernstein, E. (2007) Epigenetics: A Landscape Takes Shape. Cell 128, 635-638

22. Rivera, R. M., and Bennett, L. B. (2010) Epigenetics in humans: an overview. Current Opinion in Endocrinology Diabetes and Obesity 17, 493-499

23. Holliday, R. (1994) Epigenetics-an overview Developmental Genetics 15, 453-457

24. Bracken, A. P. (2006) Genome-wide mapping of Polycomb target genes unravels their roles in cell fate transitions. Genes & Development 20, 1123-1136

25. Cao, R., Wang, L., Wang, H., Xia, L., Erdjument-Bromage, H., Tempst, P., Jones, R. S., and Zhang, Y. (2002) Role of histone H3 lysine 27 methylation in Polycomb-group silencing. Science 298, 1039-1043

26. Francis, N. J., Kingston, R. E., and Woodcock, C. L. (2004) Chromatin compaction by a polycomb group protein complex. Science 306, 1574-1577

27. Huang, X. J., Wang, X., Ma, X., Sun, S. C., Zhou, X., Zhu, C., and Liu, H. (2014) EZH2 is essential for development of mouse preimplantation embryos. Reprod Fertil Dev 26, 1166-1175

28. Kamminga, L. M., Bystrykh, L. V., Boer, A. C., Houwer, S., Douma, J., Weersing, E., Dontje, B., and de Haan, G. (2006) The polycomb group gene Ezh2 prevents hematopoietic stem cell exhaustion. Blood 107, 2170-2179

29. Pereira, J. D., Sansom, S. N., Smith, J., Dobenecker, M. W., Tarakhovsky, A., and Livesey, F. J. (2010) Ezh2, the histone methyltransferase of PRC2, regulates the balance between self-renewal and differentiation in the cerebral cortex. Proceedings of the National Academy of Sciences 107, 15957-15962

30. Qin, G., Chen, L., Ma, Y., Kim, E. Y., Yu, W., Schwartz, R. J., Qian, L., and Wang, J. (2012) Conditional Ablation of Ezh2 in Murine Hearts Reveals Its Essential Roles in Endocardial Cushion Formation, Cardiomyocyte Proliferation and Survival. PLoS ONE 7, e31005

31. Richter, G. H. S., Plehm, S., Fasan, A., Rossler, S., Unland, R., Bennani-Baiti, I. M., Hotfilder, M., Lowel, D., von Luettichau, I., Mossbrugger, I., Quintanilla-Martinez, L., Kovar, H., Staege, M. S., Muller-Tidow, C., and Burdach, S. (2009) EZH2 is a mediator of EWS/FLI1 driven tumor growth and metastasis blocking endothelial and neuro-ectodermal differentiation. Proceedings of the National Academy of Sciences 106, 5324-5329

32. Schwarz, D., Varum, S., Zemke, M., Scholer, A., Baggiolini, A., Draganova, K., Koseki, H., Schubeler, D., and Sommer, L. (2014) Ezh2 is required for neural crest-derived cartilage and bone formation. Development. 141, 867-877. doi: 810.1242/dev.094342.

33. Su, I. H., Basavaraj, A., Krutchinsky, A. N., Hobert, O., Ullrich, A., Chait, B. T., and Tarakhovsky, A. (2003) Ezh2 controls B cell development through histone H3 methylation and Igh rearrangement. Nature Immunology 4, 124-131

34. Yu, Y. L., Chou, R. H., Chen, L. T., Shyu, W. C., Hsieh, S. C., Wu, C. S., Zeng, H. J., Yeh, S. P., Yang, D. M., Hung, S. C., and Hung, M. C. (2011) EZH2 Regulates Neuronal Differentiation of Mesenchymal Stem Cells through PIP5K1C-dependent Calcium Signaling. Journal of Biological Chemistry 286, 9657-9667

35. Hemming, S., Cakouros, D., Isenmann, S., Cooper, L., Menicanin, D., Zannettino, A., and Gronthos, S. (2014) EZH2 and KDM6A Act as an Epigenetic Switch to Regulate Mesenchymal Stem Cell Lineage Specification. Stem Cells. 32, 802-815. doi: 810.1002/stem.1573.

36. Wei, Y., Chen, Y.-H., Li, L.-Y., Lang, J., Yeh, S.-P., Shi, B., Yang, C.-C., Yang, J.-Y., Lin, C.-Y., Lai, C.-C., and Hung, M.-C. (2010) CDK1-dependent phosphorylation of EZH2 suppresses methylation of H3K27 and promotes osteogenic differentiation of human mesenchymal stem cells. Nature Cell Biology 13, 87-94

37. Wang, L., Jin, Q., Lee, J. E., Su, I. h., and Ge, K. (2010) Histone H3K27 methyltransferase Ezh2 represses Wnt genes to facilitate adipogenesis. Proceedings of the National Academy of Sciences 107, 7317-7322

38. Yang, D., Okamura, H., Teramachi, J., and Haneji, T. (2015) Histone Demethylase Utx Regulates Differentiation and Mineralization in Osteoblasts. Journal of cellular biochemistry

39. Yang, D., Okamura, H., Nakashima, Y., and Haneji, T. (2013) Histone Demethylase Jmjd3 Regulates Osteoblast Differentiation via Transcription Factors Runx2 and Osterix. Journal of Biological Chemistry 288, 33530-33541

40. Ye, L., Fan, Z., Yu, B., Chang, J., Al Hezaimi, K., Zhou, X., Park, N.-H., and Wang, C.-Y. (2012) Histone Demethylases KDM4B and KDM6B Promotes Osteogenic Differentiation of Human MSCs. Cell Stem Cell 11, 50-61

41. Huszar, J. M., and Payne, C. J. (2014) MIR146A inhibits JMJD3 expression and osteogenic differentiation in human mesenchymal stem cells. FEBS Letters 588, 1850-1856

42. Banka, S., Lederer, D., Benoit, V., Jenkins, E., Howard, E., Bunstone, S., Kerr, B., McKee, S., Lloyd, I., and Shears, D. (2015) Novel KDM6A (UTX) mutations and a clinical and molecular review of the X-linked Kabuki syndrome (KS2). Clinical genetics 87, 252-258

43. Lederer, D., Grisart, B., Digilio, M. C., Benoit, V., Crespin, M., Ghariani, S. C., Maystadt, I., Dallapiccola, B., and Verellen-Dumoulin, C. (2012) Deletion of KDM6A, a histone demethylase interacting with MLL2, in three patients with Kabuki syndrome. The American Journal of Human Genetics 90, 119-124

44. Miyake, N., Mizuno, S., Okamoto, N., Ohashi, H., Shiina, M., Ogata, K., Tsurusaki, Y., Nakashima, M., Saitsu, H., and Niikawa, N. (2013) KDM6A point mutations cause Kabuki syndrome. Human mutation 34, 108-110

45. Micale, L., Augello, B., Maffeo, C., Selicorni, A., Zucchetti, F., Fusco, C., De Nittis, P., Pellico, M. T., Mandriani, B., and Fischetto, R. (2014) Molecular analysis, pathogenic mechanisms, and readthrough therapy on a large cohort of Kabuki syndrome patients. Human mutation 35, 841-850

46. Van der Meulen, J., Speleman, F., and Van Vlierberghe, P. (2014) The H3K27me3 demethylase UTX in normal development and disease. Epigenetics 9, 658-668

47. Lan, F., Bayliss, P. E., Rinn, J. L., Whetstine, J. R., Wang, J. K., Chen, S., Iwase, S., Alpatov, R., Issaeva, I., and Canaani, E. (2007) A histone H3 lysine 27 demethylase regulates animal posterior development. Nature 449, 689-694

48. Agger, K., Cloos, P. A., Christensen, J., Pasini, D., Rose, S., Rappsilber, J., Issaeva, I., Canaani, E., Salcini, A. E., and Helin, K. (2007) UTX and JMJD3 are histone H3K27 demethylases involved in HOX gene regulation and development. Nature 449, 731-734

49. Johnston, L. D., Knutson, S., Warholic, N., Klaus, C. R., Wigle, T., Iwanowicz, D., Admirand, E. A., Littlefield, B. A., Scott, M. P., and Smith, J. J. (2013) EZH2 inhibitor EPZ-6438 synergizes with anti-lymphoma therapies in preclinical models. Blood 122, 4416-4416

50. Knutson, S. K., Warholic, N. M., Wigle, T. J., Klaus, C. R., Allain, C. J., Raimondi, A., Scott, M. P., Chesworth, R., Moyer, M. P., and Copeland, R. A. (2013) Durable tumor regression in genetically altered malignant rhabdoid tumors by inhibition of methyltransferase EZH2. Proceedings of the National Academy of Sciences 110, 7922-7927

51. van Kruijsbergen, I., Hontelez, S., and Veenstra, G. J. C. (2015) Recruiting polycomb to chromatin. The International Journal of Biochemistry & Cell Biology 67, 177-187

52. Chen, S., Bohrer, L. R., Rai, A. N., Pan, Y., Gan, L., Zhou, X., Bagchi, A., Simon, J. A., and Huang, H. (2010) Cyclin-dependent kinases regulate epigenetic gene silencing through phosphorylation of EZH2. Nat Cell Biol 12, 1108-1114

53. Easwaran, H., Johnstone, S. E., Van Neste, L., Ohm, J., Mosbruger, T., Wang, Q., Aryee, M. J., Joyce, P., Ahuja, N., Weisenberger, D., Collisson, E., Zhu, J., Yegnasubramanian, S., Matsui, W., and Baylin, S. B. (2012) A DNA hypermethylation module for the stem/progenitor cell signature of cancer. Genome Research 22, 837-849

54. Kubo, H., Shimizu, M., Taya, Y., Kawamoto, T., Michida, M., Kaneko, E., Igarashi, A., Nishimura, M., Segoshi, K., Shimazu, Y., Tsuji, K., Aoba, T., and Kato, Y. (2009) Identification of mesenchymal stem cell (MSC)-transcription factors by microarray and knockdown analyses, and signature molecule-marked MSC in bone marrow by immunohistochemistry. Genes Cells. 14, 407-424. doi: 410.1111/j.1365-2443.2009.01281.x. Epub 02009 Feb 01217.

55. Ikeda, R., Yoshida, K., Tsukahara, S., Sakamoto, Y., Tanaka, H., Furukawa, K., and Inoue, I. (2005) The promyelotic leukemia zinc finger promotes osteoblastic differentiation of human mesenchymal stem cells as an upstream regulator of CBFA1. J Biol Chem 280, 8523-8530

56. Wu, S. M., Shih, L. H., Lee, J. Y., Shen, Y. J., and Lee, H. H. (2015) Estrogen Enhances Activity of Wnt Signaling During Osteogenesis by Inducing Fhl1 Expression. J Cell Biochem

57. Hamidouche, Z., Hay, E., Vaudin, P., Charbord, P., Schule, R., Marie, P. J., and Fromigue, O. (2008) FHL2 mediates dexamethasone-induced mesenchymal cell differentiation into osteoblasts by activating Wnt/beta-catenin signaling-dependent Runx2 expression. FASEB journal : official publication of the Federation of American Societies for Experimental Biology 22, 3813-3822

58. Park, D., Spencer, J. A., Koh, B. I., Kobayashi, T., Fujisaki, J., Clemens, T. L., Lin, C. P., Kronenberg, H. M., and Scadden, D. T. (2012) Endogenous bone marrow MSCs are dynamic, fate-restricted participants in bone maintenance and regeneration. Cell stem cell 10, 259-272

59. Park, D., Spencer, J. A., Lin, C. P., and Scadden, D. T. (2014) Sequential In vivo Imaging of Osteogenic Stem/Progenitor Cells During Fracture Repair. JoVE (Journal of Visualized Experiments), e51289-e51289

60. Barna, M., Merghoub, T., Costoya, J. A., Ruggero, D., Branford, M., Bergia, A., Samori, B., and Pandolfi, P. P. (2002) Plzf mediates transcriptional repression of HoxD gene expression through chromatin remodeling. Dev Cell 3, 499-510

61. Barna, M., Hawe, N., Niswander, L., and Pandolfi, P. P. (2000) Plzf regulates limb and axial skeletal patterning. Nat Genet 25, 166-172

62. Ivins, S., Pemberton, K., Guidez, F., Howell, L., Krumlauf, R., and Zelent, A. (2003) Regulation of Hoxb2 by APL-associated PLZF protein. Oncogene 22, 3685-3697

63. Lee, H.-H., Lee, J.-Y., and Shih, L.-H. (2013) Proper Fhl1 expression as Wnt signaling is required for chondrogenesis of ATDC5 cells. Animal Cells and Systems 17, 413-420

64. Barna, M., Pandolfi, P. P., and Niswander, L. (2005) Gli3 and Plzf cooperate in proximal limb patterning at early stages of limb development. Nature 436, 277-281

65. Xu, B., Hrycaj, S. M., McIntyre, D. C., Baker, N. C., Takeuchi, J. K., Jeannotte, L., Gaber, Z. B., Novitch, B. G., and Wellik, D. M. (2013) Hox5 interacts with Plzf to restrict Shh expression in the developing forelimb. Proceedings of the National Academy of Sciences of the United States of America 110, 19438-19443

66. Fukuyo, S., Yamaoka, K., Sonomoto, K., Oshita, K., Okada, Y., Saito, K., Yoshida, Y., Kanazawa, T., Minami, Y., and Tanaka, Y. (2014) IL-6-accelerated calcification by induction of ROR2 in human adipose tissue-derived mesenchymal stem cells is STAT3 dependent. Rheumatology (Oxford) 53, 1282-1290

67. Yang, T., Zhang, J., Cao, Y., Zhang, M., Jing, L., Jiao, K., Yu, S., Chang, W., Chen, D., and Wang, M. (2015) Wnt5a/Ror2 mediates temporomandibular joint subchondral bone remodeling. J Dent Res 94, 803-812

68. Ling, L., Nurcombe, V., and Cool, S. M. (2009) Wnt signaling controls the fate of mesenchymal stem cells. Gene 433, 1-7

69. Liu, Y., Bhat, R. A., Seestaller-Wehr, L. M., Fukayama, S., Mangine, A., Moran, R. A., Komm, B. S., Bodine, P. V., and Billiard, J. (2007) The orphan receptor tyrosine kinase Ror2 promotes osteoblast differentiation and enhances ex vivo bone formation. Molecular Endocrinology 21, 376-387

70. Maeda, K., Kobayashi, Y., Udagawa, N., Uehara, S., Ishihara, A., Mizoguchi, T., Kikuchi, Y., Takada, I., Kato, S., and Kani, S. (2012) Wnt5a-Ror2 signaling between osteoblast-lineage cells and osteoclast precursors enhances osteoclastogenesis. Nature medicine 18, 405-412

71. Oguri, M., Kato, K., Yokoi, K., Yoshida, T., Watanabe, S., Metoki, N., Yoshida, H., Satoh, K., Aoyagi, Y., Nozawa, Y., and Yamada, Y. (2010) Assessment of a polymorphism of SDK1 with hypertension in Japanese Individuals. Am J Hypertens 23, 70-77

72. Jain, R., Li, D., Gupta, M., Manderfield, L. J., Ifkovits, J. L., Wang, Q., Liu, F., Liu, Y., Poleshko, A., Padmanabhan, A., Raum, J. C., Li, L., Morrisey, E. E., Lu, M. M., Won, K. J., and Epstein, J. A. (2015) HEART DEVELOPMENT. Integration of Bmp and Wnt signaling by Hopx specifies commitment of cardiomyoblasts. Science 348, aaa6071

73. Powell, A. E., Wang, Y., Li, Y., Poulin, E. J., Means, A. L., Washington, M. K., Higginbotham, J. N., Juchheim, A., Prasad, N., and Levy, S. E. (2012) The pan-ErbB negative regulator Lrig1 is an intestinal stem cell marker that functions as a tumor suppressor. Cell 149, 146-158

74. Takeda, N., Jain, R., LeBoeuf, M. R., Wang, Q., Lu, M. M., and Epstein, J. A. (2011) Interconversion between intestinal stem cell populations in distinct niches. Science 334, 1420-1424

75. Munoz, J., Stange, D. E., Schepers, A. G., van de Wetering, M., Koo, B. K., Itzkovitz, S., Volckmann, R., Kung, K. S., Koster, J., Radulescu, S., Myant, K., Versteeg, R., Sansom, O. J., van Es, J. H., Barker, N., van Oudenaarden, A., Mohammed, S., Heck, A. J., and Clevers, H. (2012) The Lgr5 intestinal stem cell signature: robust expression of proposed quiescent '+4' cell markers. EMBO J 31, 3079-3091

76. Pettersson, M., Dannaeus, K., Nilsson, K., and Jonsson, J. I. (2000) Isolation of MYADM, a novel hematopoietic-associated marker gene expressed in multipotent progenitor cells and up-regulated during myeloid differentiation. J Leukoc Biol 67, 423-431

77. Wyngaarden, L. A., Delgado-Olguin, P., Su, I. H., Bruneau, B. G., and Hopyan, S. (2011) Ezh2 regulates anteroposterior axis specification and proximodistal axis elongation in the developing limb. Development. 138, 3759-3767. doi: 3710.1242/dev.063180. Epub 062011 Jul 063127.

78. ten Berge, D., Brouwer, A., Korving, J., Martin, J. F., and Meijlink, F. (1998) Prx1 and Prx2 in skeletogenesis: roles in the craniofacial region, inner ear and limbs. Development 125, 3831-3842

79. Dudakovic, A., Camilleri, E. T., Xu, F., Riester, S. M., McGee-Lawrence, M. E., Bradley, E. W., Paradise, C. R., Lewallen, E. A., Thaler, R., Deyle, D. R., Larson, A. N., Lewallen, D. G., Dietz, A. B., Stein, G. S., Montecino, M. A., Westendorf, J. J., and van Wijnen, A. J. (2015) Epigenetic Control of Skeletal Development by the Histone Methyltransferase Ezh2. J Biol Chem

80. Atkins, G. J., Kostakis, P., Welldon, K. J., Vincent, C., Findlay, D. M., and Zannettino, A. C. (2005) Human trabecular bone-derived osteoblasts support human osteoclast formation in vitro in a defined, serum-free medium. J Cell Physiol 203, 573-582

81. Gibson, William T., Hood, Rebecca L., Zhan, Shing H., Bulman, Dennis E., Fejes, Anthony P., Moore, R., Mungall, Andrew J., Eydoux, P., Babul-Hirji, R., An, J., Marra, Marco A., Consortium, F. C., Chitayat, D., Boycott, Kym M., Weaver, David D., and Jones, Steven J. (2012) Mutations in EZH2 Cause Weaver Syndrome. American Journal of Human Genetics 90, 110-118

82. Cakouros, D., Isenmann, S., Cooper, L., Zannettino, A., Anderson, P., Glackin, C., and Gronthos, S. (2012) Twist-1 Induces Ezh2 Recruitment Regulating Histone Methylation along the Ink4A/Arf Locus in Mesenchymal Stem Cells. Molecular and Cellular Biology 32, 1433-1441

83. Nguyen, T. M., Arthur, A., Hayball, J. D., and Gronthos, S. (2013) EphB and Ephrin-B interactions mediate human mesenchymal stem cell suppression of activated T-cells. Stem cells and development 22, 2751-2764

84. Noll, J. E., Hewett, D. R., Williams, S. A., Vandyke, K., Kok, C., To, L. B., and Zannettino, A. C. (2014) SAMSN1 is a tumor suppressor gene in multiple myeloma. Neoplasia 16, 572-585

85. Kanis, J. A., Melton, L. r., Christiansen, C., Johnston, C. C., and Khaltaev, N. (1994) The diagnosis of osteoporosis. J Bone Miner Res 9, 1137-1141

86. Marcus, R., and Majumder, S. (1996) The nature of osteoporosis. Osteoporosis 1, 3-17

87. Thompson, D. D., Simmons, H. A., Pirie, C. M., and Ke, H. Z. (1995) FDA Guidelines and animal models for osteoporosis. Bone 17, 125S-133S

88. Kalu, D. N. (1991) The ovariectomized rat model of postmenopausal bone loss. Bone Miner 15, 175-191

89. Arthur, A., Panagopoulos, R. A., Cooper, L., Menicanin, D., Parkinson, I. H., Codrington, J. D., Vandyke, K., Zannettino, A. C., Koblar, S. A., Sims, N. A., Matsuo, K., and Gronthos, S. (2013) EphB4 enhances the process of endochondral ossification and inhibits remodeling during bone fracture repair. J Bone Miner Res 28, 926-935

Additional publications generated during my PhD:

Stem Cells Dev. 2015 Jun 1;24(11):1297-308. doi: 10.1089/scd.2014.0471. Epub 2015 Feb 25. **Cakouros D, Isenmann S, Hemming SE, Menicanin D, Camp E, Zannettino AC, Gronthos S**. Novel basic helix-loop-helix transcription factor hes4 antagonizes the function of twist-1 to regulate lineage commitment of bone marrow stromal/stem cells.

Stem Cells. 2014 Jul;32(7):1991-2. doi: 10.1002/stem.1710. **Hemming S, Cakouros D, Gronthos S**. Detachment of mesenchymal stem cells with trypsin/EDTA has no effect on apoptosis detection.

Sarah Elizabeth Hemming, Dimitrios Cakouros and Stan Gronthos. "Epigenetic regulation of mesenchymal stem cell growth and multi-potential differentiation". In: The Biology and Therapeutic Applications of Mesenchymal Cells. Ed K. Atkinson. John Wiley and Sons, Hoboken, New Jersey, USA. 2015, currently in press manuscript attached below.

Epigenetic regulation of mesenchymal stem cell growth and multi-potential differentiation

Sarah Elizabeth Hemming[1,2], Dimitrios Cakouros[1,2], Stan Gronthos[1,2,*]

[1]Mesenchymal Stem Cell Laboratory, School of Medical Sciences, Faculty of Health Sciences, University of Adelaide, South Australia, Australia.

[2]Cancer Theme, South Australian Health and Medical Research Institute, Adelaide, SA, Australia.

***Corresponding Author**: Professor Stan Gronthos. Mesenchymal Stem Cell Laboratory, School of Medical Sciences, Faculty of Health Sciences, University of Adelaide, Frome Road, Adelaide 5005, South Australia, Australia.

Phone: +6181284395; Fax: +61-83135384;

Email: stan.gronthos@adelaide.edu.au

Abstract

Mesenchymal Stem/Stromal Cells (MSC) are considered to be a reliable source of stem cells for cellular based regenerative medicine applications, based on their multipotent potential, pro-angiogenic and immunomodulatory properties. Whilst the use of MSC are “less controversial” than embryonic derived stem cells (ESCs), they, like all somatic stem cells have a finite lifespan ex vivo. Key master regulatory genes and signalling pathways critical for MSC self-renewal and lineage determination are the subjects of intense investigations. However, the role of epigenetic modifiers in regulating the chromatin structure and accessibility of DNA on genes of various signalling pathways has only recently been investigated. With the increasing evidence implicating epigenetic modifiers in MSC differentiation, growth, and the correlation between mutations in epigenetic modifiers resulting in human disorders with musculoskeletal phenotypes these findings suggest the importance of these proteins in skeletal development.

1. Introduction

Stem cells are characterized by their capability to self-renew and terminally differentiate into multiple cell types. Somatic or adult stem cells have a finite self-renewal capacity and are lineage-restricted. The use of adult stem cells for therapeutic purposes has been a topic of enormous interest given the ethical considerations associated with embryonic stem (ES) cells. Mesenchymal stem cells (MSCs) are adult stem cells that can differentiate into osteogenic, adipogenic, chondrogenic, or myogenic lineages. Owing to their ease of isolation and unique characteristics including lack of destructive immune responses in their host, MSCs have been widely regarded as potential candidates for tissue engineering and repair. While various signalling molecules important to MSC

differentiation have been identified, our complete understanding of this process is lacking. Recent investigations focused on the role of epigenetic regulation in lineage-specific differentiation of MSCs have shown that unique patterns of DNA methylation and histone modifications play an important role in the induction of MSC differentiation toward specific lineages. Nevertheless, MSC epigenetic profiles reflect a more restricted differentiation potential as compared to ES cells. Here we review the effect of epigenetic modifications on MSC multipotency and differentiation, with a focus on osteogenic and adipogenic differentiation. We also highlight clinical applications of MSC epigenetics and nuclear reprogramming.

2. Mesenchymal Stem Cells

Bone marrow mesenchymal stromal/stem cells (BMSC) are tissue specific postnatal stem cells which are restricted in their differentiation potentials to form functional skeletal tissues and myelosupportive stroma. Mesechymal stem-like cells have also been identified in other tissues such as peripheral adipose, umbilical cord blood, amniotic fluid, placenta, dental pulp, periodontal ligament, tendons, synovial membrane and skeletal muscle [1-1]. However, these different MSC-like populations exhibit wide variations in their multi-differentiation potentials, hematopoietic supportive properties and proliferation capacities. This variation is most likely due to the different developmental origins and tissue specific nature of the different MSC-like populations, which may be under the direct control of epigenetic patterning.

BMSC were first identified as clonogenic stromal precursor cells, termed colony forming unit-fibroblastic (CFU-F) within bone marrow aspirates of rodents [14], and subsequently in other species including humans [15]. A common feature of the ex vivo

expanded progeny of CFU-F is their heterogeneity with respect to morphology, ability to undergo self-renewal, myelosupportive capacity, lifespan and multi-differentiation potential[1,16-19].

These observations have led to the proposal that the stromal component within bone marrow is comprised of a hierarchy [20] of immature stem cells, committed progenitor cells and mature functional stromal populations (Figure 1). Since the vast majority of CFU-F demonstrate limited growth and differentiation potential, the general term describing mesenchymal stem cells only refers to the ex vivo expanded progeny of a minor subset of long lived multipotential CFU-F, with the potential to form osteoblasts, adipocytes, chondrocytes, smooth muscle cells and myelosupportive fibroblasts under inductive conditions in vitro or when transplanted in vivo. Whilst attempts have been made to establish an immunophenotype specific to MSC-like populations (HLA-ABC+/ CD73+/ CD105+/ CD29+/ CD13+/ CD44+/ CD90+/ CD45-/ CD34-/ CD31-/ CD14- (21, 22), the cell surface markers used are generic to a wide range of cultured fibroblastic cells and some vascular and haemtopoietic cell populations with different growth and developmental potentials. Moreover, none of the positive selection markers (HLA-ABC+/ CD73+/ CD105+/ CD29+/ CD13+/ CD44+/ CD90+) are capable of distinguishing between immature and committed stromal cell lineages.

The identification of multi-potential clonogenic MSC from aspirates of human bone marrow has been achieved based on their high expression of the stromal precursor cell surface antigen, STRO-1, which is down regulated in committed stromal lineages. Purification of STRO-1^{bright} BMSC was achieved by dual fluorescence activated cell sorting based on their co-expression of the perivascular markers, CD106 and CD146, and lack of expression of the haematopoietic markers, CD34, CD14, CD45, and Glycophorin-A [4, 16, 23, 24]. Therefore, the developments of immunoselection protocols to obtain

purified populations of BMSC have allowed the identification of putative regulatory genes critical for maintaining the MSC population following ex vivo expansion [25-27].

Understanding the processes that drive BMSC lineage commitment, may one day allow us to manipulate MSC to differentiate down specific lineages required for cellular therapies where stromal cells are defective in their differentiation and renewal capacity. Signalling pathways such as Wnt, Notch, bone morphogenic protein (BMP)[28] and key transcription factors, RUNX2, PPARγ2, MOYD and SOX9 have been implicated as critical drivers of MSC lineage commitment. The activation of these signalling pathways and expression of transcription factors are dependent on the regulation of chromatin, allowing the activation of these genes and their targets. Therefore, it is important to identify which epigenetic modifications are critical for the regulation of MSC growth and lineage-specification. This review will identify the relationship of important epigenetic modifications involved in MSC maintenance, self-renewal and differentiation.

3. Epigenetics

Epigenetics is the cellular modification of reversible and heritable changes in gene expression that occur without changes in the DNA code [29]. Epigenetic modifications such as DNA methylation,post-translational modifications including histone modifications and chromatin remodelers regulate the structure of chromatin, determining the accessibility of genes to transcription factors and other modulators involved in gene regulation. Chromatin is formed through the compaction of large amount of DNA where 145-146 base pairs of DNA are wrapped around a nucleosome, consisting of an octamer of histone subunit [30-31](Figure 2). Nucleosomes are joined together by linker histone 1 (H1) and a small region of DNA, which form a “beads on a string like structure”. Each

histone subunit has a specific sequence of amino acids in a tail like structure defined as a "histone tail" which protrudes out for the nucleosomes and can be post-translationally modified (Figure 2).

The functional state of chromatin can be modified through C5 methylation of DNA at cytosines within CpG dinucleotides and the post-translational modification of histone proteins and residues within the histone tails (Figure 3). DNA methylation is commonly located at the cytosine of the dinucleotides sequence CpG and is often located at genes, which have tissue-restricted expression and become stably silent. The activity of DNA methytransferases (DNMTs), is critical for genome stability, X inactivation, genomic imprinting and regulating key developmental genes during cellular differentiation [32-42]. DNA methylation can be separated in to two types, de novo and maintenance. In early mammalian development the mature oocyte, primordial germ cells and blastula DNA is relatively unmethylated. During embryogenesis and the formation of the three germ layers, DNA methylation plays a pivotal role in patterning tissue specific expression [43-45].

DNMT1 known as the "maintenance methyltransferase" is responsible for copying methylation patterns after DNA replication, imprinting, X activation and CpG methylation [38, 46]. Gene silencing can occur via DNA methylation of CpG islands to prevent the binding of proteins to DNA. This in turn acts as a marker for CpG-binding domain proteins (MBD), which recruit histone deacetylases (HDACs) and histone three lysine nine (H3K9) methyltransferase, allowing the compaction of chromatin [47-52]. DNA methylation can then be modified by DNA demethylases (dDMTase), which remove the cytosine di-methylation modification allowing the recruitment of factors involved in transcriptional activation. Ten-eleven translocation 1-3 (TET1-3) proteins are dioxgeneases that form 5 hydroxymethylation (5hmc), 5-formylcytosine (5fC) and 5-

carboxylcytosine (5caC) which are intermediates that form in the process of the removal of methylation [53, 54]. With the development of Methyl-DNA Immunoprecipitation Microarray Hybridization and bisulphite sequencing [55, 56]investigations examining the role and patterns of DNA methylation in different process such as development, stem cell self-renewal and pluripotency have yielded enormous information showing methylation of developmental genes as a cell becomes more restricted in its multipotent capacity and less stem cell like [57, 58].

Post-translational modification of histones is another level of transcriptional regulation that can result in repression or activation of gene expression. The structure of chromatin can be regulated through methylation, acetylation, phosphorylation, sumoylation and ubiquination of histone tails. Post-translational modification of 28 known residues gives rise to over 100 million differentially modified nucleosomes within cells accounting for the great diversity of signals and gene expression outcomes [59]. The regulation of DNA through epigenetic modifications allows the specification and maintenance of cellular identity in a wide range of cell types [37, 60].Acetylation of histones by histone acetyl-transferases (HATS) leads to the activation of transcription, whereas, histone methylatation by histone methyltransferases (HMTs) can regulate gene activation or repression depending on which residues are methylated. Histones can be mono- (me1), di- (me2) or tri-methylated (me3) on lysine residues and me1 or me2 on arginine residues. Methylation of histone 3 lysine 4 (H3K4), lysine 36 (H3K36) and lysine 79 (H3K79) are associated with active transcription and methylation of Histone 3 lysine 9 (H3K9) and lysine 27 (H3K27) is associated with gene repression [61] (Figure 3).

With the development of Chromatin Immunoprecipitation (ChIP) techniques researchers can now indentify histone proteins that are associated with a particular region of the genome. Recent investigations of embryonic stem cells (ESC) using microarray

and ChIP techniques have revealed the presence of both H3K27me3 and H3K4me3 specific modification patterns on chromatin termed “bivalent domains”. The presence of both these bivalent domains within ESC genomes allows the silencing of developmental regulators whist, keeping them poised for activation. Upon ESC differentiation these bivalent domains become univalent, allowing the activation of genes that drive lineage commitment [62]. Methyltransferases and demethylases are thought to be responsible for the switch between repressive H3K27 domains and active H3K4 domains. Different combinations of histone modifications can influence the recruitment of different effector proteins and transcription factors to chromatin and these combinations are known as the “histone code” which determines the functional state of chromatin [63, 64].

Furthermore, the interplay between the different epigenetic modifying enzymes (HATs, HDACs, DNMTs, MBD, and HMTs) is critical for normal gene transcription suggesting the importance of epigenetic gene regulation in many cellular processes.

4. DNA methylation and Histone modifications in MSC

The importance of key transcription factors and signalling pathways in regulating MSC differentiation, growth and life-span has been widely investigated. However, the role of epigenetic modifiers in regulating chromatin structure allowing the activation or repression of these key genes and signalling pathways in MSC has only recently been explored [65].

Studies have assessed the DNA methylation profile between MSC-like cells derived from bone marrow, adipose tissue and skeletal muscle, using bisulphite sequencing, methyl-DNA immunoprecipitation and promoter array hybridization

(MeDIP-chip)[66]. Analysis of reference sequence promoter arrays (Re-Seq) revealed that promoter DNA methylation patterns were similar in mesenchymal progenitors derived from adipose, bone marrow and skeletal muscle [67]. It was proposed that a core of hypermethylated genes constituted a common intrinsic epigenetic marking of different MSC-like populations, lending support to the common features of MSC-like cells identified in various tissues. It is suggested that promoter methylation patterns may dictate gene expression capability, where strong methylation dictates repression, while hypomethylation in some tissues determines either repressive or active gene expression when complemented with other modifying proteins.

Furthermore promoter DNA methylation is only one part of the regulation of lineage determination, since low levels of DNA methylation is not a reliable predictor of differentiation capacity [66, 68, 69]. These studies further suggest that the overall CpG methylation status of genes is not indicative of differentiation potential [70-72], suggesting that other processes other than DNA methylation, contribute to the differentiation capacity and lifespan of MSC. Therefore the role of other post-translational histone modifiers is becoming increasingly more important in the study of stem cell biology. With the use of techniques such as chromatin immune-precipitation sequencing (ChIP-Seq) it is now possible to identify the epigenetic patterns of cells during many cellular process under varying environmental conditions.

5. Epigenetic regulation of MSC osteogenic differentiation

MSC osteogenic differentiation is controlled by key signalling pathways and transcription factors, which can be regulated through epigenetic modifications [73]. For example DNA methylation and demethylation have been reported to play a role during

osteogenic differentiation, where highly methylated osteogenic associated genes, Dlx5, Runx2, Bglap, Osterix, in adipose-derived MSC, undergo demethylation and increased gene expression during osteogenic differentiation [7]. Similarly, alkaline phosphatase, Trip10 and Rank Ligand, have also been shown to be regulated by DNA methylation during BMSC osteogenic differentiation [75-77], while another report observed reduced gene expression of the stem cell associated genes, Branchyury and LIN28 by hypomethylation of the promoter during BMSC differentiation [78]. Furthermore, the intrinsic and extrinsic signals MSC receive during maturation can also govern the epigenetic regulatory outcome of MSC cell fate determination [79].

Besides DNA methylation, gene repression can be mediated through H3K27 methylation. Studies have found that the H3K27 methyltransferase, Enhancer of Zeste Homolog two (EZH2), a component of the poly comb repressor complex 2 (PCR2), can interact with DNMTs to promote gene repression [80]. EZH2 has been widely implicated as a regulator of developmental processes and differentiation associated genes [81, 82]. EZH2 activity can lead to either mono, di or tri methylation of the K27 residue of H3 tails (H3K27me1/2/3), and is associated with heterochromatin, chromatin compaction and repression of gene transcription [83-85]. EZH2 influences chromatin structure through adding a me3 modification to H3K27, where this mark is recognised by PRC1, which recruits effector proteins such as chromatin remodelers involved in compaction of chromatin [86]. EZH2 deficiencies in mice lead to peri-natal lethality due to deformities in morphological movement of ESC in the developing embryo.

More recently, over-expression of EZH2 in human BMSC inhibited osteogenic differentiation, while siRNA knockdown of Ezh2 or treatment with the methytransferase inhibitor, DZNep, promoted osteogenic differentiation, identifying a direct role for EZH2 in regulating human BMSC bone cell differentiation [87]. Furthermore, EZH2 was found

to bind and methylate the promoter regions of Runx2 and osteopontin using ChIP analysis [87], suggesting that EZH2 may be a key regulator for MSC cell fate determination. During MSC differentiation, cyclin dependent kinase 1 (CDK1) represses EZH2 methyltransferase activity through the phosphorylation of residue threonine 487, thus promoting BMSC osteogenic differentiation in vitro [88]. ChIP-on-chip analysis of adipocytes and osteoblast revealed that the myocyte enhancer factor-2 interacting transcription factor (MITR or HDAC9c) is bound by EZH2 in adipocytes but not in osteoblasts. During osteogenesis EZH2 binding to MITR is repressed allowing to MITR to complex with PPARγ2, thereby directly interrupting PPARγ-2 activity [89].These observations have led to the hypothesis that the known H3K27 demethylase (HDMs) KDM6A (UTX: ubiquitously transcribed tetra-tricopeptide repeat X) and Jumonji domain-containing protein 3 (JMJD3 also known as KDM6B) could also be pivotal in dictating the lineage specificity of MSC.

Histone methylases and demethylases control the level of methylation present within a cell. An increase in H3K27 demethylation leads to the recruitment of gene activating factors and activation of gene transcription. UTX and JMJD3 have both been identified as having potential roles in regulating MSC osteogenic differentiation [87, 90-93]. UTX over–expression in MSC was found to promote osteogenic differentiation, while siRNA knockdown of UTX resulted in decreased osteogenesis in vitro and in vivo [87]. However, the role of JMJD3 in osteogenic differentiation is thought to act by regulating RUNX2 and Osterix expression in osteoblasts [91-93], which is regulated by MIR146A during osteogenic differentiation [92]. Therefore, it is still unclear whether UTX and JMJD3 work synergistically or individually to regulate osteogenic differentiation. While it is well established that BMP, Wnt, and Notch signalling pathways all play important roles in osteoblast differentiation [28], these two demethylases could play different roles in

regulating osteogenic differentiation based on the cellular signals they encounter leading to specialised effects on cellular differentiation.

Methylation of another lysine residue on H3, H3K9, is associated with chromatin compaction and gene repression. H3K9me and H3K27me modifications are usually present on silenced genes, where H3K9 methylation can depend on the H3K4 methylation status of the adjacent lysine residue [94]. There are also multiple known H3K9 HMTs, including SUV39h, Set domain bifurcated 1 (SETDB1), G9a, Set7/Setd8, which are potentially involved in the global enrichment of H3K9Me2 during MSC osteogenic differentiation [95]. Other studies have demonstrated that the activation of the non-canonical Wnt signalling pathway resulted in promotion of osteogenic differentiation due to H3K9 methylation and repression of PPARγ2 [96]. During osteogenic differentiation the promoter regions of ALP, RUNX2 and OP were acetylated and under wend H2K9me2 demethylation. The addition of acetylation and removal of H3K9me3 facilitate in gene expression and osteogenesis. Conversely stemness genes such as OCT4 and NANOG were down regulated with a corresponding de acetylation and increase in H3K9me3 present on their promoters. Furthermore, KDM4B a H3K9 demethylase removes the H3K9me3 and H3K27me3 from osteogenic associated genes such as HOX and DLX, opening up chromatin and promoting osteogenic differentiation of MSC [90].

H3K4 methylation has been shown to positively regulate transcription by recruiting nucleosome remodelling enzymes and histone acetylases [97]. H3K4 methylation is mediated by SET domain-containing methyltransferases, such as mixed lineage leukemia 1-5 (MLL1-5), SET1A/B and SET7/9. H3K4 is critical for gene activation, where this histone modification mark is widely expressed on genes involved in differentiation, growth and self-renewal [98]. The balance of H3K4 methylation is controlled by H3K4 HMTs and H3K4 HDMs. MLL proteins often associate in a complex

with H3K27 demethylase UTX/KDM6A or JMJD3/KDM6B and Pax transactivation domain-interacting protein (PTIP; nuclear protein associated with active chromatin), allowing the rapid removal of the repressive methylation and the application of the active methylation H3K4 [99].

Opening up of chromatin allowing the gene transcription is regulated by active histone modifications such as H3K4me3. Hassan and colleges identified that H3K4me3 and hyper acetylation mediated by HOXA10 induces chromatin remodelling facilitating in RUNX2 mediated activation leading to activation of RUNX2 target genes such as osteocalcin [100]. H3K4 HDMs are associated with removal of the H3K4 active methylation modification involved in transcriptional activation. Jumonji domain-containing histone demethylases such as the JARID1 family of HDMs (JARID1A−D) remove H3K4me3 and H3K4me2 modifications. JARID1A inhibits osteogenesis through the promoter demethylation of RUNX2, Osterix, Osteocalcin and alkaline phosphatase in human adipose-derived MSC (101). The Nucleolar protein 66 is also known to have H3K4me3/2/1 demethylase activity, and has been found to demethylate the promoter region of Osterix and interact directly with Osterix preventing activation of its downstream target genes [102]. Furthermore in human adipose derived MSC, osteogenic differentiation is regulated by H3K4 demethylase Retinoblastoma binding protein 2 (RBP2). Knockdown of RBP2 increased H3K4me3 and promoted alkaline phosphatase, osteocalcin and Osterix expression. Furthermore, RBP2 directly associates with the RUNX2 protein, where knockdown of RPB2 leads to activation of RUNX2 [101].

Other modifications such as acetylation of the histone tails leads to neutralization of the partial electric charge of lysine, which in turn results in opening of the chromatin structure. HATs and HDACs are responsible for the maintenance of cellular histone acetylation. H3K9 and H4K16 acetylation (H3K9ac and H4K16ac) are commonly

associated with euchromatin and transcriptional activation. During osteogenic differentiation H3K9ac enrichment decreased on stemness genes NANOG and OCT4 and were enriched with an increases H3K9me2 [95].

Following long-term ex vivo expansion, MSC undergo spontaneous osteogenic differentiation with an increase in Runx2 and Alkaline phosphatase expression. This observation has been correlated with an increase of H3k9ac and H3K14ac modification on these osteogeneic genes [103]. There are 18 known HDACs which contribute to skeletal development and bone homeostasis. Many of these HDACs regulate bone formation and development through the regulation of Runx2 [104-107]. H3 and H4 hyperacetylation was identified on Osterix and Osteocalcin promoters leading to decreased HDAC1 recruitment to these promoters [108]. Furthermore, the treatment of MSC with the HDAC inhibitors, Vorinostat, Sodium Butyrate, Valproic acid and Trichostatin A was found to promote osteogenic differentiation [109-113].

These studies have identified a wide range of DNA and histone post-translational modifications directly involved in MSC osteogeneic differentiation, but have yet to determine the sequential and temporal activities of these epigenetic modifiers during the process of osteogenesis.

6. Epigenetic Regulation of adipogenic differentiation

Adipogenic differentiation of MSC is thought to be regulated, in part, by DNA methylation, where CpG sites have been shown to be hypomethylated in key adipogenic genes such as PPARγ2, C/EBP□, Leptin, fatty acid-binding protein 4, and lipoprotein lipase in ex vivo expanded adipose derived MSC [70].

The H3K27 methyltransferase, Ezh2 is also known to promote adipogenesis by repressing Wnt-1,-6,-10a and -10b leading to disruption of Wnt/β-catenin signalling rather than directly regulating *PPARγ2* [115]. In human studies, over-expression of EZH2 in BMSC promoted adipogenic differentiation, while siRNA knockdown inhibited adipogenic differentiation [87]. Over expression of H3K27 demethylase, UTX, inhibited adipogenesis, while siRNA knockdown promoted adipogenic differentiation of BMSC [87] possibly by demethylating Wnt associated genes therefore inhibiting adipogenesis indirectly. Ye and colleagues identified that knockdown of H3K27me3 demethylase JMJD3/KDM6B and H3K4me3 demethylase KDM4B inhibited adipogenesis further supporting the role of demethylases in adipogenic differentiation [90]. Additional research shows that during adipogenic differentiation, histones bound to adipogenic associated gene promoters undergo H4K20me1 methylation and this is mediated by methylase PR-Set7/Setd8 [116].

During MSC adipogenic differentiation the H3K9 HMT, Suv39h1, mediates AP-2alpha-dependent inhibition of C/EBPα [117]. Furthermore, PPARγ2 target gene expression is block by SUV39H1, suggesting that H3K9 methylation is a negative regulator of adipogenesis [118]. Similarly, Wnt5a induced H3K9 SETDB1 methylation was found to activate the non-canonical Wnt signalling cascade resulting in the inhibition of PPARγ2 function and adipogenesis, while promoting osteogeneic lineage commitment [119,120]. In another report, the HMT, G9a was found to be responsible for di-methylation of H3K9, which regulates gene repression [121]. Furthermore, ChIP-Seq analysis of preadipocytes revealed that H3K9me2 and H3K27me3 modifications at gene loci were largely non-overlapping [122]. In these studies, Wnt gene loci exhibited high levels of H3K27me3 and low levels of H3K9me2, while PPARγ2 had high levels of H3K9me2 and low levels of H3K27me3. Inhibition of G9a methylation activity was also found to

increase PPARγ2 gene expression, leading to the promotion of adipogenesis. Whilst G9a represses PPARγ2 expression in an HMT activity-dependent manner, it has also been shown to facilitate Wnt10a expression independent of its enzymatic activity [122]. Therefore, Wnt10a facilitates beta catenin stabilization, leading to the inhibiton of adipogenesis and promotion of osteogenic commitment.

LSD1 (lysine-specific demethylase 1), also known as KDM1 forms a complex with androgen receptors and can act as a H3K9 di-demethylase. LSD1 can regulate CEBPα by decreasing H3K9me2 and maintaining H3K4me2 at its promoter, counteracting the activity of the H3K9 methyltransferase, SETDB1 [123]. Activating methylation modifications such as H3K4 play a critical role in activation of key adipogenic differentiation genes. MLL3 and MLL4 are mono- and di-methyltransferases targeting H3K4, which are required for enhancer activation, gene activation and differentiation and are critical for PPARγ and C/EBP-α expression during adipogenesis [99, 124-126]. Moreover, H3K4 di-methylation, a mark of poised genes, has been shown to be present on the promoters of the adipose associated genes, apM1, glut4, gpd1, and leptin in preadipocytes [98,127].

Other studies have shown that H4K20 methylation, often associated with gene repression, can aid in gene activation via mono-methylation. H4K20 mono-methyltransferase PR-Set7/Setd8 gene is up-regulated by PPARγ2 gamma during adipogenesis, and the knockdown of PR-Set7/Setd8 suppressed adipogenesis [116]. These findings suggest combinations of lysine methylation patterns are required for promotion or repression of adipogenesis.

The histone 3 argine 8 methylase (H3R8) known as the protein arginine methyltransferase (PRMT) family of enzymes is divided into two classes. Type I PRMT

asymmetrically mono and di-methylate arginine residues, whereas type II PRMT symmetrically mono and di-methylate arginine residues [128]. Both types of PRMT form complexes with SWI/SNF ATP-dependent chromatin-remodelling enzymes, adding another functional layer onto chromatin regulation. Knockdown of PRMT5 inhibits adipogenic differentiation and adipogenic gene expression, whilst over-expression accelerates adipogenic differentiation [129]. The presence of PRMT5 recruits SWI/SNF binding of PPARγ2 and downstream adipose associated target genes allowing the opening up of chromatin and activation of gene transcription., Brg1 SWI/SNF remodelling enzyme appears to plays a critical role in remodelling chromatin at the PPARγ2 gene locus to facilitate PPARγ2 gene expression [130].

Histone acetylation has been reported to be an important modification in regulating white adipocyte differentiation. HATS promote the recruitment of factors involved in opening up of chromatin and the activation of key genes critical for adipogenesis [131,132]. HATS such as H3K27ac CBP/p300 have been shown to be involved in mediating PPARγ2 gene expression and promoting adipogenesis in 3T3-L1 preadipocytes. Furthermore, Genome-wide profiling of H3K9ac and H3K27ac in 3R3-L1 preadipocytes identified their presence on the *PPARγ2* gene locus during adipogenesis. However, little is known of the role of CBP/p300 and other HATS in the regulation of *PPARγ2* and other key adipogenic genes in human MSC.

The removal of acetylated histones is important for gene repression during maturation where adipogenic differentiation can be repressed through the unphosphoryated form of retinoblastoma (Rb), which recruits HDAC3 to the promoter of PPARγ2 preventing its activation of its target genes [133]. Moreover, treatment of cultured MSC with the HDAC inhibitor, Trichostatin A, decreased adipogenic differentiation [112, 134].

While it has been shown that some epigenetic modifiers act by direct activation or repression of *PPARγ2*, other modifiers such as Ezh2 regulate adipogenesis indirectly through the inhibition of signalling pathways that promote osteo/chondrogenesis [115]. Furthermore, the recruitment of epigenetic modifiers to the chromatin by other molecules can act as another level of control to further regulate the expression of adipose associated genes. Collectively, these studies depict the complexity of epigenetic modifications involved in adipogenic differentiation, where various modifiers appear to be pivotal for the switch between osteogenic or adipogenic lineage commitment (Table 1).

7. Epigenetic Regulation of myogenic differentiation

DNA methylation has been shown to be important for gene silence during MSC differentiation however, studies have found that the known myogenic differentiation 1 MyoD1 CpG islands are not methylated in many non-expressing tissues such as the brain [135]. These findings demonstrated that, in some instances, the CpG methylation status of genes did not dictate whether these genes were silenced or expressed, suggesting that other regulator mechanisms are required.

Other studies have shown that protein levels of the DNA methyl binding factors, MeCP2 and MBD-2, significantly increased during myogenic differentiation, which are known to regulate chromatin reorganisation and promotion of terminal differentiation [136]. While non-muscle derived MSC-like populations, do not normally form myotubes or constitutively express MYOD1 expression during culture, treatment with 5-azacytidine, which removes DNA methylation, was found to induce myosin heavy chain expression and myotube formation in these cells, to promote skeletal muscle differentiation [137]. Furthermore, reports have described the localization of EZH2, YY1 and HDAC1 on

silent muscle specific genes in different MSC-like populations, preventing gene muscle creatine kinase (MCK) and myosin heavy chain (MHC) transcription [138, 139]. During muscle differentiation, EZH2, Y11 and HDAC1 are removed from muscle genes allowing the recruitment of MYOD and SRF to chromatin [138, 140]. EZH2 has also been found to repress microRNA, miR-214, in MSC, where EZH2 is removed from the chromatin during myogenic induction, allowing activation of MiR-214 and activation of MYOD and MYOGENIN [141].

The role of H3K27me HDMs in MSC differentiation was first described in muscle differentiation, where recruitment of UTX by the homeodomain transcription factor, Six4, during myogenesis, resulted in H3K27 demethylation of muscle specific genes, RNA polymerase elongation and gene expression [142]. In another study, MLL5 which lacks methyltransferase H3K4 activity like its family members MLL3 and MLL4, is critical for the regulation of LSD1 and SET7/9 and the expression of muscle regulators PAX7, Myf5 and myogenin [143]. However, the role of these factors in MSC skeletal muscle differentiation remains to be determined.

Collectively, studies suggest that epigenetic modifiers may play a role in regulating lineage specific genes in myogenesis, however further investigation are needed to demine which modifiers are critical for diving myogenic lineage commitment in muscle and non-muscle derived MSC-like populations.

8. Epigenetic regulation of chondrogenic differentiation

Early studies have shown that collagen type I is methylated in fibroblasts and chrondrocytes, whilst the cartilage specific collagen type II gene exhibits reduced

methylation in chondrocytes compared to fibroblasts. In human chondrocytes, the CpG sites within the COL10A1 promoter are normally methylated, however, during MSC chondrogenic differentiation in vitro, 2 CpG regions within the COL10A1 promoter undergo demethylation [144]. In another report, DNA hypermethylation of COL9A1 down regulated its expression in osteoarthritic chondrocytes, while treatment with 5-azadeoxycytidine, which removes DNA methylation increased COL9A1 expression in these cells [145], and has previously been shown to induce chrondrogenesis [146]. In accord with these studies, the DNA methylation status of MSC chondrogenic differentiated was investigated, identifying 8 key chondrogenic CpG rich promoters, SOX9, RUNX2, CHM1, FGFR3, CHAD, MATN4, SOX4, GREM1, GPR39 which were observed to be stable through differentiation [147]. These findings are consistent with previous reports suggesting that CpG rich promoters remain stably hypomethylated in adult somatic cells, but not all methylation patterns are indicative of gene silencing or activation [148, 149].

While studies examining the epigenetic regulation of human MSC chondrogenic differentiation are scant, one report has shown that the chondrogenic specific gene, collagen type II loses H3K27me3 and gains H3K4 and H3K36 active methylation during early chondrogenic induction [150]. In mice, chondrogenesis is regulated by Sox9 and its co-regulator, AT-rich interactive domain 5b, which recruits the H3K9 demethylase, Phf2, to the Sox9 promoter to reduce H3K29me2 levels and promote chondrogenesis [151].

In other studies, the acetylase, Tat interactive protein-60 (Tip60), can activate Sox9 and H4 acetylation, promoting Sox9 mediated transcription of Col2a1 [152]. Several other transcription factors and co-activators interact directly with Sox9 to modulate Sox9 activity. For example, The Sox9 dependent transcription of cartilage associated target genes is thought to act via p300-mediated histone acetylation on chromatin [153]. Consistent with these results, the histone deacetylase inhibitor Trichostatin A was shown

to stimulate the expression of Sox9-regulated cartilage matrix genes and induced histone acetylation around the enhancer region of the collagen alpha1 (II) gene in chondrocytes [154, 155]. Therefore, it appears that Sox9 interacts with chromatin and activates transcription via regulation of chromatin modification. Other studies have demonstrated that HDAC activity promotes type II collagen expression in chondrocytes by suppressing the transcription of Wnt-5a [156]. Furthermore over expression of HDAC4 in synovial-derived MSC was found to promote chrondrogenesis in the presence of TGF□1 [157], and is thought to also function by inhibiting Runx2 activity [158].

With limited studies using MSC derived chondrocytes the impact of epigenetic modifiers on regulating chondrogenic differentiation is unclear. It is predicated that many modifications will be critical in regulating chondrogenic differentiation and maintain healthy chondrogenic tissue. Collectively, these studies have shown that epigenetic modifiers play a role in articular and synovial derived chrondrocytes and further investigation could lead to opportunity to manipulate cells with greater chondrogenic differentiation capacity for cartilage regeneration.

This review has identified the role of epigenetic modifiers driving MSC lineage commitment. It has identified the direct regulation of key transcription factors RUNX2, SOX9, PPARγ2 and MYOD for MSC differentiation as targets of epigenetic modifiers (Table 2). These findings suggest a greater level of complexity driving MSC lineage determination.

9. Epigenetic regulation of MSC lifespan and Senescence

MSC have a limited growth and differentiation potential when propagated ex vivo. DNA methylation plays critical roles in not only MSC differentiation but in regulating the life-span of MSC. DNA methylation profiles of late passage senescent BMSC and adipose derived MSC revealed highly consistent modifications at specific CpG sites. These DNA-methylation changes have been correlated with histone marks of previously published data sets, such as trimethylation of H3K9, H3K27 and EZH2 targets [159]. However, the reduced adipogenic differentiation capacity of late passage senescent MSC cannot be attributed to DNA methylation of adipogenic gene promoters alone [71]. Maharia and colleagues identified the role of ten-eleven-translocate 1/2 (TET1/2) DNA demethylases in regulating the DNA demethylation of IGFBP1. These findings suggest that TET1/2 regulate MSC self-renewal and proliferation [160].

EZH2 is important for senescence [159], where Twist-1 induces EZH2, directly or indirectly, which in turn suppresses the Ink4A/Arf locus and p16/p14 preventing senescence of human MSCs [161]. In analogy, EZH2 is involved in preventing haematopoietic exhaustion, stem cell maintenance [162]. Spontaneous transformation of rat derived MSC has been contributed to the increase of histone H3K27me and H3K9me on the p16 INK4a gene and increase DNA methylation [163]. Furthermore, MSC replicative senescence, mediated by DNA methylation has been associated more with H3K27me histone marks rather than bivalent domain [159] meaning they have lost the activating H3K4me3 mark. This is in contrast to differentiation of non-senescent cells which show many bivalent genes have increased H3K4me3 levels and decreased H3K27me3 levels while being transcriptionally activated during differentiation [66, 68-72, 164]. During long term culture, MSC undergo spontaneous osteogenic differentiation associated with down regulation of TERT and self-renewal genes Oct4 and Sox2 and an up regulation of osteogenic genes.

DNA methylation and histone modification play a role in dictating MSC life-span and sensence. It is important to understand how these modifiers can influence the life-span of MSC, which may aid in prolonging the survival and expansion capacity of MSC. Extending the in vitro expansion capacity of MSC would be highly beneficial for manufacturing process of MSC for cell based therapies.

10. Regulation of Epigenetic Modifications in MSC for clinical use.

Following on from the initial human safety trials in 1995 [165], both allogenic or auologous MSC preparations have now been used to treat patients with conditions such as graft-versus-host disease, haematologic malignancies, cardiovascular diseases, neurologic diseases, autoimmune diseases, organ transplantation, refractory wounds, and bone/cartilage defects [166,167]. Continued investigations into the molecular mechanisms which regulate MSC development, self-renewal and proliferation may help develop optimal cell expansion protocols and quality control criteria in order to overcome the consequences associated with MSCs following ex vivo expansion including donor variability, diminishing properties and limited lifespan. Therefore, a better understanding of the epigenetic modifications, which regulate the growth and multi-potential of MSC, could be used in strategies to manipulate MSC populations ex vivo in order to facilitate better tissue regeneration outcomes for specific clinical indications. The application of chemical and pharmaceutical agents that regulate epigenetic modifiers may be beneficial in priming MSC for specific therapies, and could potentially be incorporated into scaffold and cell delivery systems. However, potential therapeutic strategies such as the use of inhibitor molecules have to await the development of novel agents that target specific epigenetic modifiers to benefit tissue regenerative with minimal non-specific affects.

11. Conclusions

This review has summarised the role of epigenetic modifiers in MSC differentiation, life-span and senescence. The presence of repressive DNA methylation, H3K27me3, H3K9me3 and HDACs on the promoter regions of key genes and signalling pathways often prevents adipogenic, osteogenic, chrondrogenic and myogenic differentiation of MSC. Whereas, the presence of DNA demethylases, H3K4me3, H3K20me1, HATs on the promoter regions of key genes and signalling pathways can facilitate adipogenic, osteogenic, chrondrogenic and myogenic differentiation of MSC. Ultimately, the histone/DNA modifications lead to recruitment of chromatin remodelers which results in gene activation or repression. Whilst some chromatin remodelers have been identified during osteogenic, adipogenic, chondrogenic and myogenic differentiation, it is still unclear how and which post-translational modifications work together to determine the activation and repression of genes important for MSC lineage commitment and life-span.

With the use of genome wide sequencing techniques such ChIP-seq, RNA-seq, ChIP-on-chip and microarray, future studies may be able to correlate the epigenetic patterning during many cellular events, such as MSC multi-differentiation and growth to aid in the development of more potent MSC preparations for regenerative medicine applications. It is also hoped that increased knowledge in this field may lead to the identification of epigenetic marks associated with impaired MSC growth/ function associated with different musculoskeletal diseases such as osteoporosis and osteoarthritis, in order to develop better prognostic criteria and novel treatment regimes.

References

1. Pittenger MF, Mackay AM, Beck SC, Jaiswal RK, Douglas R, Mosca JD, et al. Multilineage potential of adult human mesenchymal stem cells. *Science 1999:*284(**5411**):143-7.

2. Rogers I, Casper RF. Umbilical cord blood stem cells. *Best Pract Res Clin Obstet Gynaecol* 2004;18(**6**):893-908.

3. Bieback K, Kluter H. Mesenchymal stromal cells from umbilical cord blood. *Curr Stem Cell Res Ther 2007*;2(**4**):310-23.

4. Shi SaG, S. Perivascular niche of postnatal mesenchymal stem cells in human bone marrow and dental pulp. *Journal of Bone and Mineral Research 2003* ;18(**4**):696-704.

5. Igura K, Zhang X, Takahashi K, Mitsuru A, Yamaguchi S, Takashi TA. Isolation and characterization of mesenchymal progenitor cells from chorionic villi of human placenta. *Cytotherapy 2004*;6(**6**):543-53.

6. De Bari C, Dell'Accio F, Tylzanowski P, Luyten FP. Multipotent mesenchymal stem cells from adult human synovial membrane. *Arthritis Rheum 2001*;44(**8**):1928-42.

7. Schipani E, Kronenberg HM. Adult mesenchymal stem cells.

8. Crisan M, Yap S, Casteilla L, Chen CW, Corselli M, Park TS, et al. A perivascular origin for mesenchymal stem cells in multiple human organs. *Cell Stem Cell 2008*;3(**3**):301-139. Gronthos S MM, Brahim J, et al. Postnatal human dental pulp stem cells (DPSCs)in vitro and in vivo. *Proc Natl Acad Sci U S A 2000*;**97**:3625-13630.

10. Seo BM, Miura M, Gronthos S, Bartold PM, Batouli S, Brahim J, et al. Investigation of multipotent postnatal stem cells from human periodontal ligament. *Lancet 2004*;364(**9429**):149-55.

11. Kuznetsov SA, Mankani MH, Gronthos S, Satomura K, Bianco P, Robey PG. Circulating skeletal stem cells. *J Cell Biol 2001*;153(**5**):1133-40.

12. Li MH, Tian D, Liu CY, Sun XJ, Wan SG, Su L, et al. [Expansion ex vivo of human bone marrow mesenchymal stem cells and cord blood CD34+ cells]. *Zhongguo Shi Yan Xue Ye Xue Za Zhi 2005*;13(**2**):235-9.

13. Bi Y, Ehirchiou D, Kilts TM, Inkson CA, Embree MC, Sonoyama W, et al. Identification of tendon stem/progenitor cells and the role of the extracellular matrix in their niche. *Nat Med 2007*;13(**10**):1219-27..

14. Friedenstein.Aj, Chailakh.Rk, Lalykina KS. Development of fibroblast colonies in monolayer culture of guinea-pig bone-marrow and spleen cells. *Cell and Tissue Kinetics 1970*;3(**4**):393-&.

15. Castromalaspina H, Gay RE, Resnick G, Kapoor N, Meyers P, Chiarieri D, et al. Characterization of human bone-marrow fibroblast colony-forming cells (CFU-F) and their progeny *Blood 1980*;56(**2**):289-301.

16. Gronthos S, Zannettino ACW, Hay SJ, Shi ST, Graves SE, Kortesidis A, et al. Molecular and cellular characterisation of highly purified stromal stem cells derived from human bone marrow. *Journal of Cell Science 2003*;116(**9**):1827-35.

17. Kuznetsov SA, Friedenstein AJ, Robey PG. Factors required for bone marrow stromal fibroblast colony formation in vitro. *Br J Haematol 1997*;97(**3**):561-70.

18. Sacchetti B, Funari A, Michienzi S, Di Cesare S, Piersanti S, Saggio I, et al. Self-renewing osteoprogenitors in bone marrow sinusoids can organize a hematopoietic microenvironment. *Cell 2007*;131(**2**):324-36.

19. Muraglia A, Cancedda R, Quarto R. Clonal mesenchymal progenitors from human bone marrow differentiate in vitro according to a hierarchical model. *J Cell Sci 2000*;113(**7**):1161-6.

20. Owen M, Friedenstein AJ. Stromal stem-cells marrow-derived osteogenic precursors. *Ciba Foundation Symposia 1988*;**136**:42-60.

21. Dominici M, Le Blanc K, Mueller I, Slaper-Cortenbach I, Marini F, Krause D, et al. Minimal criteria for defining multipotent mesenchymal stromal cells. The International Society for Cellular Therapy position statement. *Cytotherapy 2006*;8(**4**):315-7.

22. Patel DM, Shah J, Srivastava AS. Therapeutic Potential of Mesenchymal Stem Cells in Regenerative Medicine. *Stem Cells International 2013*;:1-15.

23. Zannettino ACW, Paton S, Kortesidis A, Khor F, Itescu S, Gronthos S. Human multipotential mesenchymal/stromal stem cells are derived from a discrete subpopulation of STRO-1(bright)/CD34(-)/CD45(-)/glycophorin-A-bone marrow cells. *Haematologica-the Hematology Journal. 2007* ;92(**12**):1707-8.

24. Gronthos S, Zannettino AC. A method to isolate and purify human bone marrow stromal stem cells. *Methods Mol Biol 2008*;(**449**):45-57.

25. Isenmann S, Arthur A, Zannettino ACW, Turner JL, Shi ST, Glackin CA, et al. TWIST Family of Basic Helix-Loop-Helix Transcription Factors Mediate Human Mesenchymal Stem Cell Growth and Commitment. *Stem Cells. [Article] 2009 Oct*;27(**10**):2457-68.

26. Menicanin D BM, W ZAC, et al. I. Identification of a common gene Expression Signature Associated with Immature Clonal Mesenchymal Cell Populations Derived from Bone Marrow and Dental Tissues. *Stem Cells and Development 2010*;(**19**):501-1510.

27. Kortesidis A, Zannettino A, Isenmann S, Shi S, Lapidot T, Gronthos S. Stromal-derived factor-1 promotes the growth, survival, and development of human bone marrow stromal stem cells. *Blood 2005*;105(*10*):3793-801.

28. Lin GL, Hankenson KD. Integration of BMP, Wnt, and notch signaling pathways in osteoblast differentiation. Journal *of Cellular Biochemistry2011*;112(**12**):3491-501.

29. Holliday R. Epigenetics-an overview Developmental *Genetics 1994*;15(**6**):453-7.

30. Luger K, Rechsteiner TJ, Flaus AJ, Waye MMY, Richmond TJ. Characterization of nucleosome core particles containing histone proteins made in bacteria. Journal of Molecular *Biology 1997*;272(**3**):301-11.

31. Luger K, Mader AW, Richmond RK, Sargent DF, Richmond TJ. Crystal structure of the nucleosome core particle at 2.8 A resolution. *Nature 1997*;389(**6648**):251-60.

32. Riggs AD. X inactivation, differentiation, and DNA methylation. *Cytogenet Cell Genet 1975*;14(**1**):9-25.

33. Holliday R, Pugh JE. DNA modification mechanisms and gene activity during development. *Science 1975*;187(**4173**):226-32.

34. Miniou P, Jeanpierre M, Blanquet V, Sibella V, Bonneau D, Herbelin C, et al. Abnormal methylation pattern in constitutive and facultative (X inactive chromosome) heterochromatin of ICF patients. *Hum Mol Genet 1994*;3(**12**):2093-102.

35. Okano M, Xie S, Li E. Cloning and characterization of a family of novel mammalian DNA (cytosine-5) methyltransferases. *Nat Genet 1998*;19(**3**):219-20.

36. Bird A. DNA methylation patterns and epigenetic memory. *Genes & Development 2002*;16(**1**):6-21.

37. Jaenisch R, Bird A. Epigenetic regulation of gene expression: how the genome integrates intrinsic and environmental signals. *Nature Genetics 20*03;33(**3**):245-54.

38. Li E, Beard C, Jaenisch R. Role for DNA methylation in genomic imprinting. *Nature 1993*;366(**6453**):362-5.

39. Caspary T, Cleary MA, Baker CC, Guan XJ, Tilghman SM. Multiple mechanisms regulate imprinting of the mouse distal chromosome 7 gene cluster. *Mol Cell Biol 1998*;18(**6**):3466-74.

40. Li E. Chromatin modification and epigenetic reprogramming in mammalian development. *Nature Reviews Genetics 2002*;3(**9**):662-73.

41. Shock LS, Thakkar PV, Peterson EJ, Moran RG, Taylor SM. DNA methyltransferase 1, cytosine methylation, and cytosine hydroxymethylation in mammalian mitochondria. *Proc Natl Acad Sci U S A 2011*;108(**9**):3630-5.

42. Ulaner GA, Vu TH, Li T, Hu JF, Yao XM, Yang Y, et al. Loss of imprinting of IGF2 and H19 in osteosarcoma is accompanied by reciprocal methylation changes of a CTCF-binding site. *Hum Mol Genet 2003*;12(**5**):535-49.

43. Razin A, Shemer R. DNA methylation in early development. *Hum Mol Genet 1995*;(**4**):1751-5.

44. Monk M, Boubelik M, Lehnert S. Temporal and regional changes in DNA methylation in the embryonic, extraembryonic and germ cell lineages during mouse embryo development. *Development, 1987*;99(**3**):371-82.

45. Kafri T, Ariel M, Brandeis M, Shemer R, Urven L, McCarrey J, et al. Developmental pattern of gene-specific DNA methylation in the mouse embryo and germ line. *Genes Dev 1992*;6(**5**):705-14.

46. Robertson KD. DNA methylation, methyltransferases and cancer. *Oncogene 2001*;20(**24**):3139-55.

47. Vaissiere T, Sawan C, Herceg Z. Epigenetic interplay between histone modifications and DNA methylation in gene silencing. *Mutation Research/Reviews in Mutation Research 2008*;659(**1-2**):40-8.

48. Antequera F. Structure, function and evolution of CpG island promoters. *Cell Mol Life Sci 2003*;60(**8**):1647-58.

49. Ballestar E, Wolffe AP. Methyl-CpG-binding proteins. Targeting specific gene repression. *Eur J Biochem 2001*;268(**1**):1-6.

50. El-Osta A, Wolffe AP. DNA methylation and histone deacetylation in the control of gene expression: basic biochemistry to human development and disease. Gene *Expr 2000*;9(**1-2**):63-75.

51. Fuks F, Hurd PJ, Wolf D, Nan X, Bird AP, Kouzarides T. The methyl-CpG-binding protein MeCP2 links DNA methylation to histone methylation. *J Biol Chem 2003*;278(**6**):4035-40..

52. Wolffe AP, Matzke MA. Epigenetics: regulation through repression. *Science 1999*;286(**5439**):481-6.

53. Wu H, Zhang Y. Mechanisms and functions of Tet protein-mediated 5-methylcytosine oxidation. *Genes Dev 2011*;25(**23**):2436-52.

54. Tahiliani M, Koh KP, Shen Y, Pastor WA, Bandukwala H, Brudno Y, et al. Conversion of 5-methylcytosine to 5-hydroxymethylcytosine in mammalian DNA by MLL partner TET1. *Science 2009*;324(**5929**):930-5.

55. Warnecke PM, Stirzaker C, Song J, Grunau C, Melki JR, Clark SJ. Identification and resolution of artifacts in bisulfite sequencing. *Methods 2002*;27(**2**):101-7.

56. Grunau C, Clark SJ, Rosenthal A. Bisulfite genomic sequencing: systematic investigation of critical experimental parameters. *Nucleic Acids Res 2001*;29(**13**):E65-5.

57. Bock C, Beerman I, Lien WH, Smith ZD, Gu H, Boyle P, et al. DNA methylation dynamics during in vivo differentiation of blood and skin stem cells. *Mol Cell 2012*;47(**4**):633-47.

58. Smith ZD, Meissner A. DNA methylation: roles in mammalian development. *Nat Rev Genet 2013*;14(**3**):204-20.

59. Mikkelsen TS, Xu Z, Zhang X, Wang L, Gimble JM, Lander ES, et al. Comparative Epigenomic Analysis of Murine and Human Adipogenesis. *Cell 2010*;143(**1**):156-69.

60. Fisher AG. Cellular identity and lineage choice. Nat Rev *Immunol 2002*;2(**12**):977-82.

61. Bernstein BE, Meissner A, Lander ES. The mammalian epigenome. *Cell 2007*;128(**4**):669-81.

62. Bernstein B, Mikkelsen T, Xie X, Kamal M, Huebert D, Cuff J, et al. A Bivalent Chromatin Structure Marks Key Developmental Genes in Embryonic Stem Cells. *Cell 2006*;125(**2**):315-26.

63. Sasai N, Defossez PA. Many paths to one goal? The proteins that recognize methylated DNA in eukaryotes. *Int J Dev Biol 2009*;53(**2-3**):323-34.

64. Taverna SD, Li H, Ruthenburg AJ, Allis CD, Patel DJ. How chromatin-binding modules interpret histone modifications: lessons from professional pocket pickers. Nat *Struct Mol Biol2007*;14(**11**):1025-40.

65. Teven CM, Liu X, Hu N, Tang N, Kim SH, Huang E, et al. Epigenetic Regulation of Mesenchymal Stem Cells: A Focus on Osteogenic and Adipogenic Differentiation. *Stem Cells International 2011*;(**2011**):1-18.

66. Sørensen AL, Timoskainen S, West FD, Vekterud K, Boquest AC, Ährlund-Richter L, et al. Lineage-Specific Promoter DNA Methylation Patterns Segregate Adult Progenitor Cell Types. *Stem Cells and Development 2010*;19(**8**):1257-66.

67. Sorensen AL, Jacobsen BM, Reiner AH, Andersen IS, Collas P. Promoter DNA Methylation Patterns of Differentiated Cells Are Largely Programmed at the Progenitor Stage. *Molecular Biology of the Cell 2010*;21(**12**):2066-77.

68. Collas P. Programming differentiation potential in mesenchymal stem cells. *Epigenetics 2010*;5(**6**):476-82.

69. Kang MI, Kim HS, Jung YC, Kim YH, Hong SJ, Kim MK, et al. Transitional CpG methylation between promoters and retroelements of tissue-specific genes during human mesenchymal cell differentiation. *J Cell Biochem 2007*;102(**1**):224-39.

70. Noer A. Stable CpG Hypomethylation of Adipogenic Promoters in Freshly Isolated, Cultured, and Differentiated Mesenchymal Stem Cells from Adipose Tissue. *Molecular Biology of the Cell 2006*;17(**8**):3543-56.

71. Noer A, Boquest AC, Collas P. Dynamics of adipogenic promoter DNA methylation during clonal culture of human adipose stem cells to senescence. *BMC Cell Biol 2007*;(**8**):18.

72. Collas P, Noer A, oslash, rensen AL. Epigenetic Basis for the Differentiation Potential of Mesenchymal and Embryonic Stem Cells. *Transfusion Medicine and Hemotherapy 2008*;35(**3**):205-15.

73. Deng ZL, Sharff KA, Tang N, Song WX, Luo J, Luo X, et al. Regulation of osteogenic differentiation during skeletal development. *Front Biosci 2008*;(**13**):2001-21.

74. Zhang RP, Shao JZ, Xiang LX. GADD45A protein plays an essential role in active DNA demethylation during terminal osteogenic differentiation of adipose-derived mesenchymal stem cells. *J Biol Chem 2011*;286(**47**):41083-94.

75. Kitazawa R, Kitazawa S. Methylation status of a single CpG locus 3 bases upstream of TATA-box of receptor activator of nuclear factor-kappaB ligand (RANKL) gene promoter modulates cell- and tissue-specific RANKL expression and osteoclastogenesis. *Mol Endocrinol 2007*;21(**1**):148-58.

76. Delgado-Calle J, Sañudo C, Sánchez-Verde L, García-Renedo RJ, Arozamena J, Riancho JA. Epigenetic regulation of alkaline phosphatase in human cells of the osteoblastic lineage. *Bone 2011*;49(**4**):830-8.

77. Hsiao S-H, Lee K-D, Hsu C-C, Tseng M-J, Jin VX, Sun W-S, et al. DNA methylation of the Trip10 promoter accelerates mesenchymal stem cell lineage determination. *Biochemical and Biophysical Research Communications 2010*;400(**3**):305-12.

78. Dansranjavin T, Krehl S, Mueller T, Mueller LP, Schmoll HJ, Dammann RH. The role of promoter CpG methylation in the epigenetic control of stem cell related genes during differentiation. *Cell Cycle 2009*;8(**6**):916-24.

79. Arnsdorf EJ, Tummala P, Castillo AB, Zhang F, Jacobs CR. The epigenetic mechanism of mechanically induced osteogenic differentiation. *Journal of Biomechanics 2010*;43(**15**):2881-6.

80. Vire E, Brenner C, Deplus R, Blanchon L, Fraga M, Didelot C, et al. The Polycomb group protein EZH2 directly controls DNA methylation. *Nature 2006*;439(**7078**):871-4.

81. Chambeyron S, Bickmore WA. Chromatin decondensation and nuclear reorganization of the HoxB locus upon induction of transcription. *Genes & Development 2004* ;18(**10**):1119-30.

82. Perry P, Sauer S, Billon N, Richardson WD, Spivakov M, Warnes G, et al. A dynamic switch in the replication timing of key regulator genes in embryonic stem cells upon neural induction. *Cell Cycle 2004* ;3(**12**):1645-50.

83. Francis NJ, Kingston RE, Woodcock CL. Chromatin compaction by a polycomb group protein complex. *Science [2004* ;306(**5701**):1574-7.

84. Ringrose L, Ehret H, Paro R. Distinct contributions of histone H3 lysine 9 and 27 methylation to locus-specific stability of polycomb complexes. *Mol Cell 2004*;16(**4**):641-53.

85. Ringrose L, Paro R. Epigenetic regulation of cellular memory by the polycomb and trithorax group proteins. *Annual Review of Genetics 2004*;(**38**):413-43.

86. Sparmann A, van Lohuizen M. Polycomb silencers control cell fate, development and cancer. *Nature Reviews Cancer 2006* ;6(**11**):846-56.

87. Hemming S, Cakouros D, Isenmann S, Cooper L, Menicanin D, Zannettino A, et al. EZH2 and KDM6A Act as an Epigenetic Switch to Regulate Mesenchymal Stem Cell Lineage Specification. *Stem Cells 2014*;32(**3**):802-15.

88. Wei Y, Chen Y-H, Li L-Y, Lang J, Yeh S-P, Shi B, et al. CDK1-dependent phosphorylation of EZH2 suppresses methylation of H3K27 and promotes osteogenic differentiation of human mesenchymal stem cells. *Nature Cell Biology 2010*;13(**1**):87-94.

89. Chen YH, Yeh FL, Yeh SP, Ma HT, Hung SC, Hung MC, et al. Myocyte Enhancer Factor-2 Interacting Transcriptional Repressor (MITR) Is a Switch That Promotes Osteogenesis and Inhibits Adipogenesis of Mesenchymal Stem Cells by

Inactivating Peroxisome Proliferator-activated Receptor -2. *Journal of Biological Chemistry 2011*;286(**12**):10671-80.

90. Ye L, Fan Z, Yu B, Chang J, Al Hezaimi K, Zhou X, et al. Histone Demethylases KDM4B and KDM6B Promotes Osteogenic Differentiation of Human MSCs. *Cell Stem Cell 2012*;11(**1**):50-61.

91. Yang D, Okamura H, Nakashima Y, Haneji T. Histone Demethylase Jmjd3 Regulates Osteoblast Differentiation via Transcription Factors Runx2 and Osterix. *Journal of Biological Chemistry 2013*;288(**47**):33530-41.

92. Huszar JM, Payne CJ. MIR146A inhibits JMJD3 expression and osteogenic differentiation in human mesenchymal stem cells. *FEBS Letters 2014*;588(**9**):1850-6.

93. Xu J, Yu B, Hong C, Wang C-Y. KDM6B epigenetically regulates odontogenic differentiation of dental mesenchymal stem cells. *International Journal of Oral Science 2013*;5(**4**):200-5.

94. Wu H, Sun YE. Epigenetic regulation of stem cell differentiation. *Pediatr Res 2006*;59(**4 Pt 2**):21R-5R.

95. Tan J, Lu J, Huang W, Dong Z, Kong C, Li L, et al. Genome-wide analysis of histone H3 lysine9 modifications in human mesenchymal stem cell osteogenic differentiation. *PLoS ONE 2009*;4(**8**).

96. Burdge GC, Lillycrop KA. Bridging the gap between epigenetics research and nutritional public health interventions. *Genome Med 2010*;2(**11**):80.

97. Santos-Rosa H, Schneider R, Bernstein BE, Karabetsou N, Morillon A, Weise C, et al. Methylation of histone H3K4 mediates association of the Isw1p ATPase with chromatin. *Molecular Cell 2003*;12(**5**):1325-32.

98. Musri MM, Corominola H, Casamitjana R, Gomis R, Parrizas M. Histone H3 lysine 4 dimethylation signals the transcriptional competence of the adiponectin promoter in preadipocytes. *J Biol Chem 2006*;281(**25**):17180-8.

99. Cho YW, Hong T, Hong S, Guo H, Yu H, Kim D, et al. PTIP associates with MLL3- and MLL4-containing histone H3 lysine 4 methyltransferase complex. *J Biol Chem 2007*;282(**28**):20395-406.

100. Hassan MQ, Tare R, Lee SH, Mandeville M, Weiner B, Montecino M, et al. HOXA10 Controls Osteoblastogenesis by Directly Activating Bone Regulatory and Phenotypic Genes. *Molecular and Cellular Biology 2007*;27(**9**):3337-52.

101. Ge W, Shi L, Zhou Y, Liu Y, Ma GE, Jiang Y, et al. Inhibition of osteogenic differentiation of human adipose-derived stromal cells by retinoblastoma binding protein 2 repression of RUNX2-activated transcription. *Stem Cells 2011*;29(**7**):1112-25.

102. Sinha KM, Yasuda H, Coombes MM, Dent SY, de Crombrugghe B. Regulation of the osteoblast-specific transcription factor Osterix by NO66, a Jumonji family histone demethylase. *Embo J 2010*;29(**1**):68-79.

103. Li Z, Liu C, Xie Z, Song P, Zhao RC, Guo L, et al. Epigenetic dysregulation in mesenchymal stem cell aging and spontaneous differentiation. *PLoS One 2011*;6(**6**)

104. Westendorf JJ, Zaidi SK, Cascino JE, Kahler R, van Wijnen AJ, Lian JB, et al. Runx2 (Cbfa1, AML-3) interacts with histone deacetylase 6 and represses the p21(CIP1/WAF1) promoter. *Mol Cell Biol 2002*;22(**22**):7982-92.

105. Jensen ED, Schroeder TM, Bailey J, Gopalakrishnan R, Westendorf JJ. Histone deacetylase 7 associates with Runx2 and represses its activity during osteoblast maturation in a deacetylation-independent manner. *J Bone Miner Res. 2008*;23(**3**):361-72.

106. Schroeder TM, Kahler RA, Li X, Westendorf JJ. Histone deacetylase 3 interacts with runx2 to repress the osteocalcin promoter and regulate osteoblast differentiation. *J Biol Chem 2004*;279(**40**):41998-2007.

107. McGee-Lawrence ME, Westendorf JJ. Histone deacetylases in skeletal development and bone mass maintenance. *Gene 2011*;474(**1-2**):1-11.

108. Lee TI, Jenner RG, Boyer LA, Guenther MG, Levine SS, Kumar RM, et al. Control of developmental regulator's by polycomb in human embryonic stem cells. *Cell 2006* ;125(**2**):301-13.

109. Cho HH, Park HT, Kim YJ, Bae YC, Suh KT, Jung JS. Induction of osteogenic differentiation of human mesenchymal stem cells by histone deacetylase inhibitors. J *Cell Biochem 2005*;96(**3**):533-42.

110. Lee HW, Suh JH, Kim AY, Lee YS, Park SY, Kim JB. Histone deacetylase 1-mediated histone modification regulates osteoblast differentiation. *Mol Endocrinol 2006*;20(**10**):2432-43.

111. Xu S, De Veirman K, Evans H, Santini GC, Vande Broek I, Leleu X, et al. Effect of the HDAC inhibitor vorinostat on the osteogenic differentiation of mesenchymal stem cells in vitro and bone formation in vivo. *Acta Pharmacol Sin 2013*;34(**5**):699-709.

112. Lee S, Park JR, Seo MS, Roh KH, Park SB, Hwang JW, et al. Histone deacetylase inhibitors decrease proliferation potential and multilineage differentiation capability of human mesenchymal stem cells. *Cell Proliferation 2009*;42(**6**):711-20.

113. de Boer J, Licht R, Bongers M, van der Klundert T, Arends R, van Blitterswijk C. Inhibition of histone acetylation as a tool in bone tissue engineering. *Tissue Eng 2006*;12(**10**):2927-37.

114. Di Bernardo G, Squillaro T, Dell'Aversana C, Miceli M, Cipollaro M, Cascino A, et al. Histone deacetylase inhibitors promote apoptosis and senescence in human mesenchymal stem cells. *Stem Cells Dev 2009*;18(**4**):573-81.

115. Wang L, Jin Q, Lee JE, Su Ih, Ge K. Histone H3K27 methyltransferase Ezh2 represses Wnt genes to facilitate adipogenesis. *Proceedings of the National Academy of Sciences 2010*;107(**16**):7317-22.

116. Wakabayashi K, Okamura M, Tsutsumi S, Nishikawa NS, Tanaka T, Sakakibara I, et al. The peroxisome proliferator-activated receptor gamma/retinoid X receptor alpha heterodimer targets the histone modification enzyme PR-Set7/Setd8 gene and regulates adipogenesis through a positive feedback loop. Mol *Cell Biol 2009*;29(**13**):3544-55.

117.Zhang ZC, Liu Y, Li SF, Guo L, Zhao Y, Qian SW, et al. Suv39h1 Mediates AP-2alpha-Dependent Inhibition of C/EBPalpha Expression during Adipogenesis. *Mol Cell Biol 2014*;34(**12**):2330-8. doi: 10.1128/MCB.00070-14.

118. Fu M, Rao M, Bouras T, Wang C, Wu K, Zhang X, et al. Cyclin D1 inhibits peroxisome proliferator-activated receptor gamma-mediated adipogenesis through histone deacetylase recruitment. *J Biol Chem 2005*;280(**17**):16934-41.

119. Takada I, Mihara M, Suzawa M, Ohtake F, Kobayashi S, Igarashi M, et al. A histone lysine methyltransferase activated by non-canonical Wnt signalling suppresses PPAR-γ transactivation. *Nature Cell Biology 2007*;9(**11**):1273-85.

120. Takada I, Kouzmenko AP, Kato S. Wnt and PPARγ signaling in osteoblastogenesis and adipogenesis. *Nature Reviews Rheumatology 2009*;5(**8**):442-7.

121. Wu H, Chen X, Xiong J, Li Y, Li H, Ding X, et al. Histone methyltransferase G9a contributes to H3K27 methylation in vivo. *Cell Research 2010*;21(**2**):365-7.

122. Wang L, Xu S, Lee JE, Baldridge A, Grullon S, Peng W, et al. Histone H3K9 methyltransferase G9a represses PPARgamma expression and adipogenesis. *Embo J 2013*;32(**1**):45-59.

123.Musri MM, Carmona MC, Hanzu FA, Kaliman P, Gomis R, Parrizas M. Histone demethylase LSD1 regulates adipogenesis. *J Biol Chem 2010*;285(**39**):30034-41.

124. Musri MM, Gomis R, Parrizas M. A chromatin perspective of adipogenesis. *Organogenesis 2010*;6(**1**):15-23.

125. Lee JE, Wang C, Xu S, Cho YW, Wang L, Feng X, et al. H3K4 mono- and di-methyltransferase MLL4 is required for enhancer activation during cell differentiation. *Elife (Cambridge) 2013*;(2)

126. Lee J-E, Ge K. Transcriptional and epigenetic regulation of PPARγ expression during adipogenesis. *Cell & Bioscience 2014*;4(**1**):29.

127. Okamura M, Inagaki T, Tanaka T, Sakai J. Role of histone methylation and demethylation in adipogenesis and obesity. *Organogenesis 2010*;6(**1**):24-32.

128. Bedford MT, Richard S. Arginine methylation an emerging regulator of protein function. *Mol Cell 2005*;18(**3**):263-72.

129. LeBlanc SE, Konda S, Wu Q, Hu YJ, Oslowski CM, Sif S, et al. Protein arginine methyltransferase 5 (Prmt5) promotes gene expression of peroxisome proliferator-activated receptor gamma2 (PPARgamma2) and its target genes during adipogenesis. *Mol Endocrinol 2012*;26(**4**):583-97.

130. Salma N, Xiao H, Mueller E, Imbalzano AN. Temporal recruitment of transcription factors and SWI/SNF chromatin-remodeling enzymes during adipogenic induction of the peroxisome proliferator-activated receptor gamma nuclear hormone receptor. *Mol Cell Biol 2004*;24(**11**):4651-63.

131. Johmura Y, Osada S, Nishizuka M, Imagawa M. FAD24 acts in concert with histone acetyltransferase HBO1 to promote adipogenesis by controlling DNA replication. *J Biol Chem 2008*;283(**4**):2265-74.

132. Kim EY, Kim WK, Kang HJ, Kim JH, Chung SJ, Seo YS, et al. Acetylation of malate dehydrogenase 1 promotes adipogenic differentiation via activating its enzymatic activity. *J Lipid Res 2012*;53(**9**):1864-76.

133. Fajas L, Egler V, Reiter R, Hansen J, Kristiansen K, Debril MB, et al. The retinoblastoma-histone deacetylase 3 complex inhibits PPARgamma and adipocyte differentiation. *Dev Cell 2002*;3(**6**):903-10.

134. Zych J, Stimamiglio MA, Senegaglia AC, Brofman PRS, Dallagiovanna B, Goldenberg S, et al. The epigenetic modifiers 5-aza-2'-deoxycytidine and trichostatin A influence adipocyte differentiation in human mesenchymal stem cells. Brazilian *Journal of Medical and Biological Research 2013*;46(**5**):405-16.

135. Jones PA, Wolkowicz MJ, Rideout WM, 3rd, Gonzales FA, Marziasz CM, Coetzee GA, et al. De novo methylation of the MyoD1 CpG island during the establishment of immortal cell lines. *Proc Natl Acad Sci U S A 1990*;87(**16**):6117-21.

136. Brero A. Methyl CpG-binding proteins induce large-scale chromatin reorganization during terminal differentiation. The *Journal of Cell Biology 2005*;169(**5**):733-43.

137. Nakatsuka R, Nozaki T, Uemura Y, Matsuoka Y, Sasaki Y, Shinohara M, et al. 5-Aza-2′-deoxycytidine treatment induces skeletal myogenic differentiation of mouse dental pulp stem cells. *Archives of Oral Biology 2010*;55(**5**):350-7.

138. Caretti G, Di Padova M, Micales B, Lyons GE, Sartorelli V. The Polycomb Ezh2 methyltransferase regulates muscle gene expression and skeletal muscle differentiation. *Genes Dev 2004 Nov 1*;18(**21**):2627-38.

139. van der Vlag J, Otte AP. Transcriptional repression mediated by the human polycomb-group protein EED involves histone deacetylation. *Nat Genet 1999*;23(**4**):474-8.

140. Mal A, Harter ML. MyoD is functionally linked to the silencing of a muscle-specific regulatory gene prior to skeletal myogenesis. *Proc Natl Acad Sci U S A 2003*;100(**4**):1735-9.

141. Juan AH, Kumar RM, Marx JG, Young RA, Sartorelli V. Mir-214-dependent regulation of the polycomb protein Ezh2 in skeletal muscle and embryonic stem cells. *Mol Cell 2009*;36(*1*):61-74.

142. Seenundun S, Rampalli S, Liu Q-C, Aziz A, Palii C, Hong S, et al. UTX mediates demethylation of H3K27me3 at muscle-specific genes during myogenesis. *The EMBO Journal 2010*;29(**8**):1401-11.

143. Sebastian S, Sreenivas P, Sambasivan R, Cheedipudi S, Kandalla P, Pavlath GK, et al. MLL5, a trithorax homolog, indirectly regulates H3K4 methylation, represses cyclin A2 expression, and promotes myogenic differentiation. *Proc Natl Acad Sci U S A 2009;*106(**12**):4719-24.

144. Zimmermann P, Boeuf S, Dickhut A, Boehmer S, Olek S, Richter W. Correlation of COL10A1 induction during chondrogenesis of mesenchymal stem cells with

demethylation of two CpG sites in the COL10A1 promoter. *Arthritis Rheum 2008*;58(**9**):2743-53.

145. Imagawa K, de Andres MC, Hashimoto K, Itoi E, Otero M, Roach HI, et al. Association of Reduced Type IX Collagen Gene Expression in Human Osteoarthritic Chondrocytes With Epigenetic Silencing by DNA Hypermethylation. Arthritis *Rheumatol 2014*;66(**11**):3040-51.

146. Studer D, Millan C, Ozturk E, Maniura-Weber K, Zenobi-Wong M. Molecular and biophysical mechanisms regulating hypertrophic differentiation in chondrocytes and mesenchymal stem cells. *Eur Cell Mater 2012*;(**24**):118-35.

147. Ezura Y, Sekiya I, Koga H, Muneta T, Noda M. Methylation status of CpG islands in the promoter regions of signature genes during chondrogenesis of human synovium-derived mesenchymal stem cells. *Arthritis & Rheumatism 2009*;60(**5**):1416-26.

148. Mohn F, Weber M, Rebhan M, Roloff TC, Richter J, Stadler MB, et al. Lineage-specific polycomb targets and de novo DNA methylation define restriction and potential of neuronal progenitors. *Mol Cell 2008*;30(**6**):755-66.

149. Meissner A, Mikkelsen TS, Gu H, Wernig M, Hanna J, Sivachenko A, et al. Genome-scale DNA methylation maps of pluripotent and differentiated cells. *Nature 2008*.

150. Herlofsen SR, Bryne JC, Hoiby T, Wang L, Issner R, Zhang X, et al. Genome-wide map of quantified epigenetic changes during in vitro chondrogenic differentiation of primary human mesenchymal stem cells. *BMC Genomics 2013*;(**14**):105.

151. Hata K, Takashima R, Amano K, Ono K, Nakanishi M, Yoshida M, et al. Arid5b facilitates chondrogenesis by recruiting the histone demethylase Phf2 to Sox9-regulated genes. *Nat Commun 2013*;(**4**):2850.

152.Hattori T, Coustry F, Stephens S, Eberspaecher H, Takigawa M, Yasuda H, et al. Transcriptional regulation of chondrogenesis by coactivator Tip60 via chromatin association with Sox9 and Sox5. *Nucleic Acids Res 2008*;36(**9**):3011-24.

153. Furumatsu T, Ozaki T. Epigenetic regulation in chondrogenesis. *Acta Med Okayama 2010*;64(**3**):155-61.

154. Furumatsu T, Tsuda M, Yoshida K, Taniguchi N, Ito T, Hashimoto M, et al. Sox9 and p300 cooperatively regulate chromatin-mediated transcription. *J Biol Chem 2005*;280(**42**):35203-8.

155.El-Serafi AT, Oreffo RO, Roach HI. Epigenetic modifiers influence lineage commitment of human bone marrow stromal cells: Differential effects of 5-aza-deoxycytidine and trichostatin A. *Differentiation 2011* ;81(**1**):35-41.

156. Huh YH, Ryu JH, Chun JS. Regulation of type II collagen expression by histone deacetylase in articular chondrocytes. *J Biol Chem2007*;282(**23**):17123-31.

157. Pei M, Chen D, Li J, Wei L. Histone deacetylase 4 promotes TGF-β1-induced synovium-derived stem cell chondrogenesis but inhibits chondrogenically differentiated stem cell hypertrophy. *Differentiation 2009*;78(**5**):260-8.

158. Vega RB, Matsuda K, Oh J, Barbosa AC, Yang X, Meadows E, et al. Histone deacetylase 4 controls chondrocyte hypertrophy during skeletogenesis. *Cell 2004*;119(**4**):555-66.

159. Schellenberg A, Lin Q, Schuler H, Koch CM, Joussen S, Denecke B, et al. Replicative senescence of mesenchymal stem cells causes DNA-methylation changes which correlate with repressive histone marks. *Aging (Albany NY) 2011*;3(**9**):873-88.

160. Mahaira LG, Katsara O, Pappou E, Iliopoulou EG, Fortis S, Antsaklis A, et al. IGF2BP1 Expression in Human Mesenchymal Stem Cells Significantly Affects Their Proliferation and Is Under the Epigenetic Control of TET1/2 Demethylases. Stem *Cells Dev 2014*;23(**20**):2501-12.

161.Cakouros D, Isenmann S, Cooper L, Zannettino A, Anderson P, Glackin C, et al. Twist-1 Induces Ezh2 Recruitment Regulating Histone Methylation along the Ink4A/Arf Locus in Mesenchymal Stem Cells. *Molecular and Cellular Biology 2012*;32(**8**):1433-41.

162. Kamminga LM, Bystrykh LV, de Boer A, Houwer S, Douma J, Weersing E, et al. The Polycomb group gene Ezh2 prevents hematopoietic stem cell exhaustion. *Blood 2006*;107(**5**):2170-9.

163. Zheng Y, He L, Wan Y, Song J. H3K9me-Enhanced DNA Hypermethylation of thep16INK4aGene: An Epigenetic Signature for Spontaneous Transformation of Rat Mesenchymal Stem Cells. *Stem Cells and Development 2013*;22(**2**):256-67.

164. Easwaran H, Johnstone SE, Van Neste L, Ohm J, Mosbruger T, Wang Q, et al. A DNA hypermethylation module for the stem/progenitor cell signature of cancer. *Genome Research 2012*;22(**5**):837-49.

165. Lazarus HM, Haynesworth SE, Gerson SL, Rosenthal NS, Caplan AI. Ex vivo expansion and subsequent infusion of human bone marrow-derived stromal progenitor cells (mesenchymal progenitor cells): implications for therapeutic use. *Bone Marrow Transplant 1995*;16(**4**):557-64.

166. Ikebe C, Suzuki K. Mesenchymal Stem Cells for Regenerative Therapy: Optimization of Cell Preparation Protocols. *BioMed Research International 2014*;(**2014**):1-11.

167. Lalu MM, McIntyre L, Pugliese C, Fergusson D, Winston BW, Marshall JC, et al. Safety of cell therapy with mesenchymal stromal cells (SafeCell): a systematic review and meta-analysis of clinical trials. *PLoS One 2012*;7(**10**):e47559.

Table 1. Histone modifiers which regulate MSC osteogenic and adipogenic differentiation

Epigenetic Modifier	Modification	Osteogenesis	References	Adipogenesis	References
DNA Methylation					
DMT1	5MC	Represses Runx2 & Alx5 in ADSCs. Regulates ALP, Trip10 & RANKL in MSC.	Zhang,2011 [74] Kitazawa,2007[75] Delgado-Calle, 2011 [76] Hsiao, 2010 [77]	DNA hypomethylation on PPARγ2 and Leptin in cultured adipose derived MSC.	Fu, 2005 [118]
Methylation					
EZH2	H3K27me3	CDK1 phosphorylates EZH2 promoting osteogenesis. Over-expression repressed RUNX2 & OP expression. Ezh2 represses PPARγ2 promoting osteogenesis.	Wei, 2010 [88] Hemming,2014 [87] Chen, 2011 [89]	EZH2 regulates represses non-canonical pathway promoting adipogenesis. Over-expression promotes adipogenesis.	Wang, 2010 [115] Hemming,2014 [87]
Setdb1	H3K9me3	Suppresses PPARγ2 activation by H3K9me3.	Takada, 2007 [119] Takada, 2009 [120]	Down regulated during adipogenesis.	Takada, 2007 [119] Takada, 2009 [120]
Suv39h1	H3K9me3	-		Suv39h1 mediates A2 repression of C/EBP -α	Fu, 2005
G9a	H3K9me3	-		Inhibiton promotes PPARγ2 expression.	Wang, 2013 [122]
MLL3/MLL4	H3K4me3	Promotes osteogenesis by HOXA mediated activation of Runx2 and OC.	Hassan,2007 [100]	Recruited to PPARγ2 activated gene ap2.	Musri, 2010 [123] Cho, 2007 [99] Lee, 2013 [125] Lee, 2014 [126]
PR-Set7/Setd8	H4K20me1	-		Over-expression promotes adipogenesis with methylation of PPARγ2.	Wakabayashi, 2009 [116]
PRMT5	H3R81/2	-		Knockdown inhibits adipogenesis.	Salma, 2004[130]
Demethylation					
UTX/KDM6A	H3K27me3	Over-expression promotes osteogenesis with the demethylation of RUNX2 & OP.	Hemming,2014 [87]	Over-expression inhibits adipogenesis.	Hemming,2014 [87]
JMJD3/KDMB	H3K27me3	Overexpression promotes RUNX2 & OSX expression and osteogenesis.	Yang,2013 [91] Ye,2012 [90] Xu, 2013 [93]	Knockdown promoted adipogenesis.	Ye, 2012 [90]
JARIDIA	H3K4me3	Inhibits RUNX2, ALP & OSX by demethylation.	Ge,2011 [101]	-	
KDM4B	H3K9me3	Demthylates HOX and DLX promoting osteogenesis	Ye,2012 [90]	Knockdown promoted adipogenesis	Ye, 2012 [90]
LSD1	H3K9me3	-		Promotes adipogenic by removing H3K9me3 on C/EBPα.	Musri, 2010 [98]
N066	H3K4me3	Prevents OSX activation.	Sinha, 2010 [102]	-	
RBP2	H3K4me3	Knockdown of RBP2 increased ALP, OC & OSX expression.	Ge,2011 [101]	-	
Acetylation					
HATS	H3K9ac, H3K14ac	Dysregulation leads to osteogenesis in long term cultured MSC.	Li,2011 [103]	-	
	H3ac , H4ac	Hyper acetylation prevents HDAC removal on OC & OSX. Regulates osteogenesis through Runx2	Westendorf,2002 [104] Jensen,2008 [105] Schroeder,2004 [106] McGee-Lawrence, 2011 [107]	-	
HDAC Inhibitors					
TSA, Vorinostat, Sodium Butyrate, Valproic acid	H3ac, H4ac	Promoted osteogenesis.	Cho, 2005 [109] Lee, 2006 [110] Xu, 2013 [111] Lee, 2009 [112] de Boer, 2006 [113] Di Bernardo, 2009 [114]	Inhibited adipogenic differentiation.	Zych, 2013 [134]
Deacetylases					
HDAC	H3ac H4ac	-		RB recruits HDAC3 prevents PPARγ2 activation	Fajas, 2002 [133]

H3K4me3-Histone three lysine 4 tri methylation, H3K27me3-Histone three lysine 27 tri methylation, H3K9me3,Histone three lysine 9 tri methylation, H4K20me2,-Histone four lysine 20 mono methylation. H3K9ac-Histone three lysine 9 acetylation, H3ac and H4ac, Histone 3 and 4 acetylation, HDAC-Histone deacetylases,HATS- Histone acetyltransferases,DNMT1-DNA methyltransferases 1 Runx2-Runt-related transcription factor 2,OP-Osteopontin,OSX-Osterix,OC-Osteocalcin,RB-Retinoblastoma,ALP-Alkaline Phosphatase,CEBP α-CCAAT/enhancer-binding protein alpha PPARγ2-Peroxisome proliferator-activated receptor gamma, HOX-homeotic genes,CDK1-Cyclin Depended Kinase 1.

Table 2. Epigenetic modifiers regulate DNA and histone marks on master regulatory genes during MSC differentiation

Modification	PPARγ2	RUNX2	MOYD	SOX9
5 methyl cytosine	Hypo-methylation during adipogenesis [118].	Demethylation during osteogenesis [74].	Un-methylated in non-expressing Tissues [138].	-
H3K27me3	Low methylation present in pre-adipocytes[115].	Methylated in MSC [87,88]. Removed on osteoblasts [87,91].	Prevents MYOD recruitment to muscle genes [135]. miRNA removes EZH2 from MYOD in muscle differentiation [138,140].	-
H3K9me3	Methylation on PPARγ2 promotes osteogenesis [96]. Inhibits adipogenesis. Methylation present in preadipocytes [115].	-		Demethylation activates sox9 during chondrogenesis [150,151].
H3K4me2	Promotes adipogenesis [98,99,125,126].	Promotes osteogenesis. Methylation removed in adipocytes [100].	-	-
H4K20me1	Promotes adipogenesis [116].	-		-
H3R8	Promotes adipogenesis [129]	-		-
H3K9ac	Prevent s PPARγ2 activation [133].	Dysregulated in MSC lead to spontaneous osteogenic differentiation [103] HDAC4 inhibits RUNX2 promoting chondrogenesis [157]		Acetylases inhibition promotes chondrogenesis [154]. Acetylases inhibition promotes chondrogenesis [154].

H3K4me3-Histone three lysine 4 tri methylation, H3K27me3-Histone three lysine 27 tri methylation, H3K9me3,Histone three lysine 9 tri methylation, H4K20me2,-Histone four lysine 20 mono methylation. H3K9ac-Histone three lysine 9 acetylation, H3ac and H4ac, Histone 3 and 4 acetylation, HDAC-Histone deacetylases,HATS- Histone acetyltransferases,DNMT1-DNA methyltransferases 1 Runx2-Runt-related transcription factor 2,CEBP α-CCAAT/enhancer-binding protein alpha,PPARγ2-Peroxisome proliferator-activated receptor gamma,MYOD-Myogenic Differentiation Antigen Sox9-SRY-related HMG-box 9

Figure 1. Stromal Hierarchy of MSC

Mesenchymal stem/ Stromal Cells (MSC) derived from the bone marrow contain a heterogeneous population of stem cell progenitors and committed lineage progenitors. Stem cell progenitors (MSC) express high levels of STRO-1 and low levels of lineage specific master regulatory genes. These MSC have the capacity to self-renew and differentiate. Committed lineage progenitors express low levels of STRO-1 and higher expression of specific master regulatory genes. As the committed progenitors differentiation they express key master regulator genes such as PPARγ2, RUNX2, SOX9 and MYOD as MSC differentiated into mature Adipocytes, Osteoblasts, Chondrocytes and Muscle cells respectively.

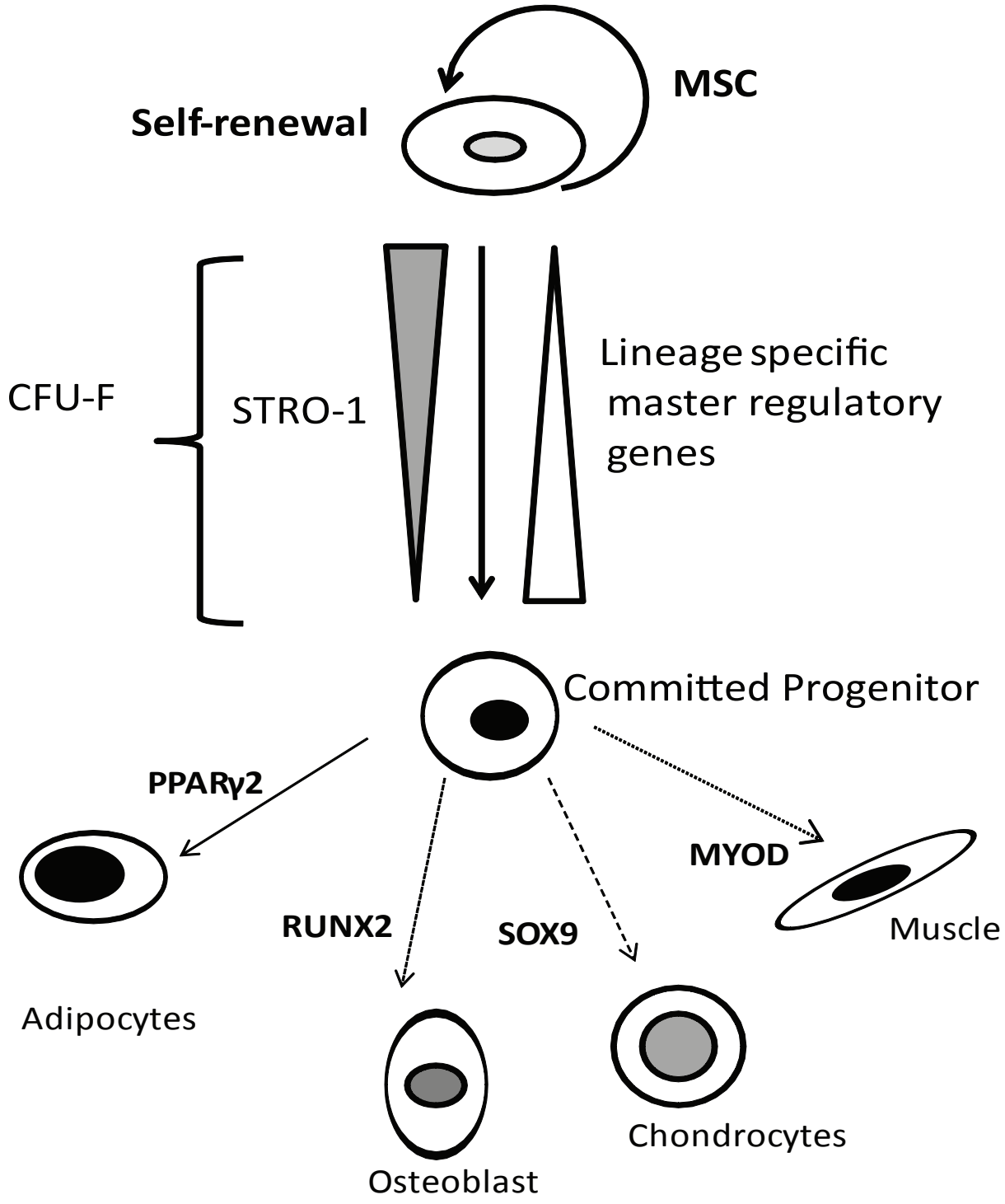
Self-renewal
MSC
CFU-F
STRO-1
Lineage specific master regulatory genes
Committed Progenitor
PPARγ2
MYOD
RUNX2
SOX9
Muscle
Adipocytes
Chondrocytes
Osteoblast

Figure 2. Compaction of DNA through the formation of chromatin

DNA is compacted within a cell through chromatin. 145-146bp DNA is wrapped around a nucleosome structure consisting of an octamer of histone subunits, 2 copies of H2 A, H2 B, H3 and H4. H1 "linker histone" anchors the DNA wrapped around the nucleosome in place. A region of DNA is present in between nucleosomes known as linker DNA. Histone tails protrude out of the histone subunits and these are regions of post-translational modifications which dictate a more open ("beads on a string") or closed chromatin structure. Nucleosomes are further compacted to form a 30 nm closed chromatin fibre structure. The structure can be further condensed to chromosomes.

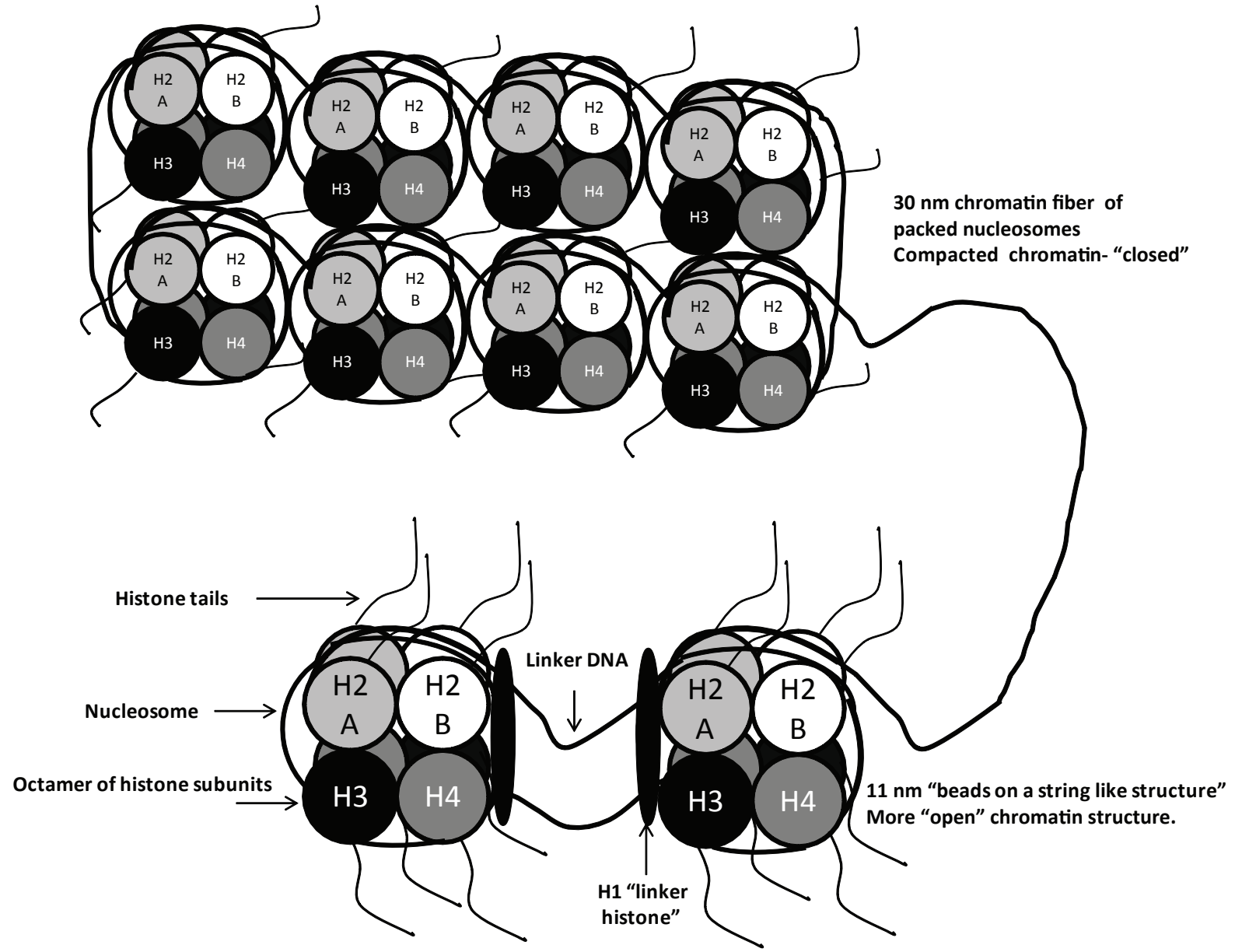
H2 A
H2 B
H3
H4
30 nm chromatin fiber of packed nucleosomes
Compacted chromatin- "closed"
Histone tails
Nucleosome
Octamer of histone subunits
Linker DNA
H1 "linker histone"
11 nm "beads on a string like structure"
More "open" chromatin structure.

Figure 3. Chromatin modifying proteins modulate chromatin structure.

DNA accessibility is dictated by chromatin structure, chromatin can be compacted or opened up leading to repression or activation of genes through DNA and post-translational histone modifications (PTMs). **A)** 5 methyl cytosine methylation (5M) of DNA by DNA methyltransferases (DNMTs). Histone three lysine 27 Histone methylation by histone methyltransferases (HMT) can tri methylate Histone three lysine nine and 27 (H3K27me3 (Ezh2)) and the removal of H3K9 acetylation (ac) by histone deacetylatases (HDACs). All these epigenetic modifications facilitate in the compaction of the chromatin structure and gene repression. **B)** Removal of 5M from DNA by DNA demethylases (dMTase) . The removal of H3K9me3 and H3K27me3 is mediated by UTX and JMJD3 histone demethylases (HDMTs). The addition of H3K4me3 and H3K420me1 methylation by HMTs and H3K9ac by acetyltransferases (HATs), lead to the opening up of chromatin and activation of gene transcription. Chromatin remodelers (CR) are recruited to chromatin by a combination of DNA and PTM leading to either the unravelling or condensation of chromatin, depending on the histone code cellular signals.

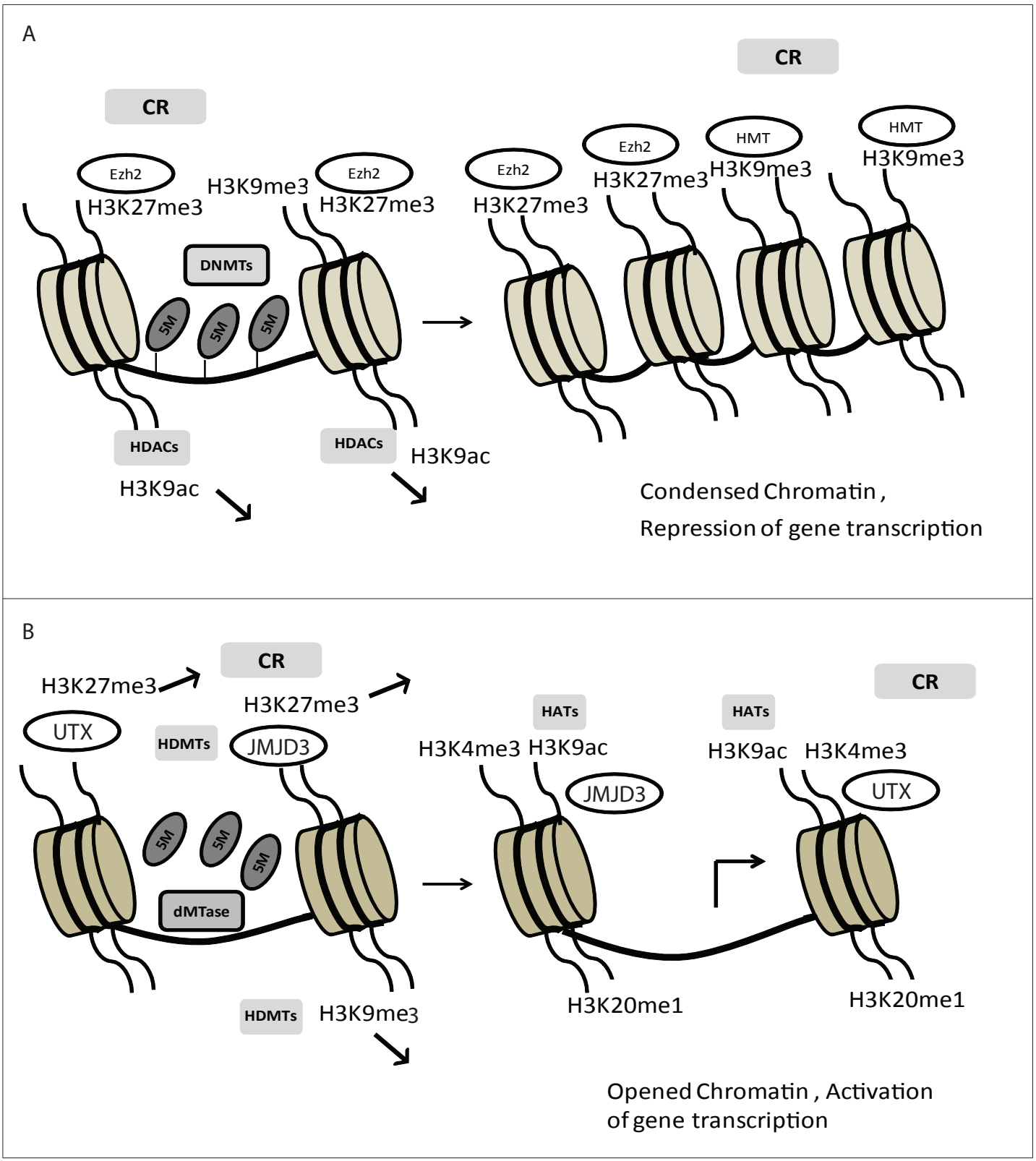
A
CR
Ezh2
H3K27me3
H3K9me3
Ezh2
H3K27me3
DNMTs
5M
5M
5M
HDACs
HDACs
H3K9ac
H3K9ac
CR
Ezh2
H3K27me3
Ezh2
H3K27me3
HMT
H3K9me3
HMT
H3K9me3
Condensed Chromatin ,
Repression of gene transcription
B
H3K27me3
CR
H3K27me3
UTX
HDMTs
JMJD3
5M
5M
5M
dMTase
HDMTs
H3K9me3
HATs
H3K4me3
H3K9ac
JMJD3
H3K20me1
CR
HATs
H3K9ac
H3K4me3
UTX
H3K20me1
Opened Chromatin , Activation
of gene transcription